SYNTHESIS AND CHARACTERIZATION OF THIOPHENES LOCKED INTO AN ANNULENE SCAFFOLD

by

MATTHEW JOHN O'CONNOR

A DISSERTATION

Presented to the Department of Chemistry
and the Graduate School of the University of Oregon
in partial fulfillment of the requirements
for the degree of
Doctor of Philosophy

March 2008

University of Oregon Graduate School

Confirmation of Approval and Acceptance of Dissertation prepared by:

Matthew O'Connor

Title:

"Synthesis and Characterization of Thiophenes Locked into an Annulene Scaffold"

This dissertation has been accepted and approved in partial fulfillment of the requirements for the Doctor of Philosophy degree in the Department of Chemistry by:

Darren Johnson, Chairperson, Chemistry
Michael Haley, Advisor, Chemistry
Marina Guenza, Member, Chemistry
James Hutchison, Member, Chemistry
Paul Wallace, Outside Member, Geological Sciences

and Richard Linton, Vice President for Research and Graduate Studies/Dean of the Graduate School for the University of Oregon.

March 22, 2008

Original approval signatures are on file with the Graduate School and the University of Oregon Libraries.

An Abstract of the Dissertation of

Matthew J. O'Connor for the degree of Doctor of Philosophy

in the Department of Chemistry to be taken March 2008

Title: SYNTHESIS AND CHARACTERIZATION OF THIOPHENES LOCKED INTO AN ANNULENE SCAFFOLD

Approved: _____

Professor Michael M. Haley

Highly conjugated carbon-rich systems have demonstrated many attractive applications for fundamental and materials science applications, including-but not limited to- probes for aromaticity, charge-transfer complexes, conducting/semi-conducting materials, linear/nonlinear optical materials, and solar cells. The bulk of this research has focused on carbon-rich fullerenes, conjugated polymers, or polycyclic aromatic hydrocarbons; however, with recent developments in cross-coupling chemistry, carbon rich chemistry, particularly dehydrobenzo[*n*]annulenes (DBAs), has grown to yield molecules of great diversity and utility.

Concurrently, materials based on conjugated heterocycles have been developed and display similar and often enhanced properties to the aforementioned carbon rich systems. The lone pair of the heterocycle often adds additional stability and polarizablity, creating novel and tunable molecules. Assimilating techniques used to produce DBAs with heteroaromatic molecules, our work has afforded a novel class of

conjugated macrocycles with the highly tunable optical-electronic properties of a DBA system. That in turn has led to the systematic study of the diverse structure-property relationships of the thiophene/DBA hybrids reported herein.

Chapter I details the synthetic advances in the field of DBA chemistry. The first section discusses the methods of synthesis, *inter-* vs. *intra*-molecular approaches, while the remaining sections provide current examples of the DBAs reported. Chapter II briefly discuses conjugated thiophene chemistry, then describes the advantages of utilizing planarized thiophenes. Several examples of thiophene macrocycles are reviewed: both planar and nonplanar. Particular attention in the review focuses on synthesis, optical properties, and some redox properties. Chapters III and IV detail the synthesis and analysis of thiophenes locked into [14]- and [15]annulene scaffolds, respectively. The dehydrothieno[14]annulenes (DTAs) and DTA/DBA hybrids of chapter III serve as aromatic probes and show significant tunabilty with respect to the number and orientation of the thiophenes. Chapter IV's dehydrobenzo[15]annulenes, which are comprised of a cross-conjugated system, also display a structure-property relationship where the optical properties encompass a wider dispersion of wavelengths. Chapter IV also explores the incorporation of pyridines and the affects on conjugation. The electronic properties of the macrocycles were explored using NMR, UV-Vis absorption and fluorescence spectroscopy, and electrochemically (cyclic voltammetry). Chapter V is devoted to further functionalization of DTAs through alkylation and further cycliziation to yield planarized terthiophene units.

This dissertation includes my previously published and co-authored material.

CURRICULUM VITAE

NAME OF AUTHOR: Matthew J O'Connor

PLACE OF BIRTH: New Haven, Connecticut

DATE OF BIRTH: June 28, 1980

GRADUATE AND UNDERGRADUATE SCHOOLS ATTENDED:

University of Oregon
University of Vermont

DEGREES AWARDED:

Doctor of Philosphy in Chemistry, 2008, University of Oregon
Bachelor of Science in Chemistry, Minor Biology, 2002, University of Vermont

AREAS OF SPECIAL INTEREST:

Organic Chemistry
Carbon-rich Chemistry
Thiophene Chemistry

PROFESSIONAL EXPERIENCE:

Graduate Research Assistant, Department of Chemistry, University of Oregon, Eugene, Oregon, 2002-2008.

Graduate Teaching Assistant, Department of Chemistry, University of Oregon, Eugene, Oregon, 2002-2007.

Undergraduate Research, Department of Chemistry, University of Vermont, Burlington, Vermont, 2002.

Research Assistant, Yale University School of Medicine, New Haven, Connecticut, 2001

GRANTS, AWARDS AND HONORS:

Merk Index Award, 2002

AEC Scholar Athlete Award, 2000

PUBLICATIONS:

O'Connor, M. J.; Yelle, R. B.; Zakharov, L. N.; Haley, M. M. "Structure-Property Investigations of Conjugated Thiophenes Fused onto a Dehydro[14]annulene Scaffold" *J. Org. Chem.*, accepted, **2008**

Johnson, C. A.; Baker, B. A.; Berryman, O. B.; Zakharov, L. N.; O'Connor, M. J.; Haley M. M. "Synthesis and Characterization of Pyridine- and Thiophene-based Platinacyclyne Topologies." *J. Organomet. Chem.* **2006**, *691,* 413-421.

Jones, C. S.; O'Connor M. J.; Haley, M. M. "Macrocycles Based on Phenyl-Acetylene Scaffolding." in *Acetylene Chemistry – Chemistry, Biology, and Materials Science*, F. Diederich, R. R. Tykwinski and P. J. Stang, Eds., Wiley-VCH: Weinheim, 2004, 303-385.

Marsden, J. A.; O'Connor, M. J.; Haley, M. M. "Synthesis and Characterization of Multiply-fused (Dehydrobenzoannuleno)annulene Topologies." *Org. Let.* **2004**, *6*, 2385-2388.

ACKNOWLEDGMENTS

I would like to thank Professor Michael Haley for the time and patience required to curate the chemist in me and allow me to not only to learn the techniques required of research, but to acquire the ability to effectively communicate my discoveries. I would like to thank my committee members: Professors Darren W. Johnson, Marina G. Guenza, James E. Hutchison, Bruce P. Branchaud, and Paul A. Wallace, for their time, advise, constructive criticism, and support. I am very grateful to Dr. Lev N. Zahkarov for his crystallographic contributions and to Dr. Robert B. Yelle for his theoretical contributions which helped immensely in my work. I would to thank Sean Mclintock, Dr. Eric Spitler, and Dr. Charles Johnson for editorial support, assistance in the laboratory, and general advice.

I would like to give much thanks and appreciation to my parents: Michael O'Connor, Kathleen Schurman as well as my step parents: David Melina, and Shaun Smith. These people molded me and instilled my stubborn "never say die" attitude that helped carried me through the program's most trying moments. Most importantly, I would like to thank my friends: Benjamin Schmidt, Jaime Sumpter, Dr. Scott Sweeney, Dr. Dave Walker, Joleen Funk, Sean Kobel, and everyone else who was there for me. I will remember them forever. These people were my life blood, cared for me, and were incessant reminders that I was never truly alone.

The investigation was supported by the National Science Foundation (CHE-0718242) and the Petroleum Research Fund for which I am very grateful.

This dissertation is dedicated to my mother Kathleen M. Schurman

TABLE OF CONTENTS

Chapter Page

Chapter Page

Chapter Page

LIST OF FIGURES

Figure Page

Chapter I

Chapter II

Figure Page

Chapter III

Chapter IV

Chapter V

Appendix A

Appendix B

Figure Page

LIST OF SCHEMES

Scheme Page

Chapter I

Scheme Page

Scheme Page

Chapter II

Scheme Page

LIST OF TABLES

CHAPTER I

MACROCYCLES BASED ON PHENYL-ACETYLENE SCAFFOLDING

1 Introduction

This chapter is a review on phenyl-acetylene macrocycles co-authored with Carissa S. Jones and Michael M. Haley composes a chapter in *Acetylene Chemistry: Chemistry, Biology, and Material Science*; Wiley-VCH: Weinheim, 2005.

The last decade of the 20th century witnessed a tremendous resurgence in the chemistry of the carbon-carbon triple bond.[1] The advent of novel synthetic methodology tailored toward the construction of the alkyne moiety, combined with use of organotransition metal complexes for carbon-carbon bond formation,[2] has revolutionized the assembly of acetylene-containing systems. In particular, recent advances in Pd-mediated cross-coupling reactions have allowed for the production of phenylacetylene derivatives from an alkyne sp-carbon atom and the sp^2 center of either an arene or an alkene,[3] while the construction of a butadiyne moiety has become routine practice in the laboratory from homo- or heterocoupling of terminal acetylene units.[4] Consequently, the assembly of novel acetylene-containing compounds including alkyne-rich marocycles, which was previously a laborious process, can now be accomplished with relative ease.

Phenylacetylene (PAM), phenyldiacetylene (PDM), phenyltri/tetraacetylene (PTM), and larger phenyloligoacetylene macrocycles are not only of theoretical importance but have also been shown to exhibit a myriad of interesting physical and chemical properties which bodes well for their use in materials applications.[5] Included in the range of fascinating properties displayed by this family of macrocycles is nonlinear optical and discotic liquid crystalline behavior, fluorescence, the ability to form host-guest complexes, while some even explode to furnish ordered carbon nanostructures. The relative ease with which phenylacetylene macrocycles can now be constructed has allowed the bench chemist to prepare a wide variety of novel derivatives that can be readily functionalized and thus allow their physical properties and chemical reactivity to be tailored.

Although a tremendous number of related aryleneethynylene macrocycles have been prepared in recent years, this report will focus on systems containing benzene and acetylene moieties only. The reader is referred to several excellent reviews regarding acetylenic macrocycles containing other arenes, metal-coordinated arenes, and heteroarenes.[6] Our review will survey the main synthetic strategies employed to prepare phenyl- and acetylene-containing macrocycles as well as provide a synopsis of the compounds prepared to date. In addition, an overview of the properties and reactivity of these novel molecules will be given.

2 Synthetic Strategies

Two main synthetic strategies exist for the preparation of phenylacetylene macrocycles and may be classified depending upon whether the ring is constructed in either an *inter-* or *intramolecular* sense. The classical approach utilizes an *intermolecular* reaction in which two or more monomers are coupled together to form the macrocycle; thus, the ring-closure involves formation of at least *two* new bonds. Whereas the starting materials are prepared with relative ease, numerous cyclooligomeric by-products are obtained in addition to the target molecule which significantly reduces the yield of the desired molecule. Conversely, the *intramolecular* approach involves building the macrocyclic precursor in a stepwise fashion. Subsequent ring-closure affords the target molecule with concomitant creation of only *one* new bond per ring formed. Although numerous steps are often required to prepare the macrocyclic synthon, the ring-closure typically proceeds in good yield and the formation of by-products is minimized. The latter has been the method of choice for phenylacetylene macrocycle construction in recent years.[5] The following subsections contain selected examples of each of these methods of macrocycle assembly

2.1 Intermolecular Approach

The initially developed (and still utilized) intermolecular approach is the cyclooligomerization technique in which several (n) monomers (X) are coupled together to form the macrocycle (Z), i.e. nX = Z. In the second approach two different components, X and Y, are coupled together to form the ring Z such that X + Y = Z.

While the former technique can afford either monoyne or diyne-linked products, this latter route has been used successfully to prepare monoyne structures only.

2.1.1 *n*X = Z

The first example of a phenyldiacetylene macrocycle (PDM) reported in the literature was described by Englinton and coworkers in the late 1950s.[7] The authors believed to have isolated the trimeric [18]annulene **1** after oxidatively coupling the terminal acetylene moieties of *o*-diethynylbenzene (**2**) using $Cu(OAc)_2$ in pyridine under high dilution conditions (Scheme 1). However, they subsequently reported that the reaction product was strained dimeric [12]annulene **3** and no evidence was obtained to support the formation of higher macrocyclic analogues such as **1**.[7] Although cyclodimer **3** proved somewhat difficult to manipulate the authors obtained a low resolution X-ray structure of the compound that showed the "bowed" diacetylenic linkages, which in turn impart significant strain upon the molecule.[9] Not surprisingly, the energy-rich hydrocarbon decomposes explosively upon grinding or upon heating above 80 °C.[8b] Although yellow crystals of **3** blacken at ambient temperature within a few days, presumably due to auto-polymerization, it can be kept in a dilute solution of benzene or pyridine for extended periods of time especially when refrigerated and stored under an inert atmosphere.

SCHEME 1. Intermolecular Synthesis of PDMs

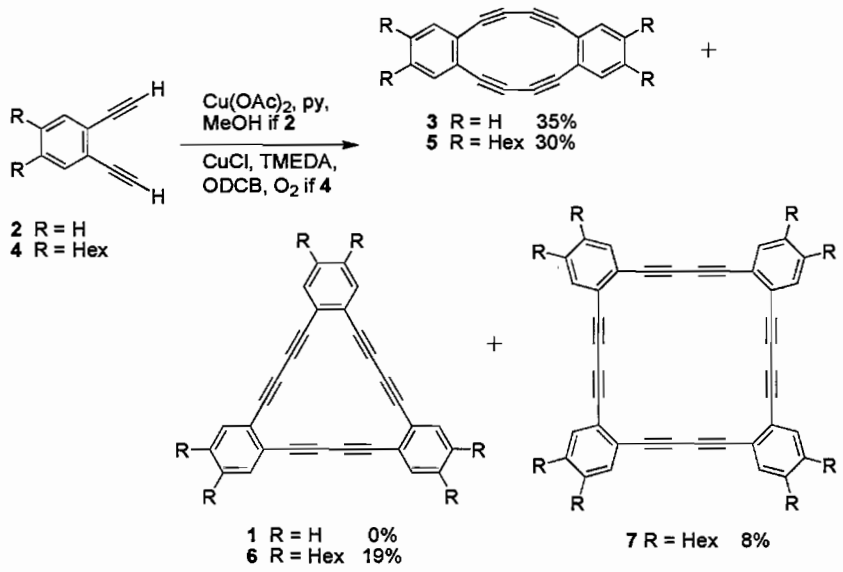

In 1994 the Swager group oxidatively homocoupled *o*-diethynylbenzene derivative **4**, which possesses two hexyl groups, to form dimer **5** as well as isolable amounts of trimer **6** and tetramer **7** (Scheme 1).[10] The successful formation of the latter two compounds can be attributed to the greater solubilizing nature of the hexyl groups and thus represents the first time that larger PDMs have been characterized from an intermolecular cyclooligomerization strategy where $n > 2$ for $n\mathrm{X} = \mathrm{Z}$.

In 1966 Eglinton et al.[11] used the Castro-Stephens reaction[12] to prepare phenylacetylene macrocycle (PAM) **8** in 26% yield (Scheme 2). The cyclization of synthon **9**, in which a Cu-acetylide group is *ortho* to a halogen, afforded only monoyne-containing macrocyclic compounds. Repetition of this work some 20 years later by Youngs and coworkers afforded the same PAM but in a somewhat higher 48% yield along with the higher macrocycles **10** and **11**.[13] Huynh and Linstrumelle have also

prepared PAM **8** (36% yield) from a Pd-mediated cross-coupling reaction of **12**.[14] In addition to **8**, the latter reaction also yields small quantities of the higher homologues **10** and **11**.[15]

SCHEME 2. Synthesis of PAMs **8**, **10**, and **11**.

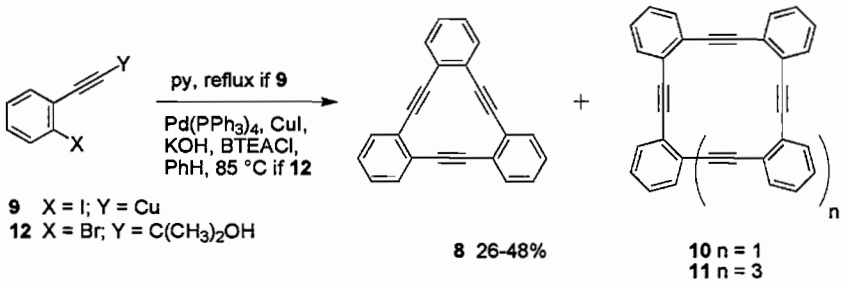

A recent report by Vollhardt and co-workers describes the synthesis of trimeric macrocycle **8** in modest yield. Alkyne metathesis of *o*-dipropynylated arene **13** was effected with the tungsten reagent [(*t*BuO)$_3$W≡C*t*Bu] to give the [12]annulene in 54% isolated yield (Scheme 3).[16]

SCHEME 3. Vollhardt Synthesis of PAM **8**

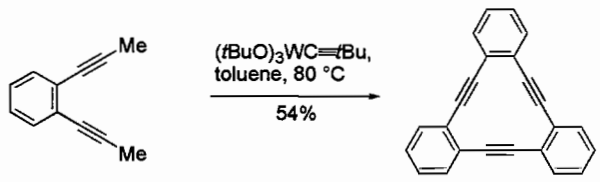

13 **8**

2.1.2 X + Y = Z

The first example of an X + Y = Z intermolecular synthesis of a phenylacetylene macrocycle was reported by Staab and Graf in 1966 (Scheme 4).[17] X and Y were the bis(ylide) derived from **14** and *o*-phthaldialdehyde, which after a double Wittig reaction,

formed intermediate **15**. Bromination of the latter compound followed by subsequent didehydrobromination with strong base gave **8** in an overall yield of 9%.

SCHEME 4. Staab Synthesis of PAM **8**.

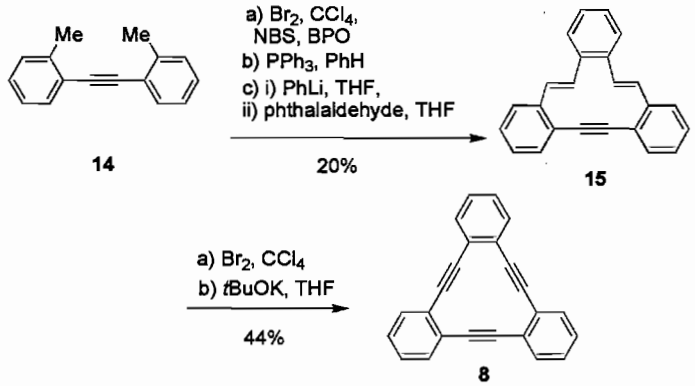

Iyoda and coworkers prepared PAM **8** in a single step by way of the intermolecular X + Y = Z approach. The authors cross-coupled 1,2-diodobenzene and excess acetylene gas, using Pd-catalysis, to give the target molecule in a modest 39% yield.[18]

The synthesis of larger oligo(phenylacetylene)s such as **16** has been accomplished by Youngs et al. from the iterative Sonogashira cross-coupling of diiodide **17** and polyyne **18** (Scheme 5).[19] In addition to isolating the 40-membered macrocycle **16** in 25% yield, the authors obtained evidence to support the formation of trace amounts of the higher derivatives $C_{160}H_{80}$, $C_{240}H_{120}$, $C_{320}H_{160}$ and $C_{400}H_{200}$.

SCHEME 5. Synthesis of PAM **16**.

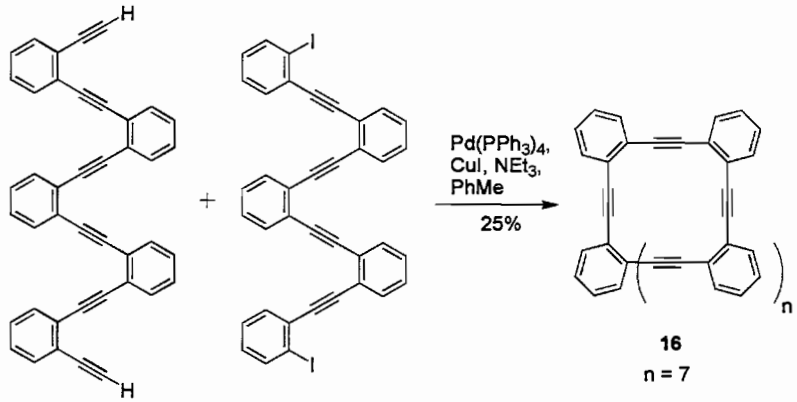

18 **17** **16**
n = 7

2.2 Intramolecular Approach

The main advantage of the intramolecular synthesis of a phenylacetylene macrocycle is that it provides a rational route towards a *single* product. Consequently, the formation of oligomeric by-products is minimized which greatly facilitates the purification of the target molecule. Although the number of steps required to prepare the macrocyclic precursor is typically high, this method allows unsymmetrical systems to be assembled. A majority of phenylacetylene macrocycles prepared recently have been synthesized by this approach.

The intramolecular synthesis can be divided into two main classes, namely, *linear* or *convergent*. In the linear approach the molecule is assembled until the ring is ready for final intramolecular ring-closure. In the convergent approach two or more components are cross-coupled together to form the macrocyclic synthon which is subjected to intramolecular ring-closure to give the target molecule.

2.2.1 Linear

The linear approach requires the greatest number to steps required for the synthesis of intermediates, most of which are obtained by way of cross-coupling reactions. Using this strategy Haley and coworkers prepared PAM **8** via a 10-step sequence (Scheme 6).[20] Thus, 2-iodoaniline was diazotized and quenched with Et_2NH (DIPA) to give the triazene which was cross-coupled with trimethylsilylacetylene (TMSA) to give the corresponding acetylene derivative. Half of this material was desilylated to give the free alkyne while the remaining material was converted into the aryl iodide by heating in MeI. Coupling of the last compound with the free alkyne gave the advanced intermediate **19**, which was converted into the triyne **20** in two steps. Finally, conversion of the triazene into the iodoarene and deprotection of the alkyne followed by intramolecular ring-closure afforded the target molecule in a modest 35% overall yield for the 10 steps. Not surprisingly, due to the significant effort required to prepare the cyclization precursor, this method is seldom used to prepare phenylacetylene macrocyclic derivatives.

2.2.2 Convergent

The first example of a convergent synthesis of a phenylacetylene macrocycle was reported by Eglinton in 1964 as proof of structure of strained PDM **1**.[21] Alkyne dimerization of the starting material with $Cu(OAc)_2$ in pyridine precluded the formation of cyclic products (Scheme 7). Didehydrobromination of the bromo intermediate furnished the terminal bisalkyne **21** which was intramolecularly homocoupled to afford **1**.

Youngs later prepared the acetylene synthon **21** from arene **22** and repeated the cyclization reaction (Scheme 7) in the presence of CuCl instead of $Cu(OAc)_2$ and aerated the solution. This modification not only afforded **1** but also the higher PDM **23**, formed in 65 and 20% yields, respectively.[22] Swager and his group obtained the [12]- and [24]annulenes **5** and **7**, respectively, from synthon **24** which was prepared from butadiyne **25**.[10] It should be noted that using the Hay catalyst (CuCl, TMEDA) in this latter reaction afforded a greater yield of tetrameric PDM **7** (45%) versus dimeric PDM **5** (13%).

SCHEME 6. Stepwise Synthesis of PAM **8**.

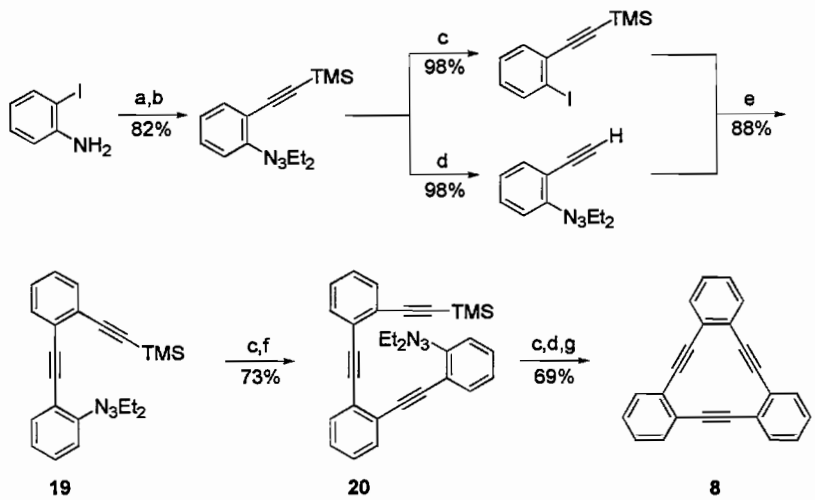

(a) i] $NaNO_2$, HCl, MeCN, H_2O, ii] Et_2NH, K_2CO_3, H_2O; (b) TMSA, $PdCl_2(PPh_3)_2$, CuI, Et_3N; (c) MeI, 120 °C; (d) K_2CO_3, THF, MeOH; (e) $PdCl_2(PPh_3)_2$, CuI, Et_3N; (f) N,N-diethyl-2-ethynylphenyltriazene, $PdCl_2(PPh_3)_2$, CuI, Et_3N; (g) $Pd(dba)_2$, PPh_3, CuI, Et_3N

By using the convergent intramolecular approach it is possible to prepare a variety of novel macrocycles that are inaccessible by the other routes. One such example is the C_{2v}-symmetric [14]annulene **26** which was prepared in an excellent 83% yield from the cyclization of tetrayne **27** with CuCl in dilute pyridine/MeOH solution (Scheme 8).[23]

SCHEME 7. Intra/Intermolecular Synthesis of PDMs.

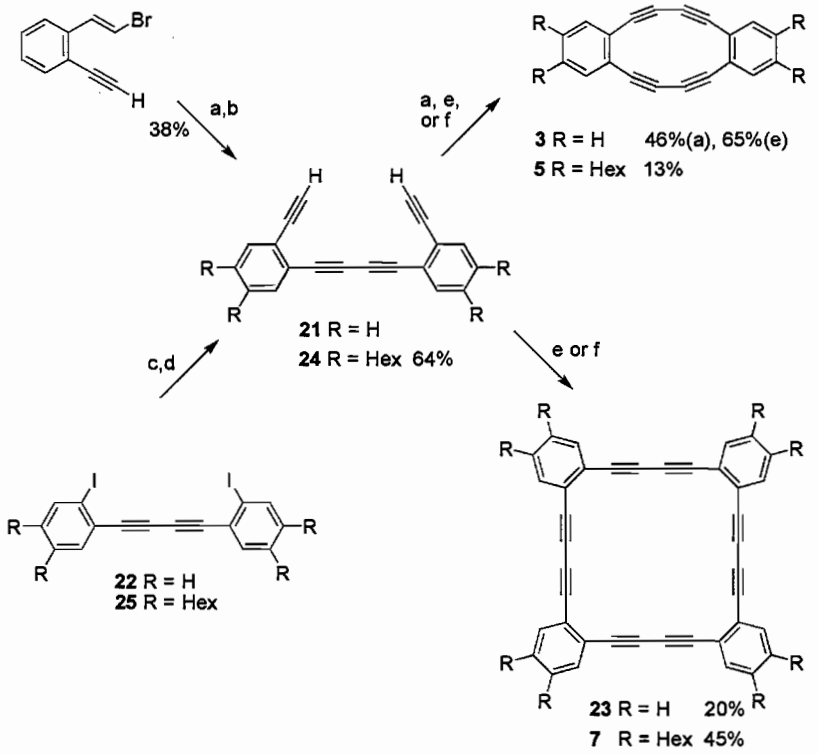

(a) $Cu(OAc)_2$, py, MeOH; (b) t-BuOK, t-BuOH; (c) TMSA, $[PdCl_2(PPh_3)_2]$, CuI; (d) KF or KOH, H_2O, THF, MeOH; (e) CuCl, py, O_2; (f) CuCl, TMEDA, ODCB, O_2.

SCHEME 8. Synthesis of PDM **26**.

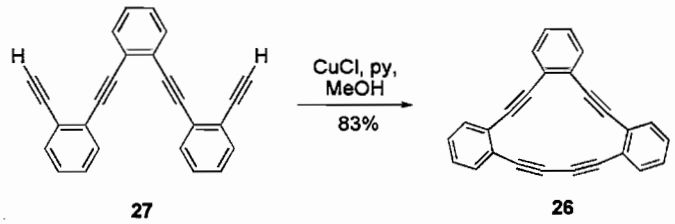

Very recently, the Haley group used a convergent intramolecular approach for the selective synthesis of bis[14]- and bis[15]annulene derivatives.[24] The authors effected macrocycle formation using the traditional Eglinton conditions ($Cu(OAc)_2$, py); however, and more importantly, ring-closure was also achieved under milder Pd-mediated

homocoupling conditions similar to those used in Sonogashira reactions to provide the appropriate PDMs in high yield. For example, cross-coupling diyne **28** with tetraiodobenzene furnished octayne **29**, which upon subsequent removal of the TIPS groups and metal-mediated ring-closure could afford either PDM **30** or **31**, or a mixture of both (Scheme 9). Interestingly, under Cu-mediated conditions, the bis[15]annulene **30** was formed as the sole product. Conversely, use of $[PdCl_2(PPh_3)_2]$ provided a mixture of **30** along with the bis[14] derivative **31**, while acetylenic homocoupling with $[PdCl_2(dppe)]$ furnished **31** exclusively.

SCHEME 9. Selective Synthesis of PDMs **30** and **31**.

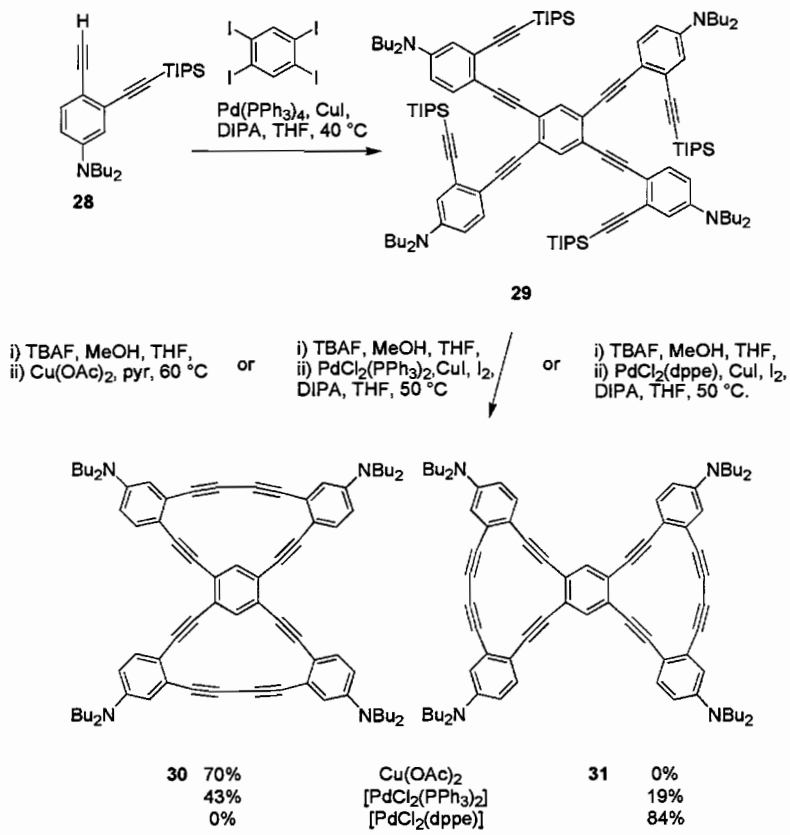

SCHEME 9

2.3 Comparison of the Two Pathways

Phenylacetylene macrocycles can be synthesized using either an inter- or an intramolecular approach. An advantage of the intermolecular approach is that the starting materials can typically be prepared in relatively few steps; however, the probability of forming numerous cyclooligomeric macrocycles is high. Unfortunately, this reduces the yield of the desired product and can make purification of the target molecule very difficult.

While the main disadvantage of the intramolecular approach is that a greater number of steps is typically required to assemble the more complex precursor molecules, this particular pathway for macrocycle synthesis allows the chemist to prepare the target compounds in a systematic manner which greatly improves the yield of the final products. Oligomeric by-products are minimized and thus purification is greatly simplified. Additionally, this route permits the preparation of novel macrocycles that would otherwise be nearly impossible to construct via intermolecular strategies, e.g., macrocycles possessing little or no symmetry, products possessing functionality at predetermined positions, and compounds with various numbers of acetylenic linkages.

3 Phenylacetylene Macrocycles

3.1 Ortho PAMs

The simplest *o*-phenylacetylene macrocycle, highly strained diyne **32**, was first reported by Sondheimer and coworkers 30 years ago.[25] The [8]annulene was prepared by brominating *sym*-dibenzocyclooctatetraene (**33**) with either one or two molar equivalents

of bromine to give **34** and **35**, respectively (Scheme 10). Subsequent treatment of the aforementioned compounds with *t*-BuOK furnished the target hydrocarbon as a yellow solid that decomposes at ~110 °C. Although the X-ray structure of **32** shows the acetylenic linkages are distorted from the normal linear arrangement by some 24.3°, the molecule decomposes only slowly over 2 days when stored under ambient conditions. Although PAM **32** has been synthesized via other methods,[26] Scheme 10 still remains the predominant route for its preparation

SCHEME 10. Synthesis of PAM **32**.

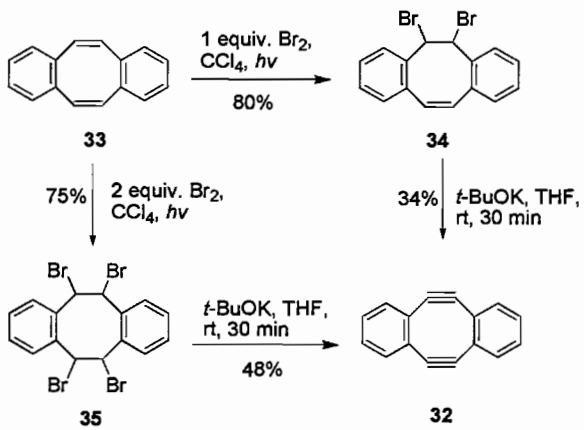

As mentioned previously, PAM **8**, which contains three phenyl rings *ortho*-linked by the same number of acetylene moieties, was prepared independently by the groups of Eglinton and Staab in 1966 by use of an intermolecular synthetic approach (see Schemes 1 and 4). Since this time two strategies have been evolved for the assembly of **8**. The first has focused on improvement of the Eglinton route by modification of the reaction condition, either by changing the method of Cu-acetylide formation[13] or by inclusion of Pd as a catalyst.[14] The second strategy has been to develop completely new synthetic

routes.[16,18,20] Very recently, Iyoda and his group prepared **8** in moderate yield using an intermolecular cross-coupling reaction between 1,2-diiodobenzene and triyne **36** (Scheme 11).[27] Thus, reflux of a DMF solution of **36** and 30 mol% of CuI and PPh_3 in the presence of K_2CO_3 afforded **8** in 51% yield. Interestingly, substituting K_2CO_3 with either $CsCO_3$ or $CaCO_3$ failed to afford significant amounts of **8** while use of Na_2CO_3 gives the target macrocycle in only 20% yield. The authors also prepared **8** in 26% yield from 1,2-diethynylbenzene **2** and bis(2-iodophenyl)acetylene (**37**) using a similar protocol (Scheme 11).

SCHEME 11. Iyoda Synthesis of PAM **8**

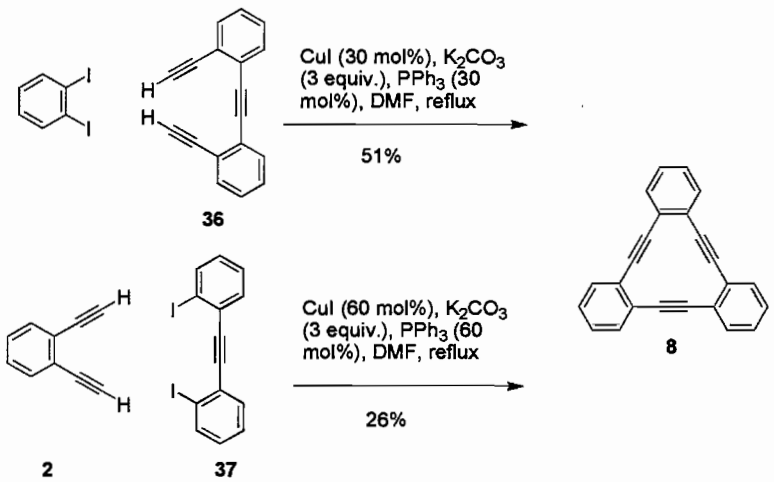

Recently Vollhardt and coworkers reported the synthesis of **8** in 54% yield by alkyne metathesis of dialkynylarene **13** and the tungsten reagent [(*t*BuO)$_3$W≡C*t*Bu] (Scheme 12).[16] The analogous treatment of other appropriately substituted 1,2-dipropynylated arenes (**38-40**) afforded the novel hexasubstituted PAMs **41-43**, respectively. Unfortunately, it was not possible to effect the above transformation with

substituents *ortho* to the acetylene groups in synthon **13**, thus limiting the synthetic utility of the procedure.

SCHEME 12. Synthesis of PAMs **8** and **41-43**.

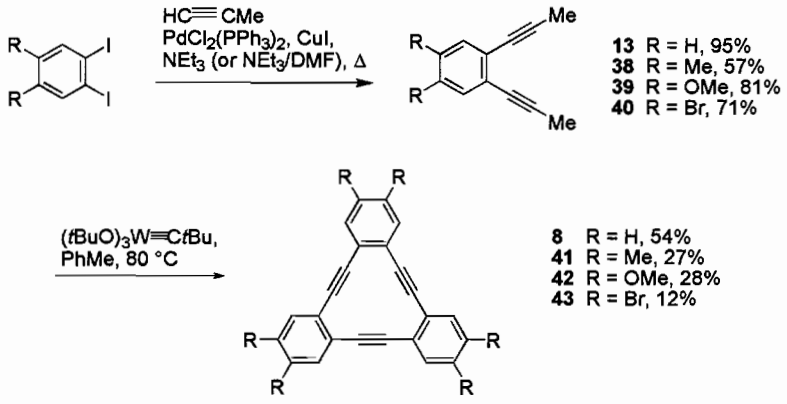

In addition to **8**, the synthesis of hexamethyl[12]annulene **41** and hexafluoro[12]annulene **44** has been accomplished by Iyoda and his group through cyclization of the appropriate 1,2-disubstituted-4,5-diiodobenzene derivative with acetylene gas in the presence of $[PdCl_2(PPh_3)_2]$ and CuI (Scheme 13).[18] The yield of product was affected dramatically by choice of solvent; thus, when 4,5-diiodo-*o*-xylene (**45**) was cyclized in morpholine, PAM **41** was obtained in trace quantities but with the solvent system DMF/NEt_3 the yield increased to 11%. The analogous treatment of 1,2-difluoro-4,5-diiodobenzene (**46**) in morpholine gave the hexasubstituted macrocycle **44** in 32% yield but in somewhat reduced 24% yield in DMF/NEt_3.

SCHEME 13. Synthesis of PAMs **41** and **44**.

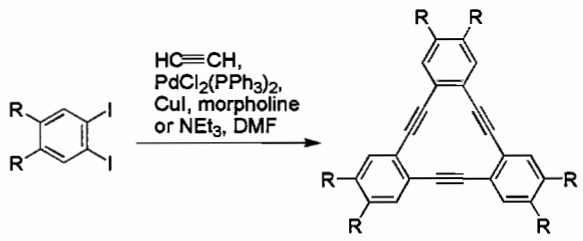

45 R = Me
46 R = F

41 R = Me, trace-11%
44 R = F, 24-32%

The intermolecular cyclotrimerization of *ortho*-ethynyliodoarenes is the most common method for *ortho*-PAM synthesis,[27] and can be effected using either catalytic or stoichiometric amounts of Cu salts (Scheme 14). Reaction of the aforementioned arenes with CuI and K_2CO_3, and either PPh_3 or P(2-furyl)$_3$ in DMF at 160 °C gives the hexasubstituted PAMs **8**, **41**, **42**, and **47** in low to moderate yield.[27a] It should be noted that choice of phosphine ligand impacts significantly upon the outcome of the reaction. For example, use of PPh_3 with *o*-ethynyliodobenzene gives macrocycle **8** in 55% yield while P(2-furyl)$_3$ gives the same compound in only 24% yield. Alternatively, cyclotrimerization via a modified Stephens-Castro reaction (in situ generation of the Cu-acetylide) furnishes trimers **48** and **49** along with equal amounts of tetramers **50** and **51** in ca. 30% combined yield.[27b] Although designed to behave as discotic mesogens, PAMs **48-51** exhibit no liquid crystalline phases.

SCHEME 14. PAM Synthesis by Cyclotrimerization.

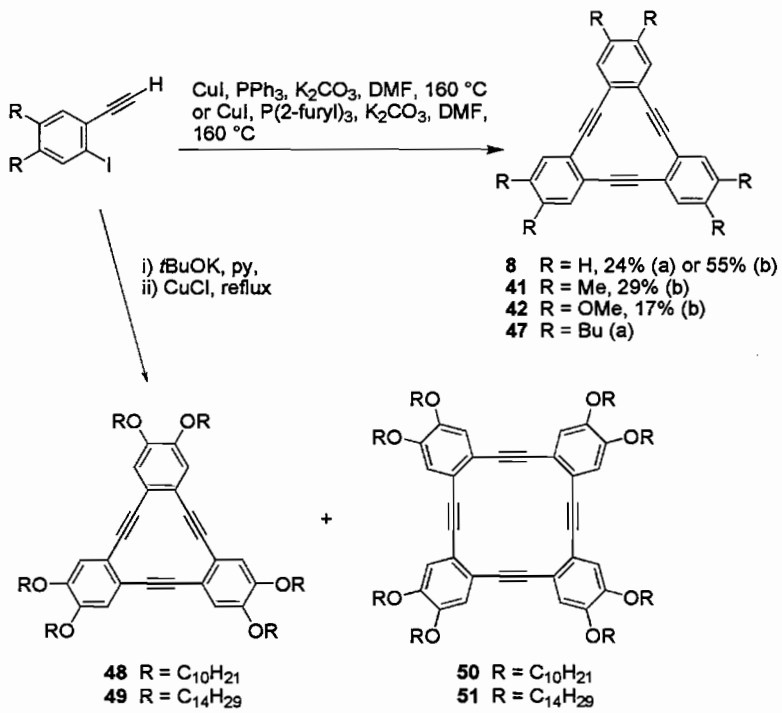

Vollhardt and his group have reported the synthesis of hexaethynylated [12]annulenes (**52-55**).[28] The synthons for cyclization were alkyne derivatives **56-58**, which were in turn prepared in a stepwise fashion from 1,2,3,4-tetrabromobenzene (Scheme 15). Regioselective alkylation of the tetrahalogenated substrate at the 1- and 4-positions afforded diacetylene derivatives **59-61**, which were monoalkynylated at the 2-position to afford compounds **62-64**. Halogen-lithium exchange of the latter, quenching the resultant anion with molecular iodine, and then removal of the trimethylsilyl protecting group with base furnished **56-58**. Conversion of **56-58** into the Cu-acetylide derivatives followed by reflux in pyridine affords PAMs **52-54**. The parent macrocycle **55** was generated by fluoride-induced desilylation of **54**.

SCHEME 15. Synthesis of Ethynyl PAMs **52-55**.

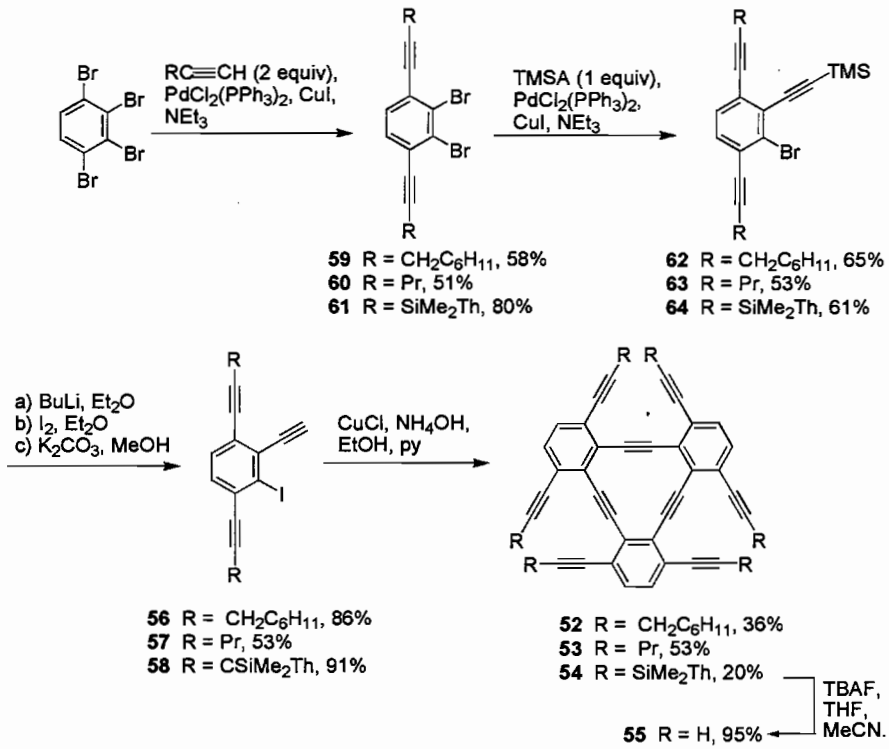

The crystal structure of [12]annulene **52** shows the molecule is locally C_2 symmetric.[28a] As a result of severe steric congestion caused by the bulky acetylenic substituents, the macrocyclic core of **52** is highly distorted with the triple bonds deviating from linearity by an average of 5.7° (cyclic) and 4.5° (exocyclic). In contrast, the crystal structure of the unsubstituted hexaethynyl macrocycle **55** shows the molecule is essentially planar and D_3 symmetric.[28b] Interestingly, the proximal alkynyl CH bonds of **55** chelate THF with supramolecular organization of the macrocycle around the occluded solvent molecules. This augers well for **55** to be used as a supramolecular synthon for crystal engineering.

The hexamethoxy[12]annulene **65** has been prepared by Youngs et al. from substrate **66**.[29] Treatment of alkyne **67** with 'superbase' followed by reaction with $Br_2Mg{\bullet}OEt_2$ and quenching with molecular iodine gives **66** (Scheme 16). Formation of the Cu-acetylide from the terminal acetylene moiety of **66** and subsequent Castro-Stephens cyclotrimerization in refluxing pyridine furnishes **65** in excellent 80% yield. The cyclization can also be effected by refluxing **66** in pyridine with $[PdCl_2(PPh_3)_2]$; however, the yield of **65** is very poor (5%). Double demethylation of one of the arene rings of **65** can be effected with ceric ammonium nitrate (CAN) to give quinone **68** in 91% yield. Further oxidation to the corresponding all-quinone derivative was not possible.

SCHEME 16. Synthesis of PAM **65**.

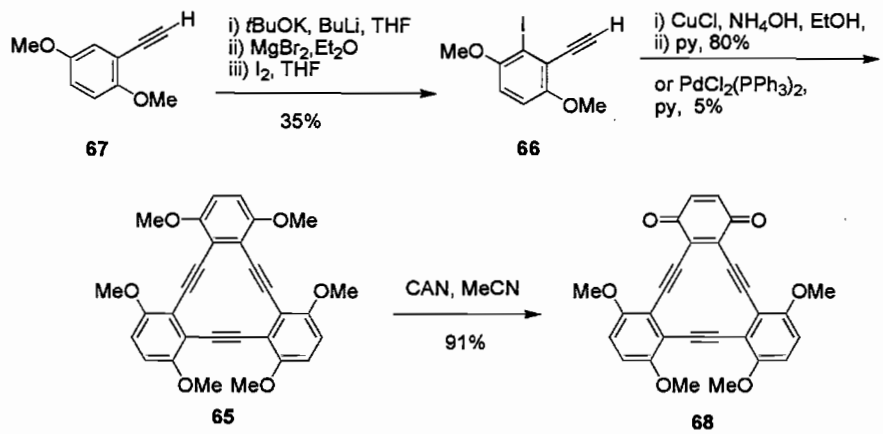

67 **66** **65** **68**

The ready availability of PAM **8** via several syntheses has allowed elucidation of the chemistry displayed by the molecule. In particular, a variety of organometallic species have been prepared in which the π–electron rich **8** participates as the ligand (Figure 1). The treatment of **8** with $Co_2(CO)_8$ furnishes the 66-electon cluster **69** which was characterized by X-ray crystallography.[30] The authors inferred that the binding of

cobalt to the macrocycle resembled the postulated transition state of a metal-mediated [2+2+2] cyclotrimerization of alkynes. The reaction of **8** and the hexamethoxy derivative **65** with $Ni(COD)_2$ results in incorporation of the Ni(0) atom into the cavity of the macrocycle to give complexes **70** and **71**, respectively, in which the metal is bound by π–alkyne/transition metal bonding interactions.[31] When a saturated solution of **8** is treated with $Cu_2(C_6H_6)(OTf)_2$, complex **72** is formed in which the Cu(I) ion is chelated by the three alkyne moieties.[32] Conversely, when stoichiometric amounts of **8** and $Cu_2(C_6H_6)(OTf)_2$ are mixed together, complex **73** is generated in which three Cu centers are bound to the face of the macrocycle.[32] Reaction of half an equivalent of AgOTf with **8** furnishes the novel macrocyclic sandwich complex **74**.[33] The latter complex was found to dissociate in solution; however, the sandwich complex formed from **8** and $AgBF_4$ is stable enough to characterize by NMR spectroscopy.[18] The hexabutyl-substituted macrocycle **47** also forms a sandwich complex with the silver cation.[26] The treatment of **47** with $AgBF_4$ generates the sandwich species which has been characterized by NMR spectroscopy.

Very recently, Iyoda and his group have shown that macrocycle **8** undergoes ruthenium-catalyzed oxidation in the presence of a variety of oxidants to give dione **75** as well as the unusual polycyclic hexaketone monohydrate **76** (Scheme 17).[34]

FIGURE 1. Compounds **69-74**.

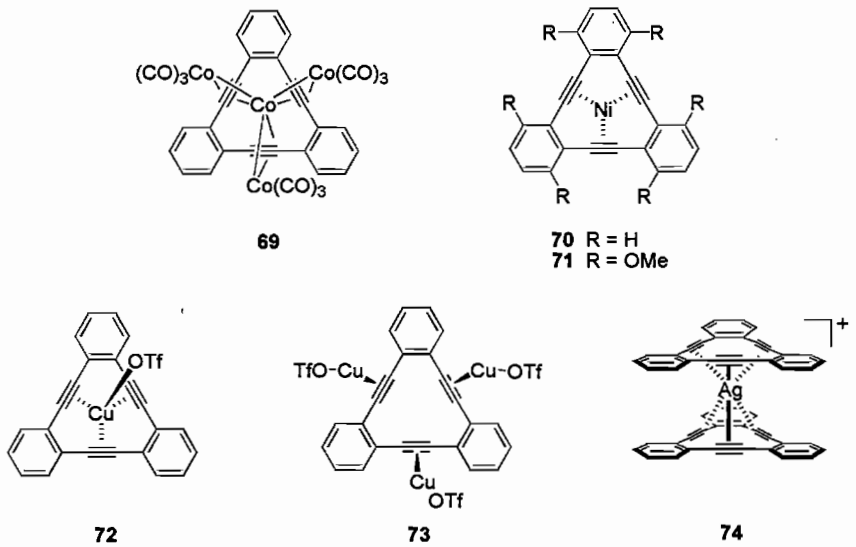

69 **70** R = H **71** R = OMe

72 **73** **74**

SCHEME 17. Oxidation of PAM **8**.

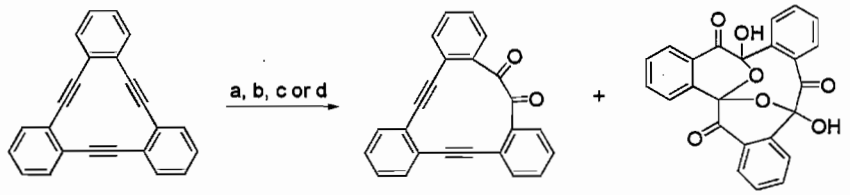

8 **75** **76**

a) $RuO_2o_2H_2O$, $NaIO_4$, CCl_4, MeCN, H_2O	27%	13%
b) $RuCl_3o_3H_2O$, PhIO, Me_2CO, H_2O	6%	31%
c) $RuCl_2(PPh_3)_2$, CH_2Cl_2	21%	trace
d) $RuCl_2(MeCN)_2(PPh_3)_2$, PhIO, CH_2Cl_2	26%	trace

The behavior of macrocycle **8** with Li metal has been studied.[35] Addition of four molar equivalents of Li to a THF solution of **8** produced the highly air-sensitive dilithiate **77**, the structure of which was confirmed by X-ray crystallography (Scheme 18). Youngs et al. proposed that the first two equivalents of Li generate the diradical dianion, which

then collapses to form the central 6-membered ring. Further reduction by two more equivalents of alkali metal and subsequent protonation by the solvent affords **77**.

SCHEME 18. Reduction of PAM **8**.

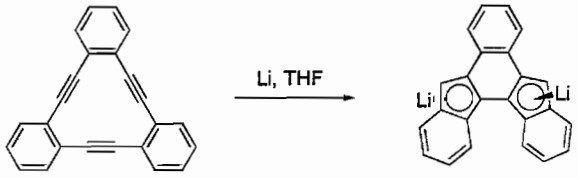

8 **77**

The syntheses of more complicated *ortho*-PAMs have been achieved recently. The driving force behind the preparation of these multiple [12]annulene derivatives has been predictions of interesting materials properties for oligomeric/polymeric structures based on **8** (Figure 2). In 1987 Baughman et al. calculated the structures of several hypothetical all-carbon networks and predicted that graphyne (**78**), comprised equally of sp and sp^2 carbons, would display promising third-order nonlinear optical properties. The material was also calculated to be a large bandgap semiconductor and, once suitable doped with alkali metals, to exhibit metallic behavior.[36] Recent semiempirical INDO/S and AM1 molecular orbital calculations have shown that molecular chains derived from [12]annulene (e.g., **79**) are also expected to display nonlinear optical properties.[37] Despite these predictions, synthetic accessibility has hampered graphyne-related research; thus, most efforts in this area have focused on smaller, soluble, discreet substructures (vide infra).

FIGURE 2. Compounds **78-79**.

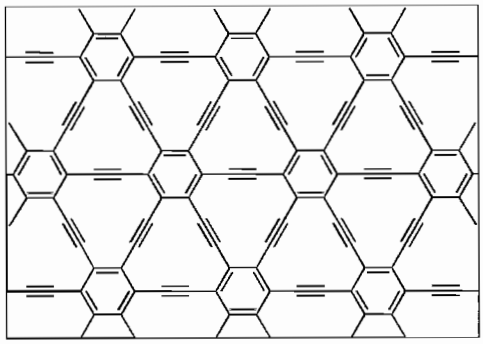

78

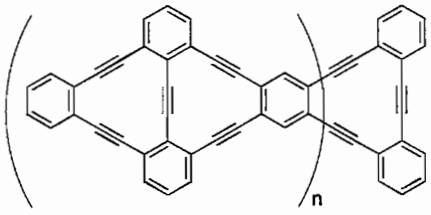

n = 1-4

79

The Haley group has prepared 'bowtie' bis[12]annulene **80** by an intramolecular stepwise strategy (Scheme 19).[20] Using an analogous set of reactions by which macrocycle **8** was prepared (see Scheme 6), the Haley group synthesized advanced intermediate **81**. Conversion of the triazene moieties into the corresponding iodo derivatives and subsequent deprotection of the free alkynes and cross-coupling gave PAM **80** as sparingly soluble yellow solid. Although the authors did not obtain NMR data for **80**, they were able to obtain UV/Vis, IR, and MS data which were fully in accord with the proposed structural assignment.

More recently, Vollhardt et al. prepared **80** by a six-fold metathesis reaction between two equivalents of **13** and tetrayne **82** (Scheme 20).[16] Not only did the authors obtain macrocycle **80** in 6% yield, which is impressive since four metathesis reactions must occur, but they were also able to secure proton NMR data of the compound.

SCHEME 19. Stepwise Synthesis of PAM **80**.

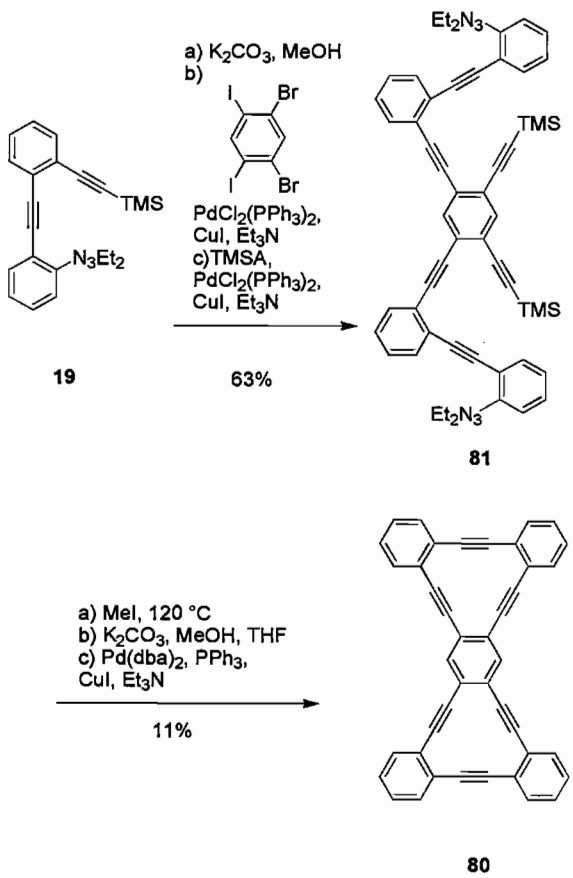

SCHEME 20. Metathesis Synthesis of PAM **80**.

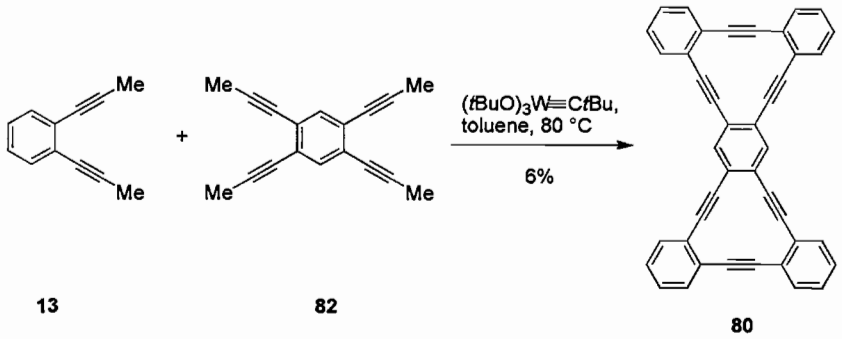

Iyoda and coworkers have prepared octasubstituted bowtie PAM **83** from Cu-mediated cross-coupling of 1,2,4,5-tetraiodobenzene and substituted triyne **84** (Scheme

21).[26] Although the yield of formation of bismacrocycle **83** is extremely low (~1%), the authors were able to characterize the first example of a substituted derivative of **80**. Not surprisingly, the eight butyl substituents aided product solubility significantly.

SCHEME 21. Synthesis of PAM **83**.

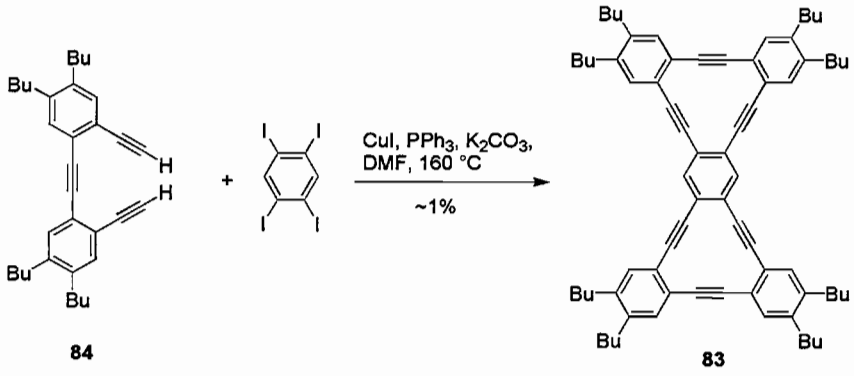

The novel PAM **85**, which contains three [12]annulenes fused to a benzene core, was prepared very recently by Tobe and his group.[38] Six-fold Pd-catalyzed cross-coupling of hexabromobenzene with phenylacetylene **86** afforded **87** in 60% yield (Scheme 22). Treatment of the latter with $VCl_3(THF)_3$/Zn furnished the all-*erythro* polycycle **88**. Chlorination/ dehydrochlorination gave the target macrocycle **85** in 10% yield for the two steps combined.

Haley and coworkers prepared 'diamond' bisPAM **89**, which contains solubilizing *t*-butyl groups, using a stepwise intramolecular approach (Scheme 23).[20] 4-*t*-Butylaniline was converted into iodoarene **90** in four steps. Part of this material was carried forward to **91**, which was then desilylated and cross-coupled to **90** to afford **92**. Iodination, desilylation and double intramolecular cross-coupling furnished the desired macrocycle **89** as a bright yellow solid in an overall yield of 0.6%.

SCHEME 22. Synthesis of PAM **85**.

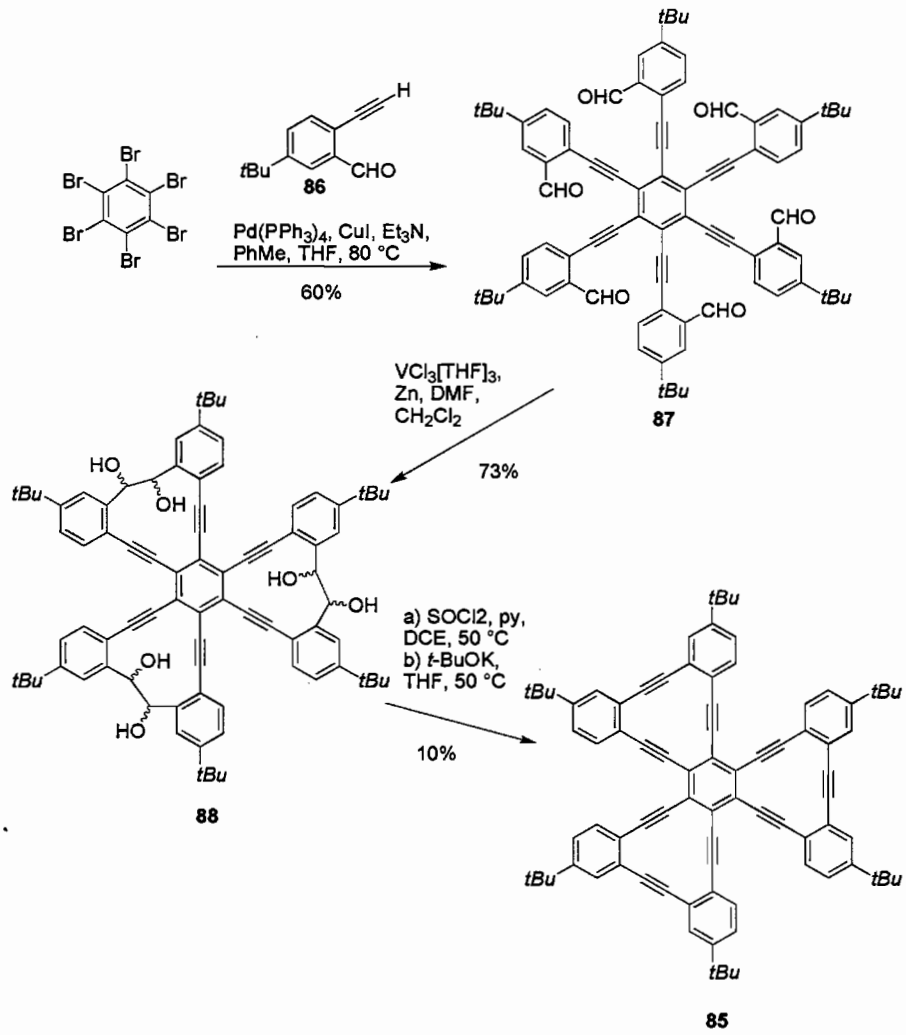

Tobe and his group very recently prepared the hexasubstituted 'diamond' PAM **93** using an intermolecular approach (Scheme 24).[38] 4-Decylaniline was converted into iodide **94** in two steps in 61% yield. Part of this material was treated with 2-methyl-3-butyne-2-ol and then KOH to afford terminal acetylene **95**, which was cross-coupled with **94** to furnish the diphenylacetylene **96**. Reflux of the latter compound in basic media

under Pd catalysis with the diacetylene (**97**), itself prepared in one step from 1,2-didecyl-4,5-diiodobenzene and 2-methyl-3-butyne-2-ol, affords target macrocycle **93** in 9% yield.

SCHEME 23. Stepwise Synthesis of PAM **89**.

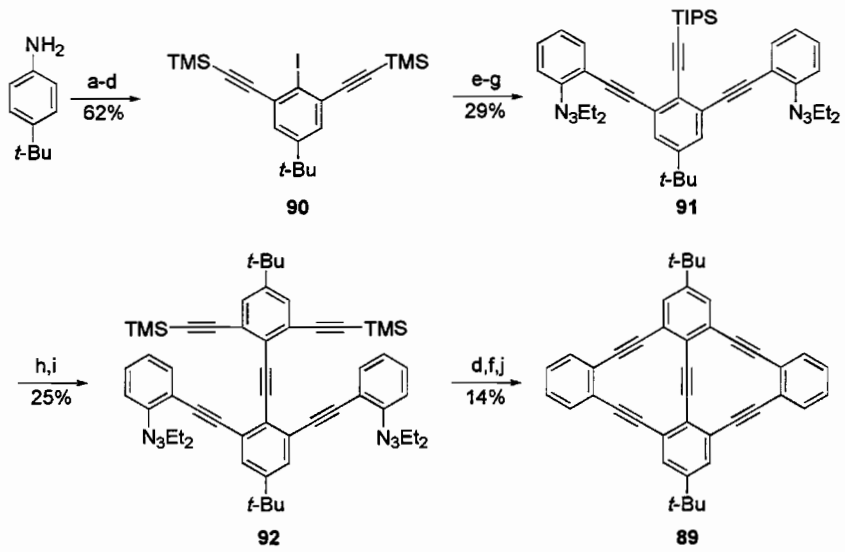

(a) $BTEAICl_2$, $CaCO_3$, CH_2Cl_2, MeOH; (b) i] $NaNO_2$, HCl, MeCN, H_2O, ii] DIPA, K_2CO_3, H_2O; (c) TMSA, $PdCl_2(PPh_3)_2$, CuI, Et_3N; (d) MeI, 120°C; (e) TIPSA, $PdCl_2(PPh_3)_2$, CuI, Et_3N; (f) K_2CO_3, THF, MeOH; (g) N,N-diethyl-^{2}-iodophenyltriazene, $PdCl_2(PPh_3)_2$, CuI, Et_3N; (h) TBAF, THF, EtOH; (i) **90**, $PdCl_2(PPh_3)_2$, CuI, Et_3N; (j) $Pd(dba)_2$, PPh_3, CuI, Et_3N.

The only *ortho*-PAMs in which the macrocycle contains greater than twelve carbon atoms to have been prepared and characterized formally are the [16]-, [24]-, and the [40]annulenes **10**, **11**, and **16**, respectively.[13,15,19] An X-ray structure has been obtained on PAM **16** and shows that the molecule contains no symmetry other than a C_1 axis.[19b] Similar to **8**, PAM **10** reacts with $Co_2(CO)_8$ to give a tetracobalt cluster and undergoes a Li-induced 'zipper' cyclization reaction.[39]

SCHEME 24. Synthesis of PAM **93**.

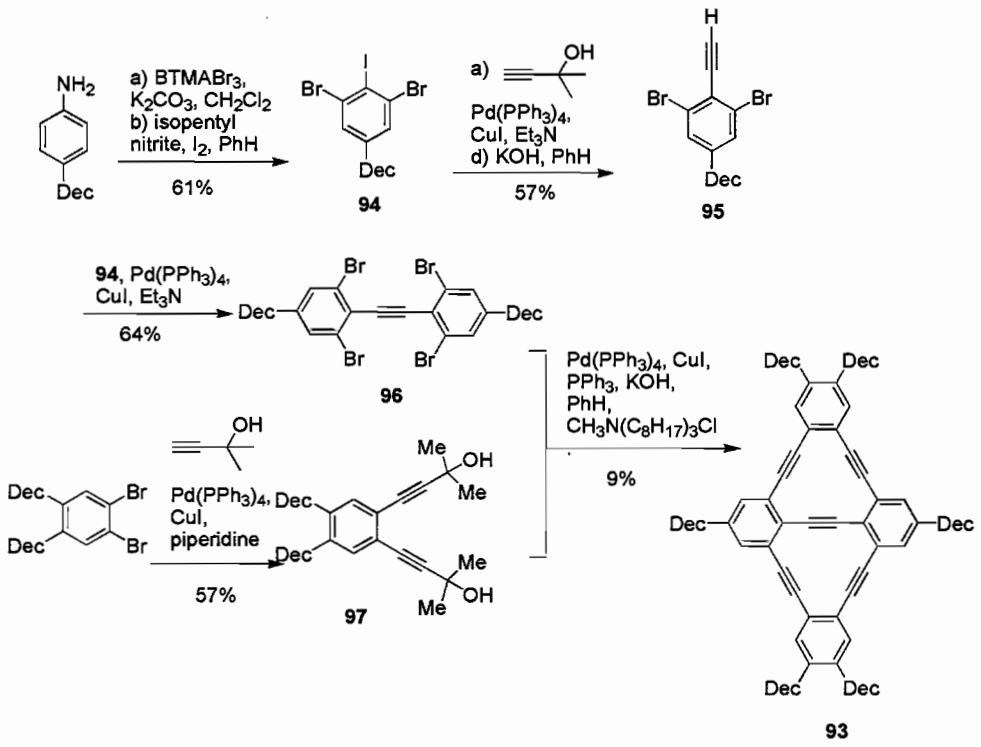

3.2 Meta PAMs

The smallest known *m*-phenylacetylene macrocycle is the [15]annulene **98** which was prepared by Oda and his group in 1997 and has a computed strain energy of 48 kcal mol^{-1}.[40] The synthon to the trimeric macrocycle **98** is triene **99** which was synthesized by an intramolecular Ti-mediated reductive coupling of the formylstyryl benzene derivative **100** (Scheme 25). Treatment of **99** with excess bromine and subsequent dehydrobromination yields macrocycle **98** as a moderately stable crystalline material which decomposes thermally above 180 °C. An X-ray structure of **98** shows the molecule is nearly planar and C_2 symmetric [40]. The benzene rings are distorted 3.3° from a regular hexagon and the torsion angles between the benzene rings and triple bonds less

than 3.5°. The alkyne moieties, which impart significant strain on the molecule, are highly distorted from linearity with an average sp bond angle of 158.6°, a value comparable to those of *sym*-dibenzocyclooctatetraene **32** (159.1°).

SCHEME 25. Synthesis of PAM **98**.

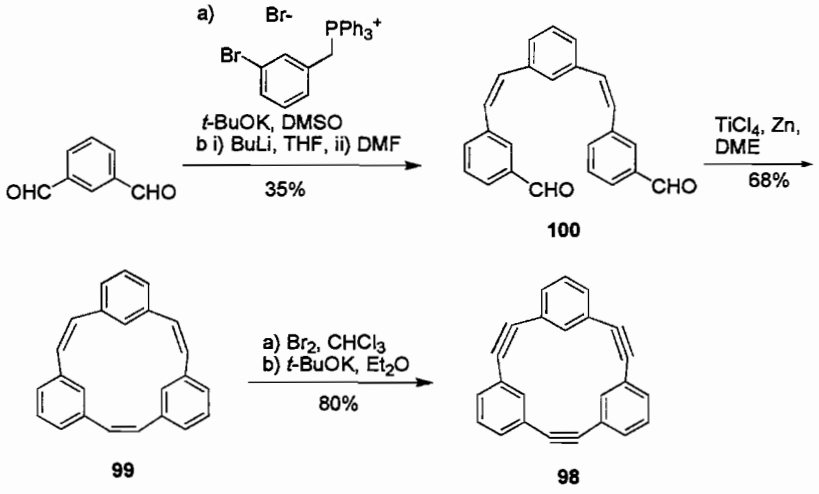

PAM **98** was found to undergo facile Diels-Alder reaction with cyclopentadiene at room temperature to afford a mixture of the *syn*/*anti* diadducts **101** in an approximate 1:1 ratio (Scheme 26). Surprisingly, no evidence was obtained to support the formation of either the mono- or triadduct.

SCHEME 26. Cycloaddition of PAM **98**.

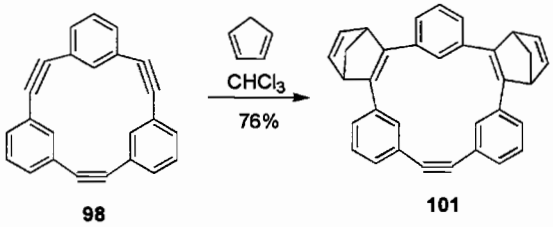

The synthesis of the *m*-phenylacetylene macrocycle **102**, which contains four alternating acetylene and phenyl moieties, was reported the previous year by Oda and his colleagues.[41] McMurry coupling of dialdehyde **103** with low valent titanium metal affords a mixture of (*Z,Z,E,E*)- and (*E,Z,E,Z*) isomers of **104**; neither the (*Z,Z,Z,Z*) nor the intramolecular coupling product from **103** were detected (Scheme 27). Reaction of **104** with molecular bromine followed by dehydrobromination of the resulting adduct with *t*-BuOK affords PAM **102** in 55% yield.

SCHEME 27. Synthesis of PAM **102**.

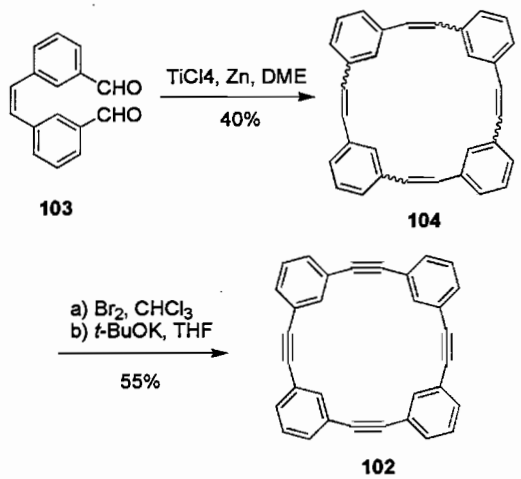

The X-ray structure of **102** reveals the molecule is non-planar, and the twist angle of the benzene rings from the plane of the macrocycle is less than 2°.[41] As anticipated, the triple bonds are distorted from linearity (167.7-169.9°), which imparts strain upon the molecule. Although the strain energy of the macrocycle has been calculated as ca. 11 kcal mol^{-1}, it is remarkably stable and decomposes above 300 °C on attempted melting. In contrast to triyne **98**, macrocycle **102** is inert towards cycloaddition reaction with either furan or cyclopentadiene.

PAM **105**, which contains four intraannular methoxy substituents, was synthesized in an analogous manner to the parent compound **102** (Scheme 28).[42] Thus, McMurry coupling of dimethoxystilbene **106** affords a mixture of cyclic dimers (**107**) from which the (*E,Z,E,Z*)-tetraene separates out as crystals in 19% yield. Bromination/dehydrobromination of the last compound furnishes **105** as a stable solid in modest 62% yield.

In contrast to the nearly planar parent macrocycle **102**, the X-ray structure of **105** reveals the molecule is non-planar with C_2-symmetry in which the first and third benzene rings lie in the plane whilst the second and forth rings are twisted out of the plane by 42°.[42] As expected, the triple bonds of **105** are bent with an average angle of 166.9° and, as a result of steric congestion, the methoxy moieties of rings one and four point upward while the other two point downward. The X-ray structure shows that macrocycle **105** has an organized cavity with a diameter of 1.2 Å which augers well for the molecule to act as an ionophone. Indeed, when **105** is treated with the alkali metal picrates (PicM) where M = Li^+, Na^+, K^+, Rb^+ and Cs^+, encapsulation occurs for all but the last ion. The association constants are large, ranging from 8.2-10.6, and the ability of macrocycle to bind K^+ ions is comparable to that of 18-crown-6.

The only reported example of a *meta*-PAM containing five alternating phenyl and acetylene units is the *n*-butyl ester substituted **108**.[43] The pentayne was prepared using a covergent stepwise approach from ester **109** (Scheme 29). Treatment of the said ester with either weak base or MeI furnishes **110** and **111**, respectively, which are cross-coupled to afford **112**. Repetition of the above transformations generates the linear

pentamer **113**. The treatment of the last compound with MeI and subsequent base-induced desilylation of the protected acetylene moiety affords synthon **114**. Cyclization of the last compound is accomplished under pseudo-high-dilution conditions by slow addition of **114** to an active solution of Pd catalyst to give macrocycle **108** in moderate yield.

SCHEME 28. Synthesis of PAM **105**.

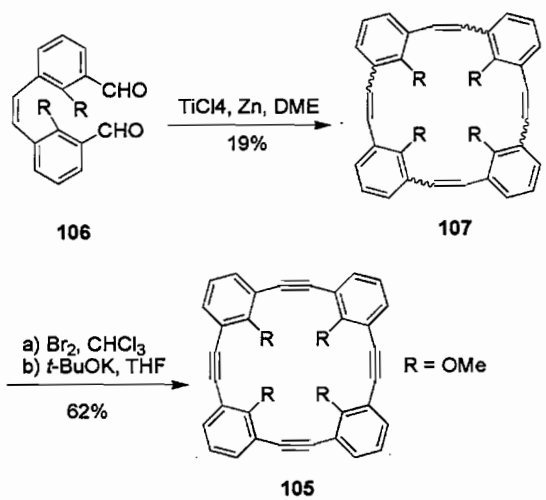

The parent hexamer **115** was first reported in the literature 30 years ago by Staab and Neuenhoeffer.[44] The authors prepared the requisite macrocycle though a six-fold Stephens-Castro coupling of Cu-acetylide **116** in 4.6% yield (Scheme 30). Synthon **116** was, in turn, generated from treatment of acetylene **117** with CuCl in aqueous ammonia/ethanol.

SCHEME 29. Synthesis of PAM **108**.

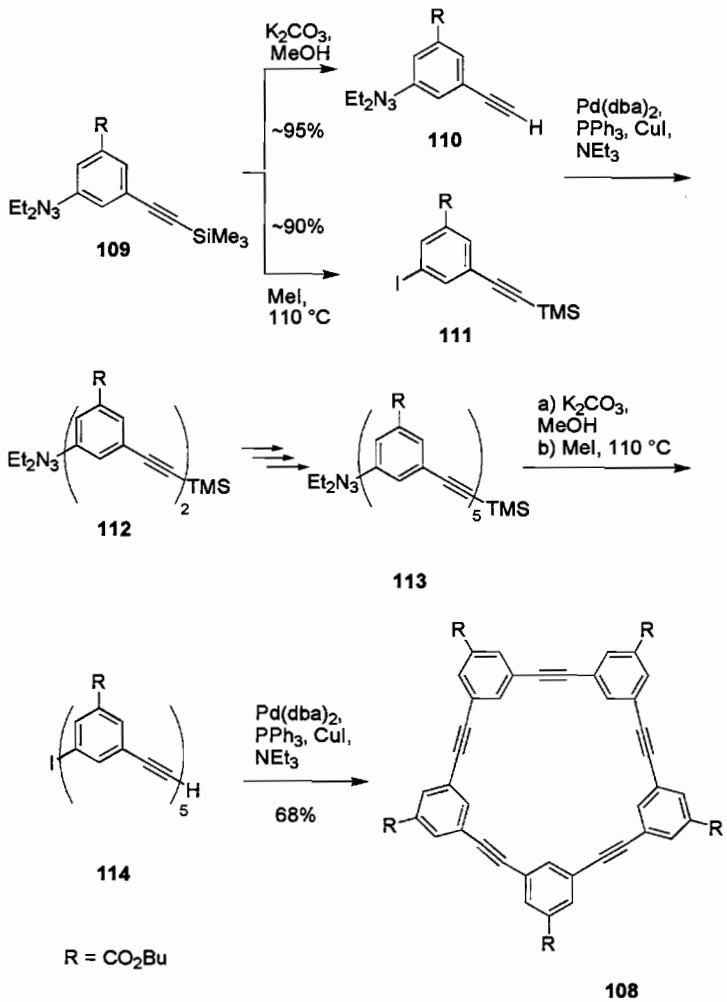

Bunz and coworkers prepared the hexasubstituted *meta*-phenylacetylene derivatives **118** and **119** using a one-pot cyclooligomerization strategy (Scheme 31).[45] Treatment of the substituted benzene derivatives **120** and **121** with the molybdenum reagent $Mo(CO)_6$ in 4-chlorophenol at elevated temperature affords six-fold alkyne metathesis hexamers **118** (6%) and **119** (1.2%), respectively. Treatment of the former macrocycle with $(MeCN)_2Os_3(CO)_{10}$ results in coordination of one acetylene moiety to

metal atoms to form a triosmiumdecacarbonyl cluster complex in 11% yield. As evidenced by an X-ray structure the attachment of the osmium cluster to the acetylene moiety disrupts the planarity of the ring significantly. An X-ray crystal structure of **118** shows that the PAM is nearly planar and essentially strain-free.[45] The molecule was found to include two equivalents of disordered hexane per molecule, one of which passes through the center of the ring while the other is located between the stacks of rings. The rings of **118** are stacked and align in columns.

SCHEME 30. Synthesis of PAM **115**.

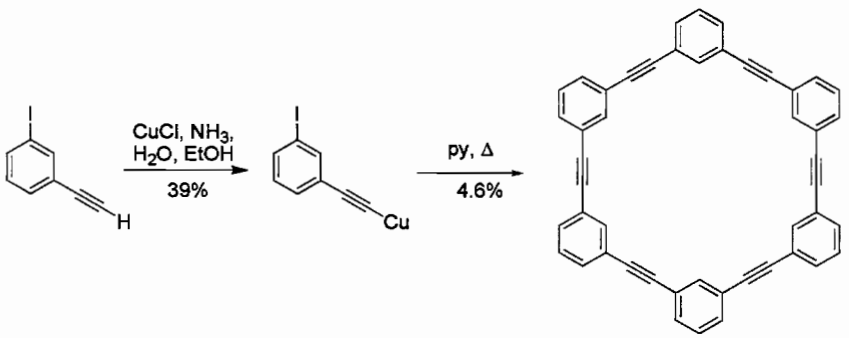

117 **116** **115**

A vast array of substituted hexameric (and other) PAMs (e.g., **122-129**) have been prepared since the early 1990s by Moore and his group.[5c,43,46] By using an iterative route it was possible to synthesize appropriately functionalized phenylacetylene macrocycles by sequential addition of derivatized monomers and subsequent cyclization of the linear hexamers to afford well-defined macrocycles with precise substituent placement on the periphery of the PAM (Scheme 32). Thus, the coupling of **130** and **131** and subsequent treatment of the derived adduct with base gives dimer **132**. Reaction of the latter compound with **133** and removal of the TMS moiety of the resultant species with base

furnishes tetramer **134**. Repetition of the aforementioned sequence of events with dimer **135** then affords precyclized hexamer **136**. Conversion of the triazene moiety of the last compound into the corresponding aryl iodide, protiodesilylation of the TMS group, and Pd-mediated ring-closure affords the geometrically well-defined PAMs **122-129**.

SCHEME 31. Synthesis of PAMs **118** and **119**.

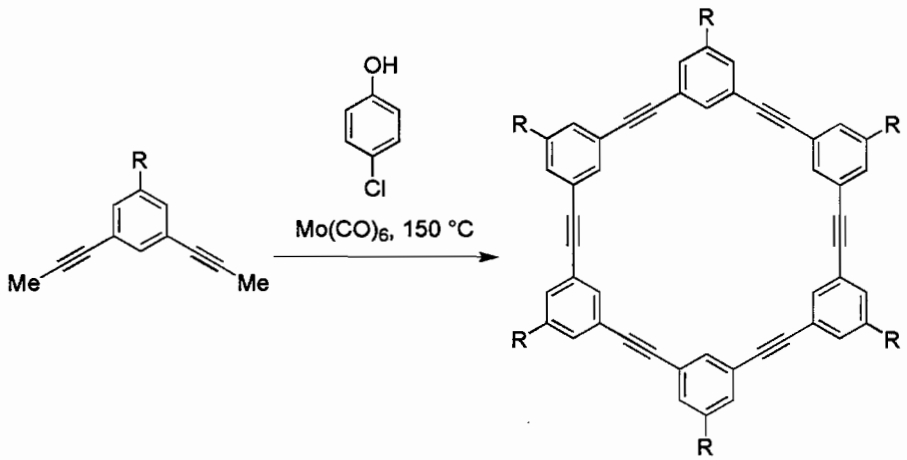

120 R = *t*-Bu
121 R = Hex

118 R = *t*-Bu 6%
119 R = Hex, 1.2%

SCHEME 32. Moore Synthesis of PAMs **122-129.**

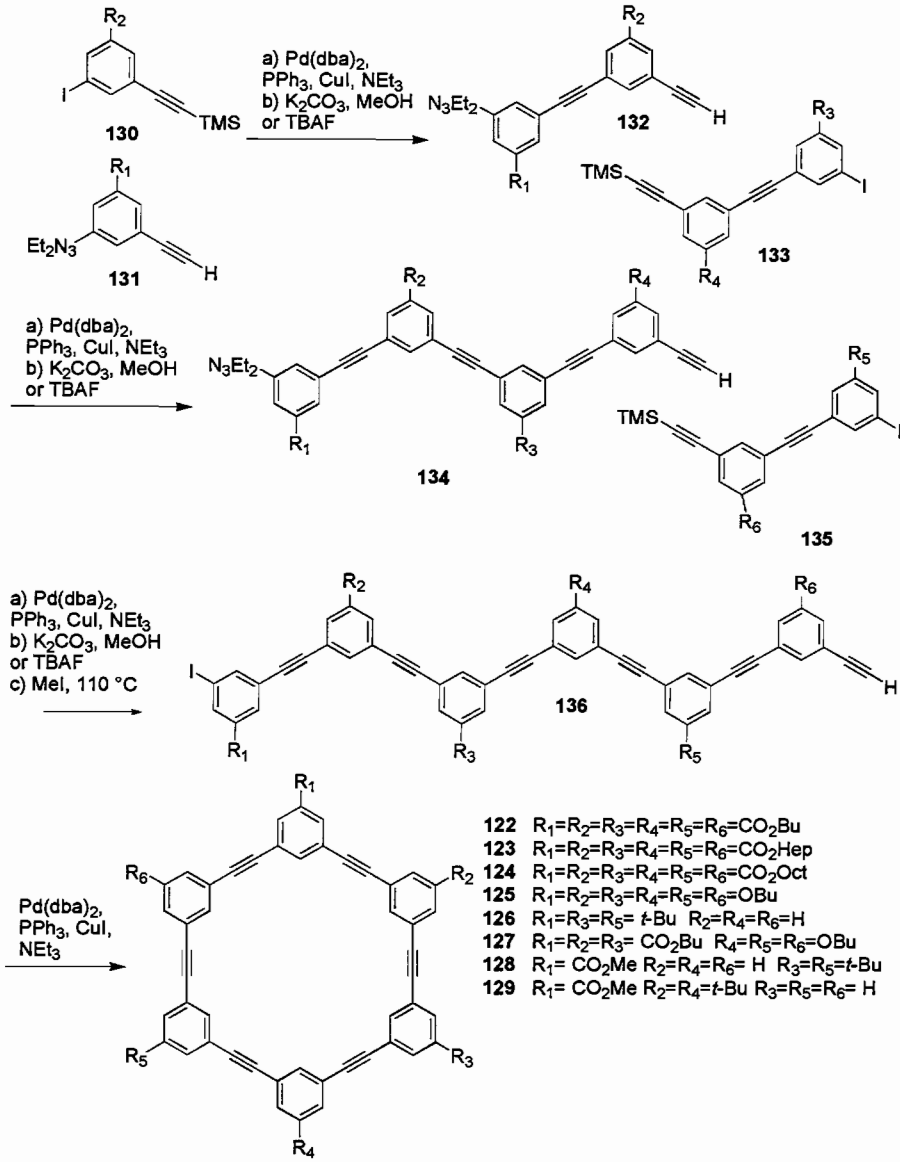

The hexameric PAMs have attracted much interest due to a slew of novel properties. In 1992 Zhang and Moore reported that the chemical shifts in the proton NMR spectrum of ester **122** were concentration dependant which indicates the compound was spontaneously aggregating into ordered assemblies in solution due to π–stacking.[47] A variety of differently functionalized phenylacetylene macrocycles were prepared for

subsequent investigation. The results show that those molecules containing ester groups with linear alkyl side chains (e.g., **123**) aggregate in solution while aggregation was reduced significantly, if not observed at all, for macrocycles not possessing electron withdrawing substituents. For example, no self association was observed for hexaether derivative **125**.[47,48]

Once suitably functionalized, phenylacetylene macrocycles such as **137** and **138** (Figure 3) display liquid crystalline behavior.[49] The aforementioned compounds were shown to xhibit both ordered isotropic and fluid phases and demonstrated self-organization in the discotic nematic phase upon cooling from the isotropic melt. More recently, PAMs have been shown to exhibit a discotic liquid crystalline phase.[50]

FIGURE 3. Compounds **137-139**.

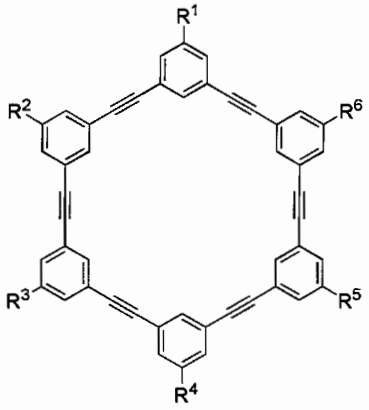

137 $R^1=R^2=R^3=R^4=R^5=R^6=$ OHep
138 $R^1=R^2=R^3=R^4=R^5=R^6=$OCOHep
139 $R^1=R^2=R^3=R^4=t$-Bu, $R^5=R^6=COO^{-+}NBu_4$

One of the rich properties displayed by phenylacetylene macrocycles is the ability of some to form ordered monolayers.[46c] For example, when the tetrabutylammonium

carboxylate salt **139** is transferred onto various substrates, it forms a stable two-dimensional organization which displays a high degree of polar and conformational order.

To date, only one example of a *meta*-hexaethynyl PAM with only internal ring substituents has been reported.[51] Macrocycle **140** was prepared in two steps from stillbene **141** (Scheme 33). McMurry coupling of **141** in DME-toluene afforded hexaene **142** along with the tetraene **143** in 14 and 23% yield, respectively. Bromination/dehydrobromination of **142** furnished **140** in 52% yield as a poorly soluble solid.

SCHEME 33. Synthesis of PAM **140**.

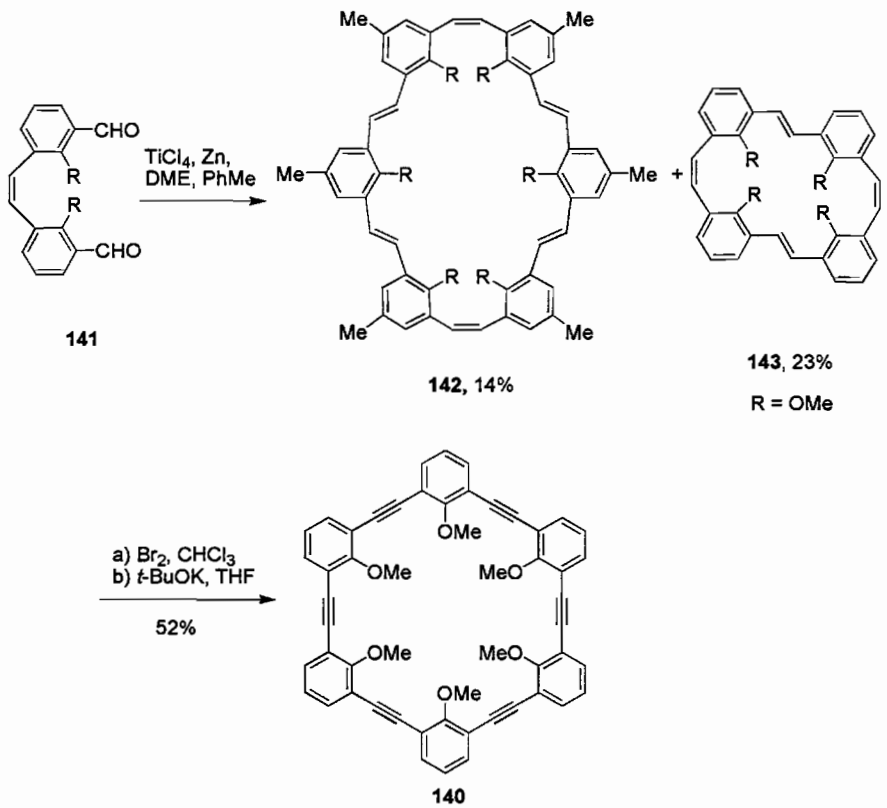

Examples of *meta*-hexaethynyl PAMs which contain both internal and external ring substituents are known. Oda and coworkers prepared macrocycle **144** by bromination/dehydrobromination of substrate **145** (Scheme 34).[51] In turn, **145** was prepared by McMurray coupling of the dialdehyde (**146**); the reaction also affords the trimeric macrocycle (**147**). An X-ray structure was obtained on macrocycle **144**.[51] The compound is essentially planar with the methoxy groups alternating *syn* and *anti*. The molecule has a cavity of ~5Å and exhibits good ionophoric selectivity for the ammonium ion.

SCHEME 34. Synthesis of PAM **144**.

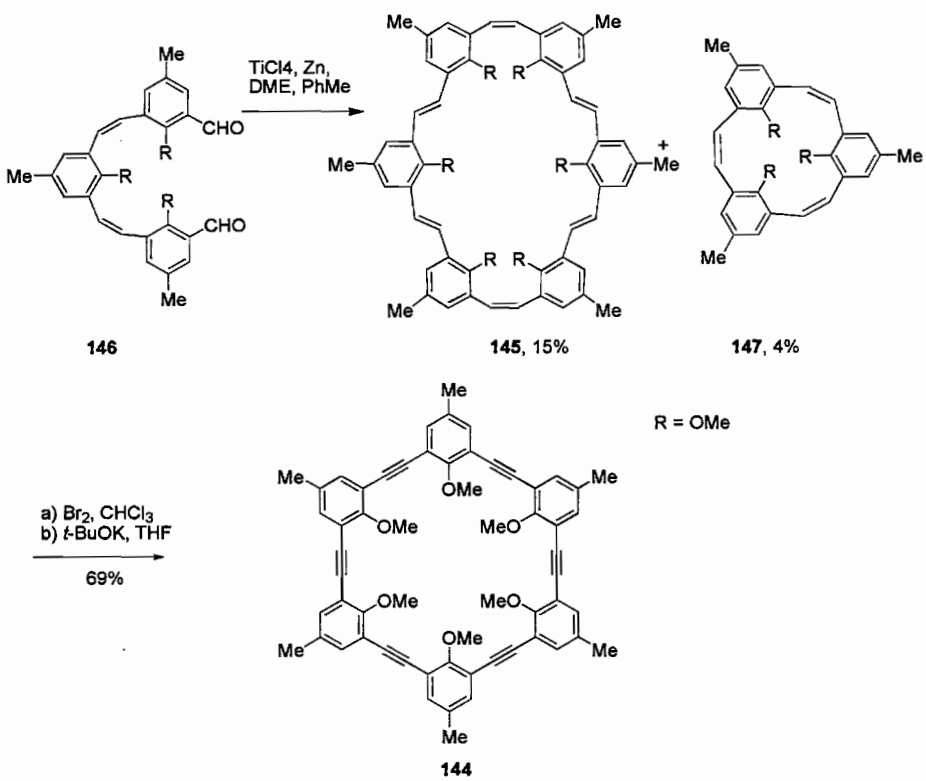

SCHEME 35. Synthesis of PAM **148**.

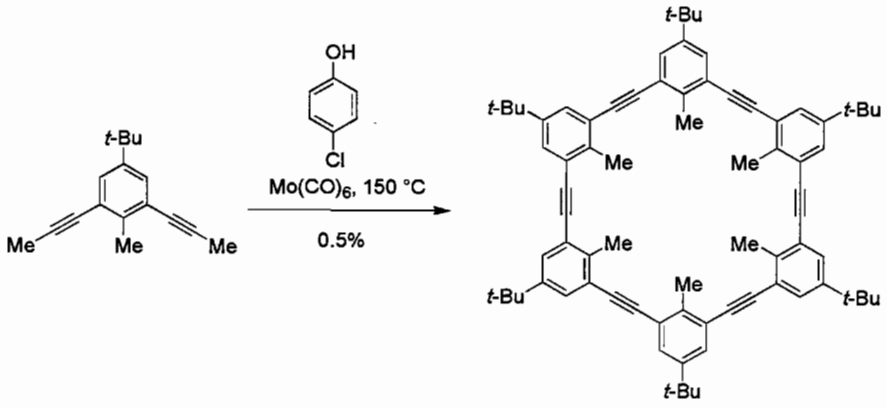

149 **148**

PAM **148** was prepared along with the heptameric analogue by Bunz et al. by way of alkyne metathesis of the dipropynylated benzene derivative **149**, albeit in 0.5% yield (Scheme 35).[45] The formation of oligomeric and polymeric by products presumably accounts for the low yield in which **148** was formed..

Very recently Cho and coworkers prepared *meta*-PAM **150** which contains two different types of donor groups, OMe and NBu_2 (Scheme 36).[52] The terminal alkyne **151** was cross-coupled with the requisite diiodobenzene to give **152**. Treatment of the latter with TMSA and then base affords **153** which, when cross-coupled with **152**, gives the target macrocycle **150** in 15% yield. A detailed investigation of the photophysical properties of **150** reveals that the molecule has a Stokes shift of 3026-4152 cm^{-1}; the value increases in more polar solvents which indicates a significant change in the charge-transfer state. The two-photon absorption cross-section of **150** is comparable to that of Rhodamine and thus, the compound may find application as a two-photon absorption chromophore.

SCHEME 36. Synthesis of PAM **150**.

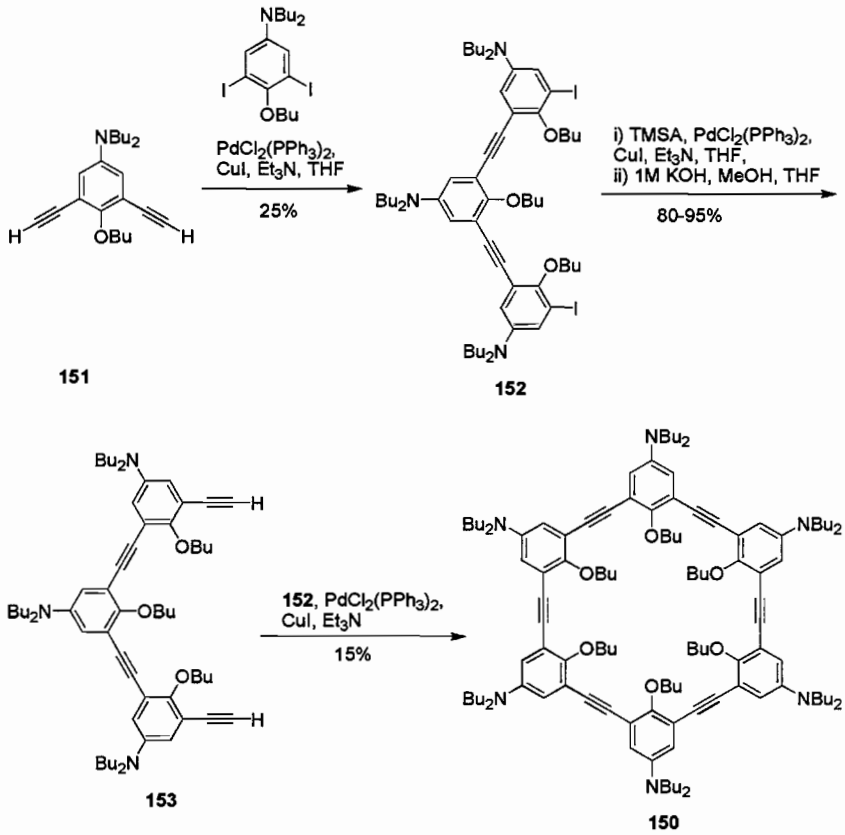

An example of a hepta *meta*-PAM, compound **154** (Figure 4), was prepared using the iterative route shown in Scheme 32.[43] Although an X-ray structure of **154** was not obtained, molecular modeling suggests the molecule has a flexible, non-planar geometry. Consequently, π–stacking interactions between the aromatic rings of the compound are disfavored.

Some of the largest *meta*-PAMs to have been prepared are the branched macrobicyclic arrays **155** and **156**[53] and the macrotricycle **157**.[54] The last compound is a freely hinged system with a sizeable (and collapsible) 36 × 12 × 12 Å molecular cavity.

FIGURE 4. Compound **154**.

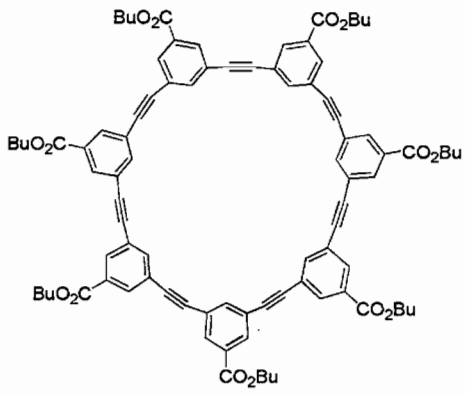

154

FIGURE 5. Compounds **155-157**.

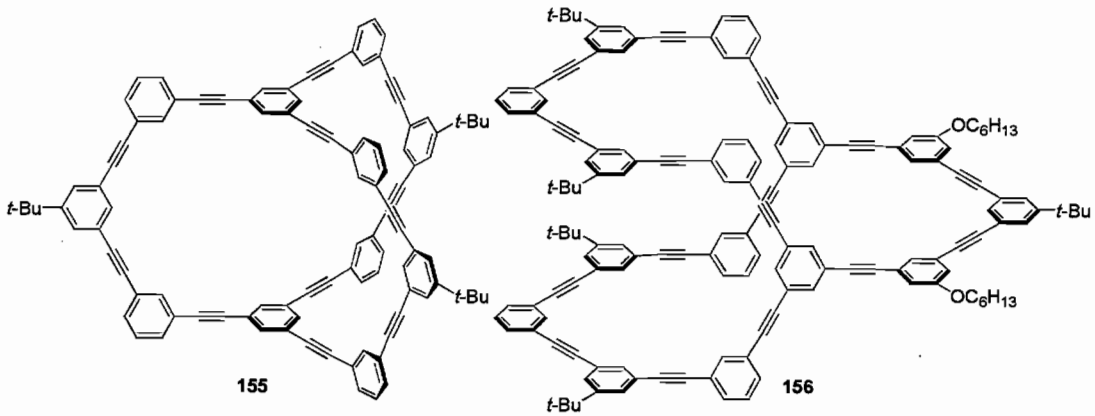

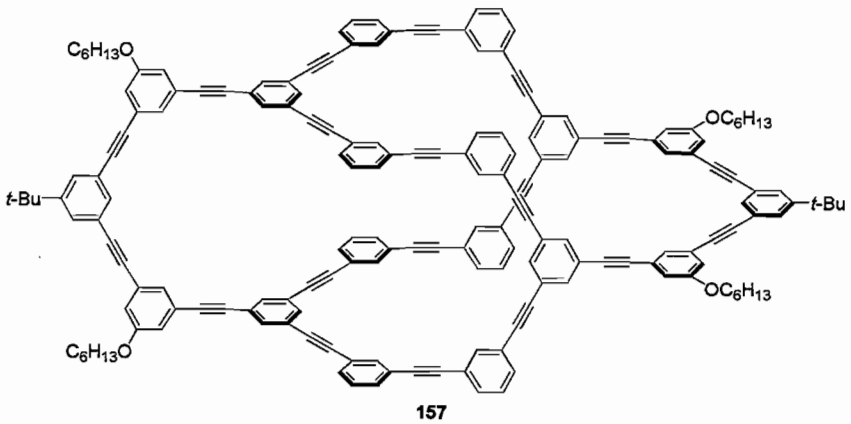

157

3.3 Para PAMs

Relatively few examples of all *para*-linked phenylacetylene macrocycles are known. The belt shaped PAMs **158-161** were prepared from the requisite macrocyclic synthons **162-165**, which in turn were obtained from the McMurray coupling of the appropriate stilbene (Scheme 37).[55] Bromination/dehydrobromination of an inseparable mixture of **162** and **163** furnishes a 4:1 ratio of the belt-shaped air-sensitive macrocycles **158** and **159** in a combined 85% yield; the compounds were separable by gel permeation chromatography. More recently, Oda et al. prepared relatively clean samples of synthons **162** and **163** which afford the appropriate macrocycles in significantly higher yield and almost pure form.[56] The belt-shaped macrocycles **160** and **161** were prepared, using the same technique, in 20 and 4% yield, respectively, from contaminated samples of synthons **164** and **165**.[56] Attempts to prepare the strained *para*-tetra(phenylacetylene) macrocycle from bromination/dehydrobromination of **166** were unsuccessful.[55]

SCHEME 37. Synthesis of PAMs **158-161**.

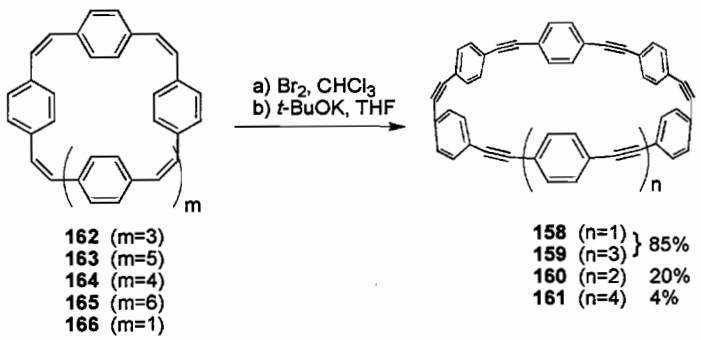

The carbon nanorings **158** and **159** possess cavities with diameters of 13.2 and 17.3 Å, respectively, and form weak inclusion complexes with toluene and

hexamethylbenzene.[57] Oda and his group reported that **158** forms a stable 1:1 crystalline complex with both C_{60} and bis(ethoxycarbonyl)methanofullerene.[58] An X-ray structure of the methanofullerene:**158** complex shows each molecule of the structure associates with two solvent molecules. The C_{60} cage is not embedded deeply in **158** and adopts a bowl-shaped conformation and the average distance between the host and guest is approximately 3.4 Å. Attempts to form host-guest complexes from the larger phenylacetylene macrocycle **159** and the aforementioned fullerenes were unsuccessful. Interestingly, nanorings **158** and **161** associate with one another to give 'onion-type' complexes .[59]

Oda and his group very recently prepared the acid- and oxygen-sensitive PAMs **167** and **168** (Figure 6) which can be stored in dilute solution at 0 °C over a month.[60] These macrocycles were shown to associate with both C_{60} and C_{70} and form extremely stable complexes. PAM **167** also associates with other nanorings in an 'onion-type' complex, which in turn includes C60 in the presence of excess fullerene.[59] Unfortunately, X-ray structures of these complexes have yet to be obtained.

FIGURE 6. Compounds **167-168**.

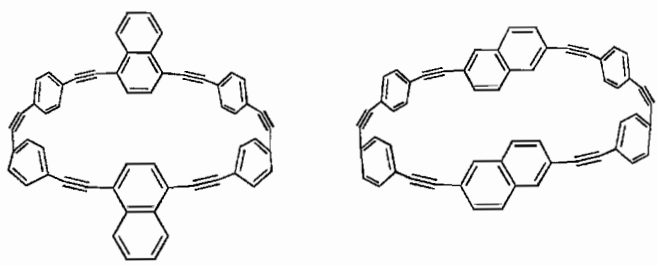

167 **168**

3.4 Mixed PAMs

Vollhardt and his group prepared PAM **169**, which contains both *ortho* and *meta* linkages, in 19% yield from alkyne metathesis of a 1:1 mixture of the dipropynylated arenes **13** and **170** with the tungsten reagent [(*t*BuO)$_3$W≡C*t*Bu] (Scheme 38).[16] An X-ray structure of **169** shows the molecule is nearly planar with the dihedral angles between the planes of the *ortho*- and *meta*- fused rings of 7.1°.

SCHEME 38. Synthesis of PAM **169**.

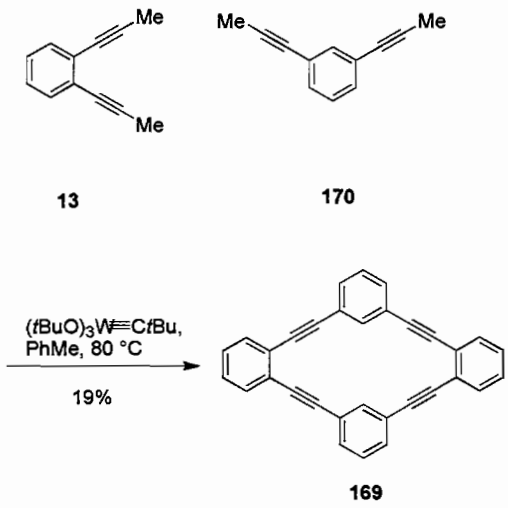

Tsuji and coworkers prepared the *ortho*/*para*-connected PAM **171** in 74% yield, from photoirradiation of Dewar benzene synthon **172**, which is in turn prepared in six steps from 1,2-diiodobenzene (Scheme 39).[61] Conversion of the last compound into **173** is accomplished using standard transformations. Protiodesilylation of **173** and subsequent Pd-catalyzed cross-coupling of the terminal alkyne with **174** affords compound **175** which upon deprotection and homocoupling under phase-transfer

conditions gives **176**. Acidic hydrolysis of **176** and subsequent treatment with TIPSOTf furnishes PAM **171** in 72% yield. An X-ray structural analysis of macrocycle **171** shows the two *p*-substituted benzene rings are nearly planar with an interplanar distance of 3.48 Å, and these are tilted 62.5 and 64.2° with respect to the plane of the macrocycle. As expected, the acetylene moieties are distorted, deviating from the normal linear arrangement by 8.6-12°.

Using combinations of *ortho*-, *meta*-, and *para*-connected phenylacetylene monomers, Moore and coworkers have prepared a number of macrocyclic geometries based on a trigonal lattice.[5c,46a,62,63] PAMs **177-179** (Figure 7) represent a few examples of the many macrocycles prepared to date. Molecular modeling of compound **177**, which contains 12 arene rings, shows the inner diameter (hydrogen to hydrogen) is slightly greater than 22 Å.[63]

Fascinating examples of PAMs containing mixed linkages are the "molecular turnstiles" (**180-182**, Figure 8) which were prepared by Moore and Bedard.[64] Models of macrocycle **180** show the inner ring can rotate freely. Indeed, variable-temperature NMR experiments suggest the spindle of the turnstile exhibits dynamic behavior. Similarly, the turnstile of **181** rotates freely at ambient temperature and has an estimated barrier to spindle rotation of ~13.4 kcal mol^{-1}. In contrast, the more sterically congested spindle of **182** is conformationally locked and no evidence for dynamic behavior was obtained.

SCHEME 39. Synthesis of PAM **171**.

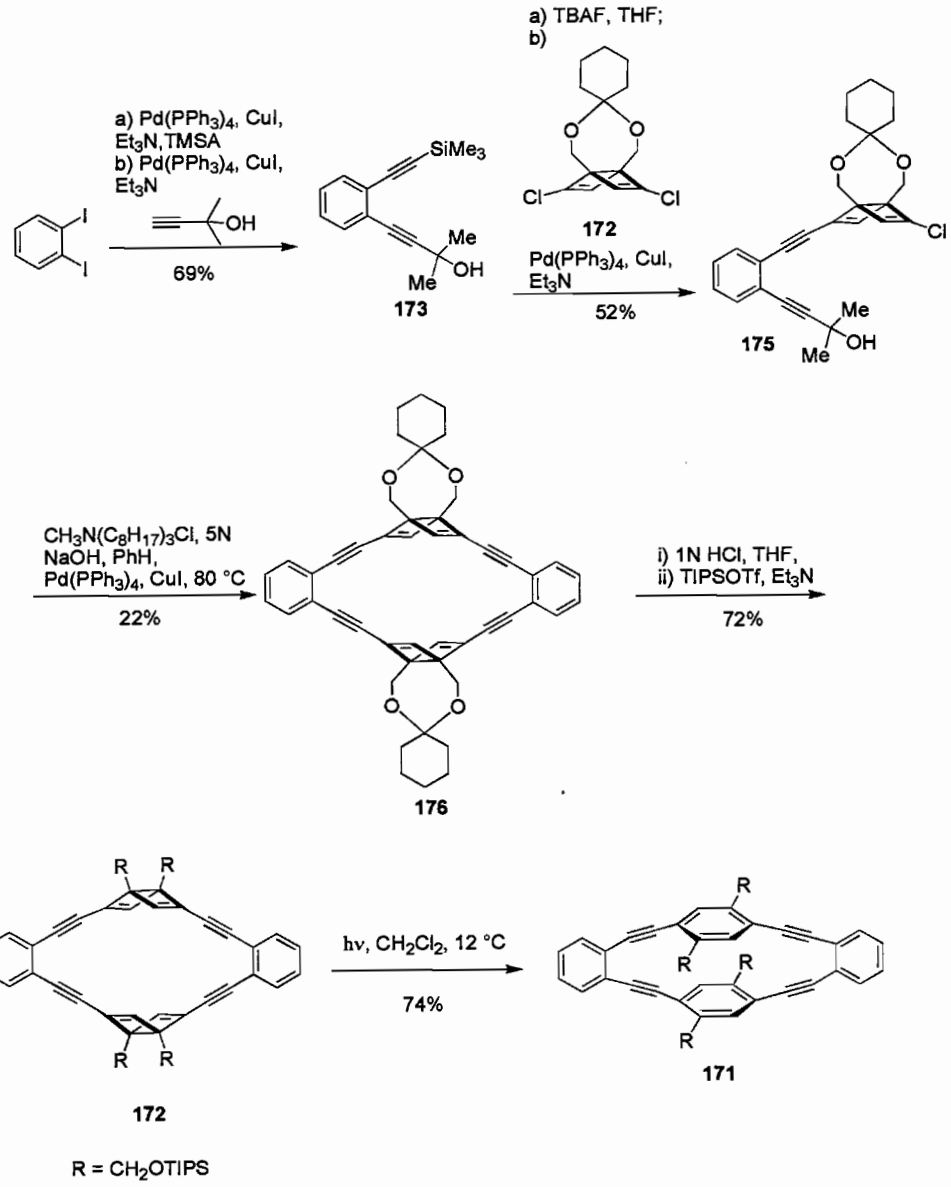

FIGURE 7. Compounds **177-179**.

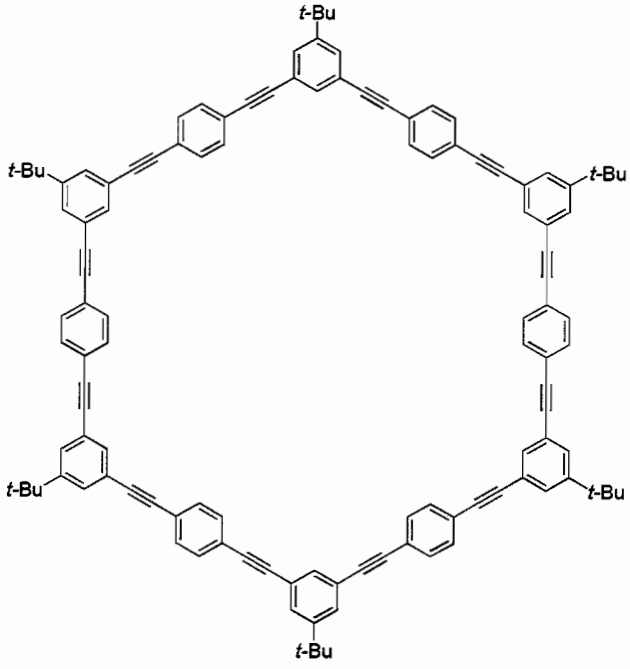

177

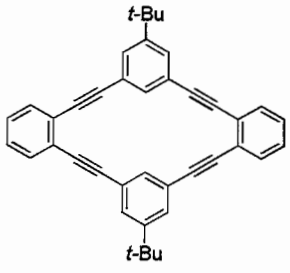

178

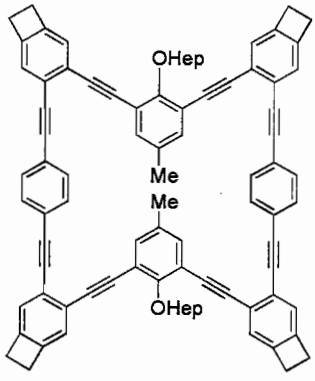

179

FIGURE 8. Compounds **180-182**.

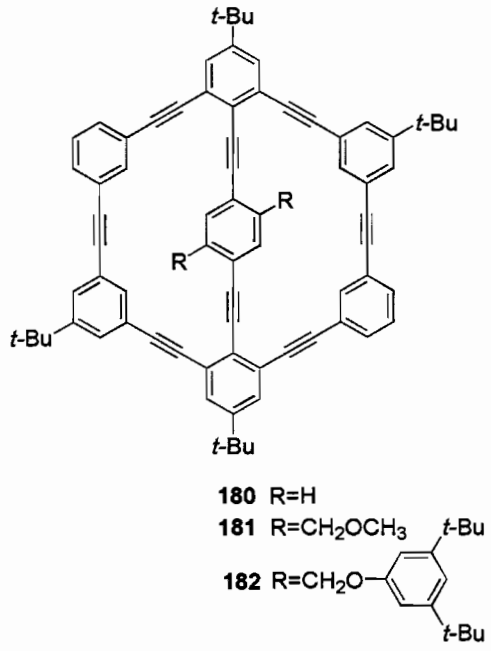

4. Phenyldiacetylene Macrocycles

In the thirty years following Eglinton's groundbreaking work on **3**, no reports were published on the preparation of related phenyldiacetylene macrocyclic systems. Since the 1990s, however, the chemistry of PDMs has witnessed an explosive resurgence concomitant with the advent of novel synthetic methodology tailored towards the construction of carbon-carbon bonds via organotransition metal complexes. Although PDMs are typically less stable thermodynamically and more reactive than the homologous PAM derivatives, they exhibit a slew of novel electronic and optical properties. As such, they serve as potential synthons for technologically important compounds such as highly conjugated polymers, nonlinear optical materials, and new carbon allotropes.

In the 1970s, diacetylene monomers were found to undergo topochemical polymerizations to generate highly ordered crystalline polymers possessing conjugated backbones which displayed interesting conductive and optical properties.[65] If this reactivity could be extended to include PDM derivatives such as **3**, a potential route to highly conjugated networks of sp and sp^2 carbon atoms, with potentially interesting properties, could be developed. With this goal in mind, several research groups have prepared over the last decade a variety of derivatized PDMs for topochemical investigation.

4.1 Ortho PDMs

Although the molecular structure of **3**, the first phenyldiacetylene macrocycle to be synthesized and characterized (Scheme 1),[8] was obtained in 1959,[9] it took another 40 years before the packing behavior of this highly strained and reactive molecule was established.[66] The flat molecules stack parallel and form columns, with the columns staggered to form a "brick wall" motif. The orientation of the molecules within the column, however, precludes a topochemical polymerization. Diffraction experiments of "polymerized" samples showed that the material had lost all single-crystalline order. PDM **3** could also be co-crystallized with hexafluorobenzene and with TCNQ.

With the polymerization goal in mind, Swager et al. prepared in 1994 annulene **3** and various derivatives for topochemical investigation.[10] In addition to diyne **2** the Swager group studied the Cu-mediated cyclooligomerizations of 4,5-disubstituted-1,2-diethynylbenzenes (**183**). The requisite dialkylbenzenes were prepared in two steps from

o-dichlorobenzene (Scheme 40). Thus, the appropriate alkyl Grignard salt was cross-coupled with ODCB in the presence of catalytic $NiCl_2$(dppp) to afford the disubstituted benzene derivative which was doubly iodinated with $I_2/NaIO_3$ in glacial AcOH. Cross-coupling the latter arene with TMSA under Sonogashira conditions followed by protiodesilylation with KOH furnished the alkylated derivatives of **183** (R = Bu, Hex, Dec, Dod). The 1,2-diiodo,4,5-didecyloxybenzene was assembled in an analogous manner; however, the cross-coupling reaction required 2 molar equivalents of CuI to furnish **183** (R = ODec) in a reasonable yield. Although the exact origin of this effect is unclear, it is possible that the lone pairs on the heteroatom act as a Lewis base and form a weakly bound aryl-copper complex which prevents the Cu-acetylide coupling partner from forming.

Cyclooligomerization of arenes **183** under Hay conditions (CuCl, TMEDA, O_2) furnished mixtures of dimeric (**184**), trimeric (**185**), and tetrameric (**186**) PDMs along with some polymeric material.[10] Purification of the different products from the mixture proved laborious and was accomplished only through repetitive chromatography and fractional crystallization. The yields of the PDMs were found to vary widely and depended upon the length of the hydrocarbon tail, the scale of the reaction, and the exact experimental conditions. Thus, while those derivatives of **183** which possess short alkyl and alkoxy groups tended to produce higher yields of larger macrocycles and polymeric material, the oligomerization of substrates possessing larger alkyl tails favored dimer formation. Moreover, fast small scale reactions were found to give the optimal overall yield of macrocyclic products. Overall yield and the product ratio of PDMs was also

dependent on the order of reagent addition. As a whole, the above problems illustrate the weakness of the intermolecular cyclooligomerization reaction.

SCHEME 40. Synthesis of PDMs **184-186**.

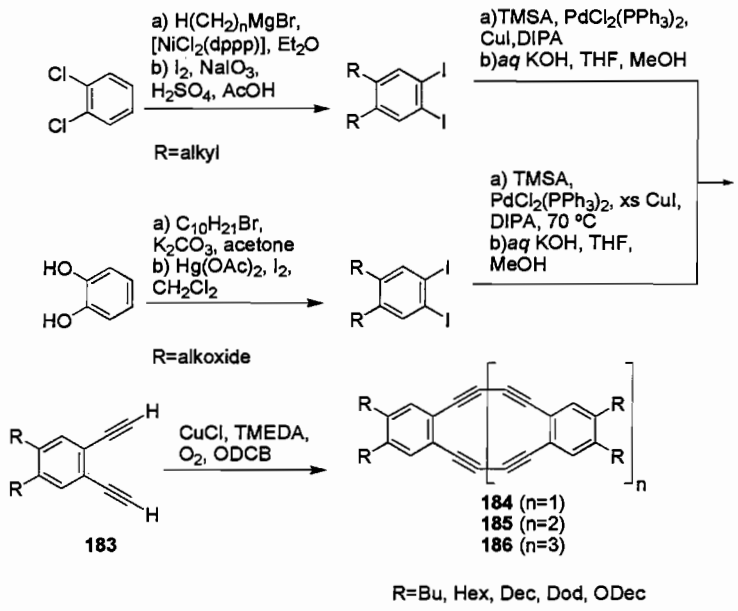

Because of the presumed unusual reactivity of the strained dimers **184**, several attempts were made to maximize their formation.[10] However, varying reaction times and decreasing substrate concentrations in the cyclooligomerization reactions failed to significantly improve upon dimer formation. Accordingly, the tetrahexyl-substituted dimer **5** (**184**, R = Hex) was synthesized by a six-step stepwise approach via synthons **24** and **25**. Ring-closure using Hay conditions furnished dimer **5** and tetramer **7** (**186**, R = Hex) in 13% and 45% yield, respectively (Scheme 7). This product distribution is surprising since intramolecular reactions are typically more facile than intermolecular reactions.

An X-ray structural analysis of dimer **184** (R = Bu) reveals similarities to **3**, in that the unsaturated portion of the molecule is planar, with the angles between adjacent acetylenic bonds deviating by 13-15° from linearity. Since the connection of the alkyne moieties to the aromatic rings is only slightly compressed (2-3°), distortion of the acetylenic linkages appears as the major source of instability in these macrocycles. Unlike **3**, the molecules no longer stack in columns but are offset in the crystal lattice because of the hexyl substituents.

Differential scanning calorimetry (DSC) experiments performed on the various dimers **184** show that the molecules abruptly thermally polymerize between 100-125 °C. While the narrow temperature range for this exothermic process is suggestive of a chain reaction, the absence of acetylenic functionalities in the IR spectra of the polymerized materials, as well as broad peaks in the X-ray powder diffraction and solid state ^{13}C NMR data, indicate that highly ordered topochemical diacetylene polymers are not formed. DSC analysis of the various trimeric PDMs **185** is even more disappointing. Although more thermally robust, these macrocycles polymerize with very broad exotherms at sufficiently high temperatures (ca. 200 °C) yielding only intractable tars.

To better understand the reactivity of PDMs **184**, their chemistry was followed in solution [10]. Addition of I_2 to an Ar-saturated benzene solution of the individual dimeric PDMs affords compounds **187**, which contain a tetraiodinated 6-5-6-5-6 fused ring system, in 50-67% yield (Scheme 41). Eglinton reported formation of the same pentacyclic architecture upon treating parent **3** with Na/NH_3.[8] Although this reaction presumably occurs through radical intermediates, attempts to trap such species led to

uncharacterizable material. Exposure of **187** to oxygen or iodine in the presence of oxygen gives dione **188**. Labeling experiments show that the carbonyl oxygen is incorporated directly by oxidation of **187** with molecular oxygen rather than as a result of hydrolysis.

SCHEME 41. Oxidation of PDM **184**.

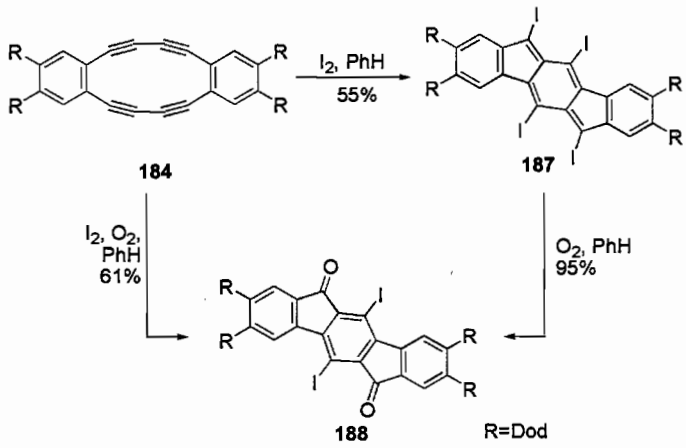

Whereas the Hay conditions in Swager's study had failed to yield the parent tetramer **23**, Youngs et al. found that highly dilute Glaser conditions with bubbling air through the pyridine solvent affords **23** in 20% yield along with a high yield of dimeric PDM **3** (Scheme 7).[22] As is often the case in Cu-mediated acetylenic homocoupling, the exact reactions conditions play an important role and can be the crucial difference between high yield or no yield of product.

The dimeric and trimeric perfluorinated analogues of **3** and **1**, PDMs **189** and **190** respectively, were recently reported by the Komatsu group.[67] Pd-catalyzed cross-coupling of TMSA with 1,2-diiodoperfluorobenzene followed by protiodesilylation with KOH

gave 1,2-diethynylperfluorobenzene (Scheme 42). Cyclooligomerization using Hay conditions affords the electron deficient π-systems **189** and **190** in 20-45% and 10-20% yield, respectively, along with minor amounts of tetramer.

SCHEME 42. Synthesis of PDMs **189** and **190**.

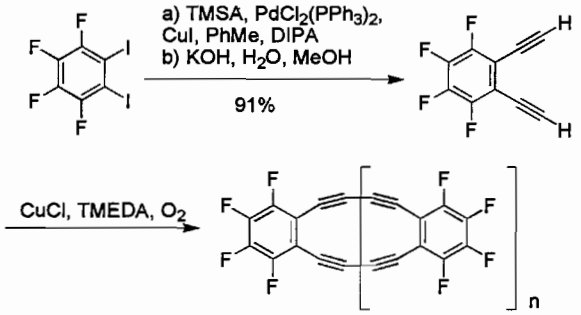

189 (n =1, 20-40%)
190 (n = 2, 10-20%)

For *trans*-topochemical polymerization of 1,3-diynes to occur most efficiently, the diyne monomers should pack in an offset manner with an intermolecular distance $d \approx$ 5 Å and a stacking angle $\Phi \approx 45°$ [65] while a $d \approx 3.5$ Å and $\Phi \approx 90°$ are required for *cis*-polymerization.[68] The X-ray data of the crystal derived from **189** in chloroform shows the PDM packs in a parallel and slanted arrangement with $d = 4.99$ Å and $\Phi = 39°$ while that obtained from the benzene solution adopts a similar arrangement but the stacks are more slanted ($d = 6.35$ Å and $\Phi = 26°$); additionally, **189** crystallizes with a solvent molecule in a 1:1 ratio. The co-crystal derived from mixing equimolar amounts of **189** and **3** packs in an unexpected 2:1 ratio in which the PDMs alternate in a face-to-face stacking array ($d =$ 3.69-3.87 Å and $\Phi = 75$-$78°$). While these results show the macrocycles stack in the proper orientation for topochemical polymerizations, attempts to induce polymerization

upon photoirradiation were unsuccessful. DSC analysis of the PDMs show strong exotherms; however, analysis of the thermoproducts suggests that they are not topological polymers but instead carbon-rich materials such as amorphous carbon and graphite, which have been shown to result from the thermal reactions of other dehydrobenzoannulenes.[69,70] To date, an ordered polymerization of the Eglinton-Galbraith dimer has yet to be observed. Attempts to grow either crystals of **190** or a co-crystal of **190** and **2** of X-ray quality have been unsuccessful.

Very recently Faust and Ott reported the synthesis of the $Ru(bpy)_2$-coordinated PDM **191** from treatment of the tetra-Boc-protected **192** with $((bpy)_2Ru(phenanthroline\text{-}5,6\text{-}dione))_2^{+}(PF_6^{-})_2$ under acidic conditions (Scheme 43).[71a] PDM **192** was generated from protiodesilylation/homocoupling of tetrayne **193** which was assembled in five steps from 1,2-diiodo-4,5-dinitrobenzene using conventional methodology. Not surprisingly, the outcome of the final Cu-mediated homocoupling reaction is concentration dependant. A 0.4 mM solution of deprotected **193** furnishes dimer **192** exclusively in 72% yield while use of a 1.5 mM solution of the terminal acetylene gives an inseparable mixture of **192** and tetramer **194** in a 2:1 ratio.[71b] The redox properties of **191** reveal two reduction waves at comparable values to that required for the first reduction of C_{60}. Furthermore, photoirradiation of **191** induces luminescence; preliminary measurements indicate the lifetime of the excited state is 28 nm.

SCHEME 43. Synthesis of PDMs **191-192,194.**

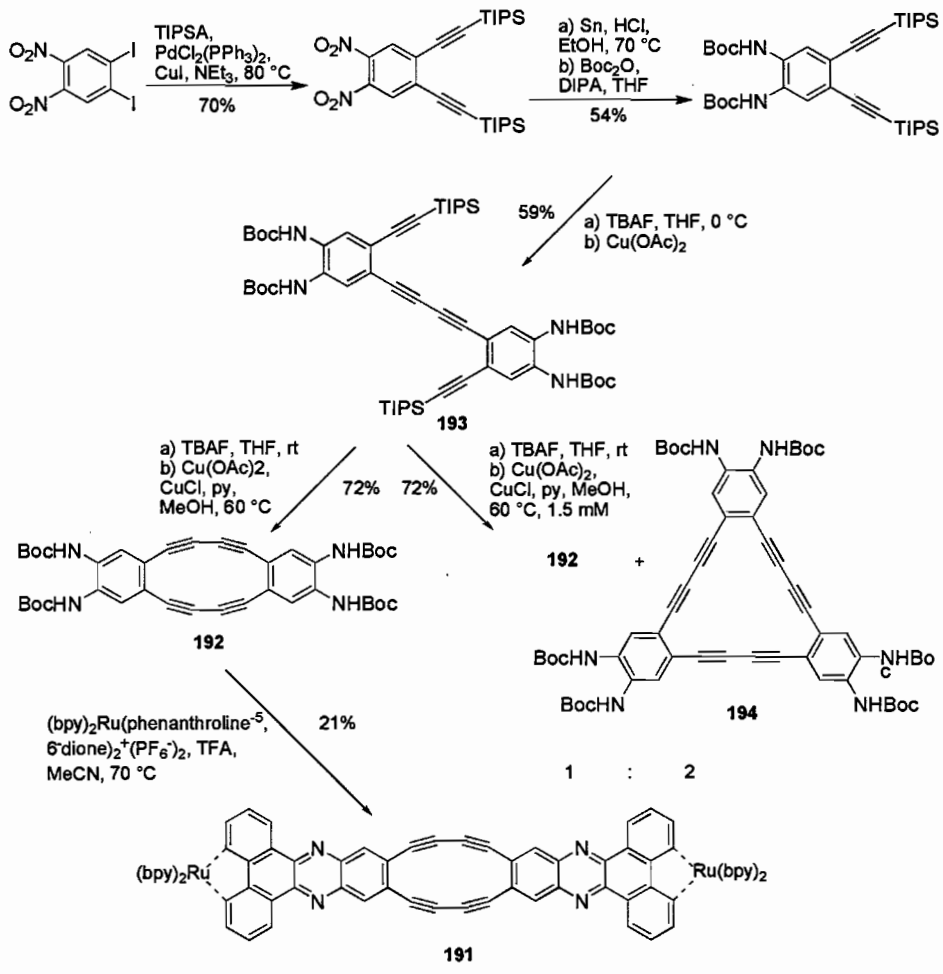

The π–framework of PDMs **192** and **194** is extended further upon treating a suspension of the annulene mixture and benzil with TFA (Scheme 44).[71b] The resultant macrocycles **195** and **196** are obtained as sparingly soluble solids. In contrast, repetition of the aforementioned reaction with 1,6-bis(TIPS)-hexa-1,5-diyne-3,4-one affords PDMs **197** and **198** which are separable readily by gel permeation chromatography. Unlike **195/196**, in **197/198** show the effect of the additional alkyne units in the absorption spectra with a bathochromic shift of ca. 20 nm compared to **195/196**.

SCHEME 44. Synthesis of PDMs **195-198**.

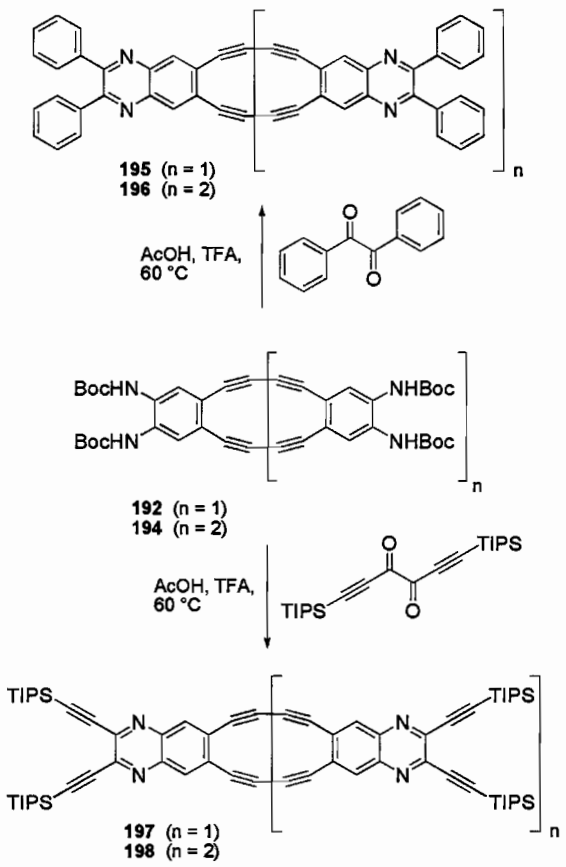

Anthony and Gallagher have synthesized a series of linearly-fused oligomers (**199-201**) based on the Eglinton-Galbraith dimer **3** (Scheme 45).[72] Starting with tetrayne **202**, partial desilylation with catalytic $AgNO_3$ and 3 equiv. NBS gave a 1:1 mixture of mono- and dibromoacetylides. Exposure of the mixture to Sonogashira conditions with **203**, followed by removal of the remaining TMS groups and oxidative alkyne coupling gave precursors **204-206** as a mixture. Removal of the TIPS groups and alkyne homocoupling under Hay conditions furnished the brightly colored cyclic oligomers, which were separated using flash chromatography. Whereas **199** and **200** are freely

soluble and can be stored for weeks, PDM **201** is only sparingly soluble and decomposes slowly in solution. The electronic absorption spectra of **199-201** show a progression of the lower energy absorptions with increased oligomer length. An estimated cut-off of the infinite polymer derived from this series is 625 nm (1.98 eV), which is comparable to other linear acetylene-based polymers.

SCHEME 45. Synthesis of PDMs **199-201**.

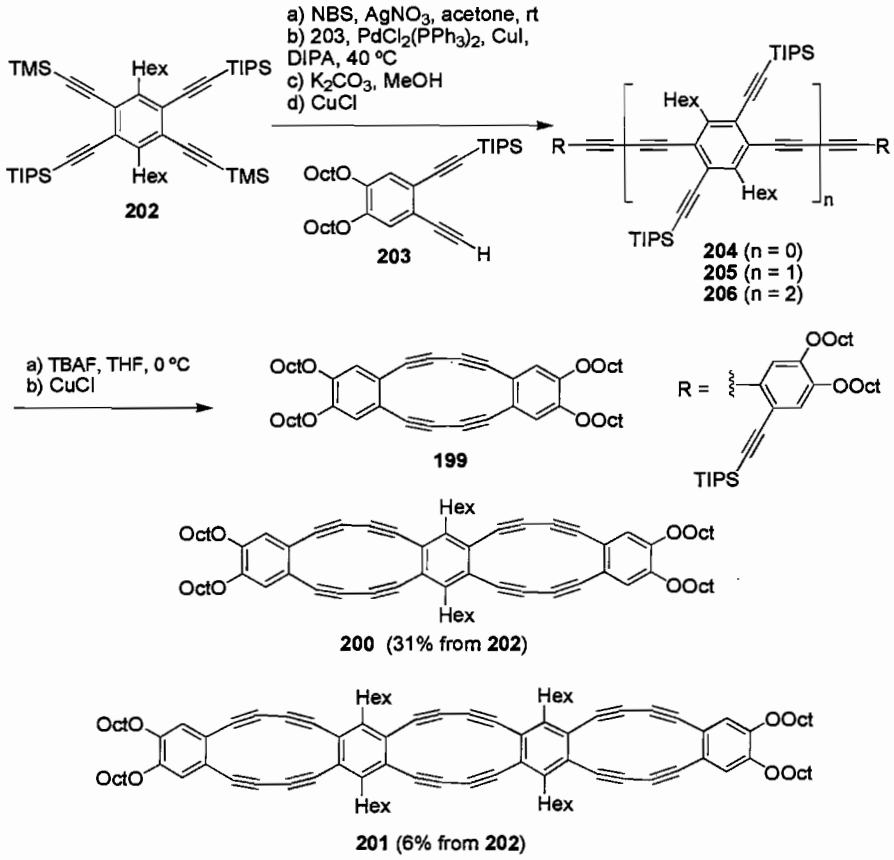

As shown in Scheme 8, Vollhardt and Youngs prepared hybrid PAM/PDM **26** via an intramolecular cyclization.[23] Similar to **3**, the molecule contains highly strained acetylene bonds which impart interesting solid-state behavior. As shown by X-ray crystallography, the monoacetylene units in **26** bow inward toward the center of the

macrocycle by 3.9-11.5° while the diacetylene moiety bows outward by 8.6-11.2°. The molecules are stacked (d = 6.3 Å, Φ = 35.5°) in the same slanted and parallel way as **3**; however, upon photoirradiation or application of pressure, **26** polymerizes to form an insoluble violet colored material with a metallic luster. Complete polymerization can be achieved through thermal annealing (150 °C by DSC) or high pressure (20,000 psi, 1 h). Solid-state ^{13}C NMR spectroscopy of the polymer displays two new peaks at 145.1 and 150.0 ppm which are assigned to the alkene carbons of the polydiacetylene chain. Additional evidence comes from TOF-MS which detects oligomers containing up to nine macrocyclic units. Despite a number of related studies, the confirmed topochemical polymerization of **26** remains unique among PDMs.

An alternate decomposition pathway for dehydrobenzoannulenes and related PDMs was reported by the Vollhardt group in 1997.[69] Treatment of the terminal acetylene **36** with $Cu(OAc)_2$ affords the non-planar dimer **207** in 13% yield along with small amounts of trimer **208** (Scheme 46). The former PDM decomposes explosively at ca. 250 °C to produce a nearly pure carbon residue. Whereas the black solid did not contain any soluble carbonaceous material (e.g., fullerenes), TEM analysis of the residue showed that "bucky onions" and "bucky tubes" had formed in addition to amorphous carbon and graphite. Although the amount of "bucky" material composed only 1-2% of the carbonaceous product, subsequent studies have shown that inclusion of metal complexes in the phenyl-acetylene starting materials results in considerably higher conversion to "bucky" compounds.[73] These results clearly validate the argument that PAMs and PDMs provide a potential route to these novel carbon-rich materials.

SCHEME 46. Synthesis of PDMs **207** and **208**.

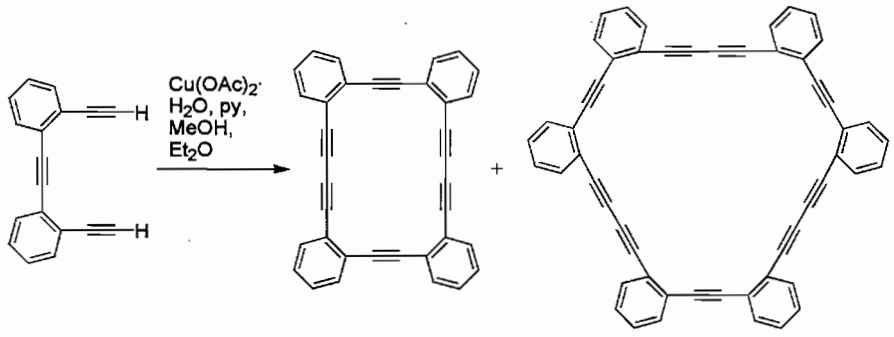

36 **207** (13%) **208** (5%)

As discussed previously, the Haley group recently synthesized bisPDMs **30** and **31** starting from the same precursor (**29**, Scheme 9), with the structure of the final molecule dependent upon the method of alkyne homocoupling.[24] Scheme 47 illustrates the selectivity for ring size between the Cu- and Pd-mediated reactions. Both the 14- and 15-membered ring precursors (**209** and **210**, respectively) are prepared by Sonogashira cross-coupling of **28** with the appropriate dibromodiiodobenzene. Protiodesilylation and alkyne homocoupling gives either **211** or **212**. While Cu-mediated ring-closure of **210** affords the 15-membered ring (**212**) in very good yield (76-80%), the analogous reaction with substrate **209** affords the 14-membered ring (**211**) in much lower yield (24-35%). Conversely, Pd-mediated ring-closure of **209** furnishes PDM **211** in very good 67-76% yield while the analogous treatment of synthon **210** furnishes the PDM **212** in a low 12-24% yield. The authors attribute this difference to the strain in the metal-containing intermediate prior to reductive elimination (alkyne homocoupling). Whereas a cis-arrangement of the alkynes in the presumed Pd-bis(σ-acetylide) complex would favor formation of **211**, a similar cis-arrangement to afford **212** would be highly strained. On

the other hand, the Cu-acetylide intermediate leading to **212** prefers a less-strained, trans-like arrangement.[4]

SCHEME 47. Comparison of Homocoupling Methods for PDMs **211** and **212**.

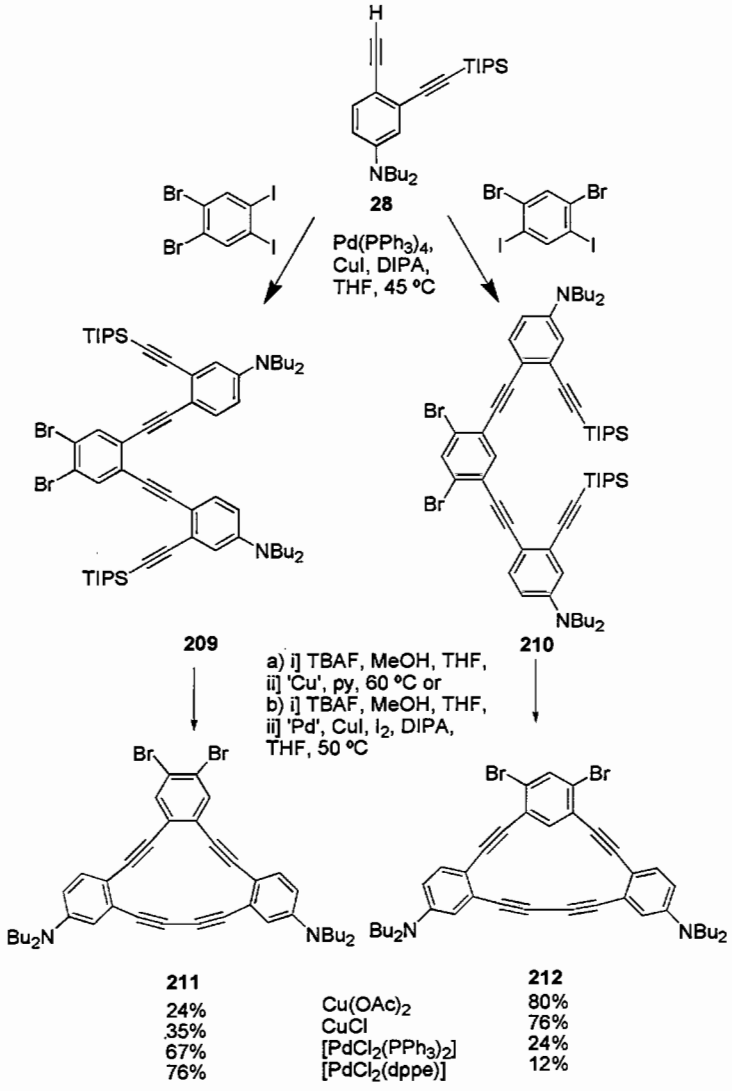

Confirmation that bisPDM **30** was indeed the product of the Cu-mediated cyclization of **29** was provided by independent synthesis of each 15-membered ring.[24]

Pd-catalyzed cross-coupling of **212** with **28** furnishes intermediate **213** in 43% yield (Scheme 48). Removal of the TIPS groups with TBAF followed by oxidative cyclization using $Cu(OAc)_2$ affords in 57% yield target molecule **30** whose spectral data are an identical match with those obtained for the compound generated by the route in Scheme 9.

SCHEME 48. Stepwise Synthesis of BisPDM **30**.

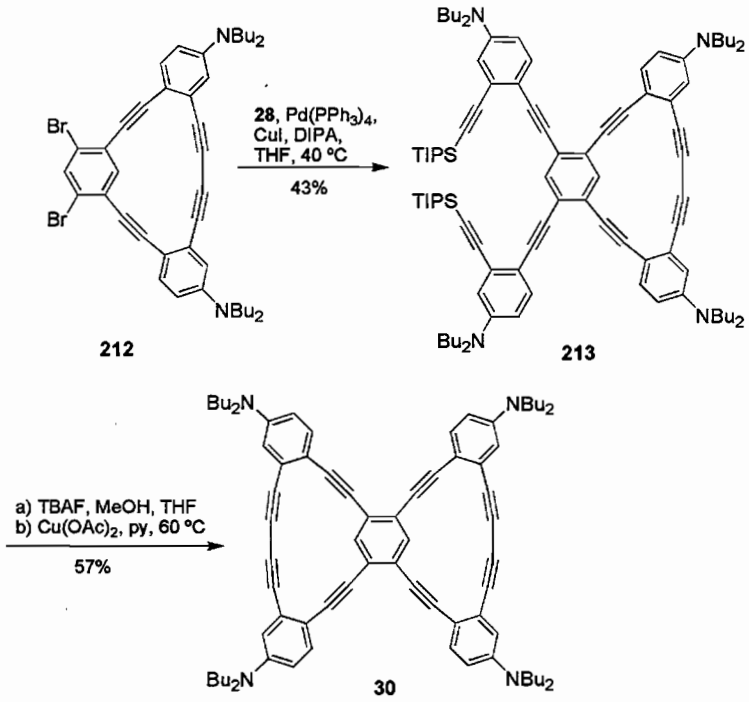

The Rubin group synthesized PDMs **214-216** from 1,2,3,4/5,6-differentially terminated hexaethynylbenzene **217** (Scheme 49).[74] Preparation of these perethynylated derivatives requires more intricate synthetic maneuvering prior to cyclooligomerization. Arene **217** was prepared though Diels-Alder reaction of suitably derivatized tetraalkynylcyclopentadienone **218** and $OHCC{\equiv}CCH(OEt)_2$ followed by expulsion of CO to afford arene **219**. This compound was then converted into **217** via **220** using

successive Corey-Fuchs alkynylation reactions. Attempts to introduce the alkynes directly by cycloaddition of **218** with bis-silylated hexatriynes were unsuccessful. Calculations suggest that the central triple bond in the triynes is sterically inhibited in the transition state by the bulky dienophile with the large capping groups on the dienone. Cyclooligomerization of **217** using Hay conditions furnished **214** in an isolated yield of 25% along with an inseparable mixture of higher homologues **215** and **216** in a combined 13% yield.

SCHEME 49. Synthesis of PDMs **214-216**.

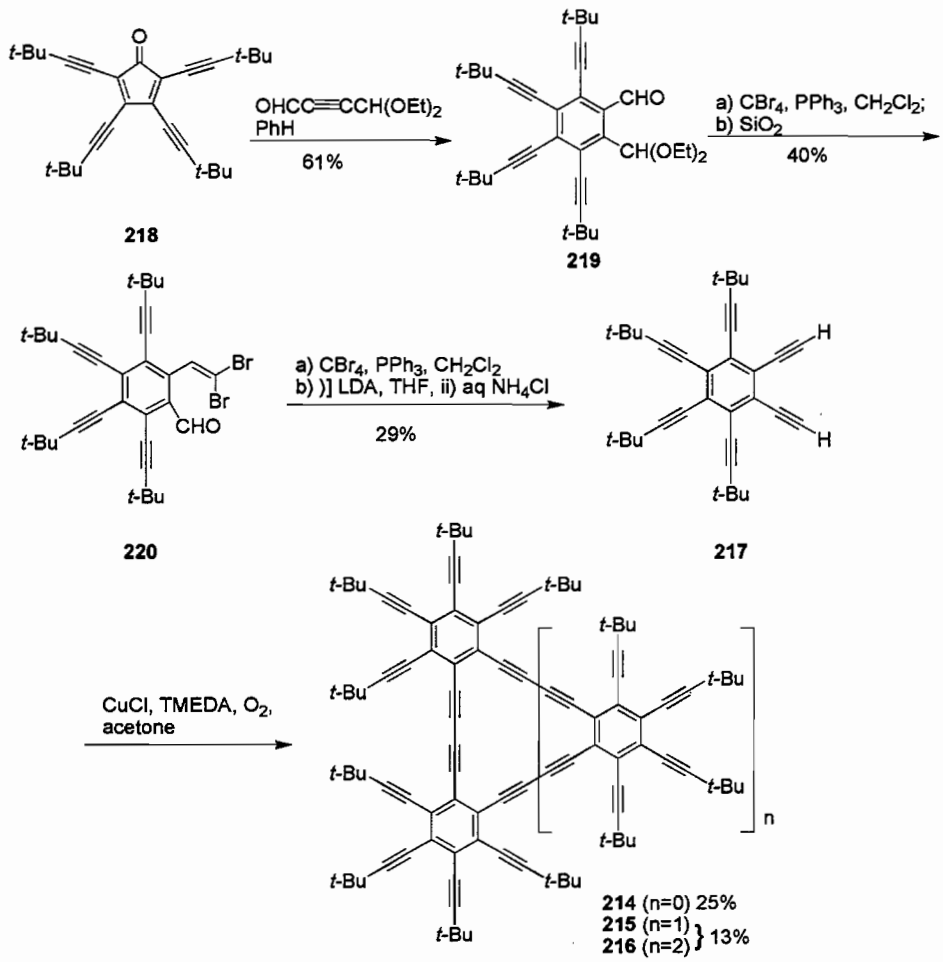

Compound **215** is a substructure of and potential precursor to the theoretical all-carbon-containing network graphdiyne (**221**), an homologue of graphyne (**78**) in which the acetylene linkages are replaced with butadiyne units. This and other diacetylenic all-carbon networks have attracted considerable attention due to predictions of technological importance, but to date have remained elusive because of synthetic difficulties.[75] PDM **215** can be considered molecular fragments of graphdiyne and features a fringe of *t*-butyl capped acetylene moieties around the periphery. This feature not only increases the potential for nonlinear optical activity by extending electron conjugation, but it also serves to stabilize the characteristically reactive dimer **214**. The difficulty of preparing the differentially terminated hexaethynylbenzenes limits this route to the above examples.

Surprisingly, the synthesis of the simplest graphdiyne subunit, PDM **1**, was not reported until 1997.[76] The Haley group prepared **1** through an intramolecular route since cyclooligomerization of *o*-diethynylbenzene purportedly failed to afford the desired macrocycle. Conversion of 1-bromo-2-iodobenzene into triyne **222** was accomplished using standard cross-coupling procedures (Scheme 50); however, attempts to monodeprotect **222** and couple it with 1,2-diiodobenzene provided intractable gums. This problem was circumvented by in situ generation of the free butadiyne under Sonogashira conditions, which then provided the bis-coupled product **223** in 71% yield. Desilylation and use of high dilution conditions in the oxidative homocoupling reaction gave **1** in 35% yield as a poorly soluble cream-colored powder. The minimal solubility of PDM **1** presumably accounts for its poor isolated yield, yet provided an important clue as to why it had not yet been reported. To best manipulate **1**, it is necessary to work-up the

homocoupling reactions using CH_2Cl_2 instead of the more traditional Et_2O. Armed with this fact, repetition of Scheme 1 utilizing this subtle modification now affords a 58% yield of **3** and an inseparable 3:2 mixture of PDMs **1** and **23** in 20% yield.[77]

SCHEME 50. Stepwise Synthesis of PDM **1**.

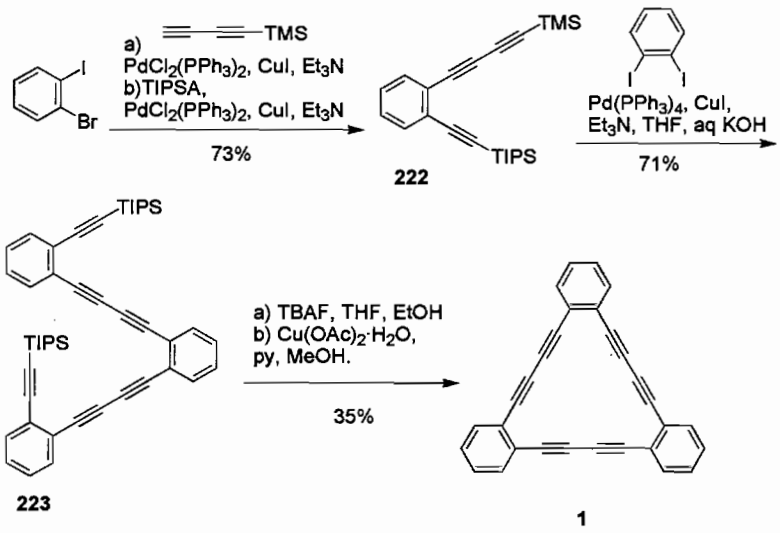

A number of larger graphdiyne substructures (Figure 9, **224-228**) have been prepared using the intramolecular cyclization technique from appropriately derivatized substrates.[77,78] From the outset, the need for solubilizing substituents was recognized. Scheme 51 illustrates the preparation of **225**. Triazene **229**, prepared from the corresponding aniline using chemistry described in Scheme 23, could be transformed into triyne **230** in 60-75% yield. Four-fold in situ desilylation/alkynylation of **230** gave dodecayne **231** in ca. 60-70% yield. Subsequent removal of the four TIPS groups with TBAF followed by two-fold intramolecular homocoupling furnished **225**. Whereas use of *tert*-butyl groups affords a solid that is virtually insoluble in common solvents, inclusion of decyl substituents solubilizes **225** effectively in that the compound is isolated

in 63% yield. The decyl versions of **224** and **226-228** were prepared in an analogous fashion.

FIGURE 9. Compounds **224-226**.

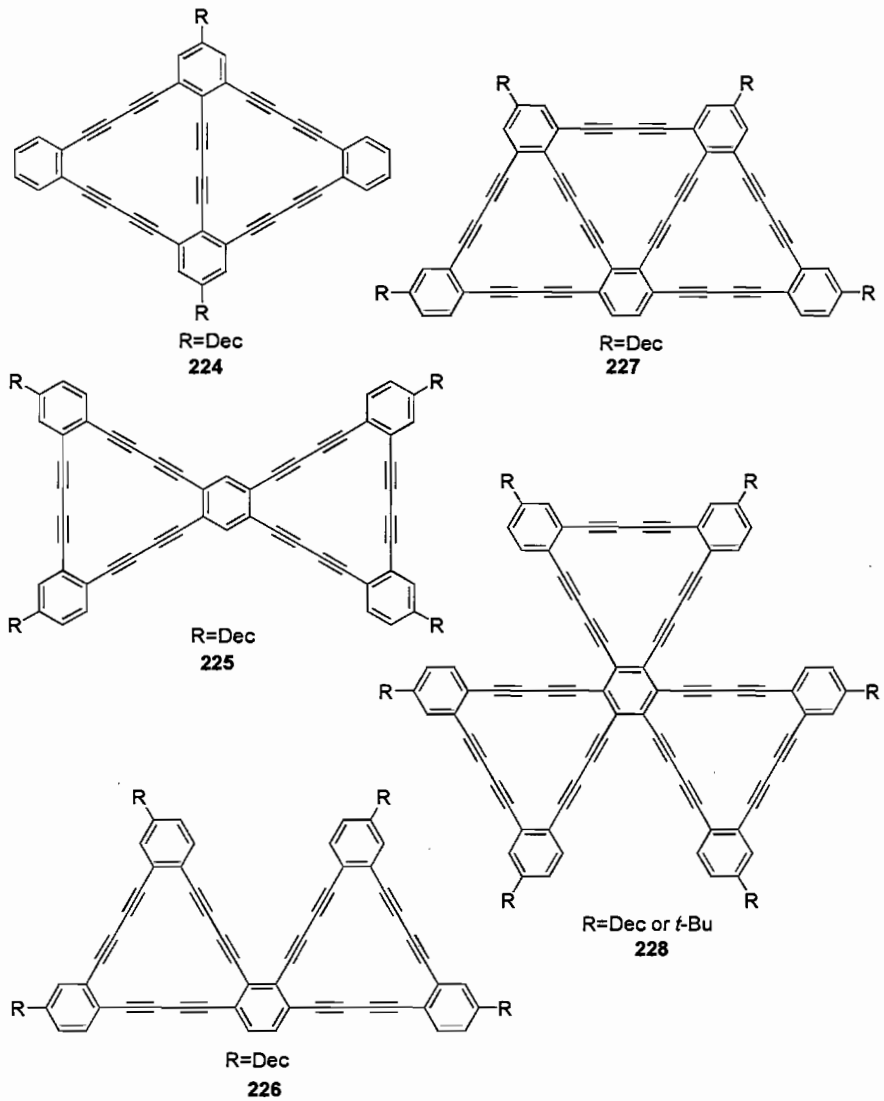

The electronic absorption data for **1** and **224-228** exhibit a characteristic pattern of four absorption bands, which are assigned primarily to $\pi \rightarrow \pi^*$ transitions in the [18]annulene skeleton. These peaks shift to longer wavelengths and possess greater

intensities as the number of longer 1,4-bis(phenylbutadiynyl)benzene chromophores is increased. Compared to **1**, the peaks of trisPDM **228** are shifted nearly 100 nm toward lower energy, thus reflecting the increased linear π-conjugation. Interestingly, the λ_{max} of **1** and **224-228** all show the effect of locking the π-electron-rich backbone into planarity. This effect is most pronounced in **228**, in which the λ_{max} is red-shifted nearly 60 nm compared to its acyclic precursor.

SCHEME 51. Synthesis of PDM **225**.

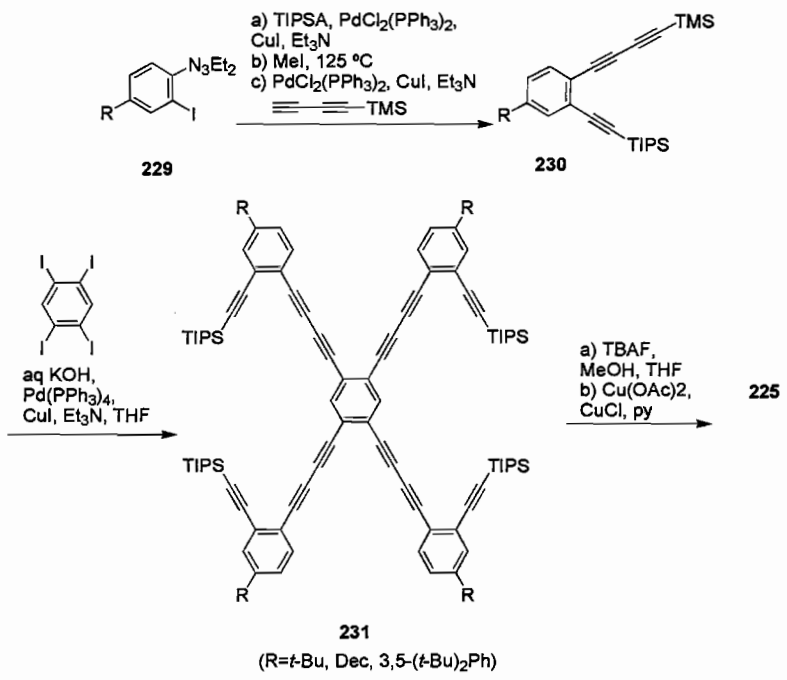

Although the size of graphdiyne subunits is limited by solubility constraints, major advances towards the synthesis of "supersize" substructures such as **232** and **233** have been made in the Haley laboratories.[79] Triazene **234**, which permits the introduction of three different alkynylated groups, is converted into the asymmetric coupling unit **235**

using standard techniques (Scheme 52). Protiodesilylation and Pd-mediated cross-coupling of the last compound with appropriately substituted benzene derivatives affords the corresponding macrocyclic precursors. Attempts to deprotect and cyclize those substrates containing decyl functionalization were unsuccessful, presumably because of the extreme insolubility of the resulting macrocycles. Whereas tetraether functionaliztion imparted greater solubility to the precursors, this route was abandoned because of the need for tedious and repeated chromatographic separations. Gratifyingly, the 3,5-di(*t*-butyl)phenyl unit imparts good solubilizing characteristics. For example, repetition of the chemistry is Scheme 51 yields the 3,5-di(*t*-butyl)phenyl version of **225** which is 10-15 times more soluble in halocarbon solvents than the corresponding decylated PDM. Use of a combination decyl tails and 3,5-(*t*-butyl)phenyl substituents furnishes tricyclic PAM **232** (R^1 = 3,5-*t*-Bu_2Ph, R^2 = Dec) in approximately 8% yield from **235**. Preparation the 3,5-di(*t*-butyl)phenyl-functionalized hexaPDM **233** is currently underway.

Using synthetic techniques similar to those described in Schemes 50 and 51, a wide variety of *ortho*-PDMs can be assembled quickly from common intermediates.[70] The key to these successes is efficient construction of the PDM carbon skeleton using in situ-generated phenylbutadiynes. The resultant polyyne can then be homocoupled under pseudo-high dilution conditions to afford a single product. Among the structures created are PDMs which are either unavailable by traditional routes (Figure 10, **236-238**) or obtainable only in low yield (**7**, **207**). Due to the nonplanarity and/or lower symmetry of the PDMs, inclusion of solubilizing groups is not needed.

SCHEME 52. Assembly of "Super-Sized" PDMs.

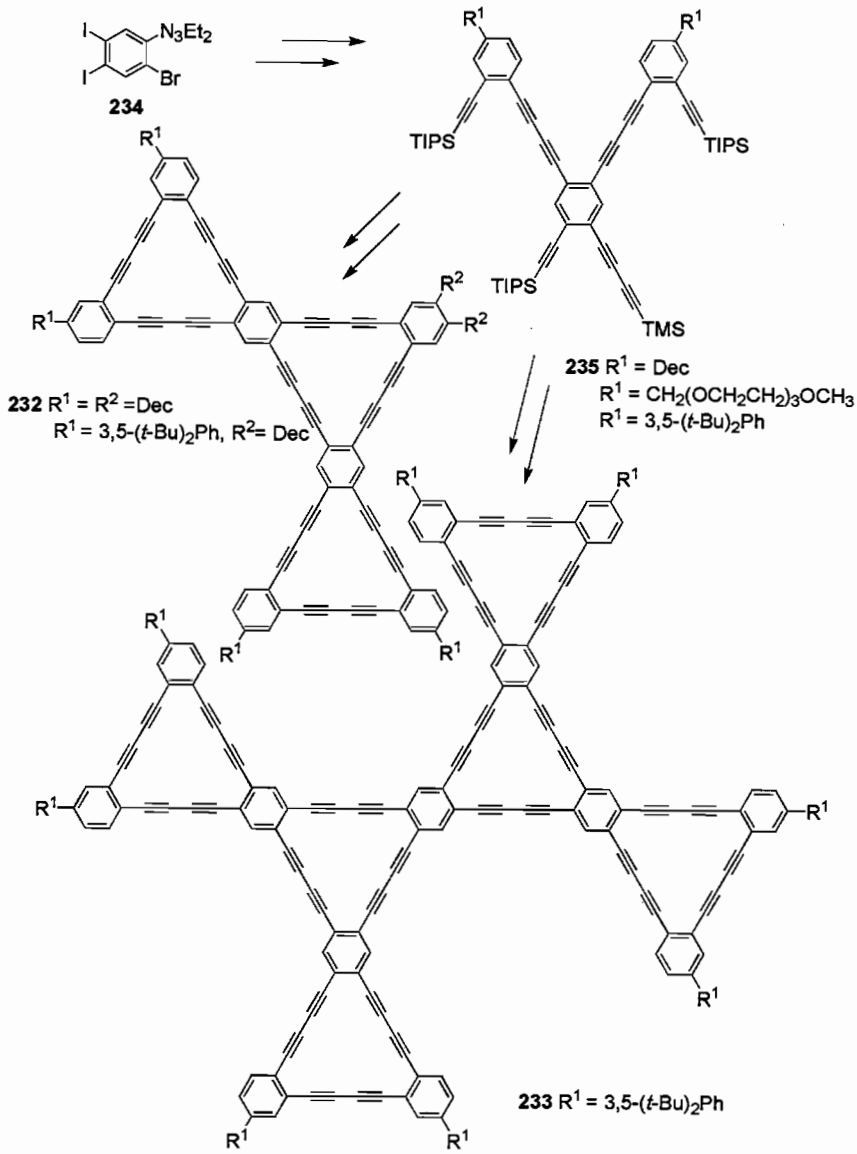

FIGURE 10. Compounds **236-238**.

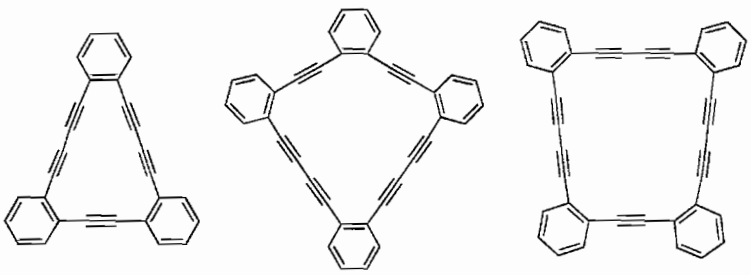

236 **237** **238**

The advent of rational synthetic techniques for PDM assembly (vide supra) now makes possible site-specific placement of functional groups on the arene rings and thus allows access to PDM topologies that would otherwise be difficult to prepare via the cyclooligomerization of functionalized 1,2-diethynylbenzenes. Structures **239-248** (Figure 11) illustrate some of the various symmetries prepared and substituents utilized to date.[80-82] A representative synthesis, that of the C_s-symmetric PDM **248**, is shown in Scheme 53. Electron-donor and -acceptor groups can be introduced at a number of positions during the initial stages of PDM assembly, either as triyne "legs" (e.g., **249-250**) or diiodoarene "heads" (e.g., **251**). In the case of **251**, selective cross-coupling reactions lead to the desired hexayne precursor **253**. Desilylation and homocoupling furnish **248** in a remarkable 52% overall yield for the four steps. More importantly, the molecule is the sole product of the cyclization reaction, making isolation/purification of the PDM trivial.

FIGURE 11. Compounds **239-247.**

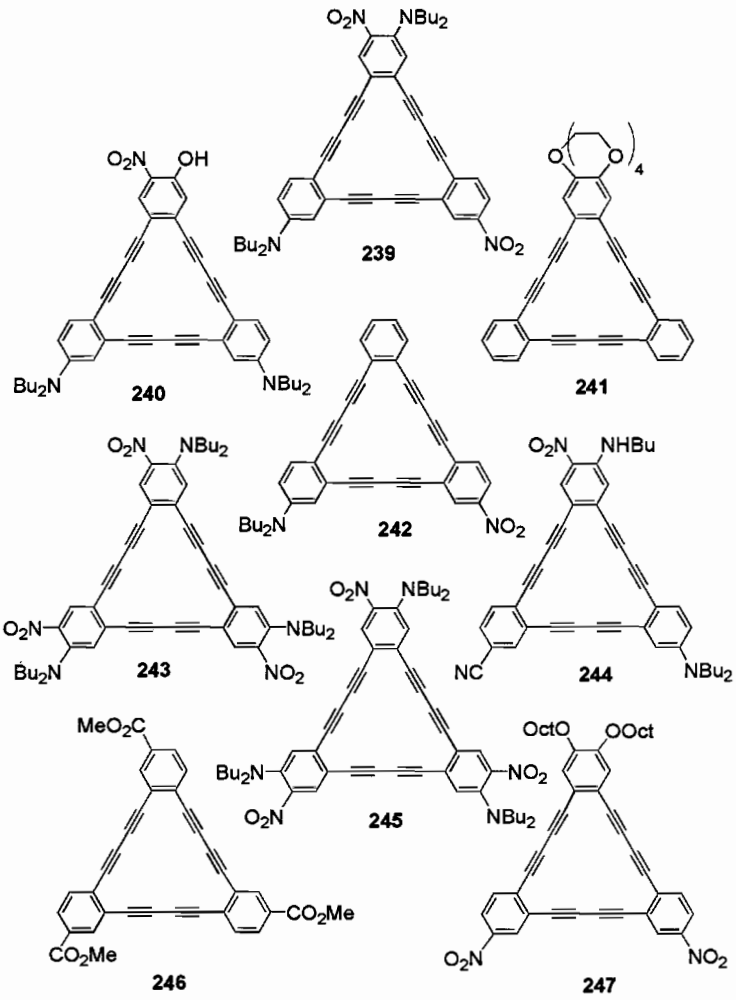

The extreme polarizability of the above donor/acceptor PDM derivatives results in novel UV-vis absorption properties. The electronic spectra display the four characteristic absorbances typical for [18]annulenes but are weakened, and the low energy bands are extended and broadened greatly. These shifts are maximized when opposing groups are positioned at each end of the macrocyclic framework, such as in **248**, and can be attributed to the increased polarization of the conjugated backbone.[80] The high polarization makes the donor/acceptor PDMs excellent candidates for nonlinear optical

materials. By strategically placing functional groups on the periphery of the macrocycle the physical properties of the material can be tuned. Furthermore, since these systems are also locked into planarity, the NLO efficiency is increased further due to an enhancement of π-conjugation and communication between chromophores. The β values for PDMs **1**, **239**, **242**, **243**, **245**, and **248** have been measured using the hyper Raleigh scattering (HRS) technique and were found to be 2-3 times greater than that of the standard 4-dimethylamino-4'-nitrostilbene (DANS) reference chromophore.[81]

SCHEME 53. Synthesis of PDM **248**.

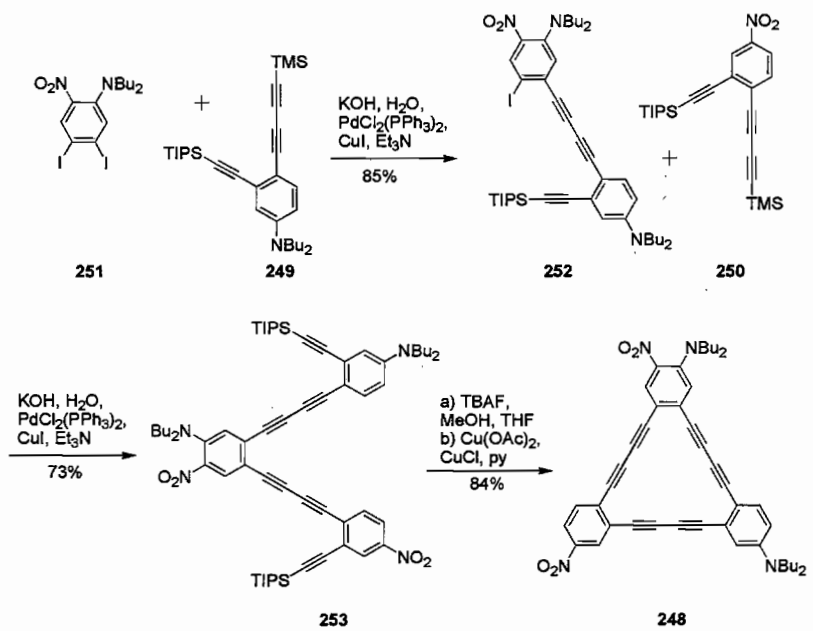

4.2 Meta PDMs

The first examples of PDMs composed of meta linkages were reported by Tobe and coworkers in 1996.[83] The diacetylenic homologues of Moore's meta-PAM derivatives, the PDMs were also expected to self-associate in solution in a manner

analogous to Moore's meta-PAMs;[47] consequently, their solution-phase self association properties were studied. The attractive force at work, π-π stacking of aromatic moieties, plays an important role in supramolecular chemistry. For example, the existence of stable DNA double helices is dependant upon the weak associative forces between vertically stacked adjacent base pairs while the packing orientation of aromatic molecules in the solid state is determined, also, by π-stacking. Consequently, understanding the structural characteristics that contribute to the ability of a molecule to engage in this type of behavior has important real-world implications.

With this goal in mind, the Tobe group prepared meta-PDMs **254-256** (Figure 12) using three different ester linkages (Scheme 54).[83] Sequential Sonogashira reactions with benzoate ester **257** affords differentially protected monomer **258**. Treatment of **258** with LiOH removes the TMS group and hydrolyzes the ester. The resultant acid is re-esterified with DCC and the appropriated alcohol, yielding **259**, which is then oxidatively dimerized to furnish dimer **260**. Initial attempts on PDM formation focused on intermolecular oxidative coupling of desilylated dimer **261b**; however, cyclization with $Cu(OAc)_2$ provided very low yields of **254b** (10%) and **256b** (2%) and none of **255b** [83a]. It was thus necessary to prepare **254-256** via stepwise assembly of the open-chain oligomers and then intramolecular cyclization. Partial deprotection of **260** gave **262** as the major product along with **261** and unreacted starting material. Homocoupling of **262** furnished tetramer **263**, which was then deprotected and cyclized to give **254a/c** and **256a/c** in considerably higher combined yield (ca. 50%) when compared to the intermolecular method (12%). Conversion of **262** to bromoalkyne **264** and cross-

coupling to **261** provided open-chain hexamer **265**. Deprotection and cyclization as before gave **255a-c**.

SCHEME 54. Synthesis of PDMs **254-256**.

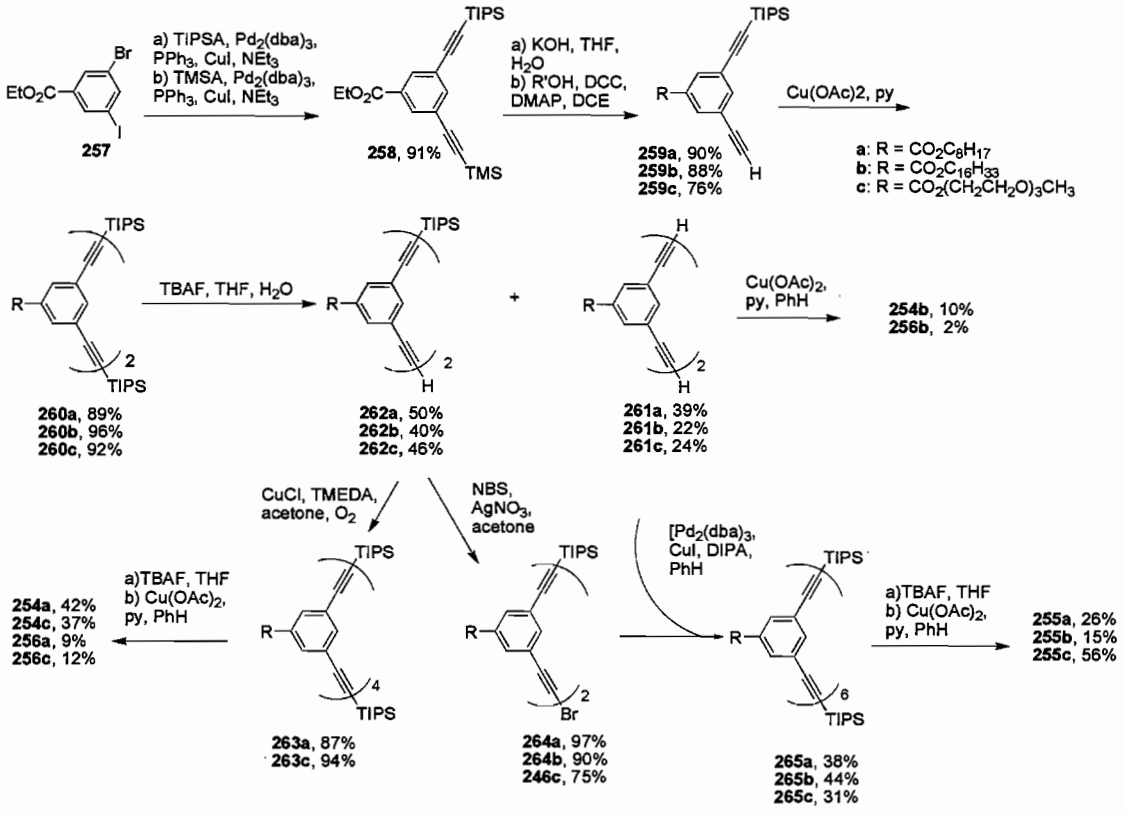

The self-aggregation behavior of the PDMs was investigated though ^{1}H NMR spectroscopy and by vapor pressure osmometry (VPO). In $CDCl_3$ solution at 303K the binding constants, K_{assoc}, for **254a-c**, **255c**, and **256a** were found to range from approximately 20-43 M^{-1} while K_{assoc} of the hexamers **255a** and **255b** were calculated as 173 and 150 M^{-1}, respectively. In more polar solvents, the association of meta-PDMs is enhanced due to solvophobic effects. In fact, evidence suggests that large, nanotubular aggregates of PDMs **254c** and **255c** are formed. Surprisingly, the meta PDMs aggregate

more strongly in aromatic solvents than in $CDCl_3$, though the reason for this is not fully understood. Overall, the study concludes that PDMs promote π–π stacking interactions effectively due to the ester's electron withdrawing nature. Furthermore, self-association properties are controlled by the size of the PDM and the cyclic hexamers with their rigid, planar backbones associate to greatest extent. The PDMs in fact aggregate more readily than the corresponding PAMs, which is attributed to withdrawal of electron density from the aromatic rings by the butadiyne linkages, thus facilitating π-π stacking interactions.

FIGURE 12. Compounds **254-256**.

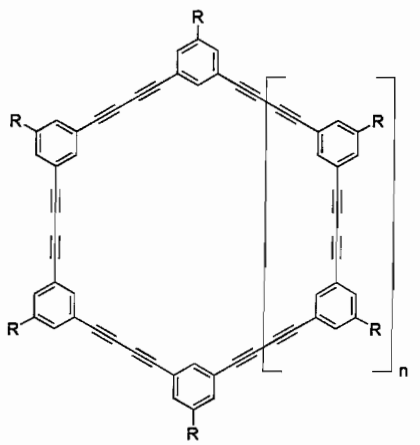

254 n = 0 **a**: R = $CO_2C_8H_{17}$
255 n = 1 **b**: R = $CO_2C_{16}H_{33}$
256 n = 2 **c**: R = $CO_2(CH_2CH_2O)_3CH_3$

PDMs **266** and **267**, where *t*-butyl groups have replaced the ester moieties, have also been prepared by Tobe's group (Scheme 55).[83a,84] The two macrocycles are synthesized in an analogous manner to those in Scheme 54. As before, intermolecular cyclization of the dimer **268** affords the PDMs in much lower combined yield than intramolecular cyclization of tetramer **269**. Both the Hay and Breslow cyclization

conditions were also attempted; however, PDM yields were lower with the former method and no PDMs were isolated via the latter procedure. Unlike the ester-substituted systems, PDMs **266** and **267** exhibit no self-association behavior in solution.

SCHEME 55. Synthesis of PDMs **266-267**.

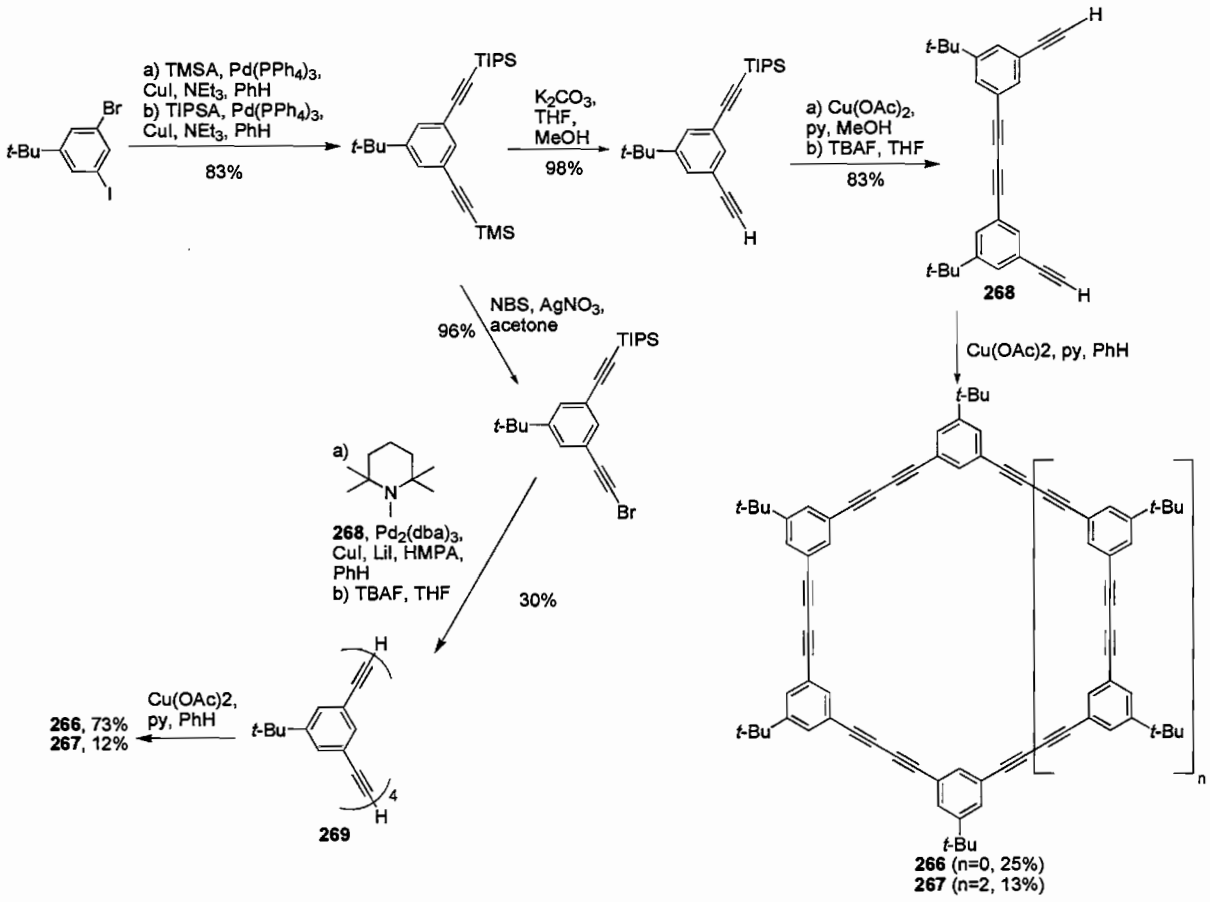

In 1998 Tobe et al. reported the synthesis of **270** which contained interior binding cyano groups.[85] PDM **270** (Figure 13) was constructed using the same stepwise methodology depicted in Scheme 54, with the sole change being inclusion of a cyano group on the benzoate ester. Unlike **255b**, **270** does not aggregate at all. The lack of self association of the latter compound is most likely due to the electrostatic repulsion of the

cyano groups. Surprisingly, upon mixing **255b** and **270** in $CDCl_3$, aggregation does indeed occur but is considerably more complex as **255b** interacts with **270** to form a heterodimer as well as higher oligomeric aggregates. Thus, while the cyano groups of **270** inhibit self-association, the electron withdrawing groups enhance attractive π-π stacking interactions with **255b**. In addition to this unusual aggregation behavior, PDM **270** forms 1:1 and 2:1 host:guest complexes with both tropylium and guanidinium cations.

FIGURE 13. Compound **270**.

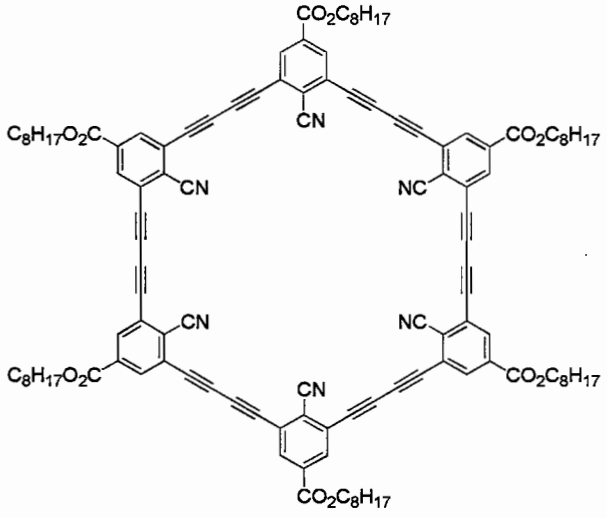

270

Mayor and Lehn created a series of phenylthio-linked tetrameric (**271**), hexameric (**272**), octameric (**273**), and decameric (**274**) meta-PDMs (Figure 14) in order to observe the electrochemical properties of the PDM-based "molecular batteries" (Scheme 56).[86] Reduction of the cyano moieties of isophthalonitrile **275** and then four-fold nucleophilic aromatic substitution with *p-tert*-butylthiophenyl anion furnishes sulfide **276**. Corey-

Fuchs alkynylation of **276** and anion quench with TBDMSCl gives monomer **277**. Partial deprotection with TBAF followed by oxidative homocoupling provides dimer **278**, which upon full deprotection and Cu-mediated cyclization affords PDMs **271-274** in 41% combined yield. Somewhat surprising, the intramolecular cyclization of desilylated **279**, prepared again by partial deprotection followed by oxidative homocoupling, gives tetrameric PDM **271** in a low 14% yield.

FIGURE 14. Compound **271-274**.

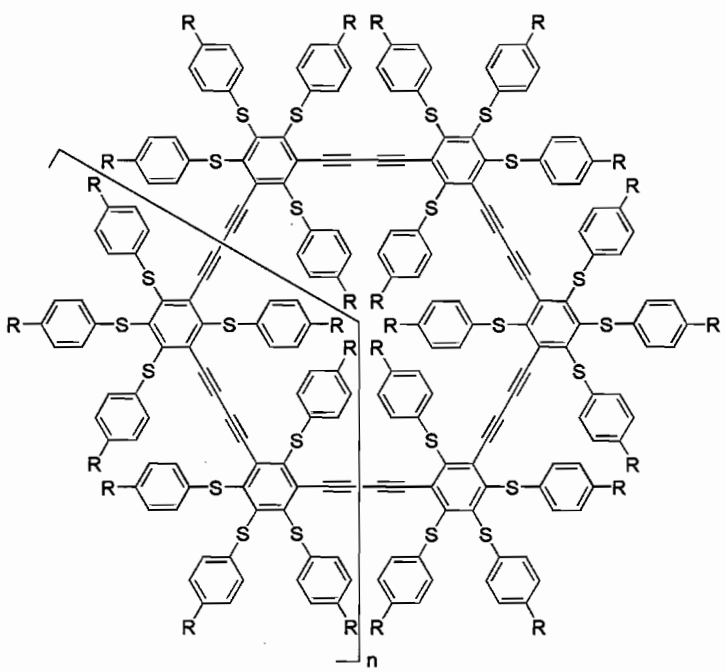

Cyclic voltammetry measurements of the sulfur-containing PDMs show no oxidation peaks up to –1.3V; however, several reversible reduction waves are observed for **271** (–1.07, –1.19, –1.44 V) and **272** (–1.09, –1.29, –1.40 V) while **273** displays one broad peak (–1.09 V) and a large shoulder toward more negative values, which

presumably arises from unresolved reduction waves. The multiple reversible reductions of these compounds allude to the ability of these macrocycles to act as "electron reservoirs" which makes them potential candidates for "molecular batteries".

SCHEME 56. Synthesis of PDMs **271-274**.

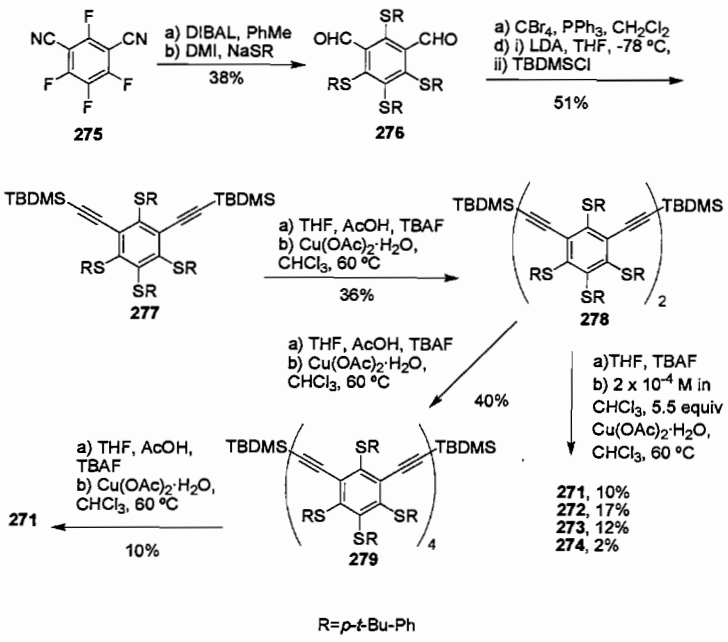

4.3 Para PDMs

The belt-shaped macrocycle **280** is the sole *para*-linked PDM reported in the literature to date and is available in six steps from substrate **174** (Scheme 57).[87] Conversion of **174** into the differently protected diacetylene **281** is accomplished using standard Pd-catalyzed cross-coupling techniques. In situ deprotection of the TMS moiety and successive homocoupling of the free alkyne affords tetrayne **282** in 85% yield. Treatment of the tetrayne with TBAF then $Cu(OAc)_2$/CuCl affords hexamer **283** which, upon acidic hydrolysis/silylation and subsequent photoirradiation, furnishes **280** as an air-

sensitive solid that decomposes gradually within several days under ambient conditions. Molecular modeling studies suggest **280** adopts a cylindrical conformation and the acetylene moieties deviate from linearity by 8.8-9.2°. Moreover, rotation of the phenyl rings at 25 °C is rapid as evidenced by the proton and carbon NMR spectra which display only four and nine lines, respectively.

SCHEME 57. Synthesis of PDM **280**.

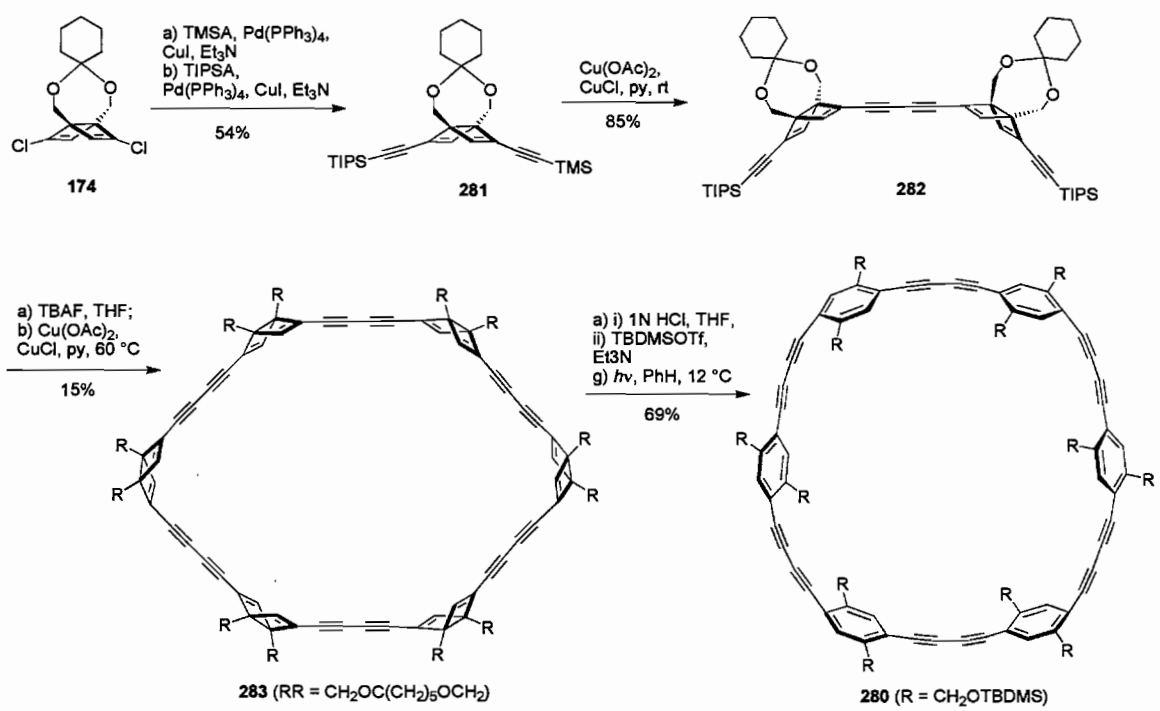

4.4 Mixed PDMs

The shape-persistent, structurally well-defined nature of macrocycles based on phenyl and acetylene building blocks makes them ideal candidates for binding guests within their cavities. Although this review illustrates a few salient examples of large,

shape-persistent macrocycles and their host-guest chemistry, the reader is referred other reviews for more detailed discussions of this topic.[88]

In 1995 Höger and Enkelmann constructed the *meta/para* PAM/PDM hybrid **284** with hydrophobic/hydrophilic functionality specifically for use in host-guest chemistry (Scheme 58).[89] The macrocycle is assembled in a straightforward manner from arene **285** via standard alkyne cross-coupling/deprotection chemistries. Cyclodimerization of **286** and hydrolysis of the THP ethers gives **284** in 45% yield for the last two steps.

SCHEME 58. Synthesis of PDM **284**.

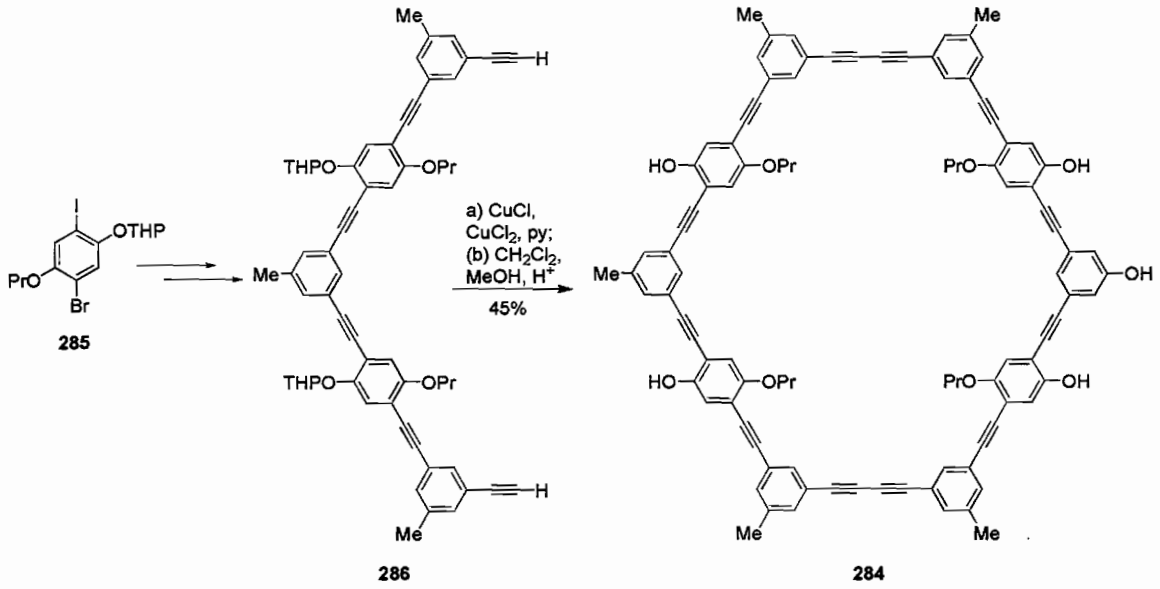

X-ray structure analysis of **284** shows the macrocycle is nonplanar with a torsion angle about the diyne units of 6.7°. The interior cavity is approximately 2.0 × 2.4 nm and is occupied by the greasy propoxy groups. Furthermore, the macrocycle cocrystallizes with four molecules of pyridine which hydrogen bond to the phenolic hydroxy groups on the exterior of the ring. Solution studies of **284** (^{1}H NMR) suggest the compound

exhibits dynamic behavior and interconverts rapidly between several different conformations; however, the authors were unable to ascertain whether the hydroxyl groups were inside or outside the macrocycle. The use of the guest molecules of a suitable size, for example, tetraamine **287**, results in reversal of the binding topology in **284**.[90] In fact, guest **287** fits extremely well in the cavity of the PDM so that hydrogen bonding now occurs exclusively in the interior of the macrocycle (K_{assoc}= 160 M^{-1}).

The cyclization of **286** was found to be the lowest yielding step in the synthesis of the macrocyclic amphiphile **284**. Höger and coworkers have investigated two strategies to overcome this problem. The simpler of the two was a study of the effect of temperature and structure on the cyclooligomerization reaction.[91] Temperatures of ca. 60 °C were found to be optimum for product formation when using $CuCl/CuCl_2$ in pyridine to promote the cyclization. Structure of the cyclization precursors was found to be equally important. The presence of groups which could possibly be templated by the Cu salts markedly increased yields.

A more ingenious method for cyclooligomerization utilized covalently bound templates to direct the cyclization reaction.[92] Condensation of **288** with 1,3,5-benzenetricarboxylic acid gave the templated ester **289** (Scheme 58). With the interior ester functionality binding the tetrayne moieties together, the terminal alkynes were then homocoupled and the template subsequently hydrolyzed to furnish PDM **290** in an excellent 89% yield. This is a significant improvement compared to the non-templated pathway which affords **290** in ca. 20% yield along with a number of inseparable cyclooligomeric byproducts. Use of a longer hydroxyundecyl tether in place of the 3-

hydroxypropyl group furnishes the target macrocycle in 84% isolated yield which suggests that as long as the geometry is preorganized, proximal spatial constraint is not necessary for the high-yield cyclization to occur.[92a]

SCHEME 59. Synthesis of PDM **290**.

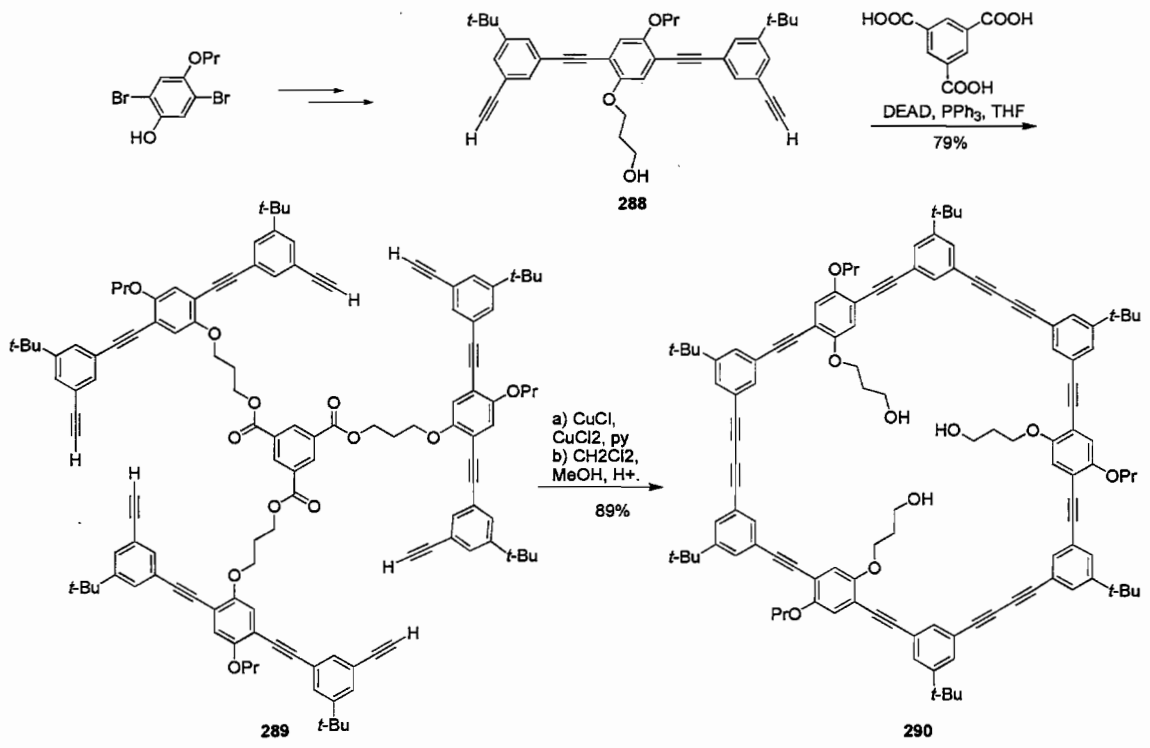

The use of "outside" templates affords PDMs in comparable impressive yields.[92b] For example, the Cu-mediated ring closure of substrate **291** furnishes PDM **292** in impressive 86% yield (Scheme 60). Subsequent experiments show that in the "outside" case tether length plays an important role in the product yield. Assuming that cyclization is a stepwise process, use of a short tether should promote the first dimerization but sterically prohibit the second. Indeed, shortening the tether of the acyclic precursor by 10

carbon atoms reduces the yield of PDM by 15%. Overall, the utilization of templates proves to be a very powerful method in PAM/PDM synthesis and is only limited by template introduction/removal. For further discussion of larger, shape persistent, mixed PDMs, please refer to the following reference by Höger.[88]

SCHEME 60. Synthesis of PDM **292**.

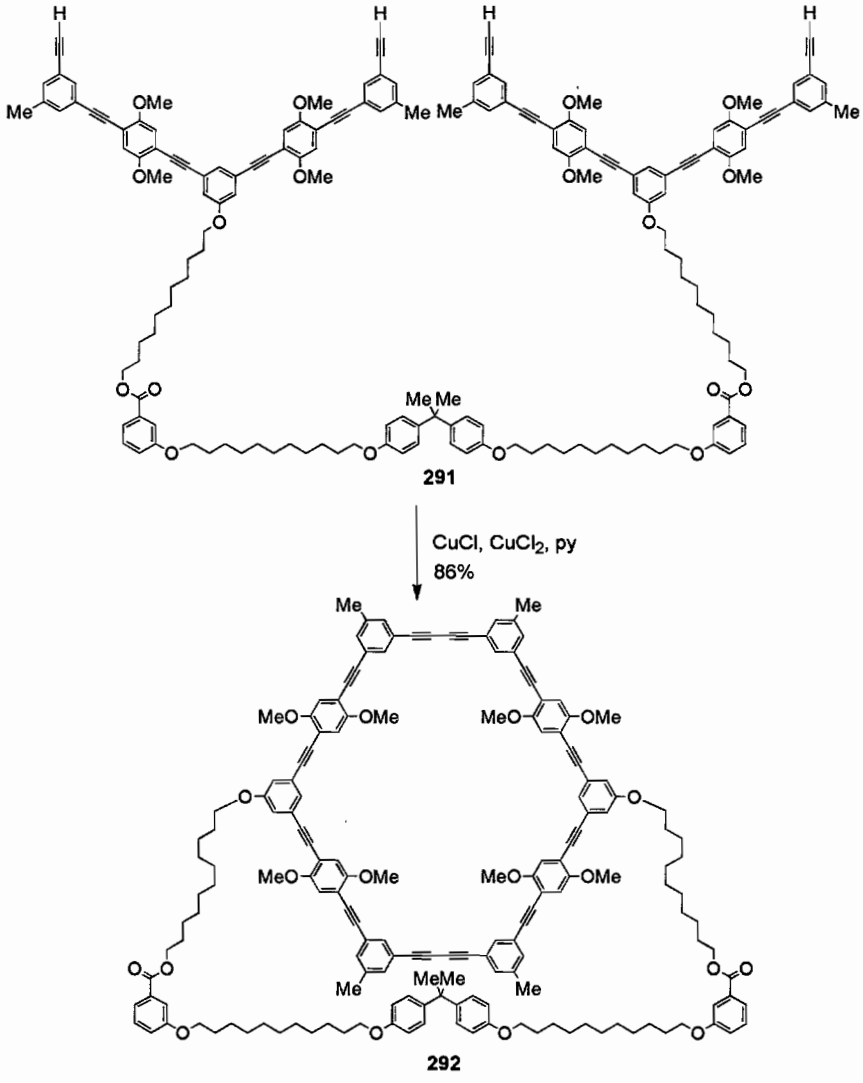

SCHEME 61. Synthesis of PDMs **295** and **296**.

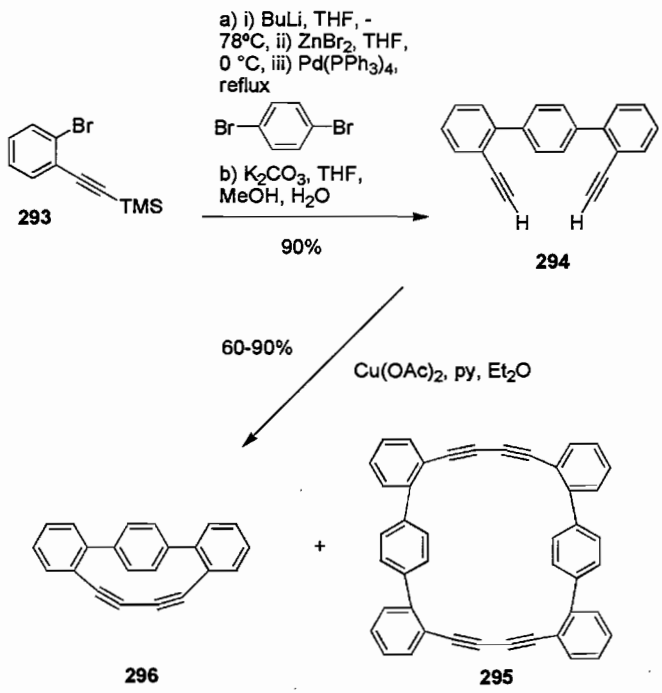

A number of considerably more simple mixed PDM derivatives have been prepared by Fallis and coworkers. Although originally sought as collapsible, helical structures, the Canadian team has made some interesting discoveries during their PDM studies. For example, cyclization of **293**, prepared from **294** by successive Suzuki coupling with 1,4-dibromobenzene and desilylation, was hoped to generate intermolecular dimer **295** but instead furnished intramolecular product **296** in 90% yield (Scheme 61).[93] If the Eglinton coupling reaction was done at room temperature for 3 days instead of 90 °C and 3 hours, **295** could be isolated in ca. 20-25% yield along with ca. 45-55% of **296**. An X-ray crystal structure of a derivative of **296** shows that the carbon backbone is highly strained, with the triple bonds distorted from linearity by about 16°. The terphenyl unit is also perturbed, deviating from planarity by ca. 18°. An X-ray

structure of **295** shows that the molecule twists and collapses to give a saddle-like structure, as similarly observed in other PAMs and PDMs with four ortho-benzo-fused vertices (e.g., **10**, **23**, **207**, **237**).

Inserting two acetylene units into the terphenyl moiety of **294** results in a different outcome of the cyclodimerization reaction (Scheme 62).[94] Unlike **294**, the terminal acetylenes in **297** are too far apart to undergo intramolecular homocoupling and thus dimer **298** is isolated as the sole product. As with **295**, PDM **298** adopts a twisted helical geometry.

SCHEME 62. Synthesis of PDM **298**.

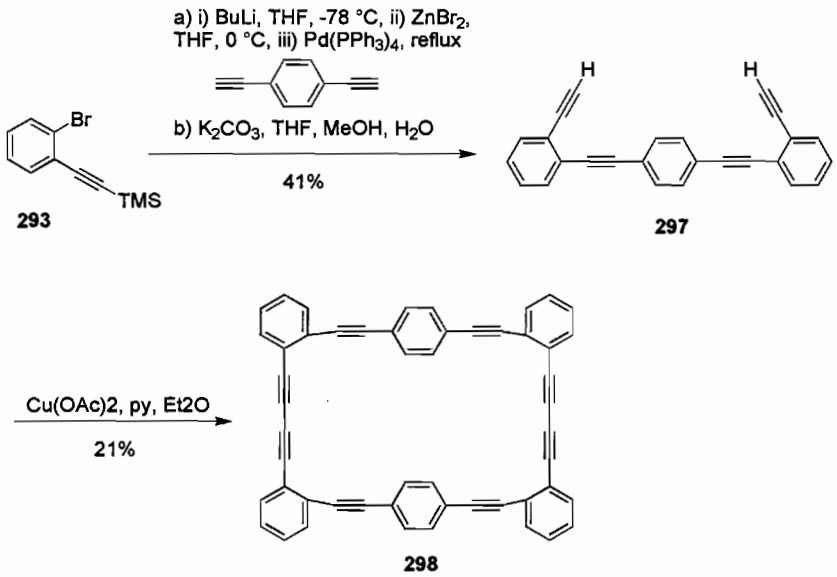

Modification of the PDM cores of **295** and **298** with long-chain groups was hoped to produce liquid crystalline materials.[94] Compounds **299-301** (Figure 15) were prepared via chemistry analogous to that in Scheme 61 and 62. As before, **299** and **300** were both produced by the Cu-mediated homocoupling whereas **301** was the sole cyclization product. The formation of **300** and **301** was more complex as both compounds were

produced as a racemic mixture of two different regioisomers. Of the whole series of PDMs, only one regioisomer of **301b** exhibited potential evidence of liquid crystalline behavior. Definitive proof will require the synthesis an enantiomerically pure product, which is not possible via the cyclooligomerization route.

FIGURE 15. Compounds **299-301**.

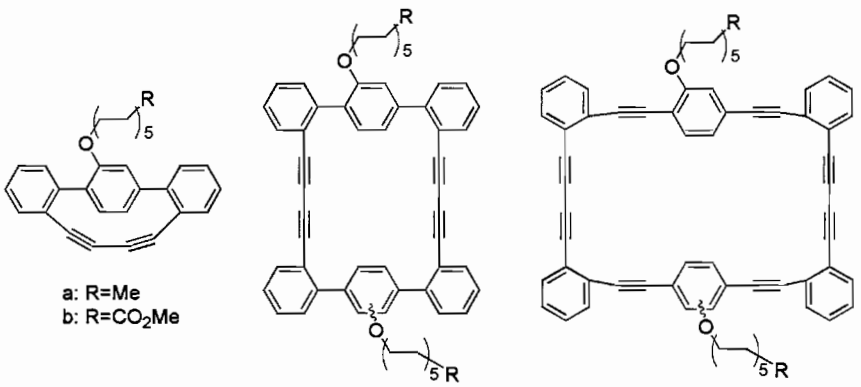

Expanding on their previous work, the Fallis group constructed PDM **302** that contains *ortho* and *meta* linkages in the 60 carbon core.[95] Compound **302** was prepared in 15% yield via in situ desilylation/dimerization of **303**, which in turn was obtained though a modified Cadiot-Chodkiewicz reaction of 1,3-bis(bromoethynyl)benzene with terminal acetylene **28** (Scheme 63). The flat cyclic representation of PDM **302** does not accurately depict its actual conformation. Computer modeling indicates that two different conformers are possible, the 'bowtie' **302a** and 'butterfly' **302b** macrocycles, respectively. The two isomers of **302** are produced by the cyclodimerization reaction in a 3:1 ratio and are separable by semipreparative HPLC. The major isomer, which displays higher symmetry in the NMR data over the minor isomer, is consistent with 'bowtie' **302a**. Attempts to interconvert the two atropisomers at 100 °C were unsuccessful, which

suggests the compounds are conformationally and configurationally stable and must have a high barrier to interconversion.

SCHEME 63. Synthesis of PDM **302**.

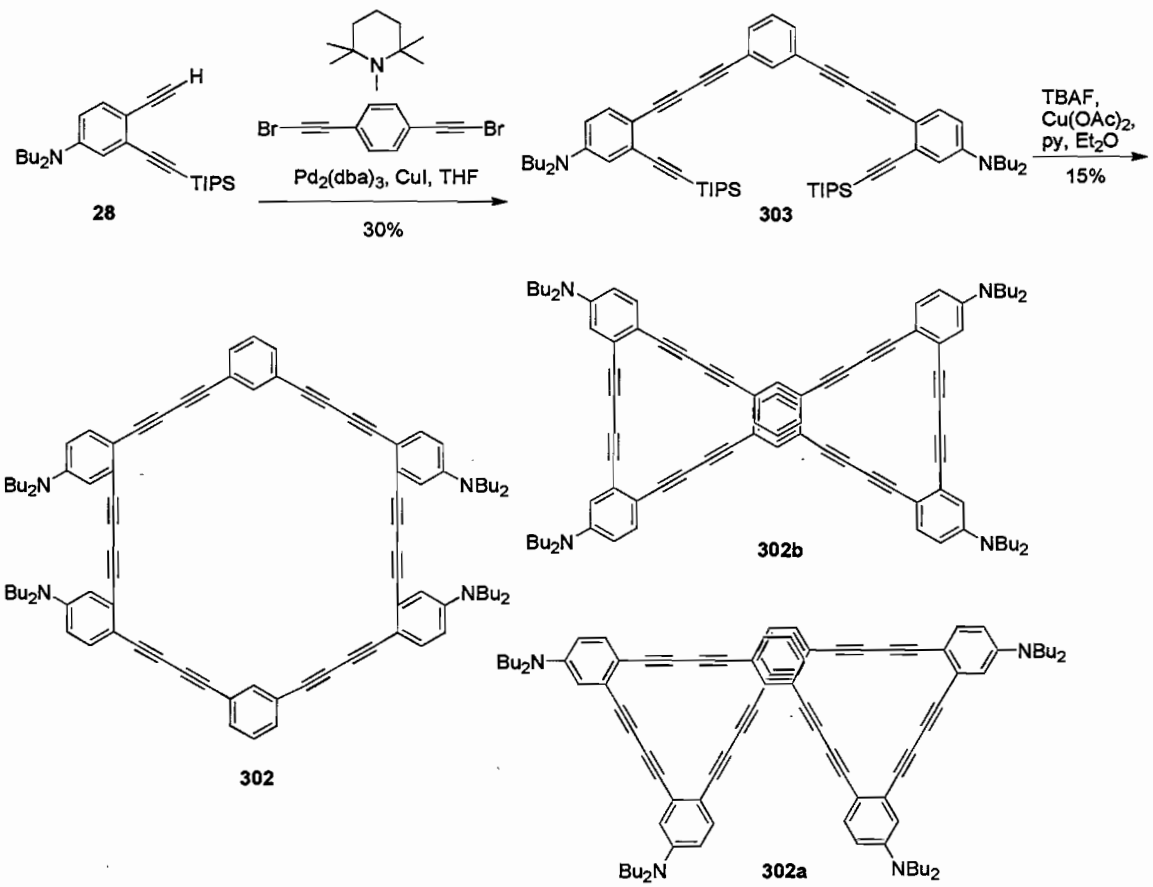

Tsuji and coworkers have reported the synthesis of the *meta/para* linked PDM **304** from photoirradiation of the dewar benzene **305** (Scheme 64).[61] Compound **305** was prepared in five steps from readily available diyne **306**. An X-ray structure of **304** shows the molecule is nearly planar and two of the silane moieties reside within the sizeable molecular cavity (7.3 × 11.5 Å). The acetylene moieties deviate by 0.1–11.3° from linearity. The proton NMR spectrum reveals the methylene protons are enantiotropic

which suggests, in solution, that the phenyl rings must rotate rapidly between rotomers **304a** and **304b**.

SCHEME 64. Synthesis of PDM **304**.

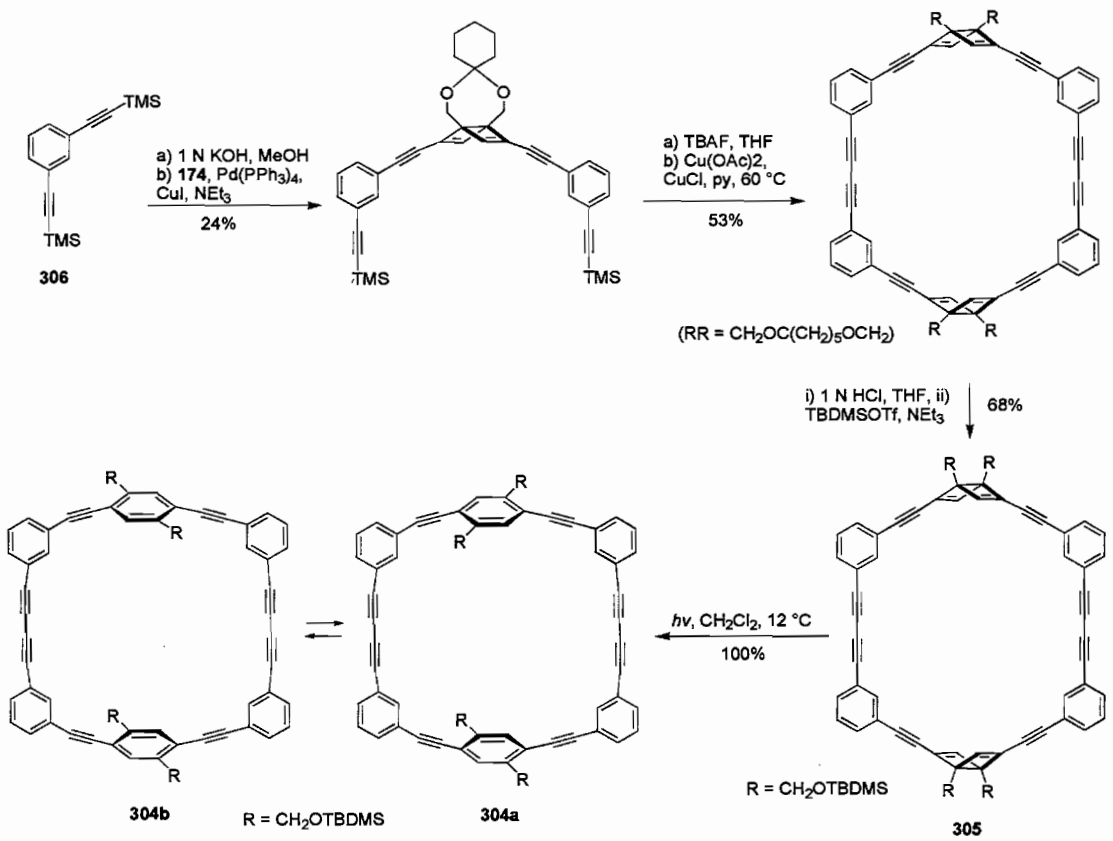

The assembly of two unusual PDM-fused PDMs is depicted in Scheme 65.[96] Both **307** and **308** were prepared from iodoarene **309**, which in turn was synthesized from the corresponding aniline in four steps using the chemistry in Scheme 23. Installation of the terminal alkyne by Stille reaction, followed by either cross-coupling or homocoupling, gave polyynes **310** and **311**, respectively. Desilylation of **310** and Pd-catalyzed homocoupling furnished PDM **307**, the first member of a previously

unattainable class of π-extended fenestranes. The molecule exhibits remarkable stability and solubility, the latter due to a slight bowl shape (as predicted by calculations). Alternatively, desilylation of **311** and Cu-mediated homocoupling furnished PDM **308**. Interestingly, intramolecular homocoupling orients the molecule in such a way that intermolecular homocoupling now occurs. Whereas the protons on the outer phenyls of **307** show a slight shielding (δ 7.06, 7.03) due to the bent alkynes, the analogous protons on **308** exhibit a much more significant upfield shift (δ 6.94, 6.74) due to the bent alkynes as well as the anti-aromatic ring current of the two fused [12]annulenes.

Attempts to prepare three-dimensional PDM structures have met with varied success. As illustrated in Schemes 61-63, the distance between the terminal acetylenes in the homocoupling reaction can be used as a qualitative measure as to whether the reaction yields intra- or intermolecularly coupled products, or both. For example, the distance between the terminal acetylenes in **312** is less than 4.3 Å and thus homocoupling yields highly strained **313** instead of **314** (Scheme 66).[97]

SCHEME 65. Synthesis of PDMs **307** and **308**.

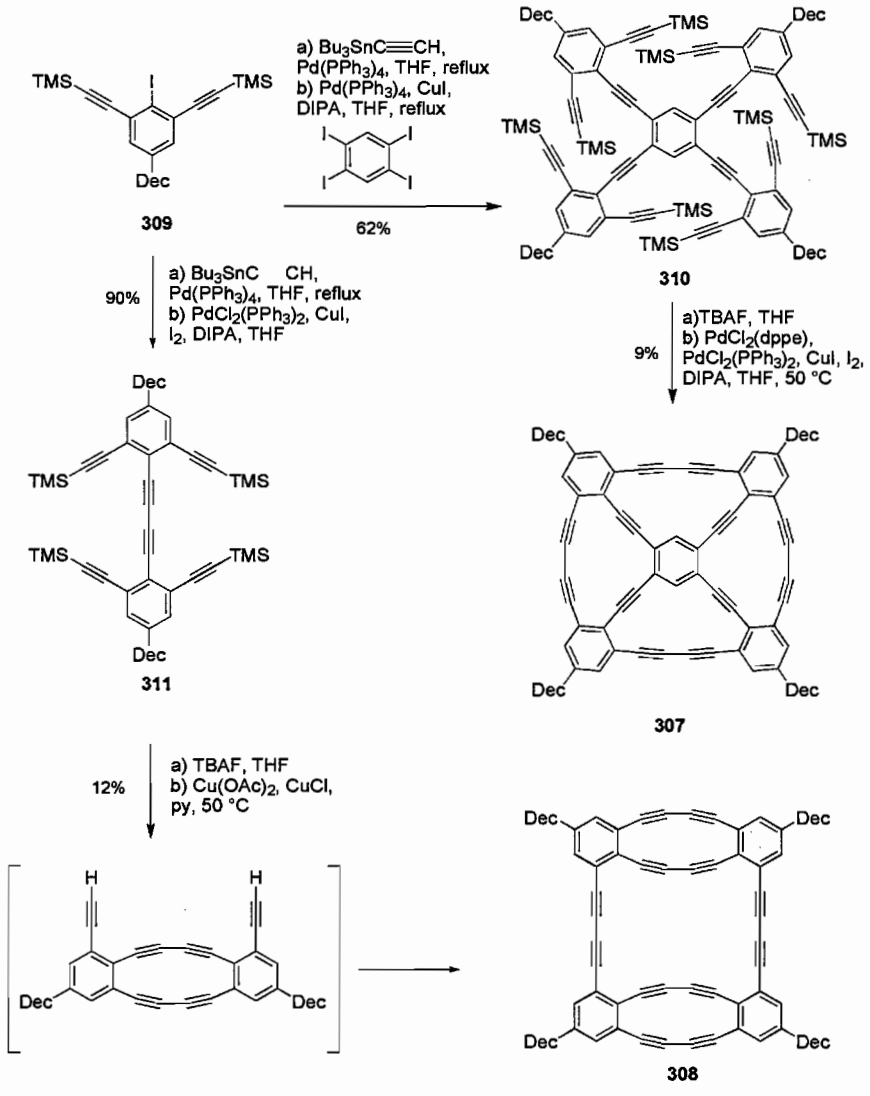

Expansion of the meta-terphenyl core with acetylene linkages, while increasing the spacing between the terminal acetylenes to 5.1 Å, is still insufficient for intermolecular reactivity. Tobe et al. discovered that tetrayne **315**, a simplified model for a 3D C_{48} precursor, furnishes intramolecular PDM **316**, analogous to reactivity shown by the C_{48} precursor (Scheme 67).[98]

SCHEME 66. Synthesis of PDM **313**.

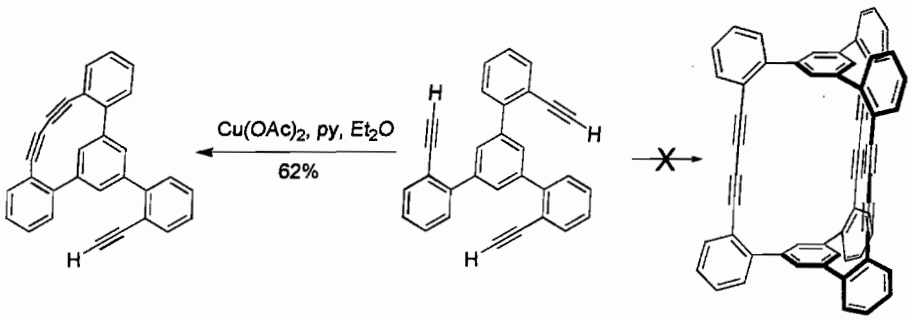

The next higher homologue, where diyne linkages connect the benzenes, was reported by Rubin in 1997.[99] Once desilylated, the terminal acetylene carbons in **317** are over 10 Å apart and thus only intermolecular PDM **318** was formed in the homocoupling reaction (Scheme 68). It was hoped that the molecule would "zip-up" to afford fullerene derivatives; however, both **318** and its ethylenic anaologue (benzene replaced by ethene)[100] possessed little propensity to loose hydrogen and, as such, fullerenes were not obtained.

SCHEME 67. Synthesis of PDM **316**.

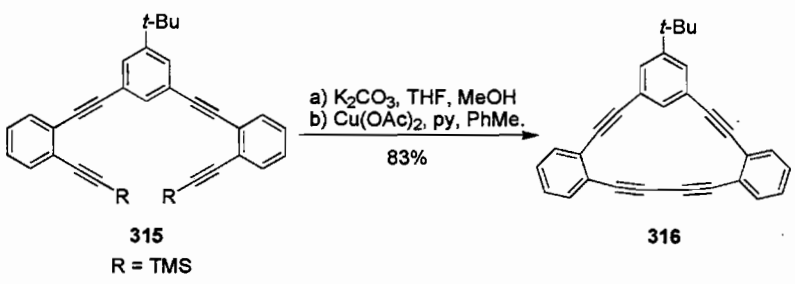

SCHEME 68. Synthesis of PDM **318**.

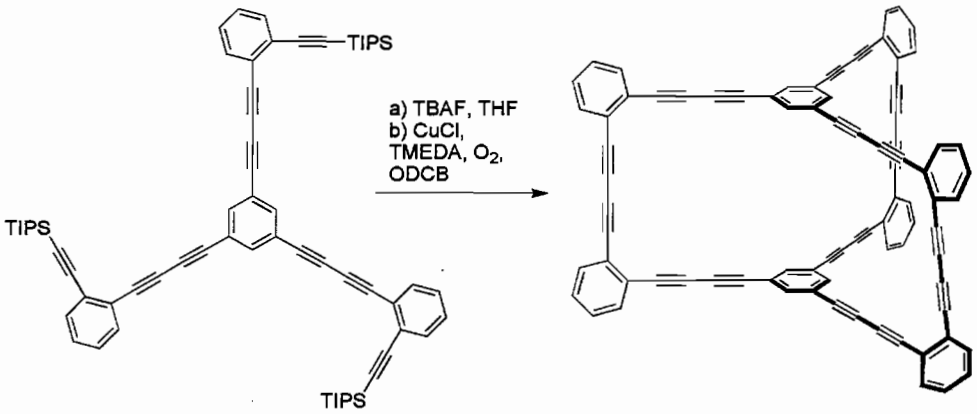

317 **318**

5. Phenyltriacetylene Macrocycles

Very recently, the Tobe group synthesized the simplest phenyltriacetylene macrocycles, PTMs **319** and **320** (Scheme 69).[101] The two macrocycles were formed by loss of indan upon irradiation of precursors **321** and **322**, respectively, at 254 nm. The precursors were in turn generated from dichloride **323** by standard procedures coupling/cyclization procedures. Highly reactive PTM **319** could be generated and trapped in solution by Diels-Alder addition with furan in 20% yield. Alternatively, **319** could be generated and characterized in an Ar matrix at 20 K by FTIR and UV-vis spectra. PTM **320** proved to be more stable and was characterized by ^{1}H NMR spectroscopy as a mixture with indan and **322** in deuterated THF.

SCHEME 69. Synthesis of PTMs **319** and **320**.

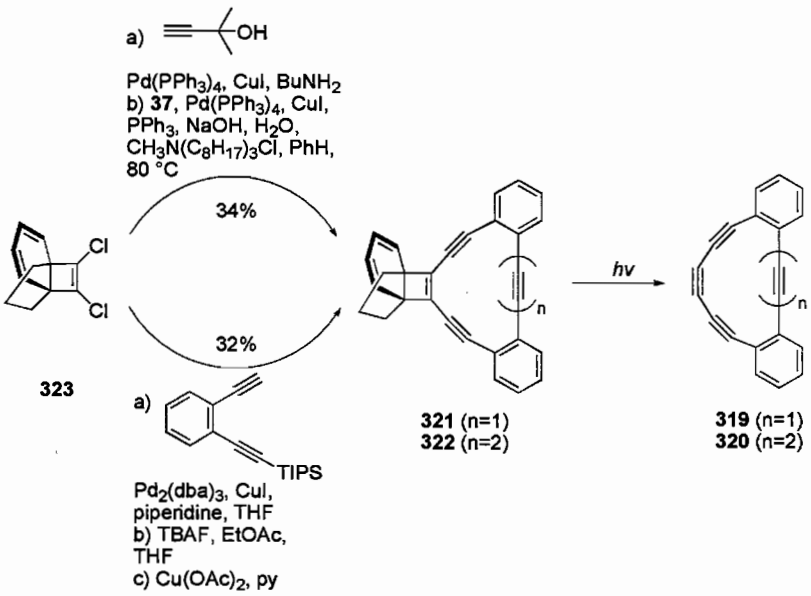

PTMs were initially reported by the Haley group in 1998.[70b,102] Because the assembly of such macrocycles was not feasible though cyclooligomerization chemistry, **324** was prepared via intramolecular acetylenic homocoupling (Scheme 70). The requisite building block **325** was prepared from **326** by selective desilylation and then a modified Cadiot-Chodkiewicz coupling with TMSC≡CC≡CBr. In situ generation of the highly unstable phenylhexatriyne under Sonogashira conditions followed by deprotection and Cu-mediated cyclization gave **324**. PTM **327** was also constructed using similar synthetic methods.

SCHEME 70. Synthesis of PTM **324**.

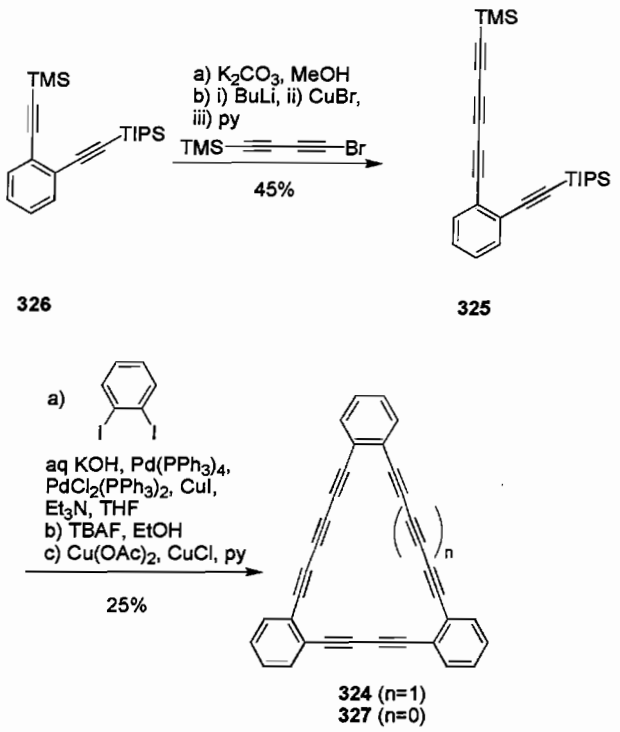

6. Phenyltetraacetylene Macrocycles

The first tetrayne-linked PTMs (**328**/**329**) were prepared in 1997 (Scheme 71).[103] Key to this success was in situ generation of the phenylbutadiynes under Eglinton homocoupling conditions, yielding **330** and **331**. Subsequent removal of the TIPS groups and cyclization under pseudo-high dilution conditions furnished PTMs **328** and **329** in moderate overall yield. No intramolecular homocoupling was observed as the terminal acetylenes are nearly 11 Å apart.

SCHEME 71. Synthesis of PTMs **328** and **329**.

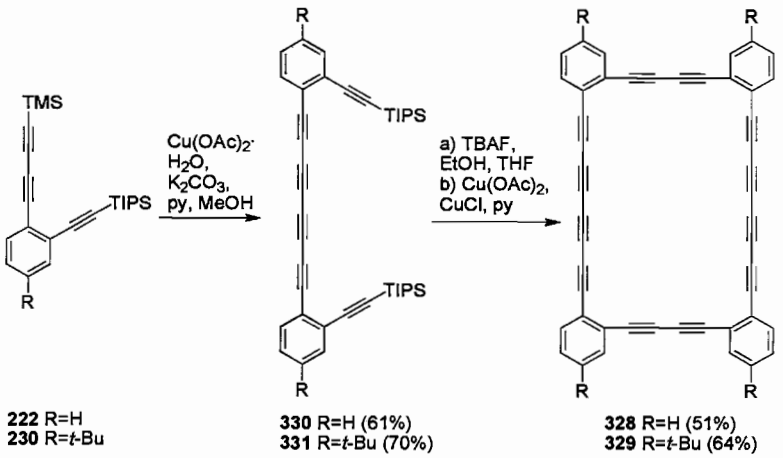

The Fallis group prepared dimeric PTM **332** as well as strained tetrayne **333** (Scheme 72).[104] Sonogashira cross-coupling of **334** with 1,4-diethynylbenzene gave hexayne **335**. Once again, the distance between the terminal acetylenes was an important factor, which in the case of **335** is ca. 7.2Å. In situ phenylbutadiyne generation with TBAF under Eglinton homocoupling conditions afforded only **333** (46%) at low concentrations, whereas higher concentrations gave **332** (5%) and **333** (26%).

SCHEME 72. Synthesis of PTMs **332** and **333**.

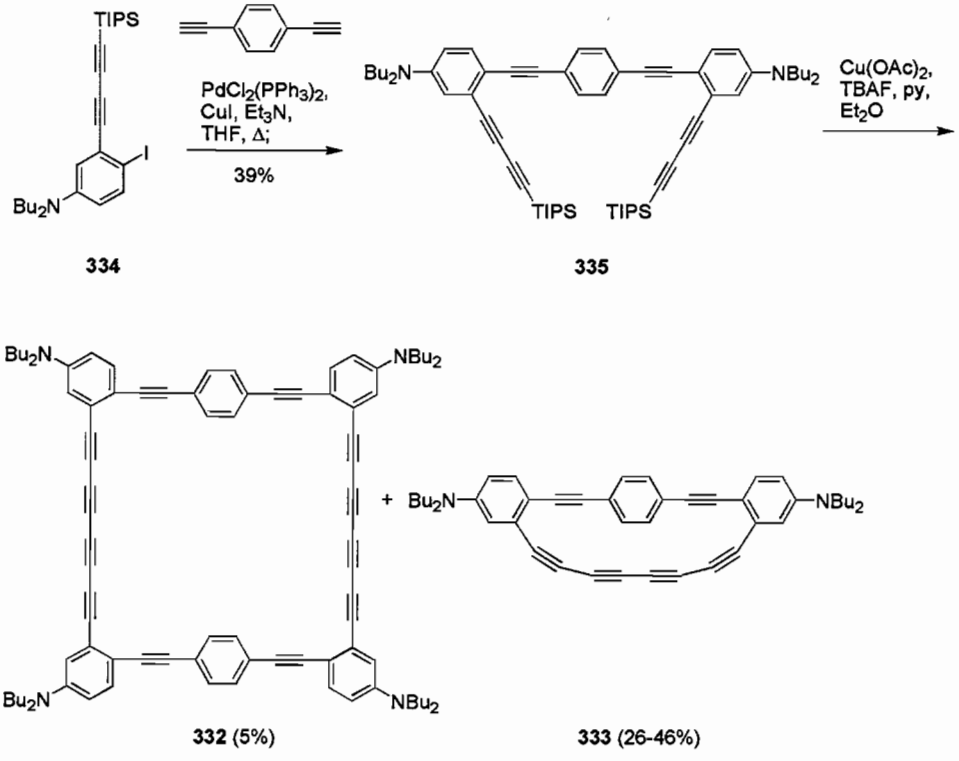

An different route to tetra-donor PTMs is shown in Scheme 73.[95] In situ desilylation/homocoupling of triyne **249** followed by removal of the TIPS groups afforded hexayne **3327**. Cross-coupling of **337** with 1-bromo-4-iodobenzene and subsequent addition of $PdCl_2(PhCN)_2$ and P(*t*-Bu)$_3$ and then dropwise addition of a second equivalent of **337** into the above mixture gave PTM **336** in low 4% yield. The proton NMR spectrum of **336** reveals the molecule adopts a highly symmetrical conformation in solution. Molecular modeling along with analysis of the NMR data suggests that **336** is C_2-symmetric.

An alternate approach to tetrayne-linked systems is the use of organometallic fragments to stabilize a strained annulene with the subsequent liberation of the

hydrocarbon. With *sp* bond angles calculated to be around 162°, PTM **338** would be highly strained and therefore was expected to be quite reactive.[105] The octacobalt complex **339**, on the other hand, should be readily isolable. Masked PTM **339** was prepared easily from **340** in five steps, and was isolated as stable, deep maroon crystals (Scheme 74). All spectroscopic data supported formation of the strain-free dimeric structure. Unfortunately, all attempts to liberate **338** from the cobalt units led only to insoluble materials. Given the high reactivity of **319** and several other strained polyynes, it is likely that **338** is too unstable to be successfully isolated and characterized.

SCHEME 73. Synthesis of PTM **336**.

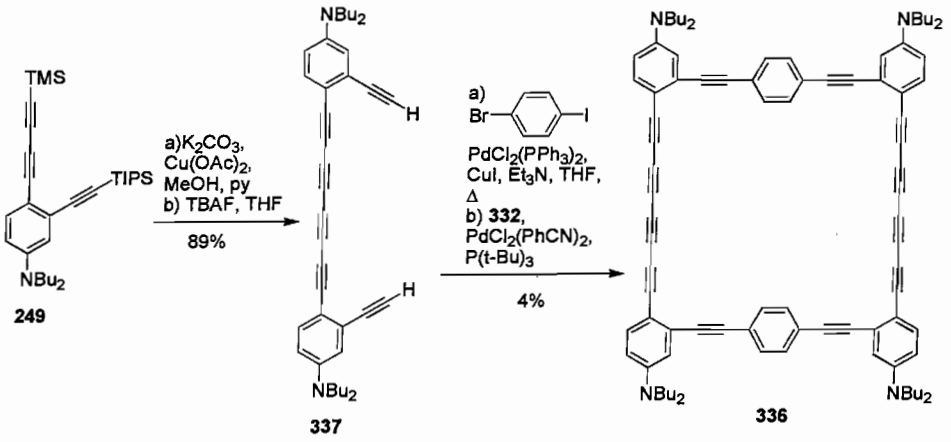

SCHEME 74. Attempted synthesis of PTM **338**.

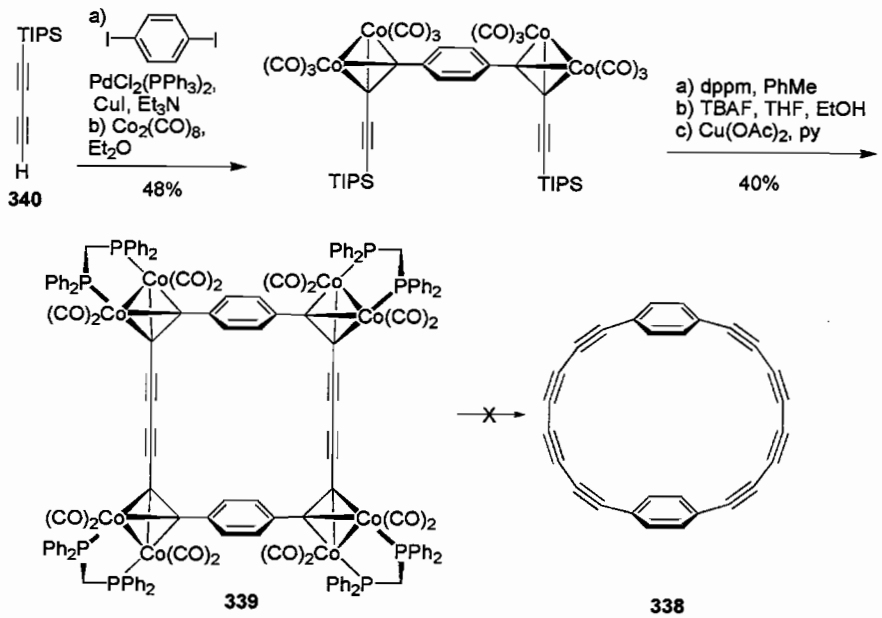

7. Phenyloligoacetylene Macrocycles

Some of the most exciting examples of macrocycles based on phenyl and acetylene units are the supercyclophanes **341-344** (Figure 16) which have been reported by both the Tobe[106] and Rubin[107] groups. In 1998 both groups generated **343** in the mass spectrometer by laser desorption of the appropriate polyyne precursors and showed that these coalesce to C_{60}. Subsequent work by the Japanese team has shown that halogenated cyclophanes **342** and **344** are superior precursors to fullerenes as the chlorine atoms are much easier to lose. Unfortunately, all attempts to generate fullerenes outside the mass spectrometer via these type of cyclophanes have not been successful. The reader is referred to an excellent reference by Tobe for a detailed discussion of this topic.[108]

FIGURE 16. Compounds **341-344**.

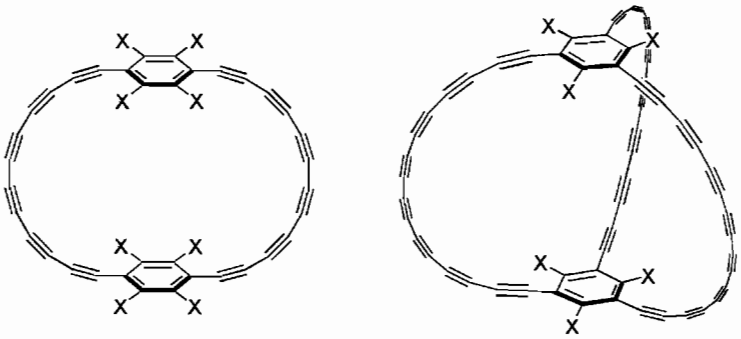

341 X=H
342 X=Cl

343 X=H
344 X=Cl

8. Conclusions

Although the groundwork for this field was laid over 45 years ago by Eglinton's pioneering studies, it has only been within the last 12-15 years that research on macrocycles comprised of phenyl and acetylene units has firmly established itself and grown at an amazing rate. Facile carbon-carbon bond formation through transition metal catalysis in conjunction with the widespread availability of silyl-protected acetylenes have made the assembly of complex macrocyclic structures a straightforward process. These synthetic developments now make it possible to tune and tailor the physiochemical properties of macrocycles, a definite first step if technological applications are to be realized. Since the early 1990s a new generation of alkyne chemists have recognized that phenylacetylene structures could be designed with technologically significant applications in mind. Numerous phenyl-acetylene macrocycles have been assembled utilizing many of the synthetic advances described over the previous pages and have shown to be useful for diverse application such as liquid crystal displays (LCD), supramolecular chemistry, self-assembly of nanostructures, nonlinear optical (NLO)

devices, and all carbon molecules and networks. Given the tremendous growth in this area in recent years, the future of phenyl/acetylene macrocycles appears to be rich with possibilities.

9. Bridge to Chapter II

Chapter II is comprehensive review on some fused and many cyclic thiophenes to show the synthetic techniques and properties of these systems. As my research is a convergence of fused thiophene systems and annulene chemistry, Chapter II will provide further background for my work.

CHAPTER II

PLANARIZED THIOPHENES AND THIOPHENE CONTAINING MACROCYCLES

1 Introduction

The following chapter is to give an overview of some fused thiophene systems and thiophene macrocycles to date. The passage presented is to review multiply fused thiophene systems and some effects and properties of the prepared compounds as reported in the literature.

While much progress has been made in materials composed of highly conjugated carbon-rich compounds,[1] there is much work that has been recently devoted to conjugated materials containing heteratoms.[2] Some advantages of working with heteroatomic aryl subunits include greater environmental stability due to resonance stabilization energy, polarizability, and enhanced optical properties. Heteroaromatic molecules have also been shown to effectively create novel polymers with conducting, semi-conducting, ion sensing, or even photovoltaic abilities.[2] With such a diverse-array of properties, the field of conjugated heteroatomic molecules continues to flourish.

While considerable work has been done and continues to be done to synthesize conjugated heteroatomic materials (pyroles, pyridines, and siloles), thiophenes possess

some key advantages. Compared to other heteroaromatic molecules, thiophenes are easier to handle and to functionalize than furans and pyrroles, which allows ready access to tailored thiophene derivatives.[2b] Thiophene is also highly aromatic and very resilient to form Diels-Alder products such as furans or the acene series. Functionalizing thiophenes with either alkyl groups or electron donating/withdrawing groups has led to facile tunability, stabilization and processablity of materials for device applications. In fact, the control and ease of thiophene synthesis has allowed for the assembly of discrete oligomers most recently up to a 96mer.[3] The optical tunability has also led to device fabrication of both optical (1^{st} and 2^{nd} order) and electronic devices with high efficiency and low band gap.[4] Thus due to the importance of thiophene chemistry to materials applications, thiophene synthetic techniques have been reviewed extensively.[2]

One strategy utilized to optimize electronic conjugated systems is to lock π-electrons into planarity, thus increasing the quinoidal character and lowering the band gap. Several techniques can be done to accomplish planarization, including conjoining thiophenes along the double bond, reducing oligomers to generate quinoidal forms, or constraining the π-bonds into a macrocycle. This review attempts to give an overview of recent achievements in creating extended planar thiophene molecules through fusion or macrocyclization.

2 Fused Thiophene Systems

2.1 Fused Thiophene Systems

Fused thiophenes are analogous to fused aromatics such as naphthalene (**1**), and anthracene (**2**). Much work was done in the 1950's because the fused thiophenes, such as **3** and **4**, were initially discovered as natural products in plants and found to be cytotoxic to various organisms in the presence of light. It was not until the current demand for extended conjugated systems and the advances in modern synthesis that many of the larger fused thiophene systems were even attempted.

FIGURE 1. Compounds **1-4**

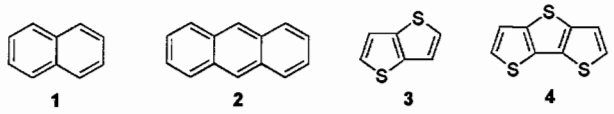

1 2 3 4

The condensed thiophenes **5** and **6,** containing greater than 3 fused thiophene units, were first published by Kobayahshi.[5] The two-step synthesis is shown in Scheme 1. Starting from an improved preparation of **7,** lithium exchange of the bromine followed by attack on dithienyldisulfide afforded **8** in 82% yield. Ring closure using $CuCl_2$ afforded crude **5** in approximately 60% yield. Pentathienoacene **6** was prepared in a similar way starting from **7**. Lithium-halogen exchange followed by treatment with bis(phenylsulfonyl)sulfide furnished precursor **9** in 23% yield. Ring closure provided acene **6** in a modest yield of 15-20%, presumably due to low solubility.

Initial studies of **5** showed that it had a low ionization potential of 7.52 eV (photoelectron spectroscopy) and formed a crystalline 1:1 charge transfer complex with

TCNQ, the conductivity of which was in the range of semiconductors at 10^{-6} S cm^{-1}. Compound **6** solubilized best in chloroform, but gradually decomposed in it to give a greenish solution. [5]

SCHEME 1. Synthesis of fused thiophenes **5** and **6**.

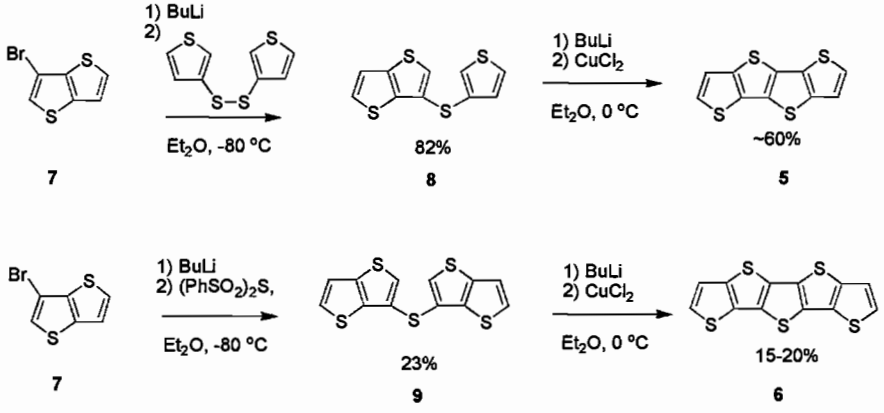

Comparison of the UV-Vis absorption spectra of **5** and **6** with thiophene and the condensed thiophenes **3** and **4** revealed a bathochromic shift and increase in absorption intensity with additional thiophene units. The plot of the absorption vs. 1/n units forms a linear relationship in the thienoacenes that is not observed in the isoelectronic angularly condensed polynuclear aromatics (naphthalene, phenanthrene, chrysene, picene). This result is suggestive that their exists a theoretical limit of a certain number of conjugated units where the additional number of monomers allows only neglibile decreases in light absorption energy.

Further work in extending condensed/fused thiophenes was done by the Matzger group[6] by preparing the thiophene equivalent of pentacene and heptacene, α-pentathiophene, and α-heptathiophene. Fused thiophenes were proposed to create more environmentally stable acene equivalents and materials that crystallize with more π-

stacking character as opposed to edge to face herringbone bonding. It is proposed that materials that associate through π-stacking have more efficient modes of electron migration than those that stack edge to face/herring bone aggregation, and thus improving the conducting/semi-conducting properties of the material.[2b] The Matzger synthesis also provides an improvement in overall yields vs. the Koboyashi method and access to fused thiophenes up to 7 rings.

The syntheses of **6** and **10** are shown in Scheme 2 starting from the condensed thiophenes **11** and **12**. Lithiation followed by silation produced **13** and **14** in 85% and 81% yield, respectively. A halogen dance reaction was then performed using LDA in THF to provide the β-brominated thiophenes **15** and **16** in 80% and 67% yield, respectively. The sulfides **17** and **18** were then synthesized using a Pd-catalyzed coupling of $Bu_3SnSSnBu_3$ with two equivalents of bromo-arene to yield **17** and **18** in 95% and 75% yield. Oxidative ring closure afforded the cyclized products **19** in 52% and **20** in 68% yield. The improved yields were attributed to the TIPS groups eliminating the deprotonation of the outer α-positions, promoting the intramolecular cyclized product. Full deprotection of **19** was achieved using TFA to yield **6** in 92% yield while **20** required TBAF to yield **10** in 96% yield.[6]

Initial X-ray studies of the TIPS protected compounds showed highly distorted molecular geometries due to the bulky TIPS groups. However, compound **6** was resolved to exhibit excellent π-stacked binding motif with a distance of 3.52 Å between planes as well as negligible atomic deviation from the mean plane of the fused ring system (<0.007 Å). Comparing the powder X-ray data of both **6** and **10** revealed that both solids were

isostructural, with compound **10** being 35% longer. Electronic properties were studied by UV-Vis and fluorescence. Generally, the absorption properties were comparable to the nonfused α-oligothiophenes with the same number of double bonds. With respect to α-oligothiophenes the condensed systems were found to possess blue shifted emissions (and thus narrower stokes shift), vibronic structure, and slight red shifts in the UV-Vis absortion (3-6 nm) which were all consistent with the planarization of the fused thiophene systems.[6]

SCHEME 2. Synthesis of fused thiophenes **6** and **10**.

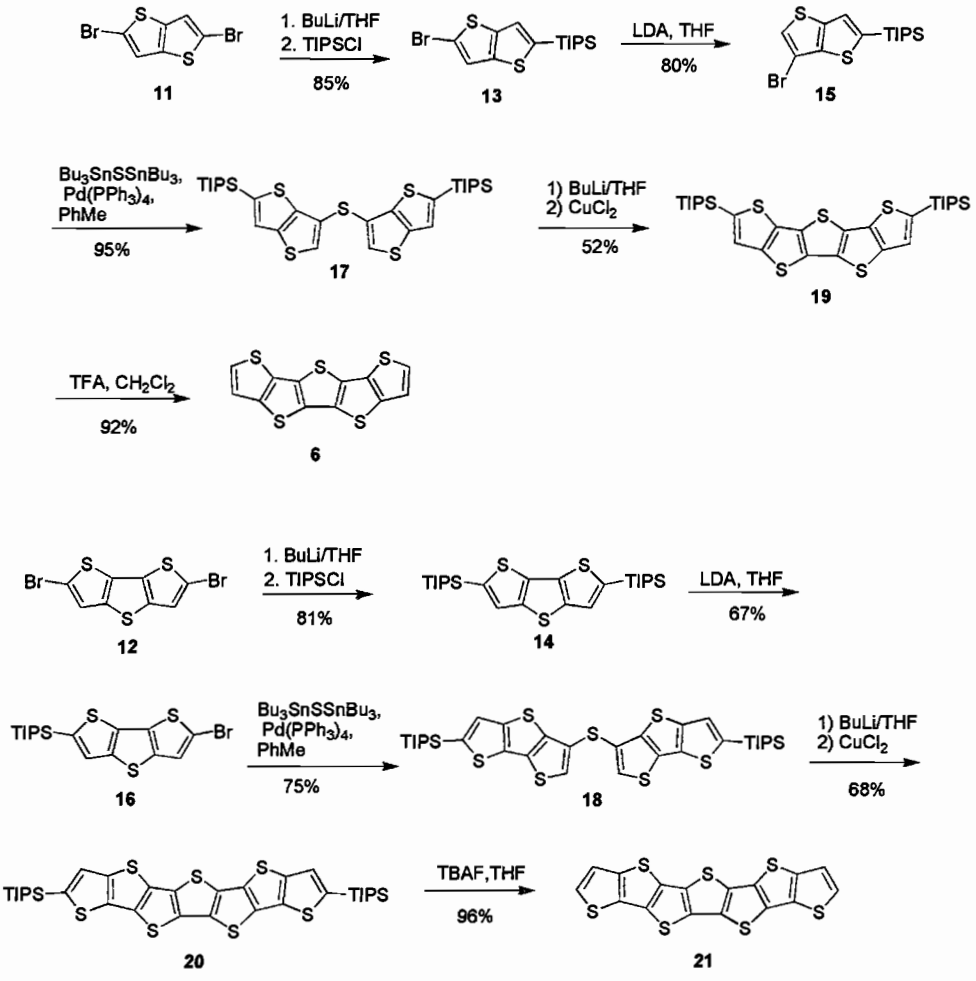

The Roncali group has done much work in fusing thiophenes together through a variety of techniques, which have been reported and reviewed.[7] Scheme 3 details the synthesis of a fused α-linked terthiophene **21**[8] with the sulfurs in proximity to each other and locked into planarity with β methylene bridges. Preparation of compound **21** is given in Scheme 3. Ketone **22** was oxidatively homocoupled with LDA followed by $CuCl_2$ to yield **23** in 30% followed by ring closure with Lawesson reagent to form **21** in 45% yield.

SCHEME 3. Synthesis of fused thiophene **21**.

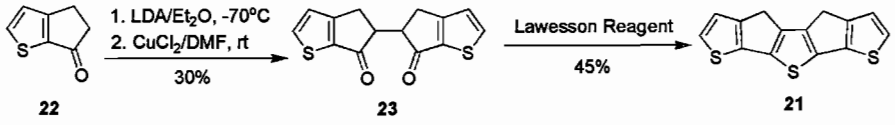

Compound **21** was characterized optically by UV-Vis absorption and electrochemically by cyclic voltammetry. The absorption spectra of **21** simply shows a 22 nm bathochromic shift with respect to α-3TP (2,2',5',3'-terthiophene) in addition to vibronic structure. The vibronic structure coming from achieving planarization while the blue shift most likely occurs from the sulfur-sulfur lone pair interactions. Cyclic voltammetry of **21** exhibits two irreversible oxidative waves at 0.60 and 0.83 V in addition to reduction waves at –0.75 and –0.90 with respect to SCE. The authors use these numbers to allude to a narrower band gap than α-3TP for perhaps making more efficient, smaller band gap materials. Preparation of a polymer film of **21** was not as easy as a typical thiophene due to the stability of the radical cation; however, repeat cyclic voltammetry scans did provide small samples to analyze. Large-scale electropolymerizations were difficult to the large amounts of non-adherent material and

only obtained with repeated scans of **21** cast onto an ITO film. The absorption spectrum of the film was found to be strongly reminiscent of that of other small linear α-oligothiophenes.[8]

2.2 Fused Benzo-Thiophene Systems

Neckers et al. reported several pentacene-like fused benzothiophene systems (**22**,**23**) in an effort to further improve on the solubility and stability of pentacene by utilizing thiophenes, yet retain some benzene character.[9] Regardless, **23** was found to be **less** stable than pentacene; therefore, resonance stabilization energy of the sulfur atom is not necessarily a stabilizing effect. The finding that thiophenes alone did not make a more stable molecule suggests there is some desired component in having benzene moieties. These molecules offered some improvement in overall conjugation by improving planarity and limiting sulfur-sulfur atom repulsions, which tilt the molecule due to overcrowding. It was also proposed that it was more important for the terminus of the acenes to be composed of thiophenes and thus offer more stability to air, be more soluble, and pack better in the solid state.

Compounds **22** and **23** differ in their synthesis by the core arene utilized. Synthesis of the aryl aldehydes is shown in Scheme 4. Lithiation of 2,2'-dibromothiophene with *n*BuLi followed by quenching with DMF forms dialdehyde **24** in quantitative yield. The 3,4-thiophene dicarboxaldyhyde **25** was not as accessible and was formed using a one-pot stepwise reaction. 3,4-Dibromothiophene was lithiated once with *n*BuLi, quenched with DMF, and then lithiated again with *t*BuLi and further quenched with DMF to form the dicarboxaldehyde in 34% yield.[9]

SCHEME 4. Synthesis of dialdehydes **24** and **25**.

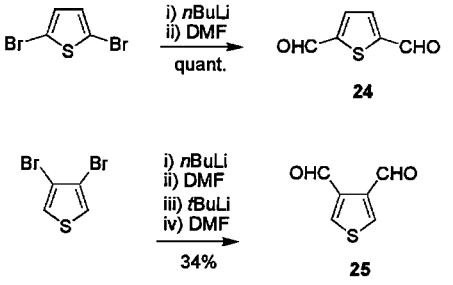

Scheme 5 shows the syntheses of compounds **22** and **23**. To form compound **22**, 3-bromo-2-lithiothiophene was added to **24** to give **26.** Hydroxyl reduction of **26** using a milder reducing reagent $NaCNBH_3/ZnI_2$ afforded **27** in 80% yield. Careful monitoring of the lithiation/carboxaldehyde formed the dialdehyde **28** in near quantitative yield. Final cyclization in benzene in the presence of Aberlyst-15 using a Dean-Stark trap furnished **22** in 46% yield.[10]

Compound **23** was prepared in an analogous manner by the reaction **25** with 3-bromo-2-lithiothiophene then reduced to form **29** in 43% yield. Bromine-lithium exchange followed by formylation gave the dialdehyde **30** in 54% yield. Cyclization furnished the product in 24% yield.[9]

Comparing the UV-Vis absorption of the two compounds, the anti isomer **23** was red shifted from the syn isomer **22** by 12 nm. Both isomers show a small Stokes shift; however, the emission of **23** had greater fluorescence quantum yield than **22** but a lower phosphorescence quantum yield due to heavy atom effects. Both molecules exhibit greater thermal stability than pentacene both with and without oxygen. When comparing the electrochemical properties, **23** shows quasi-reversible oxidation at 1.15 V while **22**

exhibits a reversible oxidation at 1.12 V vs. $Ag/AgNO_3$. The anti isomer **23** does form an intensely colored film on the surface of the electrode as well as the appearance of lower potential waves upon repeat scans showing evidence of electropolymerization.[9]

SCHEME 5. Synthesis of fused compounds **22** and **23**.

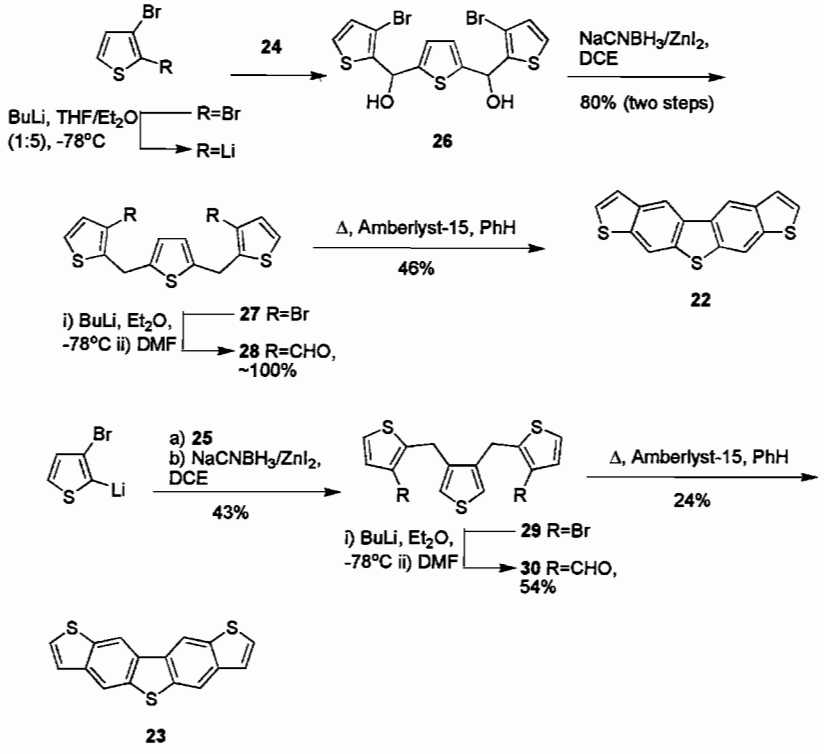

X-ray studies of **22** found the structure to pack in a herring-bone motif with favorable face-to-face packing along the c-axis of the unit cell comparable to pentacene. The molecule is nearly planar with highest deviation being ±0.174 Å. Furthermore, compound **22** also has a high packing efficiency comparable to pentacene.[9] Crystals with high packing efficiency are proposed to be excellent conducting materials with close intermolecular contacts for ideal electron transport.[9]

The Mullen group assembled the dibisbenzothienobisbenzothiophene **31** (with possible isomers **32** and **33**, Figure 2) to further enhance charge mobility by utilizing a novel intramolecular approach to create the rigid thiophene moieties.[10] The synthesis of **31** is given in Scheme 6. Commercially available dibenzothiophene was oxidized with acetic acid and hydrogen peroxide to form **34** in 99% yield. **34** was then brominated using dibromocyanuric acid to afford **35** in 57% yield. Reduction with LAH produces **36** in 59% yield. The diboronic acids **37** and **38** were furnished by addition of *t*BuLi to **36** which were then immediately cross-coupled to **39** to form **40** in 51% yield with some byproduct of **41**. Precursor **40** was cyclized with treatment of trifluormethanesulfonic acid for 12 hours forming the methylated cation as an insoluble yellow solid. Refluxing the material in pyridine for 12 h afforded **31** in 86%.[10]

FIGURE 2. Compounds **31-33**

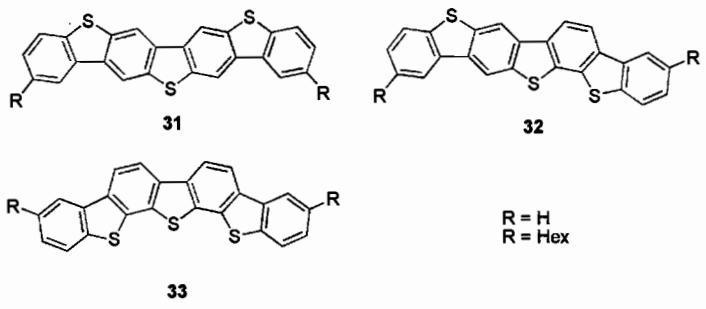

SCHEME 6. Synthesis of thienoacene **31**.

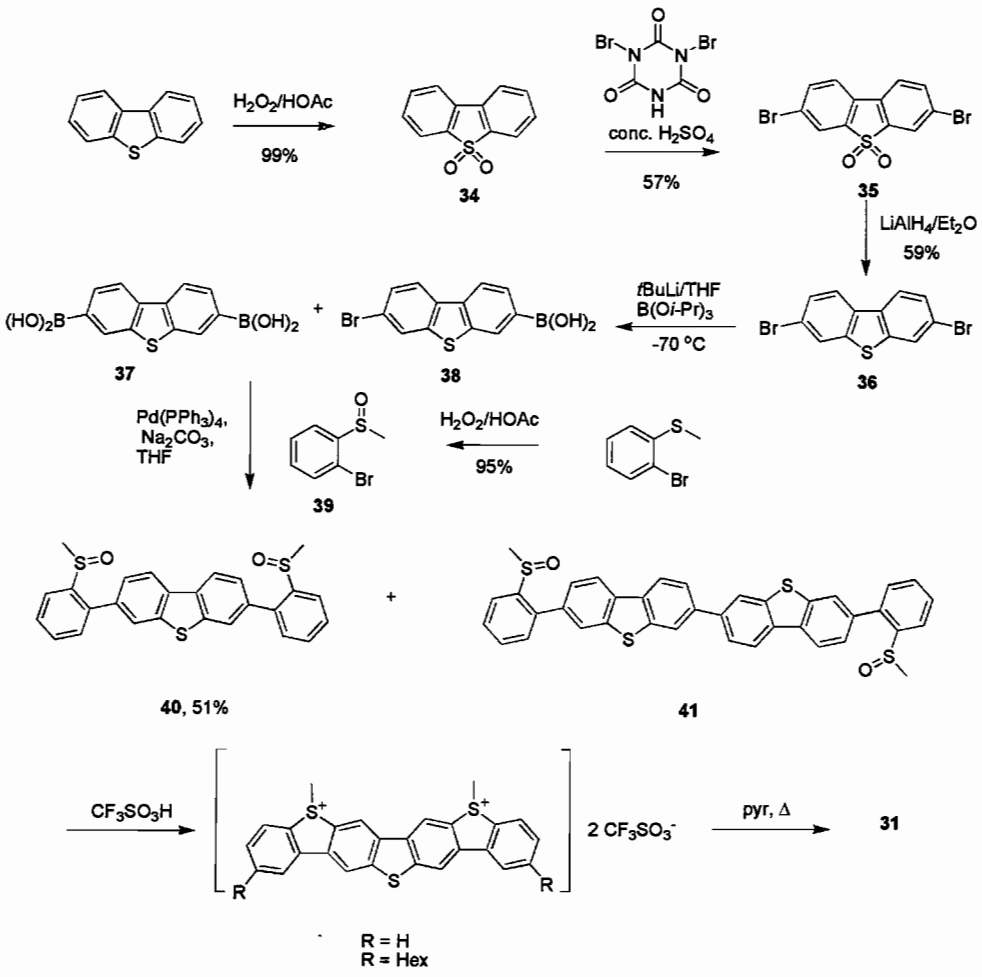

Full characterization of compound **31** (R = H) was difficult due to poor solubility and thus no NMR data was obtained. The solubility was reasonable enough in dichlorobenzene to obtain a UV-Vis spectrum with three absorption maximum at 374, 394, and 415 nm. Elemental analysis and FD-mass spectrometry were in agreement with the constitution and purity of **31** (R=H). Although **32** and **33** are also potential cyclization products, isomer confirmation or distribution were hindered by solubility issues. IR spectroscopy was suggestive of the presence of at least two of the three possible isomers with **31** being dominant. To decipher the relative amounts of isomers, *n*-hexyl units were

incorporated as solublizing groups (R = Hex). ^{1}H NMR data showed the alkylated product mixture to contain 71% of the desired compound **31** (R=Hex). Recrystallization afforded pure **31** (R = Hex) as an insoluble material; thus, definitive proton assignments could not be made. Based on the product ratios determined for **31** (R = Hex), it was then assumed that compound **31** (R = H) was the dominant product formed. Devices were made of compound **31** (R = H) and demonstrated charge mobilities of 0.15 $cm^2 V^{-1} s^{-1}$ when utilizing rigorously purified samples.[10]

The Pei group constructed several derivatives of fused benzodithiophene molecules **42a-b** and **43a-d**.[11] Compounds **42a** and **42b** were composed of 7 fused aromatic rings with a novel C_2 symmetry; whereas, compounds **43a-d** have a C_2 symmetry as well but incorporate phenyl and spiro-difluorene groups to improve solubility (although at the expense of overall conjugation.)[11]

The syntheses of **42a-b** are given in Scheme 7. 1,4-dibromo-2,5-Diiodobenzene was cross coupled to the appropriately substituted alkyne forming the aryl diynes **44a-b** in 70% (Ar =4-$C_6H_{13}O$-C_6H_4) and 60% yields (Ar =4-TIPSO-C_6H_4). Mercaptolithiation of **44** yielded methyl protected thiol in 84% and 81% for **45a-b,** respectively. Larock's iodine-induced cyclization produced the iodobenzothiophenes **46a-b** in 85% and 81% yields, respectively.[12] Sonogashira cross-coupling with TMS-acetylene followed be deprotection afforded the ethynylated compounds **47a** and **47b** in 76% and 78% respectively. Cyclization with $PtCl_2$ in toluene at 80°C afforded the fully fused ring systems **42a** and **42b** in 45% and 51% respectively.[11]

SCHEME 7. Synthesis of compounds **42a,b**.

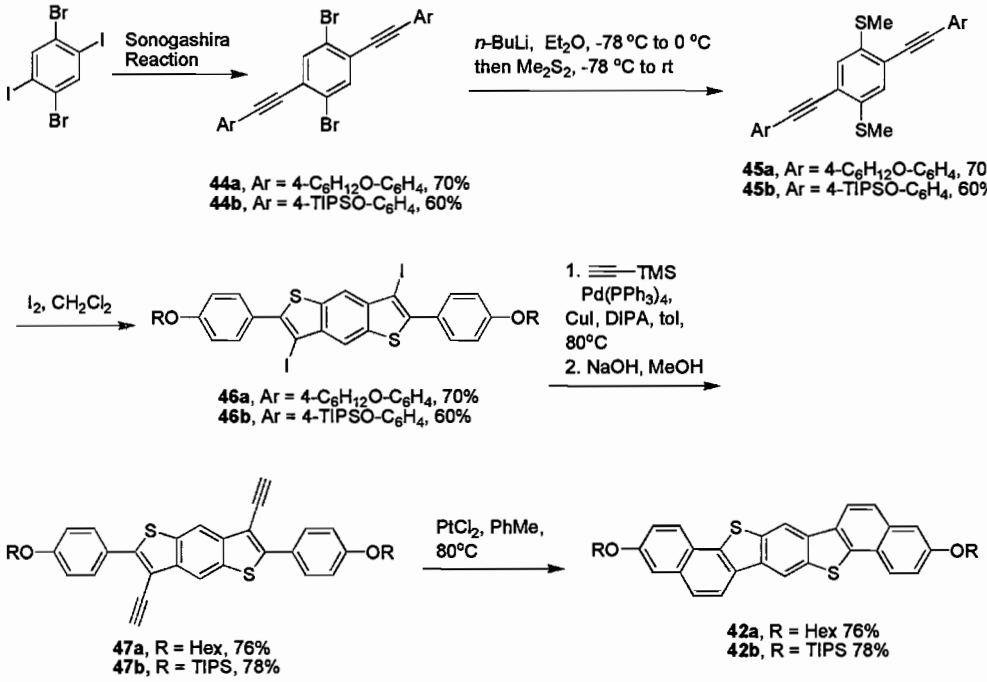

The spiro like molecules **43a-d** were synthesized to enhance solubility and shown in Scheme 8. Starting from **46a** and **46b**, lithium halogen exchange at the iodide followed by trapping with benzophenone or fluorophenenone yielded the tertiary alcohols **48a-d** in 72-85% yields. Friedel-Craft cyclization formed the spiro-compounds **43a-43d** in 58-68% yields. Compounds **48a-b** cyclized sufficiently with concentrated H_2SO_4 in AcOH while **48c-d** required BF_3 to cyclize.[11]

The UV-Vis absorption properties of the polycyclic benzothiophenes were extremely consistent. **42a** and **42b** exhibited three peaks with the most red shifted peaks at 372 and 374 nm respectively. The emission spectra were also nearly identical with a peak at 382.5 and 383.5 nm for **42a** and **42b,** respectively. The spiro-compounds **43a-**

43d all had nearly identical UV-Vis spectra absorbing at 408 nm, approximately 30 nm red shifted from **42**.

The emission spectra of **43** were unremarkably similar with a peak at 424 nm yet red shifted from **42**. The bis phenyl vs fluorenyl functionality played no role to the effective conjugation due to the sp^3 carbon atoms.[11]

SCHEME 8. Synthesis of compounds **43a-d**.

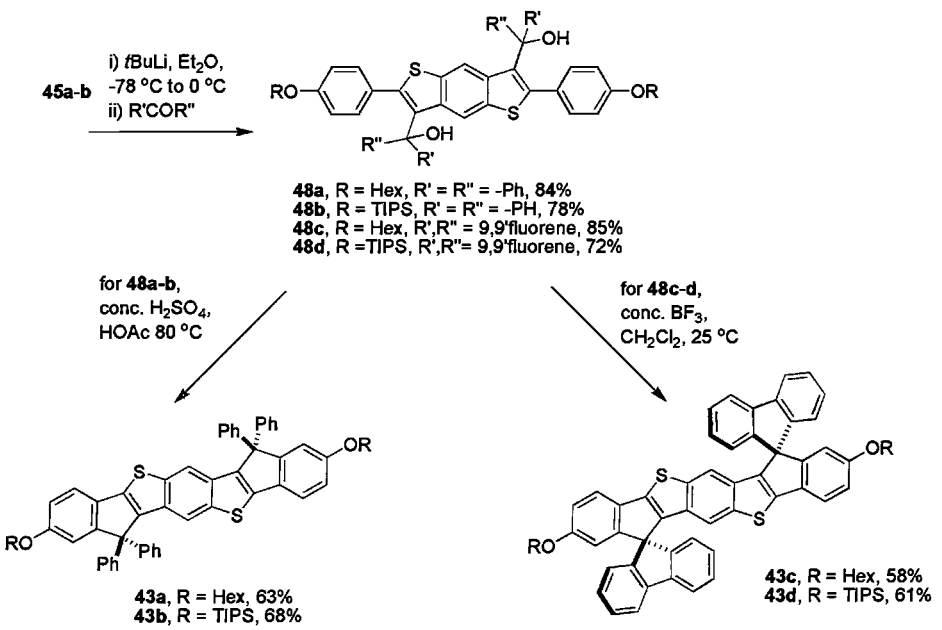

2.3 Conclusions on Fused Thiophene Systems

Due to demand in low energy band gap semi-conducting materials, exploration of compounds containing fused thiophenes and fused thiophene/benzene hybrids have been recently developed. Many of these compounds do exhibit lowering of band gap energy indicative of enhanced π-orbital overlap resulting from locking the adjacent arenes into co-planarity. Furthermore, several systems have been demonstrated to show semi-

conducting properties for device application. However, the added planarity often contributes to both loss of solubility and stability of the compounds prepared. Crystal structure obtained often exhibit more face-to-face crystal packing, which is argued to be more favorable for charge mobility. Contrasting what was initially proposed, the sulfur atom does not always offer resonance stabilization energy. Regardless, the rationale for why some fused systems afford the desired properties while others are unpredictable is elusive and warrant further exploration.

3 Thiophene Containing Macrocycles

3.1 Macrocycles Composed of Thiophenes

The fully conjugated macrocyclic oligothiophenes **49-51** and thiophene acetylene macrocycles **52-55** were prepared and studied extensively by the Bäuerle group.[13,14] These compounds offer a theoretical infinite chain of conjugation comparable to the linear thiophene polymers with further potential assembly to extend three dimensionally into novel heterocyclic nanotubes.[13] Linking the thiophenenes via α-α connections affords higher conjugation than the β-β connection or even the α-β linkages[2] and allows for a natural bend of the molecule limiting the amount of strain energy. This natural bend in heterocycles also affords direct conjugation as opposed to macrocycles composed of cross-conjugated meta-linkages[15] which limit the amount π-electron overlap. Cyclic thiophenes also self terminate the 2-positions which have been shown to stabilize the molecules from oxygen.[2]

SCHEME 9. Synthesis of dehydrothienoannulenes **52-55**.

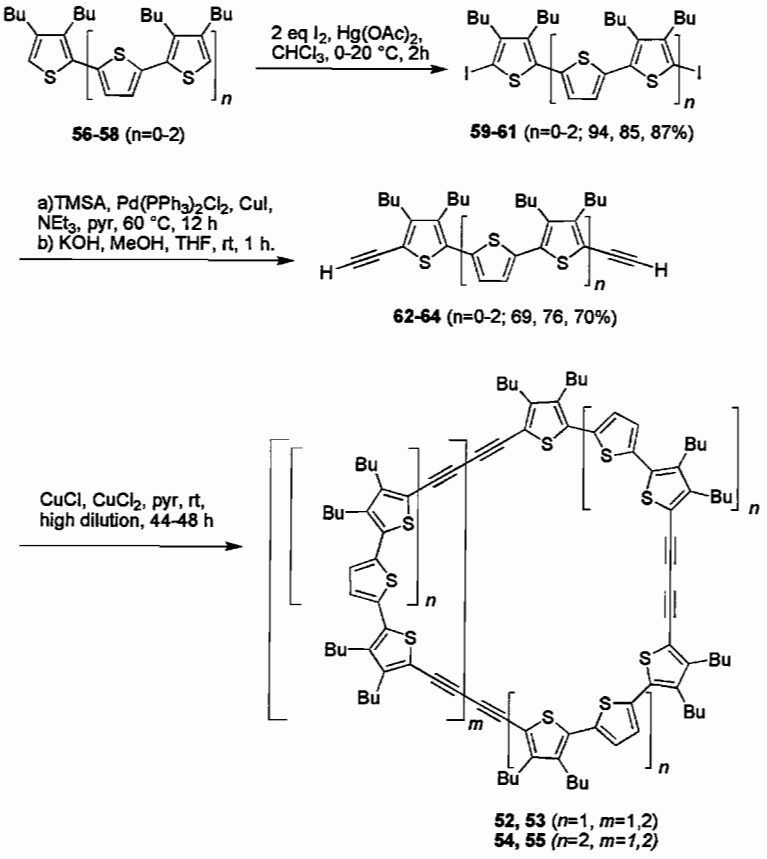

The syntheses of thiophene acetylene macrocycles **52-55** are given in Scheme 9. The butylated thiophenes **56-58** were iodinated using $Hg(OAc)_2$ in chloroform to provide **59-61** in 87-94% yields. The terminal acetylene groups were then added by Sonogashira cross coupling of TMSA to the terminal iodides followed by deprotection with KOH in THF and methanol forming free alkynes **62-64** in 69-76% yields. Macrocyclizations were performed using high dilution Eglington-Glaser conditions furnishing the dehydrothieno macrocycles **52-55** in 2-12% yields with cyclotrimers and the cyclotetramers being the main products. Definative characterization was performed using NMR spectroscopy and *MALDI-TOF* mass spectrometry. The macrocycles

isolated corresponded to 39, 52, 57, and 76 chain members for **52-55** respectively. Peak assignments of the protons were easily done to the high symmetry of the molecules formed.[13]

Scheme 10 shows the treatment of **52-54** with sodium sulfide in 2-methoxyethanol/*p*-xylene which prepared the fully sulfated thiophene macrocycles, **49-51**, in 7-27% yields. Cyclo[16]thiophene required additional purification to afford the product of the four fold reaction of the diyne molecule. The macrocycles themselves showed no significant aromatic proton shifts indicative of more benzenoid than annulenoid character. Crystals were difficult to obtain due to the large cavity of the macrocycles, which caused structural disorder when filled by solvent molecules and often led to crystal destruction when the solvent was lost. The oligothiophenyldiacetylene **50** does recrystallize from toluene forming crystals suitable for X-ray diffraction, which showed minor strain and sulfur-sulfur van der Waals interactions.[13]

The optical properties of the cyclic thiophenes were found to be somewhat unusual when compared to the absorption properties of the corresponding linear oligothiophenes. The absorption band red shifts as the chain length or macrocycle size increases, but the absorption band of the macrocycle corresponds closely to the value of a linear molecule containing half the number of thiophene units. This means that the cyclic thiophenes are blue shifted from the oligothiophenes, although the intensity for the cyclic thiophenes is twice as much. Much of this effect is likely due to the close van der Waals interactions of the sulfurs. The calculations performed to explain the phenomena involve

the Frenkel exciton theory. The rational for the differences observed in the absorption is the result of different selection rules due to their different geometry.

SCHEME 10. Synthesis of cyclic thiophenes **49-51**.

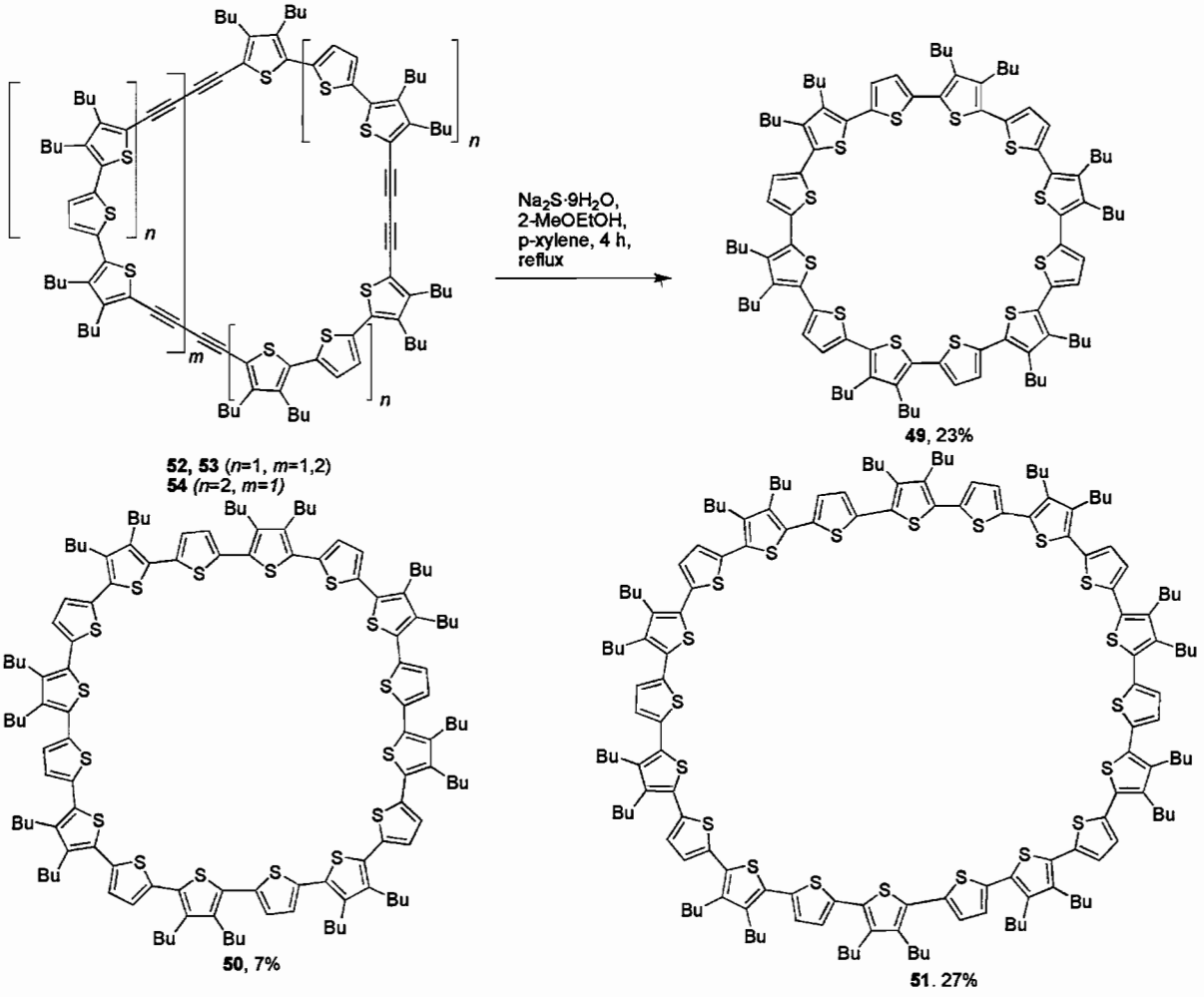

Compounds **49-51** were studied extensively through STM imaging.[14] The π-conjugated macrocycles can offer structures for molecular circuitry including site recognition and selective complexation. They also have unique absorption properties and self-assembling properties as shown by STM imaging. The macrocycles were not found

to be very rigid, but do exhibit some self association and align on the graphitic surface, butyl groups down and "spider"-like with the surface.[14a] The macrocycles associate C_{60} molecules on the graphitic surface where the interaction is described as a π-donor to π-acceptor interaction, the thiophene macrocycles donating to the buckyball. The most common binding motif is where the buckyball rests on top of the macrocyclic edge. Although the cavity is large enough to accommodate the molecule, the π overlap is not nearly as favorable.[14b]

Further developing the synthesis of the cyclic thiophene,[13] the Bäuerle group prepared the first fully conjugated interlocking molecule **65** utilizing a metal templated approach.[16] Scheme 11 shows the synthesis of both preliminary pre-catenane rings **66** and **67**. Starting from the previously reported heteroraromatic chelating ligands **68** and **69**[17] iodination afforded products **70** and **71** in 92% and 88% yields respectively. Sonagashira cross coupling with TMSA produced **72** and **73** in 91% and 89% respectively. Deprotection of the alkynes followed by metalla-macrocyclization with $Pt(dppp)Cl_2$ and CuI in Et_3N and toluene formed the macrocycles **66** and **67** (70% and 9%). Because of the low yield of **67**, pre-macrocycle **66** was used for templated synthesis of the interlocking molecule.[16]

The initial attempt at forming the catenane followed a homoleptic preparation as shown in Scheme 12. Precycle **72** was complexed with $Cu[CH_3CN]_4BF_4$ in acetonitrile/methylene chloride solution forming **74** in 95% yield. Precursor **74** was then deprotected and cyclized using Pt macrocyclization forming trace amounts of desired catenane **75** with the major product being the uninterlocked ring **66** in 52% yield.[16]

SCHEME 11. Synthesis of thiophene pre-catenanes **66-67**.

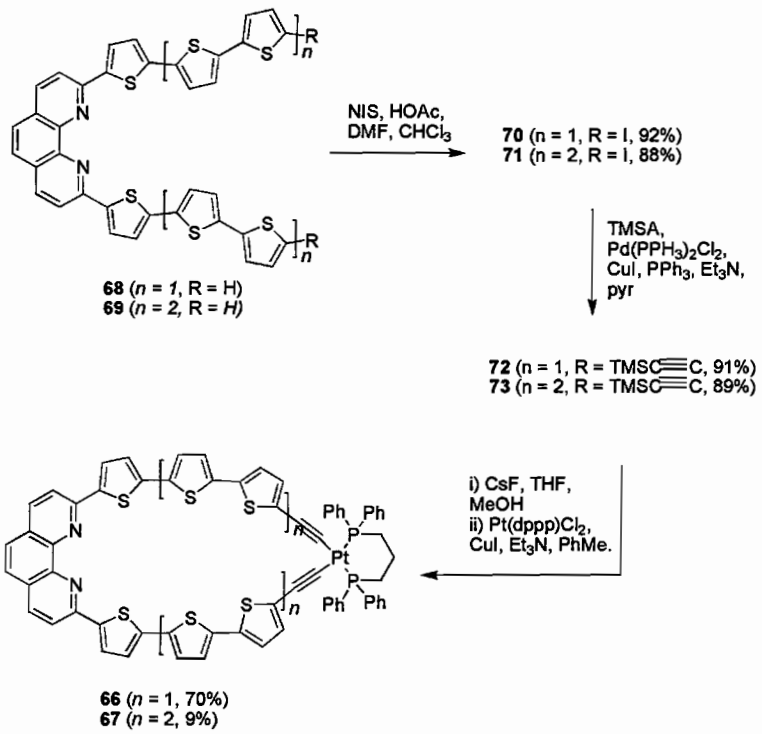

The heteroleptic synthesis is given in Scheme 13 which creates **75** at significantly improved yield. The macrocycle **66** was complexed to the open form **73** to form the pseudo-rotaxane **76** in solution. Deprotected and metalation provided **75** in 43% yield. Reductive elimination of the platinum with iodine forms the interlocking fully conjugated macrocycles **65** in 41% yield. The molecule proved impossible to demetallate due to the steric bulk surrounding the copper. Proof of structure was done using ESI-FT-ICR-MS to carefully find the exact mass and isotopic pattern of the structure, which agreed with the calculated ones.[16]

SCHEME 12. Low yielding synthesis of platino-catenane **75**.

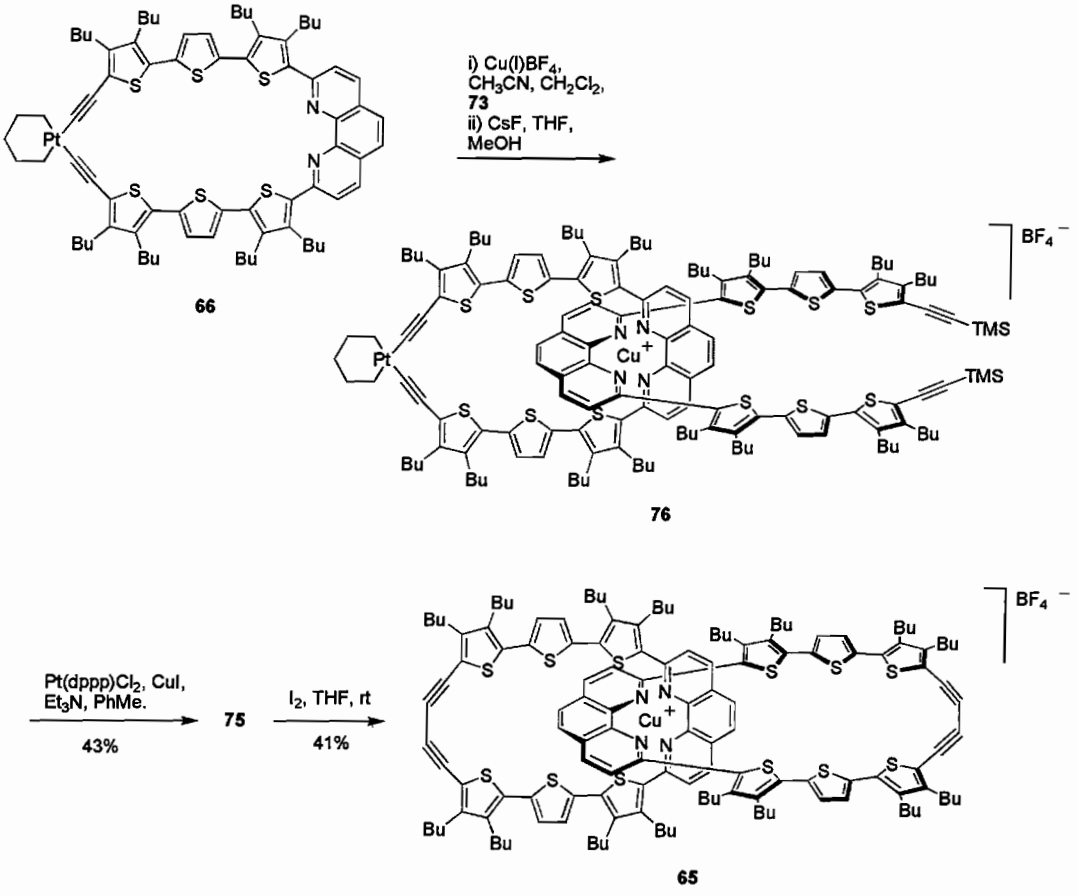

The original cyclic α-β- linked terthiophene molecule **77** was prepared by the Kauffmann group and is shown in Scheme 14. Lithiation of the dibromo-bithiophenes **78** and **79** followed by treatment with $CuCl_2$ affords compound **77** in approximately 23-24% yield.[18] Bithiophene **79** also produces the side product cyclic α-β-linked sexithiophene **80** in minor amounts. The β-β-linked macrocycle **81** was furnished from **82** utilizing $CuCl_2$ or $FeCl_3$ in comparable yields.[18]

SCHEME 13. Formation of catenane **65**.

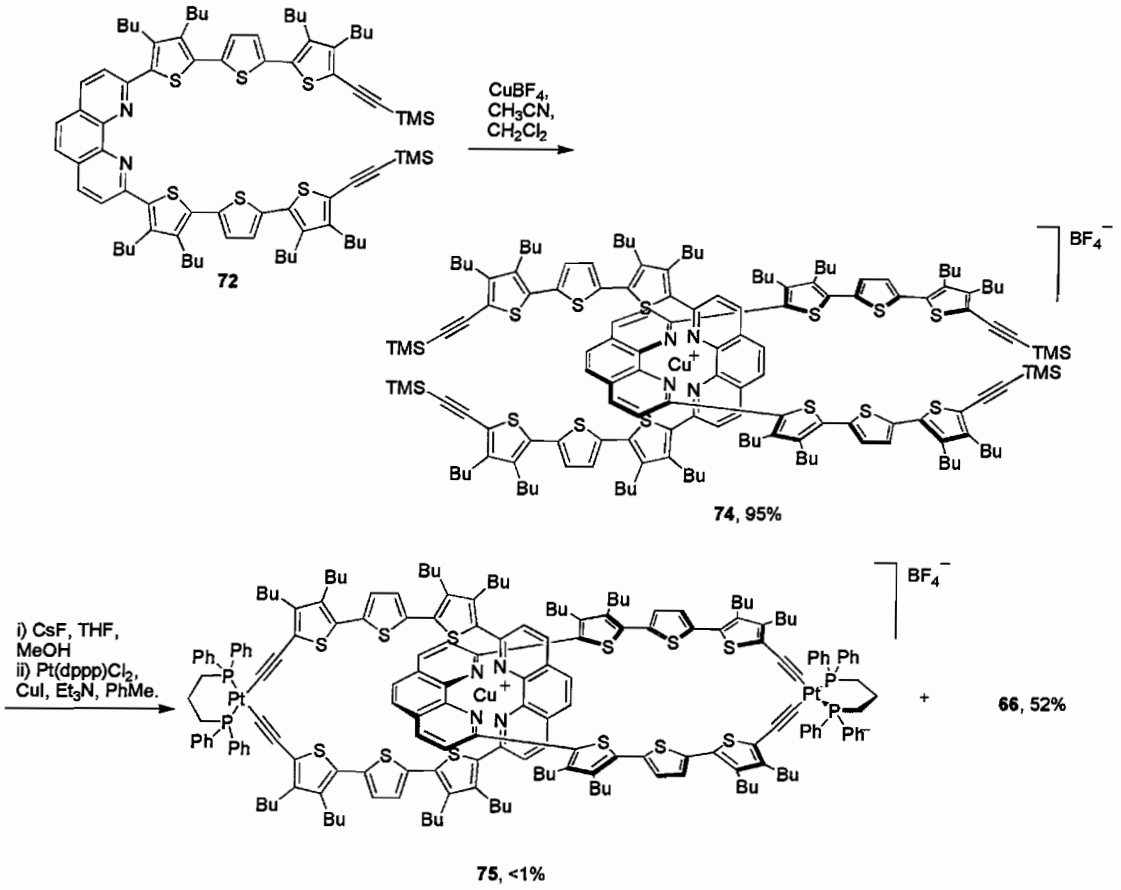

Improvements in the synthesis of **77** and **81** were done by the Iyoda group and also shown in Scheme 14. Lithiation, addition of $ZnCl_2$, then treatment of $CuCl_2$ to **79** and **82** provided **77** and **81** in 40 and 43% yield.[19]

The Marsella group has developed various molecules based on the tert-thiophene macrocycle that changes shape once oxidized.[20] Analogous to cyclooctatetraene, the molecule planarizes itself after a two electron loss and becomes aromatic. Thiophenes were utilized because they can be incorporated into a polymer scaffold, thus creating a

fluctional material. Molecule **77** that was previously prepared by Kauffman back in 1978[18] was derivatized to **83** to allow for controlled polymerizations.[20]

SCHEME 14. Formation of **77**, **80**, and **82**.

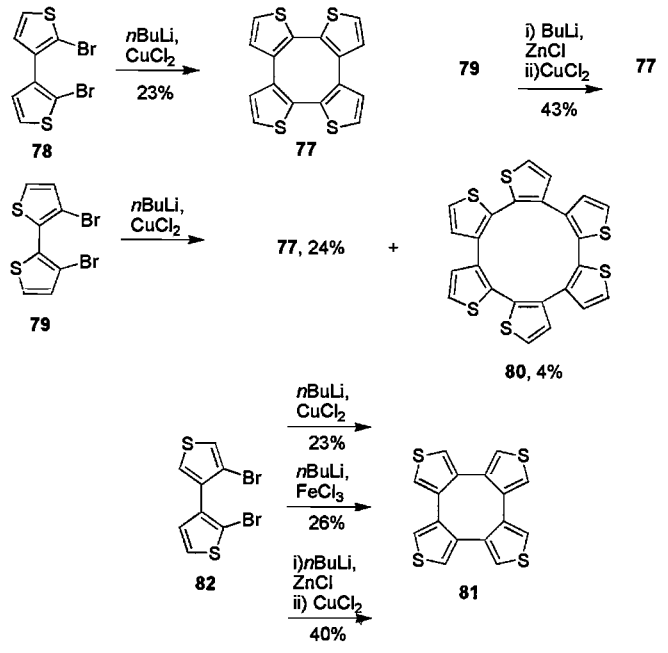

The synthesis of **83** is given in Scheme 15. Dihaloarene 2-butyl-5-bromothiophene was coupled to itself by adding 0.5 eq of *n*-BuLi, $MgBr_2$, and $NiCl_2$(dppp) to form **84**. The bithiophene **84** was dibrominated with NBS to form **85** which was then coupled to 3-thienylmagnesium bromide with $NiCl_2$(dppp) providing **86**. Tetra-thiophene **86** was then brominated again affording **87** in 31% yield (4 steps). Cyclization by treating with n-BuLi, and $FeCl_3$ furnishing macrocycle **83** in 48% yield. Iodination of **83** with BuLi preceding I_2 addition, produced **88**. Polymerization was performed by lithiation and then treatment with Ni catalyst to afford the polymer **89** in greater than 95% yield.[20]

SCHEME 15. Synthesis of macrocycle **83** and polymer **89**.

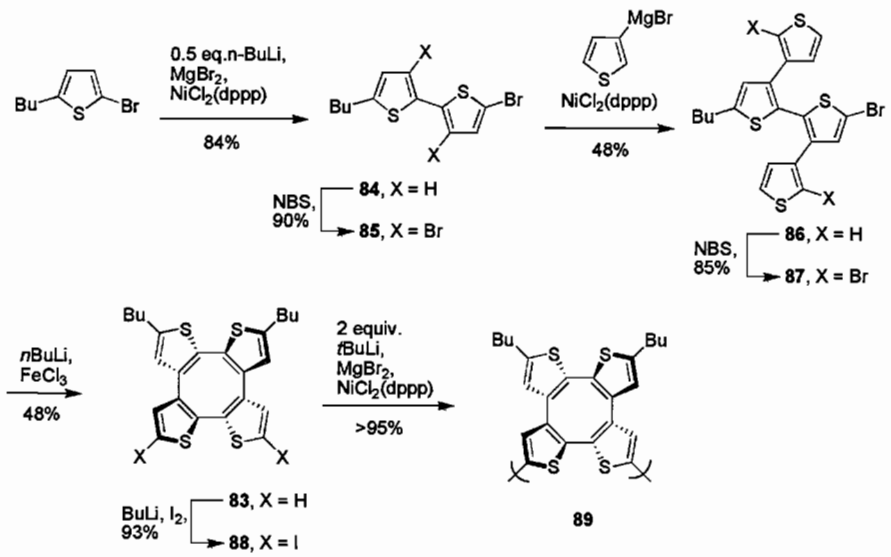

Compounds **83** and **89** were analyzed optically and electrochemically. UV-Vis spectroscopy showed the polymer **89** to be red shifted from the monomer **83** by almost 200 nm in the solution phase but not by much in the solid phase where the peaks only to broaden. Ideally, the electrochemical data should to be indicative of a fluctional polymer; however, the results were mostly disappointing due to the integrity of the material that is common with conducting polymers. Polymer **89** was found to be only irreversibly oxidizable at about 1.6 V. The irreversibility of the polymer most likely comes from the poor contact with the working electrode, as indicated by visible cracking and peeling of the polymer. The conformation of the macrocycle dihedrals was estimated from the CV by approximating the charge per repeat unit and calculating the structure of the **83-83** dimer and comparing it to the **83-83**$^{+1}$ dimer. The average charge per monomer was found to be roughly 0.6 V. Comparing that to the dimers, it was approximated that the dihedral angle in the main chain changes from 44.1° to 44.5°. It was proposed that the

conformational change of the polymer does occur but contributes to the degradation of the polymer.[20]

To determine the conformation of the molecule, AM1 semi-emperical calculations were used on sequentially oxidized versions of **83** (**83**, $\mathbf{83}^{+1}$, and $\mathbf{83}^{+2}$). As the molecule becomes more oxidized, the dihedral of the S-C-C-S bond approaches planarity. The dihedral angles for **83** are 47.6° and 46.4° which correspond reasonably with the calculated value of 45.9°. The dihedral angles for the one electron loss $\mathbf{83}^{+1}$ were calculated to be 31.7° and 44.6° while the two electron loss, $\mathbf{83}^{2+}$, was found to have a dihedral angle of 29.7°.[20]

Further studies of the further alkylated monomer **90** and dimer **91** (Figure 3) reveal oxidation peaks at 1.01 and 1.36 V showing a +1 oxidized reversible species for **90** and dimer **91** respectively. DFT calulations showed that the electron density of the oxidized species to be delocalized over the entire molecule, and that the dimensional change for **90** and **91** were 5.69% and 3.54% respectively. The delocalization of the two linked annulenes is not significant to reduce the suitability of using the molecules for single-molecule electromechanical actuaters, but the sterics of the butyl groups reduce the ablility of attenuation of the macrocycle to conform.[21]

FIGURE 3. Compounds **90**, **91**.

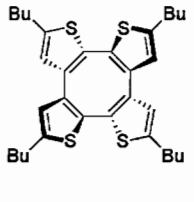

90

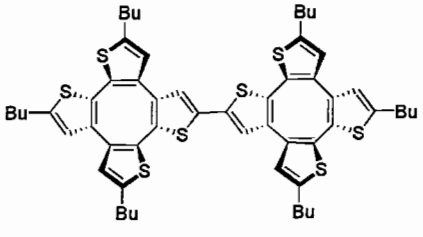

91

The Marsella group prepared a tubular sexithiophene functionalized with α-chlorides (**92**, Figure 4).[22] The chlorine atoms, while they do play a major role in the packing of the crystal, ideally were to align and resemble nanotubular structures. Kauffman previously reported the hexa[2,3-thienylene] **80**, but the research was left undeveloped for 20 years.[18]

FIGURE 4. Compounds **92**, **80**.

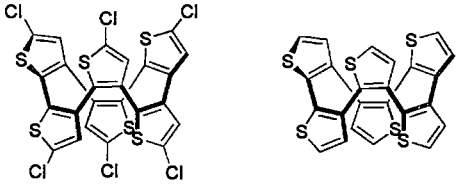

92 **80**

Synthesis of **92** was done in accordance to Scheme 16 in an alternative more direct route over the original compound **80**. In addition, the synthesis takes full advantage of the difference in reactivities of aryl bromides over aryl chlorides for lithium/palladium mediated reactions as well as the α-positions of thiophene being more reactive toward electrophilic attacks over β-positions. 3,3'-bithiophene was reacted with 2 eq. NBS followed by treatment with 2 eq. NCS to yield the tetrahalobithiophene **93** (76% yield two steps). Compound **93** was lithiated and quenched with isopropanol to proved the monobrominated **94**. Although the procedure proved troublesome, compound **94** was again lithiated and quenched with Bu_3SnCl to form the Stille adduct **95**. The resulting organotin species **95** was then cross coupled (2 eq) to the terminal bromides of **93** using $Pd(PPh_3)_4$ in toluene forming the linear sexithiophene **96** in 27% yield (two steps).

Bromination of **96** with NBS afforded the bromide **97** in 98% yield and the full cyclization was performed using a lithium halogen exchange of the bromides followed by $CuCl_2$ oxidative coupling to produce **92** in 20% yield as a colorless solid.[22]

SCHEME 16. Synthesis of macrocycle **92**.

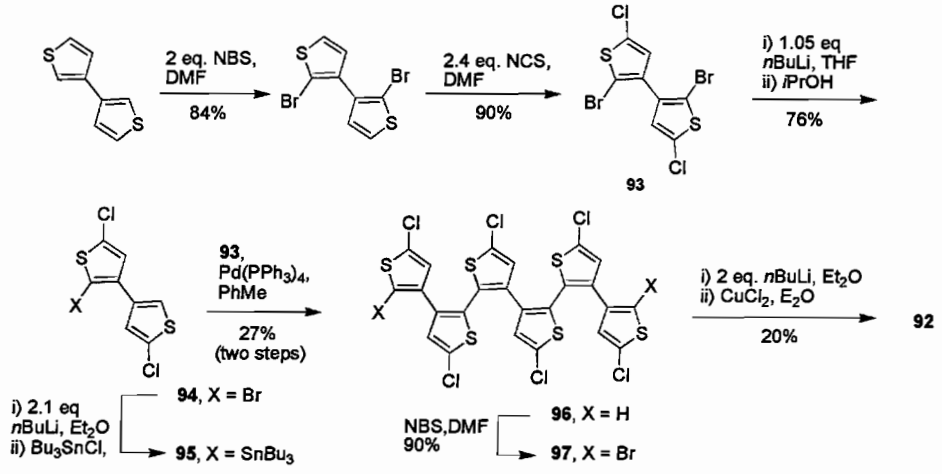

Macrocycle **92** was analyzed by X-ray diffraction and UV-Vis absorption. The compound exhibits poor π-electron overlap which is supported by the relativly high energy UV-Vis absorption spectrum (320 nm) as well as the S-C-C-S average dihedral angle of 102.7° as determined by X-ray crystallography. The compound also exhibited fairly good solubility in THF and chlorinated solvents as further evidence of nonplanarity. Crystals were obtained for X-ray diffraction from THF solutions which showed strong evidence of Cl…Cl interactions of 3.452 Å. Unfortunately the packing of the macrocycles exhibited an unexpected alternating staggered packing motif and not the desired supramolecular nanotube arrangement.[22]

Chernichenko et al. synthesized compound **98**,[23] a novel oligomeric form of carbon sulfide. The relatively strained octathio[8]circulene was prepared rather easily

and shown in Scheme 17. The tetrathiophene **82** was treated with 16 eq. LDA followed by addition of sulfur, and then quenched with HCl to form the polythiolate **99**. Vacuum pyrolysis afforded the macrocycle **98** in overall 80% yield. **98** was found to be red dark powder that was insoluble in common organic solvents.[23]

SCHEME 17. Synthesis "sulflower" **98**.

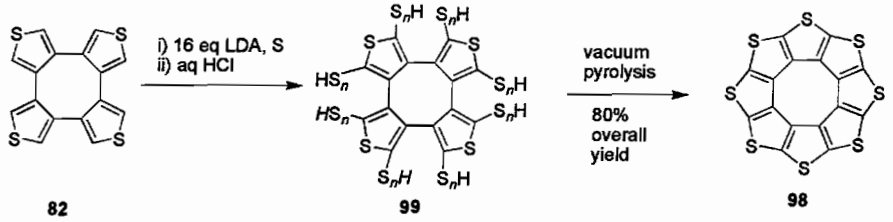

Elemental analysis and high-resolution mass spectrometry were in full agreement with the proposed structure including the predicted ratio peaks. Solid state ^{13}C NMR and IR spectroscopy confirmed **98**'s high degree of symmetry with two singlet carbon resonances at 125 and 138 ppm and intense peaks at 499, 724, and 947 cm^{-1} indicative of C-S bonds of typical of annulated thiophenes. Powder X-ray diffraction further confirmed the structure of the molecules to be relatively flat and stacked in columns separated by 3.9 Å with a tilt of approximately 131° to the adjacent stack.[23]

Macrocycle **98** was found to have rather unique magnetic properties. The compound is in fact soluble in trifluoroacetic acid and an ESR spectrum was obtained showing a broad singlet indicative of the formation of a radical cation. This radical cation should allow for further devolopment into conducting thin films.[23]

3.1 Macrocycles Composed of Thiophenes and Methyne (thioporphyrins)

The all thiophene porphyrin was prepared by Vogel and was found to have properties unique to itself, atypical of nitrogen containing porphyrins. Replacing the nitrogen atoms with sulfurs potentially lowers the band gaps in addition to further tuning the electronics of the macrocycle.[24] Although many other porphyrins containing alternative heteroatoms have been synthesized[25] this chapter will only refer to those completely composed of thiophenes. The preparation of porphyrins **100** and **101** from thiophene **102** is shown in Scheme 18. Acid catalyzed condensation of **102** formed the products **103** in 25% yield and pentacyclized product in **104** in 20% yield[24a] however the production distribution can be changed to 30% **103** and 15% **104** when using 1 eq of *p*TsOH.[24b] Compounds **103** and **104** were easily separated and purified by chromatography followed by recrystallization. Correct identification was performed with mass spectrometry as the ^{1}H NMR spectra is nearly superimpossible. Oxidation of the porphrynogens with either DDQ and $HClO_4$ for **103** and $SbCl_5$ for **104** formed the cationic porphyrins **100** and **101**. **100** was isolated as a brightly colored perchlorate salt from recrystallization in acetic acid.[24]

The formation of the thienoporphyrns as their respective cations was somewhat of a surprise and is most likely the result of a narrow HOMO-LUMO gap and possibly the sterics of the compounds. The ^{1}H NMR spectrum of the isolated porphryn dication **100** in CD_3NO_2 exhibited a far downfield shift of the *meso* protons to $\delta = 12.46$. In a less polar solvent, the proton spectrum shifts by $\Delta\delta = 0.3$, suggestive of the formation of aggregates. X-ray diffraction of suitable crystals of **100** found the compound slightly

deviated from planarity due to the steric demand of the sulfur atoms. Compound **101** was analayzed by X-ray diffraction and was found to be significantly more planar than **100**. Compound **101** as the trication still obeys Hückel's rule (π-electrons).[24]

SCHEME 18. Synthesis of porphyrins **100** and **101**.

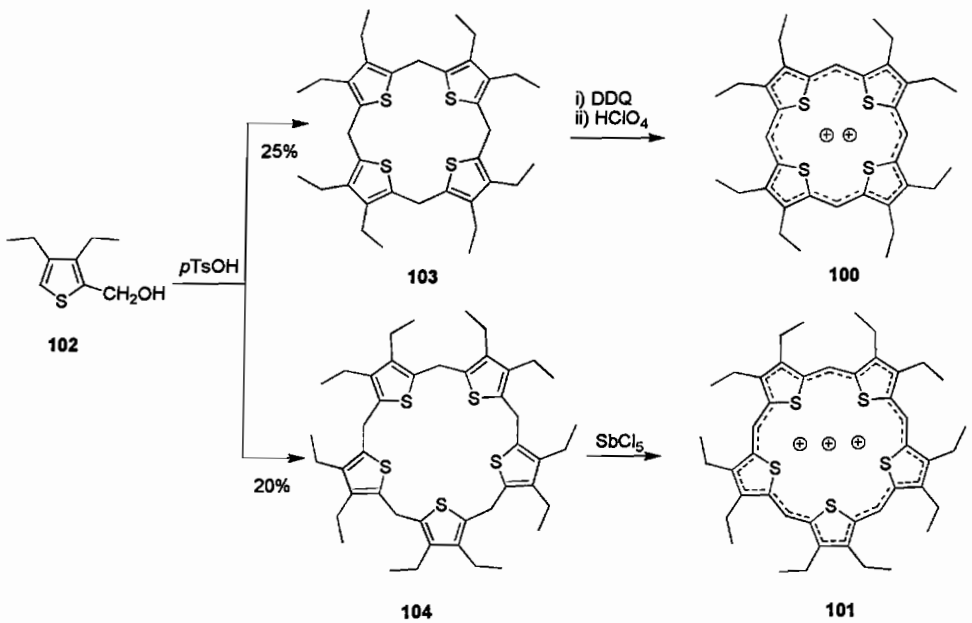

FIGURE 5. Compound **105**.

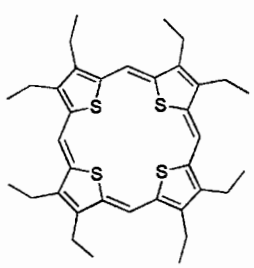

105

Electrochemistry revealed two defined half wave potentials (1 electron reduction each) of 0.37 and 0.07 V vs. Ag/AgCl in dichloromethane. Further reduction to the dianion was not observed; regardless, the formation of neutral **105** seemed feasible.[24]

Isolating the neutral porphyrin **104** was not trivial due to the instability of **104** due to extreme oxygen sensitivity. Obtaining an NMR spectrum of **105** was done by treating **100** with SmI_2 at low temperatures to yield a mixture of **100** and **105**. Due to sterics, the protons were found to be weakly paramagnetic compared to oxyporphyrins (δ = 5.26-*meso*, 2.05-methylene, 0.95-methyl). However, one simple substitution of one of the sulfurs with an oxygen produced a neutral isolable compound.[24]

Replacement of one of the *meso* protons with an electron withdrawing substituent also produces a stable neutral compound as shown in Scheme 19. The reaction of **100** with NaCN at –20 °C afforded **106** in 45% yield as a blue microcrystalline powder. The compound was found to be highly dynamic on the NMR time scale with an activation barrier between the two forms of 8.8 kcal/mol as determined by variable temperature ^1H NMR spectroscopy.[24]

SCHEME 19. Synthesis of macrocycle **106**.

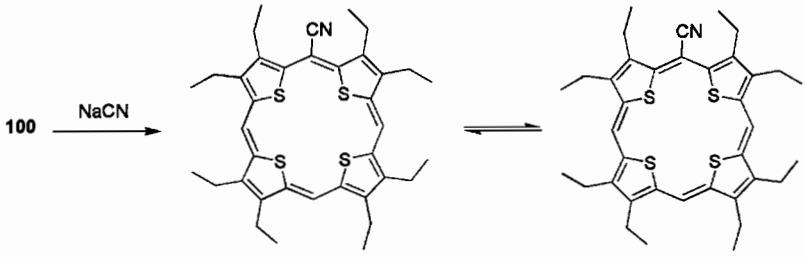

106

3.3 Macrocycles Composed of Thiophenes and Ethenes

The Cava group synthesized a number of macrocycles (**107-112**) from intermolecular McMurry homocoupling of 2,5-substituted dicarboxaldehydes.[26] The

compounds served as an aromatic probe to be compared to compound **105**; however, only a few examples gave any appreciable ring currents.[26]

FIGURE 6. Compounds **107-112**.

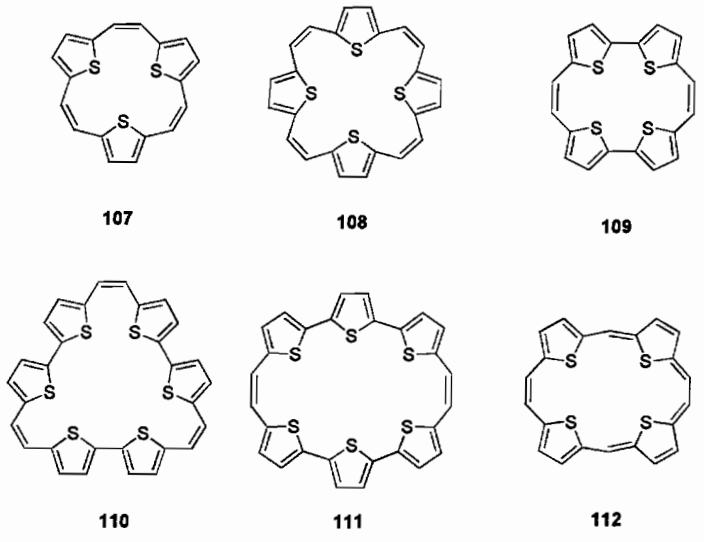

The syntheses of macrocycles **107-112** are given in Scheme 20. Compounds **107** and **108** were prepared from the McMurry coupling of 2,5-thiophenedicarboxaldehyde in 38% and 4.7% respectively among other linear oligomers and nondiscrete macrocyclic products. X-ray crystal studies confirmed that the sulfur atoms were twisted out of plane due to steric hinderance.

McMurry coupling of 2,2'-bithiophene-5,5'-dicarboxaldehyde afforded compounds **109** and **110** in 10.5% and 13.6% yields. The stability of **109** was initially suspect because of its highly strained structure and it is isomeric of **105**; however, the molecule proved to be relatively air stable and was fully characterized. **109** was isolated as a yellow solid with a UV-Vis absoporption spectrum maxima at 336, 274, 229, and 210 nm. The ^{1}H NMR spectrum showed three signals: a singlet at 6.70 ppm, and two

doublets at 6.99 and 6.78 ppm. The overall conjugation for **110** was proposed to be modest at best while attempts to further oxidize the red crystalline solid were unsuccessful. The ^{1}H NMR data was similar to **109** with peaks at 7.05 ppm, 6.98 ppm and 6.60 ppm while the electronic absorption spectrum has maximas at 384, 370, 263, and 227 nm.[26] These previous two structures were also prepared similarly and independently by Ellinger et al. in lower yield. However, the X-ray crystallography obtained by the Cava group confirmed the nonplanarity.[27]

McMurry coupling of the 5,5''terthiophenedicarboxaldehyde, **113**, afforded compound **111** in 64% yield. The macrocycle was found to be a moderately stable, dark, crystalline compound. While the ^{1}H NMR spectrum alluded to a nonplanar structure (6.94-6.26 pm), the UV-Vis absorption spectrum red shifted significantly with maxima at 431, 394, 381, 272, and 227 nm. A cyclic voltammogram of **111** produced two promising reversible oxidation peaks suggesting that the dication could be produced and isolated. Adding **111** to a H_2SO_4 solution (also Scheme 20) produced the 26π dication **114** with an ^{1}H NMR spectrum with strongly increased ring current (protons in the range of 11.28 – 12.10 ppm). The UV-Vis absorption spectrum also dramatically red shifted to produce peaks with maxima at 885, 858, and 521 nm.[26] Ellinger also reported the synthesis of compound **111** although in much lower yield (1%).[27]

Compound **112**, however, was the first reported stable, aromatic, and fully neutral all thiophene-carbon porphyrin. The synthesis, also given in Scheme 20, starts from the acid catalyzed condensation of 2-bromothiophene with dimethoxymethane to afford 2,2'methylenebis[5-bromothiophene] in 85% yield. Lithiation/formylation produces

dicarboxaldehyde **115** followed by McMurry coupling of **115** gives macrocycle **116** in 56% yield (two steps). Dehydrogenation with DDQ followed by reduction in hydrazine produced the black crystalline annulene **112** in 82% yield. Aromaticity of **112** was shown to be strong by downfield proton shifts in the ^{1}H NMR spectrum (12.34, 11.36, 10.86, and 10.84 ppm) and longer wavelength UV-Vis absorption peaks (503, 540, 579, and 771 nm). The methylene linkers of **112** limit the crowding around the sulfur atom and extend the π-electron density in the periphery thus allowing π-electron aromatic effects.[26]

SCHEME 20. Synthesis of macrocycles **108-112** and dication **114**.

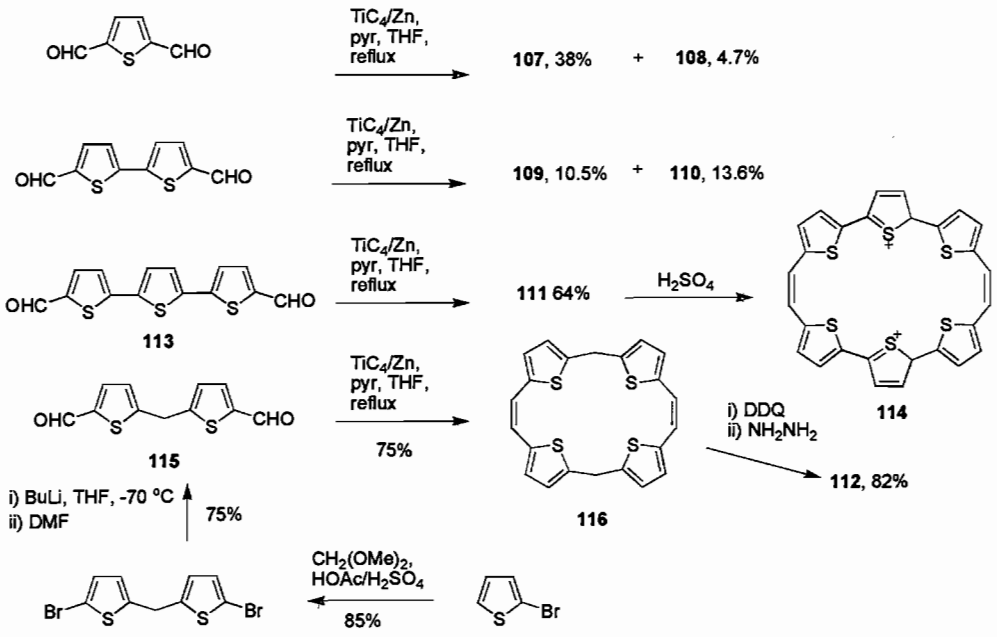

2.3.3 Macrocycles Composed of Thiophenes and Acetylenes

Expanding upon the cyclootetrathiophene model,[22] the Marsella group synthesized several subunits of the highly conjugated double helical polymer **117** (Figure

7).[28,29] Synthesize the full polymer result in significant complications due to stereochemical issues producing unproductive coupling pathways; however, the smaller subunits (**118-120**) can show promise in the development of such a polymer. [28,29]

FIGURE 7. Compound **117.**

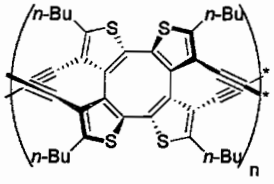

117

The tetra[2,3-thienylene] compound **118** was prepare as shown in Scheme 21.[29] Kumada coupling of the Grignard reagent from 2-methyl-5-bromothiophene (**121**) with **121** using $NiCl_{2(dppp)}$ provided the bithiophene **122** in 84% yield. NBS bromination produces **123** followed by halogen exchange yielded the iodinated compound **124** in 58% yield (two steps). Sonogashira cross coupling of TMSA produced **125** followed by deprotection furnished terminal acetylide **126** in 74% yield (two steps). Macrocycle **118** is formed from Sonogashira cross coupling of **124** to **126** in 23% yield.[28,29]

SCHEME 21. Synthesis of macrocycle **118.**

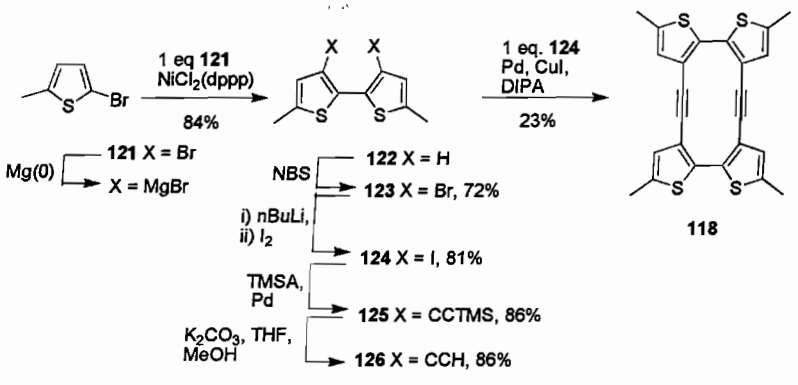

The thienomacrocycle **118** was found by X-ray crystallography to have a helical twist with two unique dihedral angles of 34.9 and 41.2 corresponding to the S—C—C—S functionalities. Ground state DFT (B3LYP/6-31G*) calculations further supported this result. Further modeling of **118** and various oxidations of **118** showed that the dihedral twisted to 0° when oxidized to $\mathbf{118}^{2+}$. This conformational change was double the predicted conformational change of **90** and results from a loss of sterics due to the extended macrocycle.[28]

The synthesis compounds **118** and **119** as further extensions of the helical polymer are shown in Scheme 22. Macrocycle **118** is a synthon to the proposed extended helical ladder polymer **117** while macrocycle **119** was shown to be a synthon to a supramolecular polymer. Previously reported bithiophene **85** was homocoupled with itself using BuLi and $FeCl_3$ to form the helical directing macrocycle **127**. Bromination of the remaining ∃-positions with bromine afforded macrocycle **128** in 90% yield. Lithium halogen exchange was performed to allow for more labile cross coupling at the ∃ position forming **129** in 85% yield. Cross-coupling **129** with TMSA under Sonogashira conditions formed synthon **118** in 82% yield while cross coupling with phenylacetylene gave compound **126** in 35% yield. The methylene protons adjacent to the thiophene rings showed by ^{1}H NMR diastereotopic protons. Interconversion of the rings is suppressed under ambient temperature.[29]

Recrystallization of compound **119** from ethanol readily afforded a supramolecular polymer bound by edge to face interactions of the phenyl groups along

the crystallographic c-axis. Such an interaction could potentially play a role in synthesizing a helical polymer.

SCHEME 22. Synthesis of macrocycles **118** and **119**.

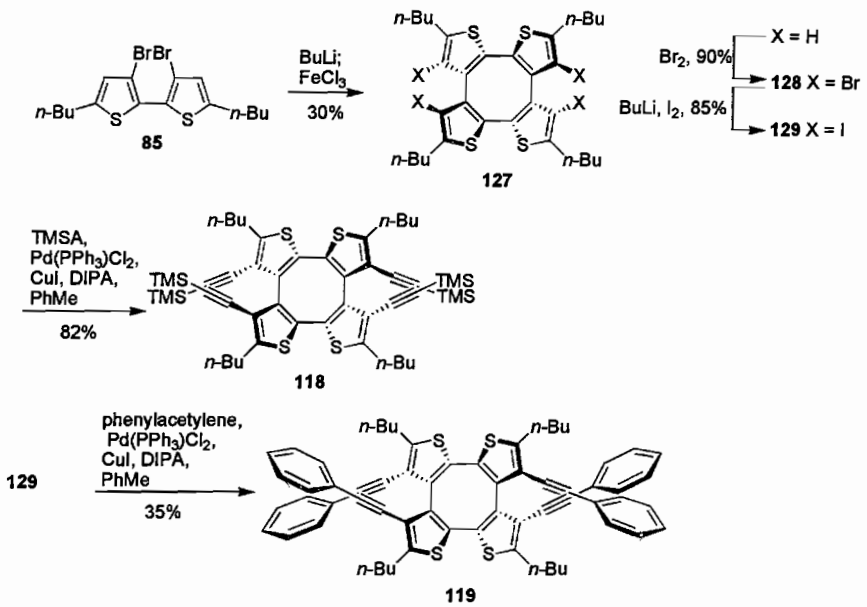

Sonogashira cross-coupling of **118** and **129** to give **117** proved to be unproductive; however, the subunit **120** can be prepared (scheme 23) thus demonstrating the viability of **117**. Lithium halogen exchange of **85** furnished **130** which was then cross-coupled TMSA under Sonogashira conditions to form the diyne **131** in 46% yield (two steps). Deprotection of the molecule with K_2CO_3 provides **132** which was then cross-coupled to **130** under highly dilute conditions to furnish **120** in 28% yield. Productive coupling of **132** occurs on average 73% yield showing that accessibility of **117** is possible.[29]

Mayor and Didschies reported the giant completely conjugated ring **133** (Figure 8) composed of acetylenes, benzenes, and thiophenes of a diameter of 11.8 nm.[30] The

giant structure was proposed to allow persistent magnetic currents in a large organic macrocycle. To observe this physical property, it was important that the ring be fully conjugated to allow total overlap of all the wave-functions and have about 6 nm radius.[30]

SCHEME 23. Synthesis of helical polymer subunit **120**.

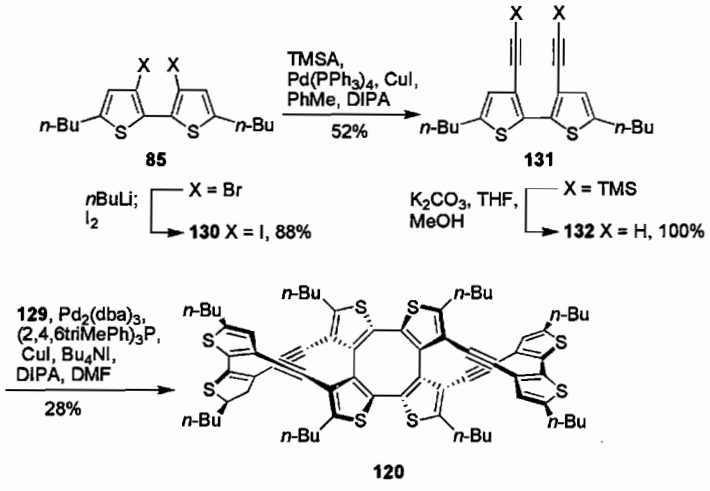

FIGURE 8. Compound **133**.

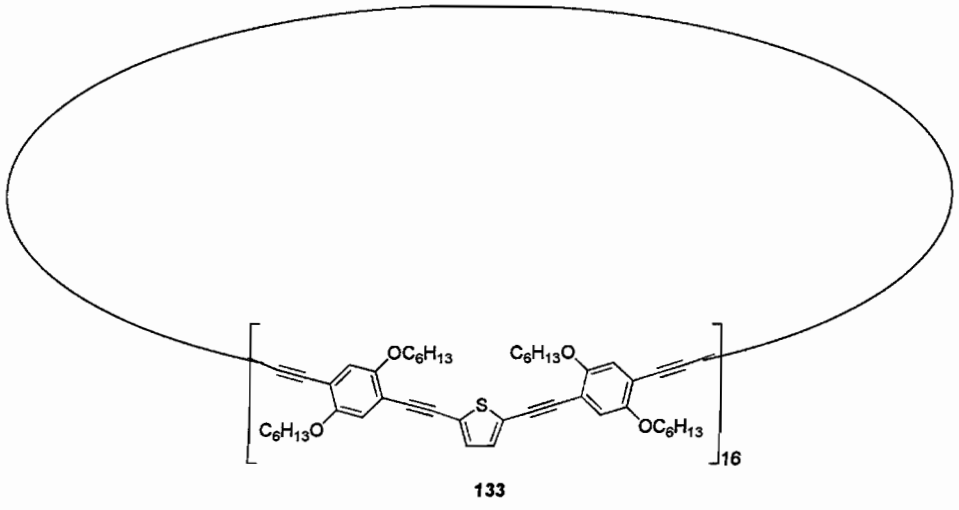

The synthesis of **133** is shown in Schemes 24 and 25. Scheme 24 shows the synthesis of the base unit **134** and begins with hydroxyquinone treated with hexylbromide

in acetonitrile which provided 1,4-dihexyloxybenzene **135**. Iodination of **135** gave 1,4-diiodo-2,5-dihexyloxybenzene (**136**) followed by mono cross-coupling with TMSA under Sonogashira conditions to afford **137**. Cross-coupling with TIPSA under similar conditions produced **138** followed by deprotection of the TMS groups gave **139.** This compound was then cross coupled at both α positions of 2,5-dibromothiophene to afford the TIPS-protected building block **134** in 19% overall yield (6 steps).[30]

SCHEME 24. Synthesis of subunit **134**.

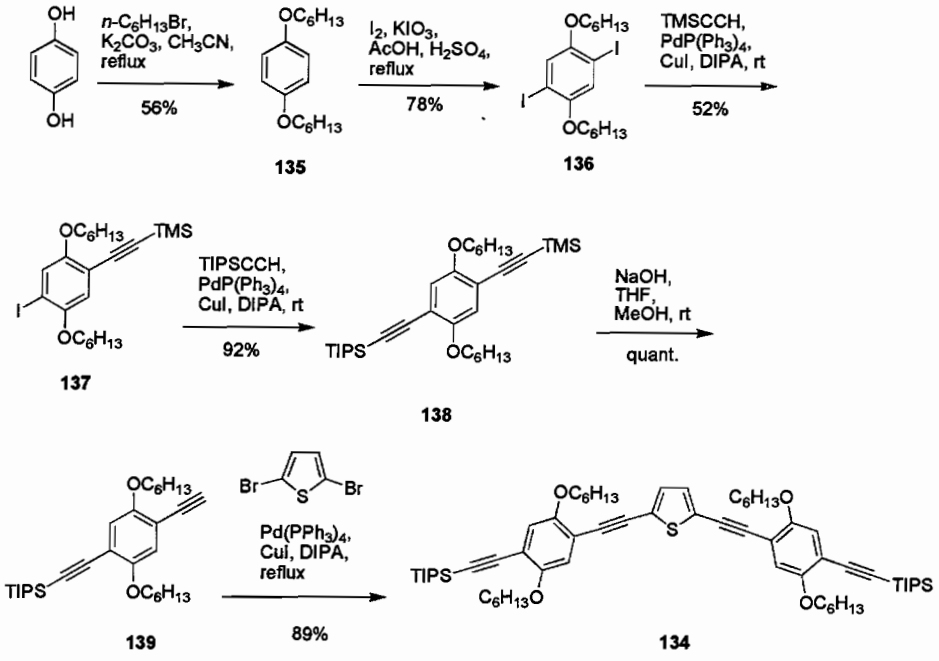

Building up the large macrocycle was done using a combination of controlled TBAF monodeprotections and diacetylenic homocouplings. Mono deprotection of **134** with TBAF in THF, trace water and acetic acid produced **140**, which was followed by oxidative homocoupling to give **141** in 47% yield (two steps). Similar monodeprotection of **141** formed **142** (and excess fully deprotected oligomer) which was subsequently oxidatively homocoupled to produce **143** (43% two steps). Monodeprotection of **143**

formed **144** in 48% yield and then homocoupled to form **145.** Deprotection of **145** furnished **146** (45% yield) and **147** the doubly deprotected precycle in 30% yield.[30]

Formation of the macrocycle was not trivial. The bis-deprotected precycle **147** was reacted under highly dilute conditions with copper acetate and pyridine to afford various cyclic oligomers. The desired product **133** was detectable under MALDI-TOF, but it was impossible to isolate discreet products. Monodeprotected **146** was then dimerized under copper oxidative conditions to form **148** (86%) which was then deprotected and cyclized under very dilute conditions (8.3 x 10^{-6}) using copper acetate and pyridine to form **133** in 38% yield as an orange glassy enamel.[30]

SCHEME 25. Synthesis of macrocycle **133**.

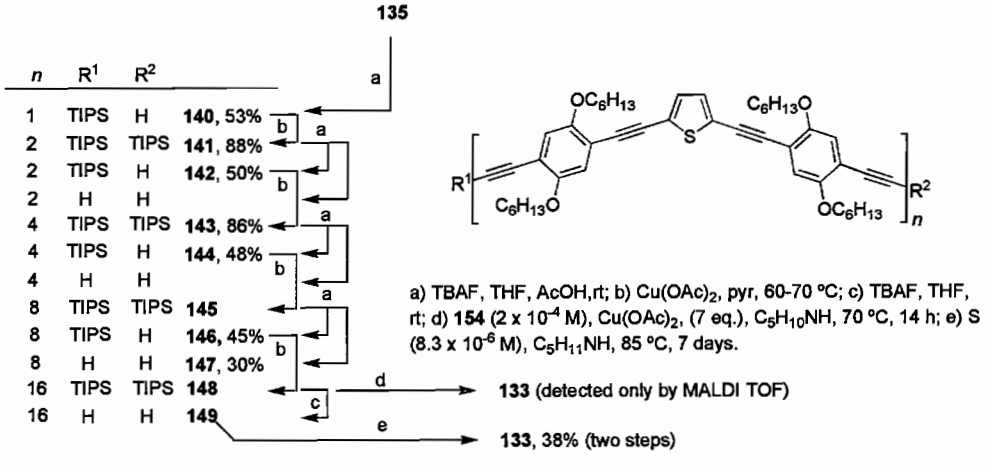

Structure **133** was characterized using ^{13}C and ^{1}H NMR spectroscopy, MALDI-TOF mass spectrometry, and UV-Vis spectroscopy. Compound **130** showed only 3 signals by ^{13}C NMR in $CDCl_3$, which resolved nicely in [D_8]THF to produce four signals (80.23, 80.54, 88.73, and 92.33 ppm). The MALDI-TOF-MS spectrum displayed one peak at *m/z* 11697 indicative of the parent peak.[30]

When UV-Vis spectra of the various oligomers of **134**, the precycle **149**, and the full macrocycle **133** were compared, there was a gradual bathochromic shift until about 461 nm. Comparison of the wavelength vs. reciprocal number of units, shows a linear fit with the maximum wavelength at infinite number units being around 462 nm, perfectly in agreement with the observed spectroscopic trend.[30]

SCHEME 26. Synthesis of Youngs' DTA **150**.

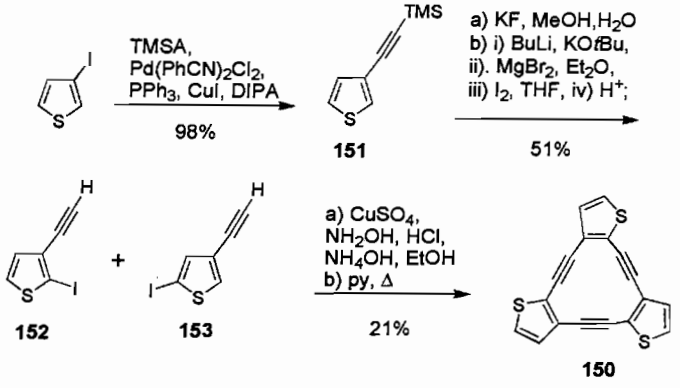

The first annulene composed entirely of thiophene and acetylene linkages (**150**) was synthesized by the Youngs group in 1990 (Scheme 26)[31]. Starting from 3-iodothiophene, cross coupling with trimethylsilylacetylene under Sonogashira conditions gave **151** in 98% yield. Deprotection and then three-step iodination afforded a mixture of **152** and **153** in a 3:1 ratio. After difficult separation, **152** was obtained in only 51% yield. Intermolecular cyclotrimerization of **152** using Cu and pyridine afforded annulene **150** in 21% yield. Yields could be improved using Sonogashira/palladium conditions.[32] The molecule was structurally characterized by X-ray crystallography and found to have a larger cavity than the [12]DBA **154** due to the outward bend of the acetylene molecules. This outward bend allowed the Youngs group to bind various metals inside the cavity

with higher affinity than **154**.[32b] It was also proposed that **150** had more electron delocalization than **154** due to lower energy IR resonance for the acetylene moieties by 14 cm^{-1}.[32] Treatment of **150** with $Co(CO)_8$ afforded a tetracobalt complex with two of the three cobalts bound to the acetylene moieties and thus distorting the geometry.

FIGURE 9. Compound **154**.

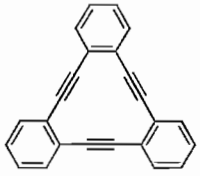

154

Further synthesis of intermolecular cyclized DTAs were performed by the Youngs group for macrocycles **155a-d** (Scheme 27).[33] Tetraiodothiophene was Sonogashira cross-coupled to two equivalents of differentially terminated alkynes to afford compounds **156a-d**. Compounds **156a-156c** were cross coupled to TMSA to afford triynes **157a-c**. **157a** and **157b** were sticky orange oils that turned darker upon standing. Compounds **157a-c** were then deprotected using KF in THF and MeOH to yield **158a-c**. In the case of the TMS terminated diyne **156d**, a Stille coupling was used to produce the free alkyne **158d**. Compound **158c** was prepared analogously to **158a,b** except being that **157c** was not purified or isolated but simply taken to the next step. Cyclizations of the triynes were all done intermolecularly to afford the macrocycles **155a-d** in 25%, 13%, 1% and 5% respectively. All compounds were isolated as white solids which gradually turned yellow and eventually brown upon standing in the air and exposed to light.[33]

Compounds **155a-d** are connected by the 3,4-thiophene bond and do not exhibit remarkable electronic delocalization in the macrocyclic ring. However, due to the long

alkyl substitutions compared to the small rigid core, it was proposed that these molecules would create excellent discotic mesophases and thus behave as liquid crystals. X-ray crystallography of **155a** showed a high degree of disorder due to the thermal motion of the alkyl groups. The disorder in the alkyl chains solvates the molecules and does not allow for interaction of the rigid cores, thus preventing the discotic mesophases from forming.[33]

SCHEME 27. Synthesis of Youngs' DTAs **155a-d**.

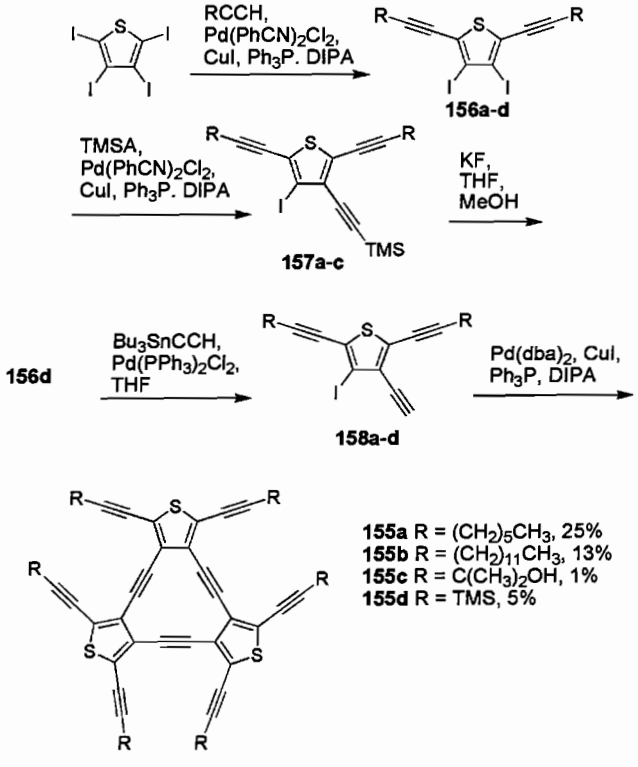

A facile synthesis of the parent 3,4 thiophene bond fused DTA **159** is shown in Scheme 28.[34] The simple reaction, where the diiodoarene was heated in either morpholine, piperidine or triethylamine/DMF mixture, afforded the macrocycle **159** in

30% yield. Addition of Ag^+ ions via $AgSO_3CF_3$ produced the alternating sandwich complex **160** as evidence by ^{13}C NMR spectra.[34]

SCHEME 28. Synthesis of Iyoda's DTA **159** and complex **160**.

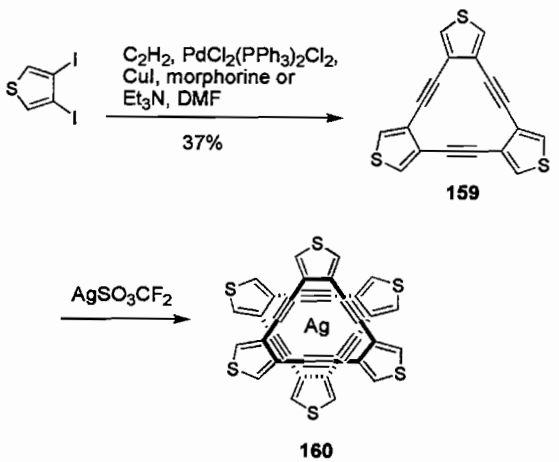

The first thiophene macrocycles containing diacetylenes **161** and **162** (Scheme 29) were synthesized by the Haley group as a probe for aromaticity in the [14]annulene framework.[35] 3,4-Diiodothiophene was cross coupled to 1-(triisopropylsilyl)-6-(trimethylsilyl)-3-hexen-1,5-diyne using an in situ deprotection and palladium catalyst to afford the precursor **163** in 67% yield. Cyclization of **163** was performed using TBAF deprotection followed by $Cu(OAc)_2$ diacetylenic homocoupling in acetonitrile furnished **161**. To produce **162**, diyne **164** was deprotected with K_2CO_3 in MeOH/THF and then cross coupled to (Z)-(4-chloro-3-buten-1-ynyl)trimethylsilane to afford the precycle **165** in 55% yield. Similar cyclization using an in situ deprotection of **165** provided **162**. Both compounds were found to polymerize very quickly when concentrated and therefore yields were not reported.[35]

SCHEME 29. Synthesis DTAs **161** and complex **162**.

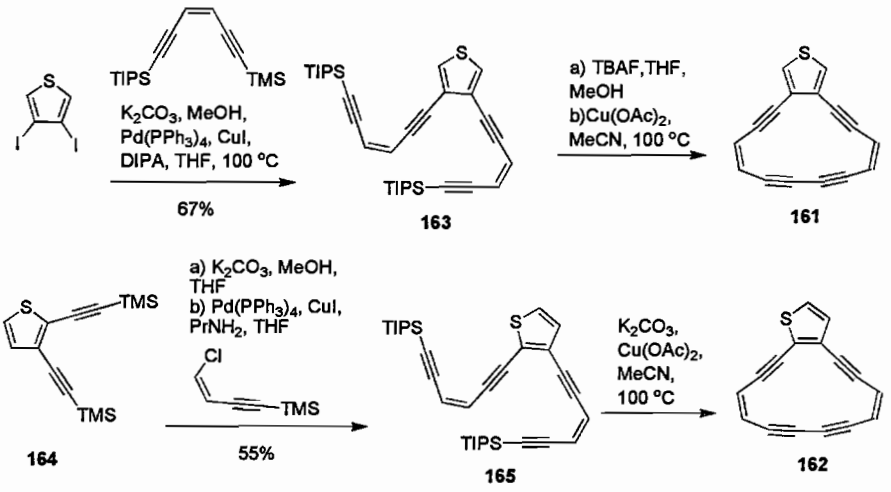

The NMR results of these two systems showed conclusively that the C3-C4 does not sustain as much conjugation in the macrocycle as does the C2-C3 bond when fused to the macrocycle. The alkene protons of **162** (7.60, 7.58, 7.02, and 6.97 ppm) are all significantly downfield shifted from **161** (6.93 and 6.32 ppm) while the UV-Vis absorption spectrum shows a slight bathchromic shift (**162**, 318 nm and **161**, 304 nm).[35]

Sarkar and Haley published some preliminary results of the synthesis of [18]DTAs **166-168** (Figure 10).[36] Macrocyles **166** and **167** both contain thiophene linkages with the C2-C3 bond fused to the macrocycle while **168** contains two thiophenes with a C3-C4 linkage in the macrocycle. The [18]DTAs were assembled intramolecularly, an example of which, **167**, is given in Scheme 30. 2-Bromo-3-iodothiophene (**169**) was cross coupled to trimethylsilylbutadiyne followed by cross coupling to triisopropylsilylacetylene to form triyne **170** in 31% yield. Triyne **170** was then deprotected in situ followed by cross coupling to 3-bromo-2-iodothiophene (**169**) to form **171** in 40% yield. **171** was then cross coupled to triyne **172** (prepared in an

analogous manner) to synthesize precursor **173** in 42% yield. Deprotection of **173** followed by ring closure furnished macrocycle **167** in 50% yield. In the UV-vis absorption of **166-168,** a slight 20 nm blue shift was observed when the C3-C4 bond was fused to the macrocycle (**168**). This is due to less double bond character in the macrocycle and thus lowering of the overall conjugation.[36]

FIGURE 10. Compounds **166-168**.

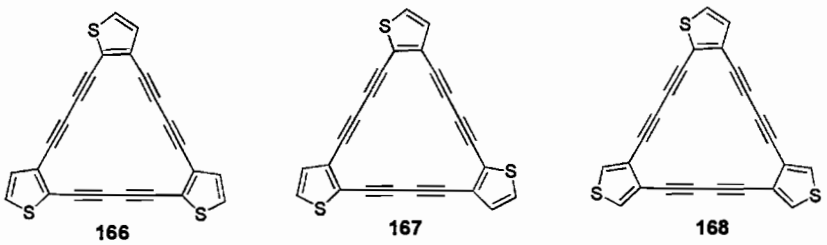

SCHEME 30. Synthesis of macrocycle **167**.

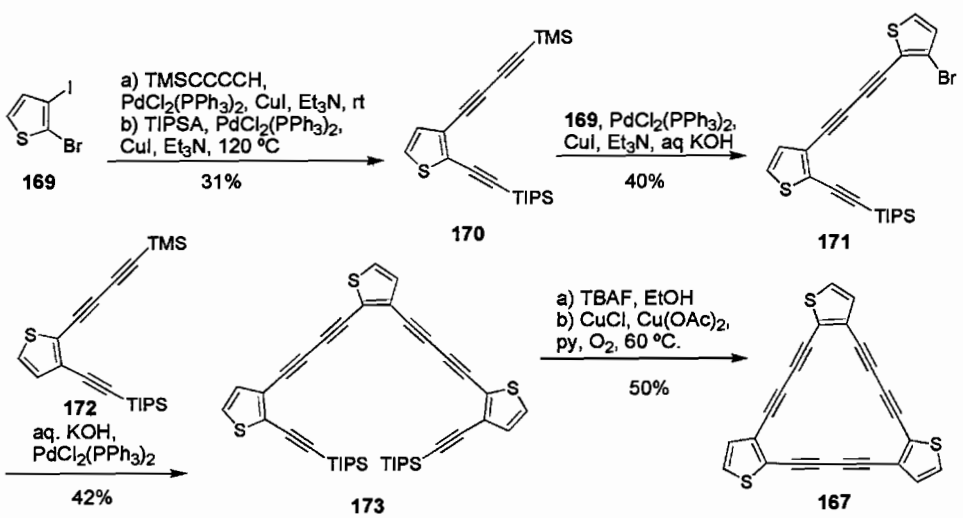

Several other [18]DTAs and [18]DTA/DBAs (Figure 11, **174-188**) were prepared by Sarkar and Haley.[37a] The [18]DTAs, when heated, exhibit sharp exotherms as shown by DSC, forming shiny black materials that were insoluble in common organic solvents.

In the case of the decylated DTA/DBAs (**178**, **180**, and **182**), heating produced an endotherm followed by an exotherm. The endotherm for the macrocycles was about 7 kcal/mol which is suggestive of a liquid crystalline phase.[37a]

Electrochemical reactivity of these [18]DTAs has also been explored. The [18]DTA hybrid **177** was oxidized irreversibly at E_{pa} = 1.31 V which is typical of thiophene polymerization; however, after each successive scan, polymer was created at the surface of the electrode that eventually passivated it, effectively creating an electron blockade in excess of 95%.[37b] The passivating polymer layer was believed to be the result of the insulating, long chain decyl groups.[37b]

FIGURE 11. Compounds **174-185**.

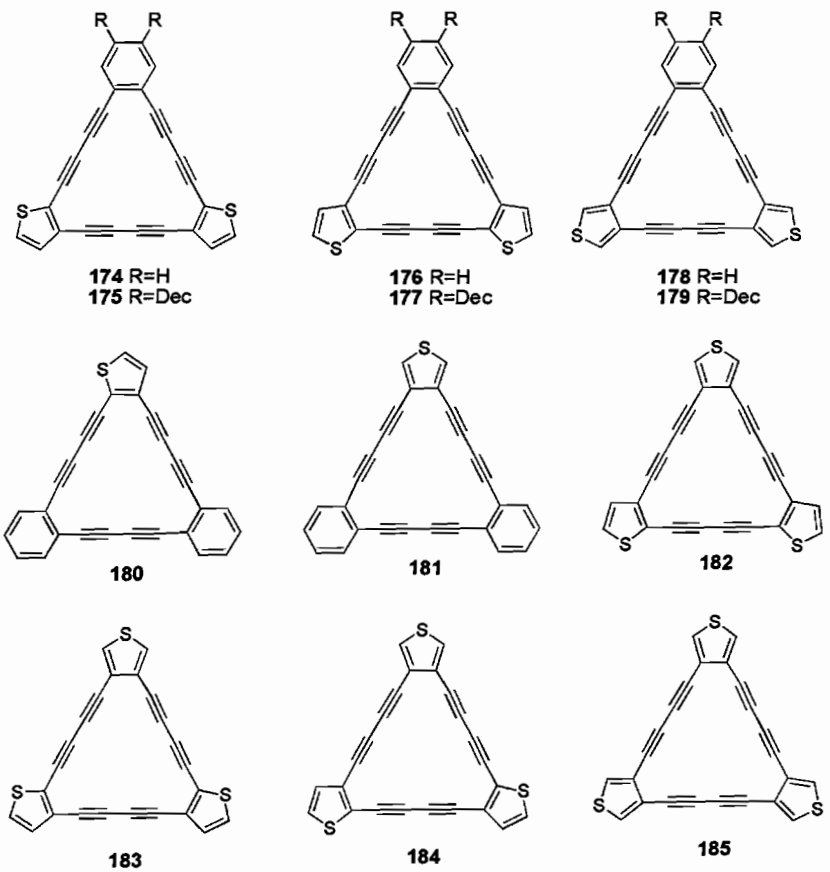

3.4 Conclusions on Thiophene Containing Macrocycles

The macrocycles presented in this review containing thiophene units all conserve conjugation around the ring to afford electron rich structures with varying degrees of electron delocalization. Assembly of these compounds were performed in a variety of stratagies to afford an array of topologies. The majority of the macrocycles were constructed using spacers such as acetylenes, ethylenes, or methynes and assembled so that the C2-C3 bonds or C3-C4 bonds were fused into the molecules. This incorporation of thiophene is not the most ideal compound for macrocycle construction due to the fact that the ideal path for electronic delocalization lies across the C2-C5 bond which does not lend itself to ideal macrocycle construction. Compounds containing the thiophene incorporation via the C2-C5 bond are usually designed to be quite large due to the strained geometries resulting from smaller macrocycles. Many thiophene systems can exhibit excellent, and sometimes quite novel, redox chemistry by stabilizing delocalized charges. Co-planarized compounds show excellent π-electron overlap and rigid character, which can perhaps be further tailored to offer enhanced optical character, including NLO. Further optimization of these systems can provide a variety of materials with tunable optical and electronic properties which warrant further investigation.

4 Conclusions

The synthesis of conjugated, cyclic, and fused thiophenes has developed significantly in the past decade, evolving well beyond the initial studies of the smaller

novel natural condensed thiophene natural products. The previously described molecules in this review have been demonstrated to be unusual and exciting targets that can serve as probes for aromaticity, nonlinear optical materials, conducting films and electrodes, and semi-conducting materials. Development of this work will continue to expand as the demand for organic materials grows. Incorporation of heteroatoms, particularly thiophenes, will continue to offer a diverse alternate avenue of highly conjugated organic systems to explore.

4 Bridge to Chapter III

Chapter III is the convergence of the aryl-diacetylene chemistry in Chapter I and the thiophene macrocyclic chemistry in Chapter II to a form a selection [14] dehydrothienoannluenes (DTAs) and DTA/DBA hybrids. These molecules exhibit behaviors similar to both annulenes and planarized thiophenes. The library of 12 macrocycles was synthesized using a convergent strategy and studied by solid-state calorimetry, x-ray crystallography, electrochemistry, UV-Vis spectroscopy, and further supported by DFT calculations.

CHAPTER III

STRUCTURE-PROPERTY INVESTIGATIONS OF CONJUGATED THIOPHENES FUSED INTO A DEHYDRO[14]ANNULENE SCAFFOLD

1 Introduction

This Chapter contains previously published material written by myself with editorial assistance from Prof. Michael M. Haley. DFT calculations were provided Robert B. Yelle and crystallography performed by Lev N. Zakharov. All substances in this report were prepared and characterized by myself.

Highly unsaturated conjugated compounds have attracted considerable attention from both synthetic and theoretical chemists in recent years.[1] In particular, alkyne-containing systems[2] have garnered the bulk of this interest, which can be attributed to two main factors. First, the advent of new synthetic methodologies for the preparation of such molecules based on organometallic cross-coupling reactions[3] has provided access to a vast array of compounds whose preparation was not possible before. Second, many of these carbon-rich molecules and macrocycles of higher dimensionality have been shown to exhibit interesting materials properties such as nonlinear optical (NLO) activity,[4] liquid crystalline behavior,[5] and molecular switching.[6] Furthermore, it has recently been demonstrated that dehydrobenzoannulenes[7] and related phenyl-acetylene macrocycles[8]

are useful precursors to a number of carbon-rich polymeric systems, such as molecular tubes,[9] ladder polymers,[10] and novel allotropes of carbon.[11] It is therefore imperative to have ready access to a wide variety of these high carbon content molecules in sufficient quantities via easy synthetic processes if their technological potential is to be harnessed.

We have been investigating alkyne-rich dehydrobenzoannulenes (DBAs)[7,12] with the aim of exploring their diverse chemical and physical properties. Over the last decade, our group has developed new or improved existing synthetic techniques for the preparation of such macrocycles. As one particular consequence, it is now possible to introduce donor and/or acceptor functional groups on the phenyl rings of the DBA in a discrete manner, thus effectively "tuning" the electronic and optical properties of the annulene.[12a] In our continuing endeavor to introduce more variations in the DBA structure for detailed structure-property relationship studies, we elected to incorporate thiophene moieties onto the dehydroannulene skeleton.[13] The choice of thiophene as the fused aromatic ring was inspired by factors such as the chemical and electrochemical polymerizability of thiophene, the ability to form two-dimensional π-systems useful for electronics and photonics, the easier polarizability of thiophene, and the interaction among the individual macrocycles due to the lone pairs on the sulfur in each thiophene ring.[14] Compared to other heteroaromatic molecules, thiophenes are easier to handle and to functionalize than furans and pyrroles, allowing ready access to tailored thiophene derivatives. By locking the conjugated unit into planarity, thiophene-containing macrocycles[15] and cyclic thiophene-acetylene hybrids[16-18] have the potential to be more

efficient materials due to enforced π-orbital overlap, increasing the quinoidal character of the delocalized system and thus lowering the optical band gap.[1]

FIGURE 1. Examples of known dehydrothienoannulenes.

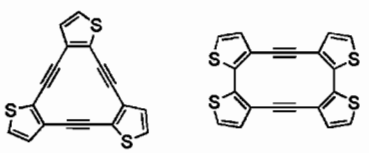

Previous work on dehydrothienoannulenes (Figure 1) by the groups of Youngs (e.g., **1**)[17] and Marsella (e.g., **2**)[18] relied on metal-mediated intermolecular couplings for molecule assembly. By virtue of the structure of the starting materials, only C_{nh}- and D_{nh}-symmetric macrocycles were produced. In order to probe the structure/property relationships among the various structural isomers, it is necessary to introduce the thiophene moieties in a systematic, stepwise manner to produce dehydrothienoannulenes (DTAs) possessing lower symmetries (C_{2v}, C_s). Our initial communication focused on the [18]DTA skeleton;[13] however, stability problems with the thienyldiyne intermediates forced us to examine other topologies. This article describes the design and stepwise preparation of thiophene-containing [14]DBAs **3-9** and the corresponding all-thiophene containing [14]DTAs **10-14** starting with a few common synthons (Figure 2). The solid state properties of **8** and **13** are investigated by X-ray crystallography. We also report the effect of structural variations on the overall effective conjugation of the macrocycles as determined by electronic absorption spectroscopy, electrochemistry, and DFT computations. Finally, we discuss the thermal properties of these macrocycles.

FIGURE 2. Target thieno-fused dehydro[14]annulenes **3-14**.

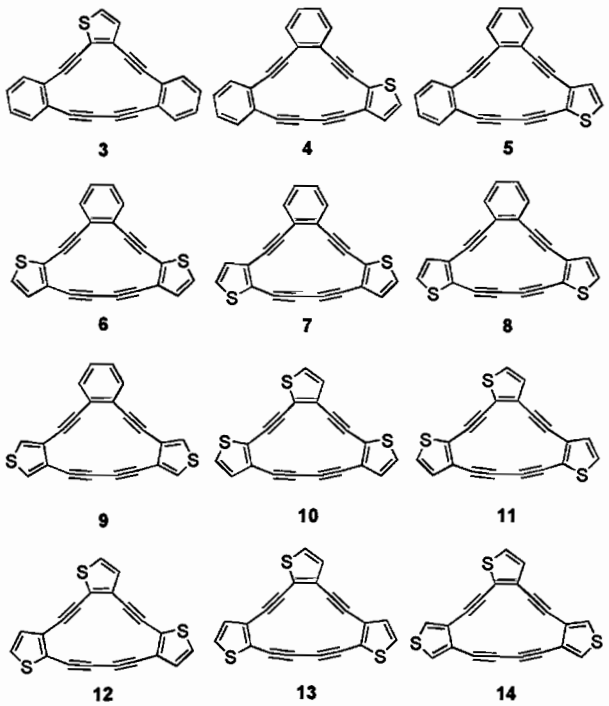

2 Results and Discussion

2.1 Macrocycle Synthesis

The use of building blocks **15-24** (Figure 3), which conforms to our previous strategies, is significant for streamlining synthetic efforts and making the assembly of thiophene-based dehydro[14]annulenes relatively convenient and facile. All macrocycles reported herein were constructed starting from the appropriate dihalothiophenes **15-18**, which were in turn prepared from commercially available thiophenes following known procedures.[20] Halides **14-16** were subsequently converted into differentially-protected diynes **20-22** by sequential Sonogashira cross-coupling with (trimethylsilyl)acetylene (TMSA) and (triisopropylsilyl)acetylene (TIPSA) in excellent yields (Table 1). The

remaining pieces were either commercially available (**19**) or prepared by literature methods (**23**, **24**).[21]

FIGURE 3. Building blocks **15-24**.

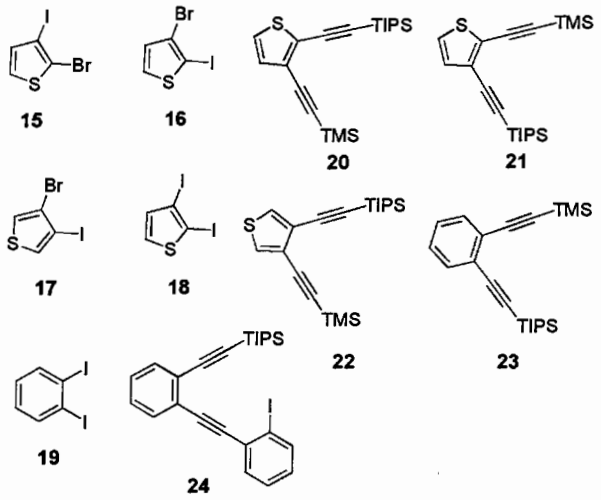

TABLE 1. Yields for Preparation of Differentially-protected Diynes 20-22.

dihalothiophene	yield TMSA cross-coupling	yield TIPSA cross-coupling (pdt)
15	96%	95%, **20**
16	94%	92%, **21**
17	95%	93%, **22**

[14]DTAs **10**, **13**, and **14** and [14]DTA/DBA hybrids **3**, **6**, **8**, and **9** possess two fused benzenes or two fused thiophenes in a symmetrical orientation on the lower portion of the annulene, and thus were assembled using a twofold coupling of the respective diyne to a central dihaloarene core. Scheme 1 illustrates a representative synthesis starting from **16**. Sequential Sonogashira reactions with TMSA and TIPSA (the latter requiring elevated heating over several days for completion) afforded diyne **21** in 91%

yield for the two steps. Selective removal of the TMS group with K_2CO_3 in MeOH followed by cross-coupling to 1,2-diiodobenzene (**19**) furnished tetrayne **25** in 86% yield. Protiodesilylation with TBAF and subsequent acetylenic homocoupling utilizing $PdCl_2(PPh_3)_2$ catalyst, CuI co-catalyst, and iodine as an oxidant[22] gave hybrid **6** in 53% yield.

SCHEME 1. Synthesis of 'symmetrical' DBA/DTA hybrid **6**.

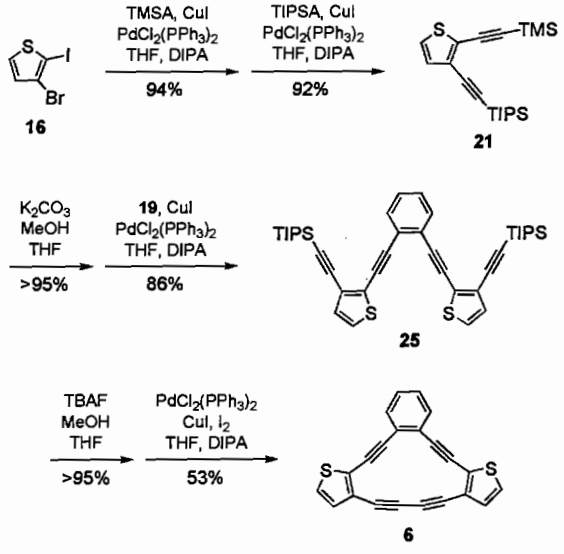

[14]DTAs **11** and **12** and [14]DTA/DBA hybrids **4**, **5**, and **7** possess two different fused arenes or two fused thiophenes in unsymmetrical orientations on the lower portion of the annulene, and are thus formed by sequential cross-couplings to the dihaloarene 'crown'. The DTA/DBA hybrids **4** and **5** were prepared by cross-coupling **21** and **22** to previously reported halodiyne **24**.[21] Scheme 2 shows a representative synthesis of an 'unsymmetrical' macrocycle, DTA **12**. Starting diyne **21** was desilylated with mild base and then immediately cross-coupled to **15**. The resultant halodiyne was cross-coupled to monodesilylated **21** to give **26** in a combined 80% yield. The macrocyclization step was

performed as before utilizing the Pd(II)/Cu(I) catalyst system under oxidizing conditions, affording **12** in 64% yield. Use of more traditional CuCl/$Cu(OAc)_2$ in pyridine for the homocoupling reactions[22b] afforded the DTAs in comparable yields. A summary of the syntheses off all twelve macrocycles is given in Table 2.

SCHEME 2. Synthesis of 'unsymmetrical' DTA **12**.

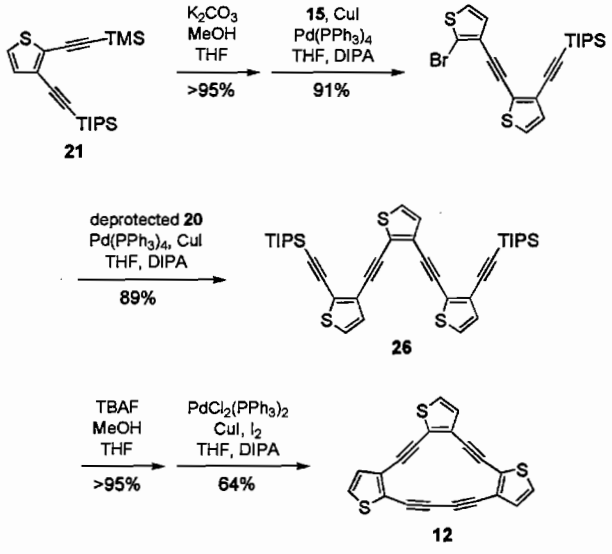

Unlike related DBA structures, the thieno-fused annulenes exhibit only moderate stability during workup and are sensitive to acid, light, and silica, which accounts for the lower than normal cyclization yields. Workups were most successful when avoiding halogenated solvents and utilizing fast chromatographic methods (chromatotron or flash chromatography). NMR characterization of the annulenes was done primarily in deuterated benzene, dichloromethane, or tetrahydrofuran. In general, those molecules with UV-vis absorptions greater than 400 nm showed the most sensitivity and/or where both sulfurs are oriented 'down' (sulfur α to the diacetylene linkage) as is the case with **8**

and **13**. Most macrocycles could be stored in solution or in the solid state for several weeks if kept cold and dark under argon.

TABLE 2. Synthesis and Yields of DTAs and DBA/DTA Hybrids 3-14.

	"equivalents" of monodesilylated diyne				precursor,	annulene,
haloarene	**20**	**21**	**22**	**23**	yield	yield
18				2	pre**3**, 90%	**3**, 62%
24		1			pre**4**, 89%	**4**, 29%
24	1				pre**5**, 64%	**5**, 33%
19		2			pre**6** (**25**), 86%	**6**, 53%
19	1 (second)	1 (first)			pre**7**, 15%	**7**, 33%
19	2				pre**8**, 90%	**8**, 32%
19			2		pre**9**, 61%	**9**, 37%
18		2			pre**10**, 67%	**10**, 30%
15	1 (first)	1 (second)			pre**11**, 28%	**11**, 30%
15	1 (second)	1 (first)			pre**12** (**26**), 81%	**12**, 64%
18	2				pre**13**, 52%	**13**, 45%
18			2		pre**14**, 47%	**14**, 38%

DSC analyses of **3-14** show that the macrocycles polymerize/decompose prior to melting to afford black solids. Hybrids **3-8** exhibit somewhat sharp exotherms, with **6** where the sulfurs are oriented 'up' reacting at a higher temperature (190 °C) than isomer **8** where the sulfurs are oriented 'down' (120 °C). In the case of the [14]DTAs **10-14**, the thermograms show two broad transitions occurring near 150 °C. All of the data are indicative of fairly disordered polymerizations. Complete decomposition of **3-14** proceeds rapidly after 200 °C.

2.2 X-Ray Structural Data

Single crystals of **8** and **13** suitable for x-ray diffraction were obtained by slow vapor diffusion of pentane into THF solutions of the macrocycle. The x-ray structure and the crystal packing of hybrid **8** are shown in Figure 4. The main structural unit of **8** consists of layers of four molecules joined by intermolecular $\pi....\pi$ and S...S interactions. Two molecules lie in the same plane (planar within 0.12 Å) and are additionally connected by two S...S interactions (S...S distances of 3.61 Å). The remaining two molecules are above and below the average plane of the pair in such a fashion that the four S atoms in these molecules form a rectangle with S...S distances in the range 3.75-3.88 Å. In the crystal these structural units are connected by S...S contacts (4.10 Å), forming infinite chains. The arrangement of the molecules clearly indicates that intermolecular S...S interactions play an important role in the association of the molecules in the crystal structure of **8**, and are in good agreement with known directional preferences of non-bonded atomic S...S contacts with divalent sulfur which could be explained based on its orbital orientation.[23]

The packing of the molecules in the crystal structure of [14]DTA **13** is different than that found in **8**. The two nearest molecules have opposite orientation to form pairs (Figure 5a) and these pairs are stacked in the crystals of **13** in columns (Figure 5b). Some of the S...S intermolecular contacts are in the range 3.60-3.82 Å and thus comparable with typical intermolecular S...S contacts;[23] however, other S...S contacts in **13** are significantly longer (4.37 Å). The four-molecule packing arrangement found in **8** is not present in **13**. The S(3) atoms in both symmetrically independent molecules are

disordered over two positions which indicates that there are no directional preferences of non-bonded atomic S...S contacts in **13**. Interestingly, neither crystal structure contains the packing motif conducive for topochemical polymerization,[24] which is found in the parent [14]DBA **28**,[25] nor are the α-positions of the thiophenes in reasonable proximity for subsequent reactivity. This likely explains the broad featureless exotherms observed in the DSC scans.

FIGURE 4. (a) X-ray structure of [14]DTA/DBA hybrid **8**; ellipsoids at the 30% probability level. (b) Fragment of the crystal packing of **8** showing S…S interactions.

(a

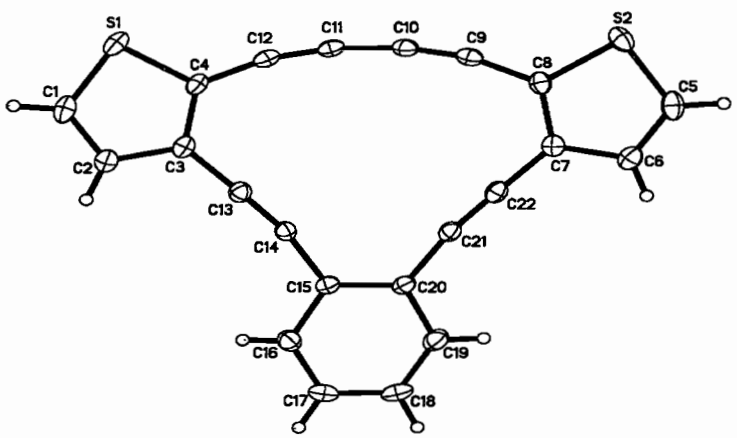

(b)

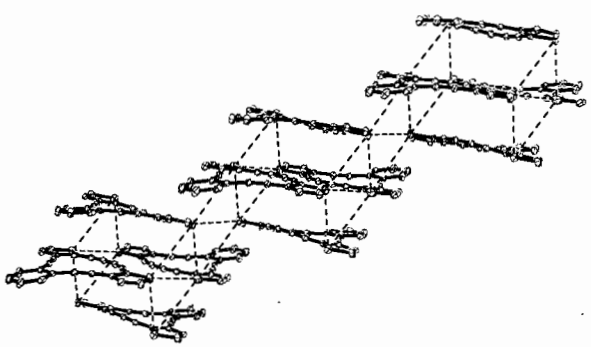

The molecular structures of **8** and **13** are essentially planar and show the typical bowed diacetylenic linkage found in a strained dehydro[14]annulene core.[25,26] The sp-carbon bond angles of the diyne bridges in **8** (166.2-169.9°) and **13** (166.0-170.9) are nearly the same as those in **28** (168.8-171.4°). For the monoyne linkages less strain is contained in the sp-carbon nearer the diyne unit (175.2-178.9°) than the sp-carbon proximal to the arene 'crown' (168.5-174.2°).

FIGURE 5. (a) X-ray structure of [14]DTA **13**; ellipsoids drawn at the 30% probability level. Only one position for the disordered atoms is shown. (b) Crystal packing of **13**.

(a)

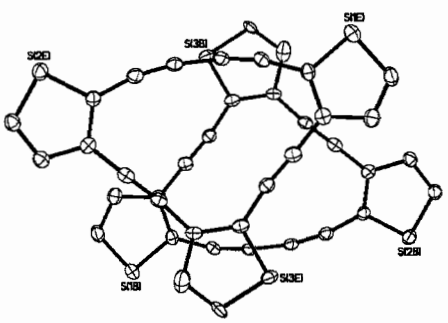

(b)

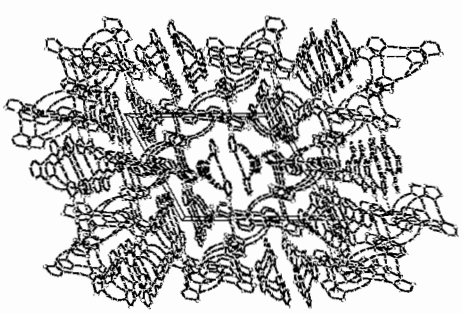

2.3 NMR Analysis

Previous work on the octadehydro[14]annulene framework, common to molecules **3-14** as well, examined the effects of thienoannelation and successive benzannelation (e.g., **27-29**, Figure 6) upon the diatropicity of the 14-membered ring.[27] Experimentally these alterations were studied by analyzing the changes of the NMR chemical shifts of the alkene protons within the series of macrocycles and with their acyclic precursors. Such effects can also been observed on the fused-benzene and thiophene protons due to ring-current competition, though to a smaller degree.[28] Although they do not possess sensitive alkene protons, annulenes **3-14** exhibit distinct downfield shifts of their arene protons upon cyclization, indicative of a diatropic current in the central 14-membered core. As opposed to an exhaustive discussion of all twelve annulenes, we will focus on [14]DTA/DBA hybrids **6-9** due to the two different aryl groups and C_{2v}-symmetry (or near symmetry), which makes interpretation of the data easier. The arene proton chemical shifts of **6-9** and of their acyclic precursors along with the corresponding data for **27-29** are given in Table 3.[29] The proton labeling scheme is shown in Figure 6.

FIGURE 6. Proton labeling scheme in Table 3 for hybrids **6-9** and known [14]annulenes **27-29**.

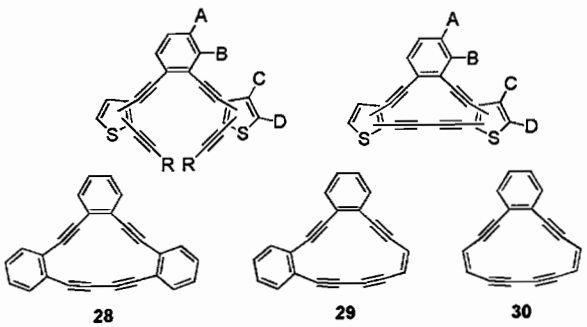

TABLE 3. ^{1}H NMR Chemical Shifts (δ, ppm) of [14]Annulenes 6-9 and Their Precursor Tetraynes in CD_2Cl_2, and Comparison with Known [14]Annulenes 28-30

	Benzene		Thiophene	
Cmpnd	proton A	proton B	proton C	proton D
25 (pre-6)	7.36	7.55	7.24	7.07
6	7.61	8.10	7.53	7.26
pre-7	7.34	7.53, 7.51	7.22, 7.15	7.13, 7.07
7	7.61, 7.58	8.12, 8.09	7.60, 7.53	7.50, 7.25
pre-8	7.33	7.52	7.19	7.04
8	7.60	8.12	7.60	7.51
pre-9	7.30	7.52	7.49	7.45
9	7.39	7.75	7.75	7.47
Pre-27[a]	7.34	7.56		
27[b]	7.43	7.89		
Pre-28[c]	7.33	7.54		
28[c]	7.64, 7.56	8.11, 7.99		
Pre-29[c]	7.32	7.50		
29[c]	7.72	8.28		

[a]Reference 29; in C_6D_6. [b]Reference 25; in $CDCl_3$. [c]Reference 27b.

Examination of the ^{1}H NMR spectra of all seven precyclized molecules shows that the range of chemical shifts of the distal and proximal benzene protons (A and B, respectively) is extremely small – 7.30-7.36 ppm for A and 7.50-7.56 ppm for B. These values are essentially the same as in 1,2-diethynylbenzene (7.29 and 7.50 ppm),[28b] suggesting very little or no influence from the group(s) appended at the end of the 1,2-diethynyl linkages. Upon macrocyclization, protons A and B in hybrids **6-8** move downfield to 7.58-7.61 and 8.09-8.12 ppm, respectively. Although **6-8** differ in the orientation of the thiophene rings, the results show that this structural variation has no effect on the remotely located benzene protons. The change in shifts, $\Delta\delta \approx 0.25$ ppm for

A and 0.55 ppm for B, are similar in magnitude to those in **28**, which suggests that two 2,3-fused thiophene rings have approximately the same bond-fixing ability as one fused benzene ring.[30]

Interestingly, 3,4-fusion of the two thiophenes in **9** results in downfield shifts of protons A and B about half as large as those in **6-8**, and slightly smaller than in **27**. The 3,4-bond in a thiophene ring well known to possess less double bond character than the 2,3-bond.[31] This results in less efficient delocalization in the 14-membered nucleus of **9** and thus poorer bond-fixing ability compared to **6-8**. Alternatively, the difference in character between **6-8** and **9** can also be explained by viewing **9** as a dehydrobisthia[20]annulene with two zero-bridges, in which 22 π-electrons are delocalized over the whole periphery, while **6-8** are bisthieno-annelated dehydro[14]annulenes. Following the usual trend, the larger annulene **9** is less aromatic than the effectively smaller annulenes **6-8**.[7b]

Thiophene protons C and D resonate in the range of 7.04-7.13 and 7.15-7.24 ppm for the precyclized molecules, and move ca. 0.3-0.4 ppm downfield upon forming **6-8**. In general the thiophene doublets are farther downfield where the thiophenes are oriented 'down' (e.g., **8**) are than isomers with thiophenes oriented 'up' (e.g., **6**). As with the benzene proton shifts above, asymmetric **7** displays features that are a combination of both **6** and **8** (Table 3). In the case of **9**, the thiophene proton shifts and change in shifts are comparable to **6-8**. While puzzling, we will table further discussion to avoid the possibility of overinterpretation.

2.4 Electronic Absorption Spectra

The electronic absorption spectrum of parent [14]DBA **28** shows a weak, low-energy absorption at 365 nm.[25] In comparison, the analogous band in the spectra of monothiophene [14]DTA/DBAs **3-5** (Figure 7a) displays a gradual bathochromic shift indicative of a narrowing optical band gap. Replacing the benzene 'crown' with a 2,3-fused thiophene as in hybrid **3** shifts this absorption to 378 nm. Macrocycles **4** and **5**, where a 2,3-fused thiophene has replaced one of the side benzene rings, afford absorption bands at 386 and 391 nm, respectively. Incorporating a thiophene into the macrocycle slightly increases the dipole moment, while thiophene orientation affects the net dipole moment as the sulfur orientation changes from 'up' in **4** to 'down' in **5**.

FIGURE 7. UV-vis absorption spectra of (a) **3-5**, (b) **6-9**, and (d) **10-14**. All spectra recorded in CH_2Cl_2 at analyte concentrations of 15-25 μM.

(a)

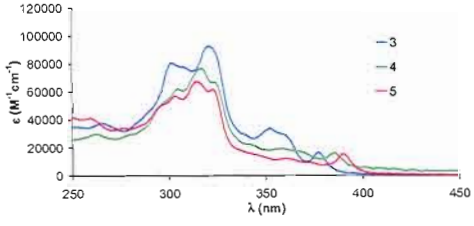

(b)

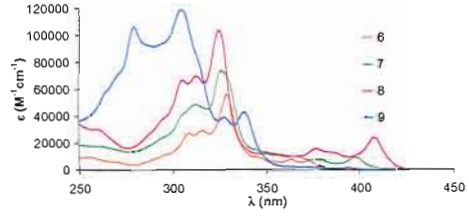

(c)

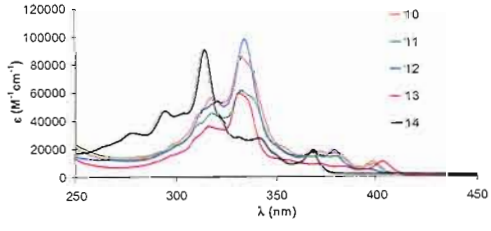

The UV-vis spectra of the macrocycles incorporating two thiophenes are given in Figure 7b. As noted above, changing the sulfur atom orientation from 'up' to 'down'

progressively shifts the low-energy absorption further into the red, from 373 nm for **6** (both 'up') to 398 nm for **7** ('alternating'), then to 408 nm for **8** (both 'down'). The extinction coefficients for similar bands also increase correspondingly. In the case of [14]DTA **9**, however, this band blue shifts to 339 nm, reflecting the weaker conjugation of the 3,4-fusion of both thiophenes and analogous to behavior previously observed for the larger [18]DTAs.[13]

Interestingly, the absorption spectra show little difference between **6-8** and **10-13**, where in the latter series three thiophenes are 2,3-fused onto the dehydro[14]annulene backbone (Figure 7c). The most red-shifted is DTA **13** at 408 nm (sulfurs 'down'), the same wavelength as **8**, while the most blue-shifted annulene is **12** at 395 nm (sulfurs 'alternating'). DTAs **10** and **11** share approximately the same peak at 400 nm and have very similar UV-Vis absorption spectra. As before, switching to 3,4-fusion as in **14** results in weaker overall conjugation and thus the lowest energy band appears at 368 nm. Changing solvents from CH_2Cl_2 to toluene results in nearly identical absorption spectra for **3-14**. The observed electronic transitions for this class of macrocycles are most likely $\pi \rightarrow \pi^*$ with small variations in vibronic structure.

2.5 Electrochemistry

Cyclic voltammograms (CV) were taken of macrocycles **6-14** using a Pt disk working electrode, Ag wire reference, and Pt swirl auxiliary in CH_2Cl_2 solutions of TBAHFP and referenced to ferrocene. Table 4 lists the energies for the first oxidation and first reduction waves for **6-14**. Unlike a majority of thiophenes, which produce well-

behaved CVs, the CVs of the DTAs and DBA/DTA hybrids were complex. Scanning in the positive potential direction generated one and perhaps two irreversible oxidations, while scanning negatively produced three (sometimes more) quasi-reversible reductions. The oxidation peak became more difficult to find when the oxidation peak occurred either at or concurrently with the CH_2Cl_2 solvent window. Unlike previous studies,[16,17] inclusion of multiple acetylene linkages alters the typical redox behavior of thiophenes in a deleterious manner.

TABLE 4. Optical Band Correlations of Selected [14]DTAs and [14]DBA/DTA Hybrids.

Cmpd	Lowest Energy Abs. $\lambda_{max.}$ [nm] (cut-off)	Optical Band Gap [eV]	Electro-chemical Band Gap [eV]	DFT Calculated Band Gap [eV]	Epa (ox) (vs. Fc)(*calc.*) [V]	Epa (red) (vs. Fc) [V]	Calculated Dipole [D]
6	374 (380)	3.26	3.26	3.53	1.39 (1.10)	-1.87	1.46
7	398 (410)	3.12	3.12	3.39	1.38 (1.04)	-1.74	2.91
8	408 (420)	3.04	2.93	3.26	1.12 (0.97)	-1.81	3.99
9	339 (360)	3.66	3.39	3.97	1.60 (1.24)	-1.79	2.33
10	399 (410)	3.10	2.87	3.37	1.13 (1.01)	-1.74	1.02
11	399 (410)	3.10	2.72	3.41	1.19 (0.97)	-1.54	2.58
12	395 sh (410)	3.16	3.09	3.48	1.32 (1.06)	-1.77	2.08
13	404 (414)	3.06	2.82	3.34	1.18 (1.05)	-1.64	3.53
14	368 (370)	3.37	3.39	3.63	1.62 (1.13)	-1.81	1.66

Thiophenes are well known to form conductive polymers and films, either chemically or electrochemically, that possess appreciable charge mobilities and can be used to sense ions with a very high degree of selectivity.[14] Small amounts of these films can be easily prepared from a monomer solution by applying a potential and then observing the behavior of the film formed on the electrode. Unfortunately, **6-13** did not behave in an analogous manner, instead yielding uncharacterizable, non-conducting

materials. Only DTA **14** polymerized on the electrode with repeated oxidative scans to afford a shiny black material that is still under study.

2.6 Computations

DFT calculations (B3LYP/6-311G**)[32] were performed on [14]DTA/DBA hybrids **6-9** and [14]DTAs **10-14** to help elucidate the observed trends. The calculated HOMO-LUMO energy gaps from the optimized structures, along with the HOMO-LUMO gaps experimentally determined from optical and electrochemical data, are given in Table 4. Although the computed values overestimate the experimental HOMO-LUMO gaps, the numbers are in good overall agreement with the observed trends. For hybrids **6-9**, the ordering of the band gaps is in excellent agreement among all three methods. The narrowest band gap (2.93-3.26 eV) corresponds to **8** with the sulfurs 'down', while the widest band gap (3.39-3.97 eV) corresponds to **9**, attributable to the 3,4-fusion of the thiophenes. Macrocycles **6** (sulfurs 'up') and **7** (sulfurs 'alternating') lie in between these bookend values (Table 4).

For all-thiophene DTAs **10-14**, there is excellent agreement of band gap ordering between the calculated and optically determined numbers. Given the aforementioned difficulties in obtaining the CVs, it is not surprising that ordering in the electrochemical data is slightly off for the 2,3-fused systems. Nonetheless, 3,4-fused DTA **14** has the widest band gap (3.37-3.63 eV) analogous to **9**. As with **8**, the sulfurs 'down' orientation of **13** is the smallest value of the all-thiophene series, in excellent agreement with the optical band gap trend, and in close agreement with the electrochemical band gap trend.

The pattern of relative sulfur orientation ('up', 'down', 'alternating') and the resultant effect on optoelectronic properties, while not observed for the [18]DTAs,[13] is an unmistakable feature in the [14] series. One possible correlation is the increase in dipole moment (Table 4): as the sulfur orientation switches from 'up' to 'alternating' then to 'down', there is a small increase in the dipole moments and thus diminishing band gaps. The dipole moments, however, are sufficiently small to begin with, which accounts for apparent lack of solvatochromism. Another consideration is the repulsion between the sulfur electrons adjacent to the bowed alkynes. When examining thiophene cyclooligomers, the sulfur-sulfur repulsion of a bent chain, as in the case of Bäuerle's cyclic thiophenes,[15] blue shifts the absorption spectra of the molecule with respect to a linear oligomer containing the same number of repeat units. This could be similar to a lone pair-alkyne interaction that could be causing the hypsochromic shifts.

The computed molecular orbital plots for **6-14** (Figure 8) show that there is little charge separation in the HOMOs and LUMOs across the entire series of molecules, thus confirming the $\pi \rightarrow \pi^*$ nature of the transitions in the electronic absorption spectra. For example, macrocycles **6-8** have HOMOs and LUMOs that topologically look very similar; thus, it is difficult to glean any meaningful information regarding the effects of sulfur orientation. The same can be said for DTAs **10-13**. The orbital plots for **9** and **14**, however, illustrate the dramatic difference between 2,3-fused and 3,4-fused macrocycles. The order of the HOMOs and LUMOs is swapped, i.e., the HOMO and LUMO of **6-8** and **10-13** correspond to the HOMO–1 and LUMO+1, respectively, of macrocycles **9** and **14**. In addition, HOMO-LUMO electron density of **9**/**14** is concentrated on the 1,2-

bis(thienylethynyl)benzene portion of the molecule, not the diacetylene linkage. The electron density shifts to the diacetylene in the HOMO–1 and LUMO+1. The 3,4-fusion, and thus reduced double bond character, significantly disrupts the net conjugation of the entire macrocycle

FIGURE 8. Calculated HOMO/LUMO plots of (a) [14]DBA/DTA hybrids **6-9** and (b) [14]DTAs **10-14**.

a)

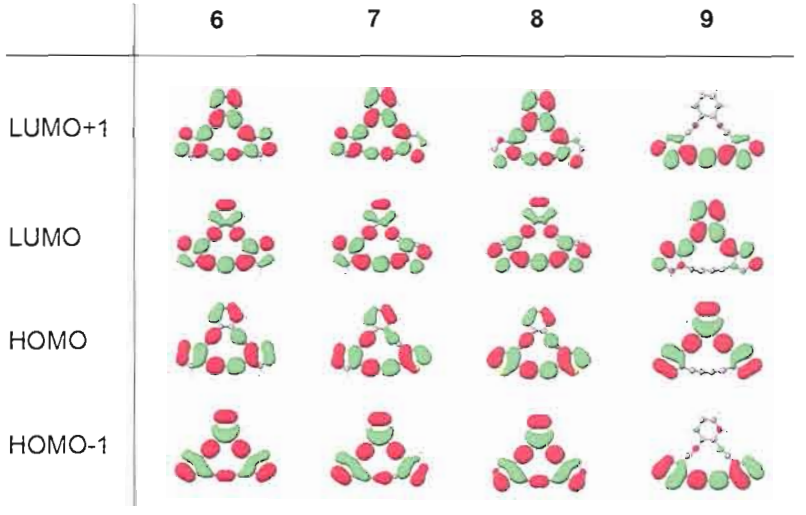

b)

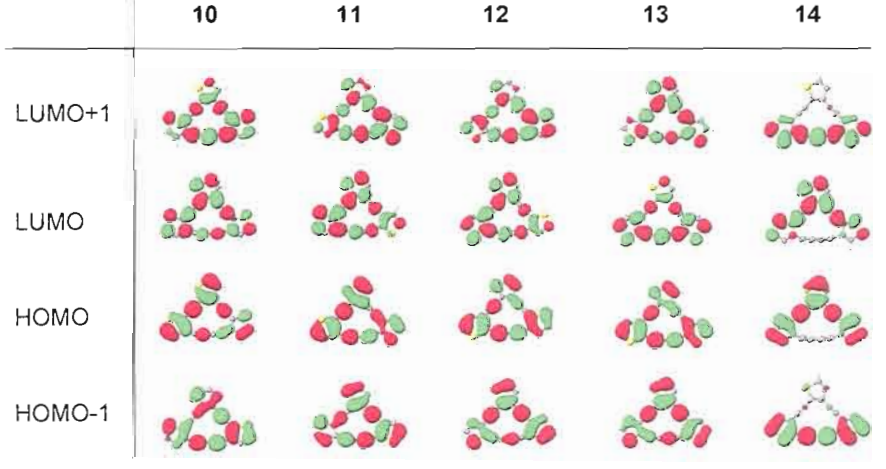

3 Conclusions

A series of twelve dehydro[14]annulene macrocycles successively fused with one (**3-5**), two (**6-9**), or three thiophene rings (**10-14**) has been prepared. Locking the entire π-system into planarity helps to promote orbital overlap, optical tunability, and increased ring currents in the macrocycles. The net electronic delocalization of these annulenes is greater than previously reported thiophene macrocycles, attributable to the rigid structure and aromatic nature of the [14]DBA ring further enhanced by the electron richness of the thiophenes themselves. The downfield chemical shifts in the ^{1}H NMR spectra show evidence of increased delocalization and enhanced ring current. Furthermore, the arrangement and number of thiophenes in the macrocycle dramatically affects the HOMO-LUMO band gaps of the molecules, with the 'down' orientation of the sulfurs in 2,3-fused systems (**8**, **13**) affording the lowest energies, as confirmed by UV-vis, electrochemical, and computational data. These data also show that the 3,4-fused macrocycles (**9**, **14**) possess the highest HOMO-LUMO energy gaps. X-ray crystal structures of **8** and **13** exhibit solid-state packing behavior unfavorable towards topochemical polymerization, thus explaining the broad exotherms found from DSC scans. While the electronic delocalization most likely creates molecules more similar to annulenes than thiophenes oligomers, this class of macrocycles is unique in its own way. Further studies are focusing on alkyl-stabilized [14]DTAs and on closely related [15]DTAs; this work will be reported in due course.

4 Experimental Section

General Methods. These are described in reference 12a. Dihalothiophenes **15-17**[20] and diynes **21**,[12c] **23**,[21] and **24**[21] were prepared according to known procedures.

2-(Triisopropylsilylethynyl)-3-(trimethylsilylethynyl)thiophene (20). 2-Bromo-3-iodothiophene (**15**, 3.0 g, 10 mmol), CuI (125 mg, 0.7 mmol), and $PdCl_2(PPh_3)_2$ (251 mg, 0.033 mmol) were dissolved in DIPA (100 mL) and THF (100 mL). The solution was degassed under Ar for 30 min. Through a syringe, TMSA (1.5 mL, 10.6 mmol) was added and the mixture stirred at room temperature in a sealed vessel overnight. The solvent was removed under reduced pressure and the crude mixture was run through a silica plug (5:1 hexanes/CH_2Cl_2, 300 mL) and then concentrated. The residue was dissolved in DIPA (100 mL) and THF (100 mL), CuI (125 mg, 0.7 mmol) and $PdCl_2(PPh_3)_2$ (251 mg, 0.033 mmol) were added, and the mixture was degassed under Ar for 30 min. Through a syringe, TIPSA (10 mL, 47 mmol) was added and the mixture stirred at room temperature in a sealed vessel overnight. The solvent was removed under reduced pressure and the residue chromatographed on silica (hexanes) to afford **20** (3.2 g, 91%) as an orange oil. ^{1}H NMR (300 MHz, $CDCl_3$) δ 0.24 (s, 9H), 1.15 (s, 21H), 6.98 (d, J = 5.3 Hz, 1H), 7.08 (d, J = 5.3 Hz, 1H); ^{13}C NMR (75 MHz, $CDCl_3$) δ –0.1, 18.8, 98.0, 98.3, 98.7, 100.0, 125.5, 127.0, 127.2, 129.8; IR (NaCl) ν 2153, 2865, 2993, 2943 cm^{-1}; MS (APCI) *m/z* (%) 431.2 (100, M^+ + THF), 359.1 (30); HRMS (EI) for $C_{20}H_{23}SSi_2$ $[M]^+$: calcd 360.1770, found 360.1763.

3-(Triisopropylsilylethynyl)-4-(trimethylsilylethynyl)thiophene (22). 3-Bromo-4-iodothiophene (**17**, 4.7 g, 15.4 mmol), CuI (29 mg, 0.15 mmol), $PdCl_2(PPh_3)_2$ (61 mg,

0.075 mmol) and TMSA (2.40 mL, 17.0 mmol) were reacted as described above for **20**. The solvent removed under reduced pressure and the crude mixture was run through a silica plug (hexanes) and then concentrated. The residue was dissolved in THF (20 mL) and DIPA (20 mL), CuI (29 mg, 0.15 mmol) and $Pd(PPh_3)Cl_2$ (41 mg, 0.05 mmol) were added, and the mixture was degassed under Ar for 30 min. $Pd(PPh_3)_4$ (26 mg, 0.025 mmol) and TIPSA (4.48 mL, 20.0 mmol) were added next. The reaction mixture was stirred in a sealed pressurized vessel at 115 °C for 4 d. Upon cooling, the solvent was removed in vacuo and the residue chromatographed (hexanes) to afford **22** (4.2 g, 88%) as an orange oil. ^1H NMR (300 MHz, $CDCl_3$) δ 0.23 (s, 9H), 1.14 (s, 21H), 7.38-7.42 (m, 2H); ^{13}C NMR (75 MHz, $CDCl_3$) δ –0.1, 18.7, 92.8, 96.4, 98.1, 99.8, 125.0, 125.2, 129.0, 129.3; IR (NaCl) ν 2158, 2865, 2893, 2944, 3110 cm^{-1}; MS (APCI) *m/z* (%) 431.2 (40, M^+ + THF); HRMS (EI) for $C_{20}H_{23}SSi_2$ $[M]^+$: calcd 360.1763 found 360.1763.

General Procedure For Preparation of 'Symmetrical' Annulene Precursors. To a solution of diyne (2.5 equiv.) dissolved in MeOH/THF (10:1, 0.05 M) was added K_2CO_3 (10 equiv.) and the mixture stirred for 30 min. The solution was filtered and then Et_2O added. The solution was washed successively with H_2O, 10% NaCl soln. and water, and then dried ($MgSO_4$). Solvent was removed in vacuo and the residue added to a solution of THF/DIPA (1:1, 0.1 M) and dihaloarene (1 equiv.). The mixture was degassed under Ar for 30 min after which CuI (6 mol%) and $Pd(PPh_3)_4$ (3 mol%) were added. The sealed vessel was stirred at room temperature until TLC showed the reaction complete (12 h – 2 d). The solvent was removed in vacuo and the crude product chromatographed on silica to afford the annulene precursor.

Precursor to 3 (pre-3). Chromatography on silica (30:1 hexanes:CH_2Cl_2) furnished **pre-3** (240 mg, 90%) as an light orange oil. ^{1}H NMR (300 MHz, $CDCl_3$) δ 1.16 (s, 21H), 1.18 (s, 21H), 7.11 (d, J = 5.3 Hz, 1H), 7.25 (d, J = 5.3 Hz, 1H), 7.24-7.32 (m, 4H), 7.52-7.61 (m, 4H); ^{13}C NMR (75 MHz, $CDCl_3$) δ 11.4, 18.7, 85.6, 87.7, 92.3, 95.2, 95.5, 96.4, 105.1, 105.2, 125.53, 125.58, 125.63, 125.9, 126.0, 126.5, 127.1, 127.89, 127.95 (2), 128.1, 129.4, 132.3, 132.5, 132.7 (2); IR (NaCl) ν 2157, 2864, 2891, 2942 cm^{-1}; MS (ACPI) *m/z* (%) 717.4 (50, MH^+ + THF), 645.3 (100, MH^+); HRMS (EI) for $C_{42}H_{52}SSi_2$ $[M]^+$: calcd 644.3328, found 644.3330.

Tetrayne 25 (pre-6). Chromatography on silica (10:1 hexanes:CH_2Cl_2) furnished **25** (251 mg, 86%) as an orange oil. ^{1}H NMR (300 MHz, $CDCl_3$) δ 1.13 (s, 42H), 7.04 (d, J = 5.3 Hz, 2H), 7.17 (d, J = 5.3 Hz, 2H), 7.30 (*AA*'BB'm, 2H), 7.51 (AA'*BB*'m, 2H); ^{13}C NMR (75 MHz, $CDCl_3$) δ 11.3, 18.7, 86.3, 95.2, 95.8, 100.7, 125.4, 126.3, 126.90, 126.92, 128.1, 129.9, 131.5; IR (NaCl) ν 2149, 2213, 2863, 2941 cm^{-1}; MS (ACPI) *m/z* (%) 723.3 (20, M^+ + THF), 651.2 (100, MH^+); HRMS (EI) for $C_{40}H_{50}S_2Si_2$ $[M]^+$: calcd 650.2892, found 650.2901.

Precursor to 8 (pre-8). Chromatography on silica (10:1 hexanes:CH_2Cl_2) furnished **pre-8** (700 mg, 90%) as an orange oil. ^{1}H NMR (300 MHz, $CDCl_3$) δ 1.12 (s, 42H), 7.02 (d, J = 5.3 Hz, 2H), 7.12 (d, J = 5.3 Hz, 2H), 7.29 (*AA*'BB'm, 2H), 7.52 (AA'*BB*'m, 2H); ^{13}C NMR (75 MHz, CD_2Cl_2) δ 11.8, 19.0, 88.5, 92.3, 98.6, 100.5, 126.0, 126.7, 126.9, 127.6, 128.7, 130.2, 132.4; IR (NaCl): ν 2143, 2206, 2865, 2890, 2943 cm^{-1}; MS (APCI) *m/z* (%) 723.3 (20, MH^+ + THF), 651.2 (100, MH^+); HRMS (EI) for $C_{40}H_{50}S_2Si_2$ $[M]^+$: calcd 650.2892, found 650.2895.

Precursor to 9 (pre-9). Chromatography on silica (12:1 hexanes:CH_2Cl_2) furnished **pre-9** (725 mg, 61%) as an orange oil. ^{1}H NMR (300 MHz, $CDCl_3$) δ 1.11 (s, 42H), 7.28 (*AA'*BB'm, 2H), 7.44 (d, J = 3.2 Hz), 7.46 (d, J = 3.2 Hz), 7.52 (AA'*BB'*m, 2H); ^{13}C NMR (75 MHz, $CDCl_3$) δ 11.6, 18.9, 87.6, 90.4, 93.4, 100.2, 125.4, 125.5, 126.2, 128.1, 128.8, 129.2, 131.9; IR (NaCl): ν 2154, 2215, 2864, 2891, 2942, 3108 cm^{-1}; MS (APCI) *m/z* (%) 721.3 (100, M^+ + THF), 651.3 (45, MH^+); HRMS (EI) for $C_{40}H_{50}S_2Si_2$ $[M]^+$: calcd 650.2892, found 650.2896.

Precursor to 10 (pre-10). Chromatography on silica (12:1 hexanes:CH_2Cl_2) furnished **pre-10** (737 mg, 67%) as an orange oil. ^{1}H NMR (300 MHz, $CDCl_3$) δ 1.15 (s, 42H), 7.01-7.05 (m, 3H), 7.17 (d, J = 5.3 Hz, 1H), 7.19 (d, J = 5.3 Hz, 1H), 7.23 (d, J = 5.3 Hz, 1H); ^{13}C NMR (75 MHz, $CDCl_3$) δ 11.3, 18.69, 18.73, 86.2, 89.4, 90.2, 91.6, 95.4, 95.9, 100.4, 100.6, 126.0, 126.3, 126.5, 126.6 (2), 126.7, 126.9, 127.1, 129.2, 129.87, 129.91; IR (NaCl) ν 2143, 2202, 2864, 2942, 3108 cm^{-1}; MS (APCI) *m/z* (%) 729.2 (100, MH^+ + THF + H_2O), 657.2 (90, MH^+ + H_2O); HRMS (MALDI) for $C_{38}H_{48}S_3Si_2$ $[M]^+$: calcd 656.2457, found 656.2456.

Precursor to 13 (pre-13). Chromatography on silica (10:1 hexanes:CH_2Cl_2) furnished **pre-13** (384 mg, 52%) as an orange oil. ^{1}H NMR (300 MHz, $CDCl_3$) δ 1.12 (s, 42H), 7.02-7.05 (m, 3H), 7.14 (bd, J = 5.3 Hz, 2H), 7.21 (d, J = 5.3 Hz, 1H); ^{13}C NMR (75 MHz, $CDCl_3$) δ 11.2, 18.65, 18.70, 85.4, 87.82, 87.84, 91.9, 98.0, 98.1, 100.4, 100.9, 125.65, 125.71, 126.2, 126.5, 126.6, 126.9, 127.2, 129.5 (2), 129.7; IR (NaCl): ν 2149, 2864, 2942 cm^{-1}; MS (APCI) *m/z* (%) 729.2 (62, MH^+ + THF + H_2O), 657.2 (100, MH^+ + H_2O); HRMS (MALDI) for $C_{38}H_{48}S_3Si_2$ $[M]^+$: calcd 656.2457, found 656.2455.

Precursor to 14 (pre-14). Chromatography on silica (10:1 hexanes:CH_2Cl_2) furnished **pre-14** (353 mg, 47%) as an orange oil. ^{1}H NMR (300 MHz, $CDCl_3$) δ 1.23 (s, 42H), 7.05 (d, J = 5.3 Hz, 1H), 7.20 (d, J = 5.3 Hz, 1H), 7.44-7.48 (m, 4H); ^{13}C NMR (75 MHz, $CDCl_3$) δ 11.6, 19.0, 83.9, 86.0, 87.4, 91.4, 93.5, 93.8, 100.0, 100.2, 125.2, 125.35, 125.36, 125.5, 126.2, 126.6, 127.0, 128.9, 129.2 (2), 129.8; IR (NaCl): ν 2156, 2202, 2864, 2942, 3108 cm^{-1}; MS (APCI) *m/z*(%) 727.3 (100, MH^+ + THF), 657.2 (30, MH^+); HRMS (MALDI) for $C_{38}H_{48}S_3Si_2$ $[M]^+$: calcd 656.2457, found 656.2454.

General Procedure For Preparation of 'Asymmetrical' Annulene Precursors. To a solution of diyne (1.0 equiv.) dissolved in MeOH/THF (10:1, 0.05 M) was added K_2CO_3 (2.5 equiv.) and the mixture stirred for 30 min. The solution was filtered and then Et_2O added. The solution was washed successively with H_2O, 10% NaCl soln. and water, and then dried ($MgSO_4$). Solvent was removed in vacuo and the residue added to a solution of THF/DIPA (1:1, 0.1 M) and dihaloarene (1 equiv.). The mixture was degassed under Ar for 30 min after which CuI (6 mol%) and $Pd(PPh_3)_4$ (3 mol%) were added. The sealed vessel was stirred at room temperature until TLC showed the reaction complete (12 h – 2 d). The solvent was removed in vacuo and the crude product chromatographed on a short plug silica to afford the halodiyne precursor. This material was redissolved in THF/DIPA (1:1, 0.1 M) and the second diyne (1.5 equiv.), desilylated in the manner described above was added. The solution was degassed under Ar for 30 min and then CuI (6 mol%) and $Pd(PPh_3)_4$ (3 mol%) were added. The sealed vessel was stirred at room temperature until TLC showed the reaction complete (12 h–2 d). The solvent was

removed in vacuo and the crude product chromatographed on silica to afford the annulene precursor.

Precursor to 4 (pre-4). Chromatography on silica (15:1 hexanes:CH_2Cl_2) furnished **pre-4** (536 mg, 89%) as a pale orange oil. ^{1}H NMR (300 MHz, $CDCl_3$) δ 1.12 (s, 42H), 7.02 (d, J = 4.9 Hz, 1H), 7.14 (d, J = 4.9 Hz, 1H), 7.20-7.29 (m, 4H), 7.49-7.57 (m, 4H); ^{13}C NMR (75 MHz, $CDCl_3$) δ 11.3, 18.7, 85.9, 91.7, 92.8, 95.0, 95.2, 96.2, 100.7, 105.4, 125.61, 125.65, 125.7, 125.9, 126.1, 126.8, 127.0, 127.4, 127.87, 127.92, 128.0, 129.9, 131.5, 131.8, 132.65, 132.70; IR (NaCl) ν 2151, 2204, 2864, 3088 cm^{-1}; MS (APCI) *m/z* (%) 645.3 (100, MH^+), 717.4 (50, MH^+ + THF); HRMS (MALDI) for $C_{42}H_{53}SSi_2$ $[MH]^+$: calcd 645.3401, found 645.3404.

Precursor to 5 (pre-5). Chromatography on silica (15:1 hexanes:CH_2Cl_2) furnished **pre-5** (714 mg, 64%) as a pale orange oil. ^{1}H NMR (300 MHz, $CDCl_3$) δ 1.11 (s, 21H), 1.12 (s, 21H), 7.00 (d, J = 5.3 Hz, 1H), 7.10 (d, J = 5.3 Hz, 1H), 7.24-7.33 (m, 4H), 7.50-7.58 (m, 4H); ^{13}C NMR (75 MHz, $CDCl_3$) δ 11.3, 18.7, 87.9, 91.92, 91.96, 92.5, 95.1, 98.2, 100.3, 105.3, 125.3, 125.6, 127.3, 127.7, 127.8, 127.89, 127.96, 128.03, 129.7, 129.9, 131.5, 131.7, 131.8, 132.3, 132.5, 132.7, 132.8; IR (NaCl) ν 2154, 2211, 2864, 2890, 2942 cm^{-1}; MS (APCI) *m/z* (%) 644.9 (100, M^+), 716.9 (43, MH^+ + THF); HRMS (MALDI) for $C_{42}H_{53}SSi_2$ $[MH]^+$: calcd 645.3401, found 645.3406.

Precursor to 7 (pre-7). Chromatography on silica (12:1 hexanes:CH_2Cl_2) furnished **pre-7** (201 mg, 15%) as an orange oil. ^{1}H NMR (300 MHz, $CDCl_3$) δ 1.34 (bs, 42H), 7.04 (d, J = 5.3 Hz, 1H), 7.10-7.15 (m, 2H), 7.17 (d, J = 5.3 Hz, 1H), 7.31 (*AA'*BB'm, 2H), 7.52 (AA'*BB'*m, 2H); ^{13}C NMR (75 MHz, $CDCl_3$) δ 11.3, 18.7, 85.9, 88.3, 91.7,

95.3, 96.1, 98.2, 99.9, 100.6, 125.3, 125.6, 125.7, 126.1, 126.4, 126.8, 127.0, 127.1, 127.9, 128.1, 129.9, 130.0, 131.5, 131.8; IR (NaCl) ν 2143, 2210, 2890, 2864, 2942, 3108 cm^{-1}; MS (APCI) *m/z* (%) 650.8 (100, MH^+); HRMS (EI) for $C_{40}H_{50}S_2Si_2$ $[M]^+$: calcd 650.2892, found 650.2898.

Precursor to 11 (pre-11). Chromatography on silica (10:1 hexanes:CH_2Cl_2) furnished **pre-11** (169 mg, 28%) as an orange oil. ^1H NMR (300 MHz, $CDCl_3$) δ 1.13 (s, 42H), 7.04 (d, J = 5.3 Hz, 2H), 7.09 (d, J = 5.3 Hz, 1H), 7.14 (d, J = 5.3 Hz, 1H), 7.19 (d, J = 5.3 Hz, 1H), 7.23 (d, J = 5.3 Hz, 1H); ^{13}C NMR (75 MHz, $CDCl_3$) δ 11.3, 18.7, 87.4, 88.3, 89.6, 89.8, 95.9, 98.2, 99.9, 100.4, 125.6, 126.3, 126.5, 126.6, 127.0, 127.15, 127.18, 129.5, 129.7, 129.9, 130.0, 130.3; IR (NaCl) ν 2145, 2177, 2884, 2942, 2890, 3108 cm^{-1}; MS (ACPI) *m/z* (%) 657.2 (100, MH^+), 729.3 (80, MH^+ + THF); HRMS (MALDI) for $C_{38}H_{49}S_3Si_2$ $[MH]^+$: calcd 657.2529, found 657.2548.

Tetrayne 26 (pre-12). Chromatography on silica (10:1 hexanes:CH_2Cl_2) furnished **27** (702 mg, 81%) as an orange oil. ^1H NMR (300 MHz, $CDCl_3$) δ 1.11 (s, 21H), 1.12 (s, 21H), 7.03 (d, J = 5.3 Hz, 1H), 7.04 (d, J = 5.3 Hz, 1H), 7.08 (d, J = 5.3 Hz, 1H), 7.14 (d, J = 5.3 Hz, 1H), 7.17 (d, J = 5.3 Hz, 1H), 7.28 (d, J = 5.3 Hz, 1H); ^{13}C NMR (75 MHz, $CDCl_3$) δ 11.3, 18.66, 18.73, 85.3, 85.8, 91.7, 92.4, 95.4, 98.0, 100.6, 100.9, 125.7, 126.2, 126.27, 126.30, 126.58, 126.60, 126.76, 126.82, 129.2, 129.6, 129.9, 130.1; IR (NaCl): ν 2146, 2192, 2864, 2890, 2942 cm^{-1}; MS (ACPI) *m/z* (%) 657.2 (100, MH^+), 729.3 (90, MH^+ + THF); HRMS (MALDI) $C_{38}H_{48}S_3Si_2$ $[M]^+$: calcd 656.2457, found 656.2455.

General Procedure for Annulene Formation. To a solution of annulene precursor (1 equiv.) in THF (0.1 M) was added TBAF (20 equiv., 1.0 M THF). The mixture was

stirred for 5 min and then Et_2O was added. The solution was washed 4–6 times with brine and then water, and the organic layer was dried ($MgSO_4$). The solution was concentrated, rediluted with 1:1 THF/DIPA to ca. 50 mL, and then injected over 8 h via syringe pump into a THF/DIPA solution (1:1, 0.05 M) containing $PdCl_2$(dppe) (3 mol%), CuI (6 mol%), and I_2 (0.5 equiv.). Once TLC showed completion of the reaction, the solvent was removed under reduced pressure and the residue was run through a silica plug (1:1 hexanes:CH_2Cl_2). The product was further purified on a chromatotron (8:1 hexanes:EtOAc).

[14]DBA/DTA 3. 15 mg, 62% yield. ^{1}H NMR (500 MHz, C_6D_6): δ 6.62 (d, J = 5.3 Hz, 1H), 6.77-6.88 (m, 3H), 6.93 (t, J = 7.8 Hz, 1H), 7.16 (d, J = 5.3 Hz, 1H), 7.28 (d, J = 7.7 Hz, 1H), 7.33 (d, J = 7.8 Hz, 1H), 7.46 (d, J = 7.8 Hz, 1H), 7.62 (d, J = 7.9 Hz, 1H); ^{13}C (125 MHz, C_6D_6): δ 81.4, 81.7, 85.9, 86.1, 87.9, 90.2, 93.3, 98.2, 123.3, 123.9, 125.0, 125.5, 127.4, 128.9, 129.4, 129.65, 130.0, 130.2, 132.5, 132.8, 133.0; IR (KBr) ν 2139, 2171, 2201, 2864, 2942 cm^{-1}; UV (CH_2Cl_2) λ_{max} (log ϵ): 302 (4.91), 322 (4.96), 353 (4.53), 378 (4.21) nm; MS (APCI) *m/z* (%) 403.1 (100, M^+ + THF); HRMS (EI) $C_{24}H_{10}S$ $[M]^+$: calcd 330.0503, found 330.0501.

[14]DBA/DTA 4. 18 mg, 29% yield. ^{1}H NMR (300 MHz, THF-d_8) δ 7.22 (d, J = 5.3 Hz, 1H), 7.51-7.57 (m, 3H), 7.59 (dt, J = 7.5, 1.2 Hz 1H), 7.64 (d, J = 5.3 Hz, 1H), 7.70 (d, J = 8.0 Hz, 1H), 7.94-7.98 (m, 1H), 8.03-8.09 (m, 2H); (125 MHz, THF-d_8) δ 80.6, 83.1, 83.3, 87.5, 88.5, 94.2, 94.6, 99.7, 123.2, 123.6, 124.0, 125.8, 126.9, 129.07, 129.16. 129.19 (2), 129.7, 130.0, 130.1, 133.5, 134.5, 135.8, 137.1; IR (KBr) ν 2113, 2139, 2863, 2942, 2969, 3083, 3104 cm^{-1}; UV (CH_2Cl_2) λ_{max} (log ε) 305 (4.79), 317 (4.89), 321

(4.83), 360 (4.28), 386 (4.21) nm; MS (APCI) *m/z* (%) 401.1 (100, M^+ + THF – H); HRMS (EI) $C_{24}H_{10}S$ $[M]^+$: calcd 330.0503 found 330.0502.

[14]DBA/DTA 5. 17 mg, 33% yield; product was unstable if left too long in solvent or in light. ^{1}H NMR (300 MHz, THF-d_8) δ 7.51 (d, J = 5.3 Hz, 1H), 7.52-7.57 (m, 3H), 7.59 (t, J = 7.5 Hz, 1H), 7.64 (d, J = 5.2 Hz, 1H), 7.72 (d, J = 7.5 Hz, 1H), 7.94-7.99 (m, 1H), 8.04-8.11 (m, 2H); (125 MHz, THF-d_8) δ 80.5, 81.6, 86.1, 89.7, 90.2, 93.9, 94.9, 95.4, 123.0, 123.9, 124.1, 124.4, 128.5, 129.0, 129.1, 129.2, 129.8, 129.9, 130.1, 131.2, 124.6, 135.3, 136.2, 137.2; IR (KBr) ν 2169, 2195, 2860, 2972, 3047, 3106 cm^{-1}; UV (CH_2Cl_2) λ_{max} (log ϵ) 304 (4.75), 315 (4.83), 323 (4.79), 391 (4.17) nm; MS (APCI) *m/z* (%) 403.1 (100, M^+ + THF); HRMS (EI) $C_{24}H_{10}S$ $[M]^+$: calcd 330.0503 found 330.0507.

[14]DBA/DTA 6. 9.7 mg, 53% yield. ^{1}H NMR (300 MHz, C_6D_6) δ 6.50 (d, J = 5.3 Hz, 2H), 6.68 (d, J = 5.3 Hz, 2H), 6.95 (*AA*'BB'm, 2H), 7.71 (AA'*BB*'m, 2H); ^{13}C NMR (75 MHz, CD_2Cl_2) δ 81.9, 85.3, 87.5, 99.2, 122.3, 124.6, 126.4, 128.3, 128.6, 132.6, 135.4; IR (KBr) ν 2102, 2924, 3102 cm^{-1}; UV (CH_2Cl_2) λ_{max} (log ε): 309 (4.44), 316 (4.46), 329.0 (4.74), 363 (4.74), 373 (3.90) nm; MS (APCI) *m/z* (%) 409.0 (100, MH^+ + THF); HRMS (EI) $C_{22}H_8S_2$ $[M]^+$: calcd 336.0067, found 336.0067.

[14]DBA/DTA 7. 11 mg, 33% yield. ^{1}H NMR (500 MHz, C_6D_6) δ 6.50 (d, J = 5.5 Hz, 1H), 6.51 (d, J = 5.5 Hz, 1H), 6.99 (dt, J = 7.5, 1.5 Hz, 1H), 7.03 (dt, J = 7.5, 1.5 Hz, 1H), 7.13 (d, J = 5.5 Hz, 1H), 7.76 (dd, J = 7.5, 1.5 Hz, 1H), 7.89 (dd, J = 7.5, 1.5 Hz, 1H); ^{13}C NMR (75 MHz, CD_2Cl_2) δ 81.9, 83.6, 85.0, 87.0, 87.3, 89.7, 94.8, 99.5, 122.7, 122.8, 123.3, 124.4, 126.3, 127.3, 128.3, 128.58, 128.64, 131.1, 132.7, 134.2, 135.5, 135.9; IR (KBr) ν 2147, 2190, 2850, 2926, 2959, 3106 cm^{-1}; UV (CH_2Cl_2) λ_{max} (log ε):

312 (4.69), 326 (4.87), 366 (4.69), 398 (4.06) nm; MS (APCI) *m/z* (%) 408.8 (100, MH^+ + THF), 337.8 (50, MH^+); HRMS (EI) $C_{22}H_8S_2$ $[M]^+$: calcd 336.0067, found 336.0065.

[14]DBA/DTA 8. 33 mg, 32% yield. ^1H NMR (300 MHz, C_6D_6) δ 6.49 (d, J = 5.3 Hz, 2H), 7.05 (*AA'*BB'm, 2H), 7.11 (d, J = 5.3 Hz, 2H), 7.92 (AA'*BB'*m, 2H); ^{13}C NMR (75 MHz, CD_2Cl_2) δ 84.8, 85.2, 89.4, 95.0, 123.00, 123.03, 127.5, 128.5, 131.5, 134.1, 135.9; IR (KBr) ν 2149, 2188, 2849, 2917, 3107 cm^{-1}; UV (CH_2Cl_2) λ_{max} (log ε): 306 (4.82), 313 (4.84), 325 (5.01), 377 (4.20), 408 (4.37) nm; MS (APCI) *m/z* (%) 409.0 (100, MH^+ + THF); HRMS (EI) $C_{22}H_8S_2$ $[M]^+$: calcd 336.0067 found 336.0071.

[14]DBA/DTA 9. 15 mg, 37% yield. ^1H NMR (300 MHz, C_6D_6) δ 6.62 (d, J = 3.1 Hz, 2H); 6.91 (*AA'*BB'm, 2H), 7.04 (d, J = 3.1 Hz, 2H), 7.62 (AA'*BB'*m, 2H); ^{13}C NMR (75 MHz, C_6D_6) δ 80.1, 82.2, 88.9, 93.0, 123.4, 124.5, 126.3, 129.3, 130.1, 136.4; IR (KBr): ν 2105, 2143, 2863, 2942, 3106 cm^{-1}; UV (CH_2Cl_2) λ_{max} (log ϵ) 280 (5.12), 304 (6.02), 328 (4.71), 339 (4.75) nm; MS (APCI) *m/z* 407.1 (100, M^+ + THF); HRMS (EI) $C_{22}H_8S_2$ $[M]^+$: calcd 336.0067, found 336.0068.

[14]DTA 10. 10 mg, 30% yield. ^1H NMR (300 MHz, THF-d_8) δ 7.41 (d, J = 5.4 Hz. 2H), 7.66 (d, J = 5.4 Hz, 1H), 7.73 (d, J = 5.4 Hz, 1H), 7.75 (d, J = 5.4 Hz, 1H), 7.77 (d, J = 5.4 Hz, 1H); ^{13}C NMR (75 MHz, THF-d_8) δ 82.4, 82.7, 84.8, 85.0, 87.8, 92.4, 93.1, 95.6, 124.1, 124.3, 125.4, 125.8, 127.0, 127.1, 128.9, 129.2 (2), 131.9, 132.3, 132.5; IR (KBr) ν 2140, 2201, 2866, 2975 cm^{-1}; UV (CH_2Cl_2) λ_{max} (log ε) 314 (4.75), 335 (4.93), 370 (4.25), 382 (4.21), 398 (4.04) nm; MS (APCI) *m/z* (%) 414.2 (20, M^+ + THF), 396.5 (70); HRMS (MALDI) $C_{20}H_6S_3$ $[M]^+$: calcd 341.9632, found 341.9626.

[14]DTA 11. 10 mg, 30% yield. ^{1}H NMR (300 MHz, C_6D_6) δ 6.48 (d, J = 5.3 Hz, 1H), 6.52 (d, J = 5.3 Hz, 1H), 6.62 (d, J = 5.3 Hz, 1H), 6.72 (d, J = 5.3 Hz, 1H), 7.18 (d, J = 5.3 Hz, 1H), 7.30 (d, J = 5.3 Hz, 1H); ^{13}C NMR (75 MHz, $CDCl_3$) δ 81.9, 82.5, 84.8, 85.7, 89.1, 90.2, 91.5, 92.5, 123.3, 123.5, 123.6, 124.1, 125.8, 126.3, 127.0, 127.1, 129.7, 131.1, 131.9, 132.9. IR (KBr) 2135, 2187, 2961, 3104 cm^{-1}; UV (CH_2Cl_2) λ_{max} (log ε): 318 (4.66), 333 (4.79), 373 (4.18), 399 (3.96) nm; MS (APCI) *m/z* (%) 415.0 (100, MH^+ + THF), 343.1 (10, MH^+); HRMS (MALDI) $C_{20}H_6S_3$ $[M]^+$: calcd 341.9632, found 341.9628.

[14]DTA 12. 34 mg, 64% yield. ^{1}H NMR (300 MHz, C_6D_6) δ 6.46 (d, J = 5.3 Hz, 1H), 6.53 (d, J = 5.3 Hz, 1H), 6.61 (d, J = 5.3 Hz, 1H), 6.77 (d, J = 5.3 Hz, 1H), 7.02 (d, J = 5.3 Hz, 1H), 7.18 (d, J = 5.3 Hz, 1H); ^{13}C NMR (75 MHz, C_6D_6) δ 82.9, 83.3, 86.5, 87.0, 87.9, 89.9, 95.0, 96.0, 123.2, 123.9, 124.3, 125.5, 126.4, 127.0, 127.3, 129.8, 132.2, 133.4; IR (KBr) ν 2140, 2183, 2871, 2959, 2982, 3109 cm^{-1}; UV (CH_2Cl_2) λ_{max} (log ε): 335 (4.99), 319 (4.74), 379 (4.28), 385 (4.26) nm; MS (APCI) *m/z* (%) 415.0 (100, MH^+ + THF); HRMS (MALDI) $C_{20}H_6S_3$ $[M]^+$: calcd 341.9632 found 341.9636.

[14]DTA 13. 23 mg, 45% yield. ^{1}H NMR (300 MHz, C_6D_6) δ 6.47 (d, J = 5.3 Hz, 1H), 6.52 (d, J = 5.3 Hz, 1H), 6.66 (d, J = 5.3 Hz, 1H), 7.02 (d, J = 5.3 Hz, 1H), 7.18 (d, J = 5.3 Hz, 1H), 7.33 (d, J = 5.3 Hz, 1H); ^{13}C NMR (75 MHz, C_6D_6) δ 85.0, 85.2, 86.0, 86.3, 89.3, 89.9, 91.5, 94.8, 123.6, 124.1, 124.7, 125.0, 127.0, 127.1, 127.2, 129.8, 130.0, 132.4, 133.4, 133.6; IR (KBr) ν 2133, 2187, 2854, 2923, 3103 cm^{-1}; UV (CH_2Cl_2) λ_{max} (log ε): 317 (4.56), 333 (4.59), 408 (4.03) nm; MS (APCI) *m/z* (%) 415.0 (100, MH^+ + THF); HRMS (MALDI) $C_{20}H_6S_3$ $[M]^+$: calcd 341.9632, found 341.9627.

[14]DTA 14. 20 mg, 38% yield. ^{1}H NMR (300 MHz, C_6D_6) δ 6.49 (d, J = 5.6 Hz, 1H), 6.62 (d, J = 3.2 Hz, 1H), 6.67 (d, J = 2.9 Hz, 1H), 6.85 (d, J = 3.2 Hz, 1H), 7.00 (d, J = 5.6 Hz, 1H), 7.02 (d, J = 2.9 Hz, 1H); ^{13}C (75 MHz, C_6D_6) δ 79.7, 79.9, 81.1, 82.9, 86.1, 88.2, 88.4, 93.0, 123.3, 123.7, 124.8, 125.2, 126.6, 126.7, 127.1, 129.10, 129.14, 132.7; IR (KBr) ν 2136, 2205, 2869, 2973, 3105 cm^{-1}; UV (DCM) λ_{max} (log ϵ) 314 (4.96), 331 (4.45), 342 (4.44), 368 (4.28) nm; MS (APCI) *m/z* (%) 415.0 (100, MH^+ +THF); HRMS (EI) $C_{20}H_6S_3$ $[M]^+$: calcd 341.9632 found 341.9626.

X-ray Crystallography. X-Ray data for **8** and **13** were collected on a Bruker SMART APEX CCD diffractometer at 173(2) K with MoKa radiation (λ = 0.71073 Å). The crystallographic data for **8** and **13** and summary of the data collection and structure refinement details are given in the Supporting Information. Absorption correction was applied by SADABS.[33] The structure was solved using direct methods and completed by subsequent difference Fourier syntheses and refined by full matrix least-squares procedures on F^2. All non-hydrogen atoms were refined with anisotropic displacement coefficients. H atoms were placed in calculated positions and refined in a riding group model. In both crystal structures there are two symmetrically independent molecules. The five-membered 'C(9)-C(12)/S(3)' ring in both molecules of **13** are disordered over two positions corresponding two opposite orientations of the molecules. Atoms in the disordered rings were refined with restrictions: the standard S-C and C-C distances were used as targets for the corresponding bond lengths. All software and sources scattering factors are contained in the SHELXTL (6.10) program package.[34]

Computational Methods. Geometry optimizations were performed using the B3LYP[35] functional and 6-31G* basis set. HOMO-LUMO gaps and dipole moments were taken from single-point energy calculations which were carried out on the optimized structures using B3LYP/6-311G**, in a solvent modeled using the Cosmo reaction field model[36] with a dielectric corresponding to methylene chloride (ε=9.08). The set of atomic radii optimized by Stefanovich and Truong[37] were used for the solvation energy calculations. The NWChem (v4.7 and v5.0)[38] program was used for all geometry optimizations and single-point energy calculations. Building and modeling of all compounds was done using the program Ecce v3.2.4.[39]

Redox potentials were approximated by taking the difference in total energy (electronic and solvation) between the optimized ground state structure, and the optimized oxidized structure. These redox potentials were referenced against the calculated redox potential for the ferrocenium/ferrocene couple.

Electrochemistry. Electrochemical measurements were taken in a solution of 100mM TBAHFP and 1mM macrocycle using Pt disc working electrode, Pt wire auxiliary electrode, and silver wire reference. Measurements were then referenced with respect to an internal ferrocene standard.

Acknowledgement. We thank the ACS Petroleum Research Fund and the National Science Foundation (CHE-0718242) for financial support. We thank Prof. J. E. Hutchison for use of his group's potentiostat.

5 Bridge to Chapter IV

Chapter IV builds on the successful synthesis of the [14] DTAs and [14] DTA/DBA hybrids and assembles isomeric [15] macrocycles to observe the effects of ring expansion on the electronic properties of the materials. The library of six reported compounds was convergently assembled and studied electrochemically, UV-Vis absorption and emission, and further supported by DFT calculations.

CHAPTER IV

SYNTHESIS AND PROPERTIES OF CONJUGATED THIOPHENES FUSED INTO A DEHYDRO[15]ANNULENE SCAFFOLD

1 Introduction

This chapter is a coauthored written by myself and with much thanks to Michael M. Haley for editorial assistance. Most of the synthetic work and characterization was performed by myself with some assistance from Thomas M. Linz. Robert B. Yelle, performed the all the DFT calculations work.

Highly unsaturated conjugated compounds have attracted substantial interest from synthetic, theoretical, and materials chemists in recent years.[1] Alkyne-containing systems[2] have garnered the bulk of this attention, which can be attributed to two main factors. First, the development of new synthetic methods based on organometallic cross-coupling reactions[3] has provided access to a vast array of compounds whose preparation was not previously possible. Second, many of these carbon-rich molecules and macrocycles of higher dimensionality exhibit interesting materials properties such as nonlinear optical (NLO) activity,[4] liquid crystalline behavior,[5] and molecular switching.[6] More recently, it has been shown that dehydrobenzo-annulenes[7] and related phenyl-acetylene macrocycles[8] are useful precursors to a variety of carbon-rich polymeric

systems, such as molecular tubes,[9] ladder polymers,[10] and novel allotropes of carbon.[11] It is therefore imperative to have ready access to a wide array of these high carbon content molecules in sufficient quantities via easy synthetic processes if their technological potential is to be harnessed.

We have been studying acetylene-rich dehydrobenzoannulenes (DBAs)[7,12] with the goal of exploring their diverse chemical and physical properties. Over the last decade, our group has developed new or improved existing synthetic techniques for the assembly of such macrocycles. As one particular result, it is now possible to introduce donor and/or acceptor functionalities on the phenyl rings of the DBA in a judicious manner, thus effectively "tuning" the optoelectronic properties of the annulene.[12a] To introduce additional variations for detailed structure-property relationship studies, we chose to incorporate thiophene moieties onto the dehydroannulene skeleton.[13] The choice of thiophene as the fused aromatic ring was inspired by features such as the chemical/electrochemical polymerizability of thiophene, the ability to form two-dimensional π-systems useful for electronics and photonics, the easier polarizability of thiophene, and the interaction among the individual macrocycles due to the lone pairs on the sulfur in each thiophene ring.[14] In contrast to other heteroaromatics, thiophenes are easier to handle and to functionalize than pyrroles or furans, permitting ready access to tailored thiophene derivatives. By locking the conjugated system into planarity, thiophene-containing macrocycles[14d-e,15] and cyclic thiophene-acetylene hybrids[16-19] have the potential to be more efficient materials because of geometrically enforced π-orbital

overlap, increasing the quinoidal character of the delocalized system and thus lowering the optical band gap.[20]

FIGURE 1. Examples of known thieno-fused dehydroannulenes.

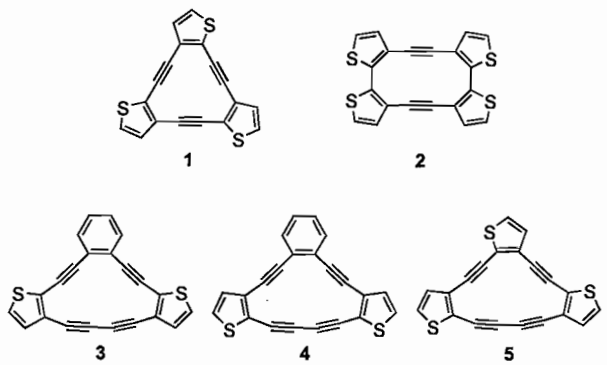

Prior studies on thieno-fused dehydroannulenes by the groups of Youngs (e.g., **1**, Figure 1)[17] and Marsella (e.g., **2**)[18] relied on metal-mediated intermolecular couplings for molecule construction. The structures of the starting materials, however, limited the resultant macrocycles to either C_{nh}- or D_{nh}-symmetry. In 2000 we reported the preparation of dehydro-thieno[18]annulenes ([18]DTAs) possessing lower symmetries (C_{2v}, C_s).[13a,b] While these macrocycles could be constructed in a systematic, stepwise manner, poor stability of the thienyldiyne intermediates forced us to examine other topologies. More recently, we described the synthesis and optoelectronic properties of a series of thiophene-containing [14]DBA/DTA hybrids (e.g., **3** and **4**, henceforth DBTAs) and the corresponding all-thiophene containing [14]DTAs (e.g., **5**).[13c] This study showed that subtle changes in molecule symmetry can "tune" the properties of annulenes. For example, the UV-vis spectra of this class of macrocycles showed that the large transitions remain essentially the same, but displayed distinct differences in the low-energy vibronic

region. Expanding on our success with [15]DBAs[12a,c,e] and our further understanding of thieno-fused annulenes, this report details the synthesis and characterization (thermal, optical, electro-chemical, computational) of [15]DBTA hybrids **6-9** (Figure 2) and [15]DPTA (dehydropyridothienoannulene) hybrids **10**[12c] and **11**.

FIGURE 2. Target thieno-fused dehydro[15]annulenes **6-11**.

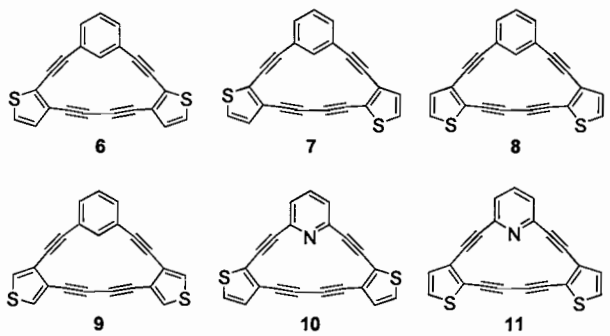

2 Results and Discussion

2.1 Macrocycle Synthesis

All six macrocycles were constructed in a convergent fashion from the synthons given in Figure 3. Dihaloarenes **12-14** are commercially available, whereas diynes **15-17** were prepared starting from the appropriate dihalothiophenes using our previously reported syntheses.[12c,13c]

FIGURE 3. Building blocks **12-17**.

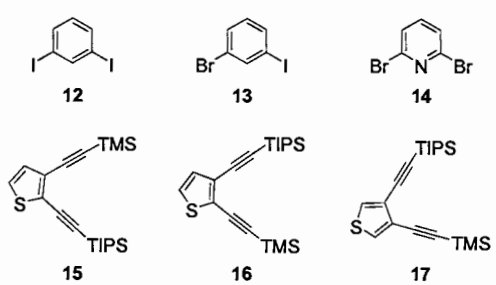

An example of symmetrical macrocycle synthesis is given in Scheme 1. Selective removal of the TMS group in diyne **16** with K_2CO_3 in MeOH/THF followed by cross-coupling to 1,3-diiodobenzene (**12**) afforded precursor **18 (pre-6)** in 86% yield. Desilylation with TBAF and cyclization using modified Glaser-Eglinton conditions generated hybrid **6** in 55% yield.

SCHEME 1. Synthesis of 'symmetrical' [15]DBTA **6**.

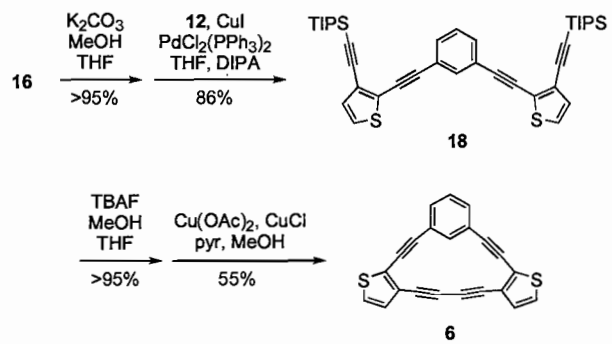

SCHEME 2. Synthesis of 'unsymmetrical' [15]DBTA **7**.

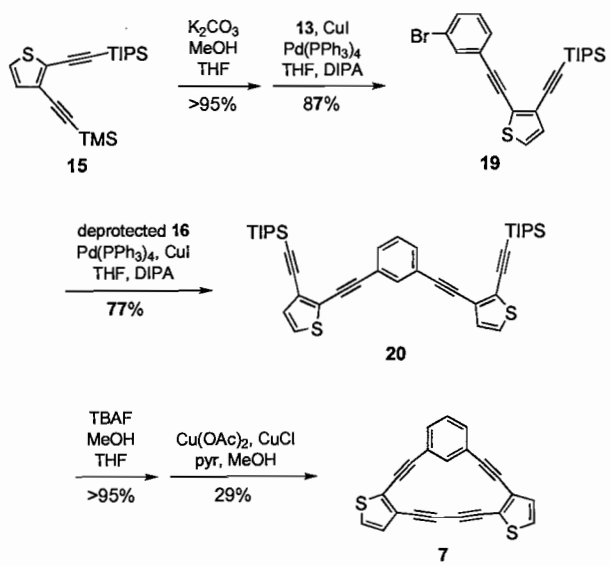

Preparation of the only unsymmetrical macrocycle, **7**, is shown in Scheme 2. Selective desilylation of diyne **15** as described above and then cross-coupling to 1-bromo-3-iodobenzene (**13**) yielded **19**, which proved to be moderately sensitive to silica. After rapid purification, compound **19** was then cross-coupled to monodesilated **16** to furnish precursor **20** (**pre-7**), which was fully characterized. Desilylation and cyclization afforded **7** in 29% yield. A summary of the various syntheses is given in Table 1.

TABLE 1. Synthesis and Yields of Macrocycles 6-11.

	"equivalents" of monodesilylated diyne			precursor,	annulene,
haloarene	**15**	**16**	**17**	yield	yield
12	2			pre-**6** (**18**), 86%	**6**, 55%
13	1 (second)	1 (first)		pre-**7** (**19**), 67%	**7**, 29%
12		2		pre-**8**, 47%	**8**, 50%
12			2	pre-**9**, 79%	**9**, 53%
14	2			Pre-**10**, 74%[a]	**10**, 73%[a]
14		2		Pre-**11**, 67%	**11**, 32%

[a]Reference 12c.

As with the previously reported [14]DBTAs, the thieno-fused [15]annulenes are only moderately stable during workup and are sensitive to acid, light, and silica, which accounts for the lower than normal cyclization yields. Workups were most successful when avoiding halogenated solvents and utilizing fast chromatographic methods (chromatotron or flash chromatography). NMR characterization of the annulenes was accomplished primarily in THF-d_8 for both stability and solubility. In general, those molecules with UV-vis absorptions past 400 nm and/or where both sulfurs are oriented 'down' (sulfur α to the diacetylene linkage), as is the case with **8** and **11**, showed the most sensitivity. Most could be stored in solution or in the solid state for several weeks if

kept cold and dark sealed under argon. The most difficult macrocycle to work with was **9**, which was found to decompose gradually over 3-4 d. The instability could be due to the more exposed α-positions of the 3,4-fused thiophenes, which have been shown to affect the integrity of samples.[13c,21]

Thermal analysis of **6-9** by DSC revealed broad exotherms with onset after 200 °C and maxima ca. 225 °C, with decomposition above 300 °C. Thermal scans of pyridine macrocycles **10** and **11**, however, showed larger and sharper exotherms between 175-200 °C. These data as a whole suggest nonetheless random, disordered polymerizations that yield black amorphous materials.

2.2 Spectroscopic Properties

NMR analysis of the [15]DBTAs shows only one significant difference between the macrocycles and their respective precursors: upon cyclization the triplet signal for the intraannular arene proton shifts from a range of 7.7-7.8 to 8.5-8.9 ppm. This large change is readily attributed to an increased anisotropic deshielding effect of the transannular triple bonds;[12a,c,e,22] otherwise, the NMR data for the [15]annulenes are unremarkable.

Compared to the [14]DBTAs, the peaks in the electronic spectra of the [15]DBTAs (Figure 4a) are bathochromically shifted, some up to 40 nm. For example, [14]DBTA **3** has its main peak at 329 nm with two low energy absorptions at 363 and 373 nm and cut-off by 390 nm. The analogous [15]DBTA, **6**, has a main peak at 337 nm and cut-off around 450 nm, with no readily discernable low energy bands. These bands do become apparent and grow in as the thiophene orientation relative to the annulene ring

changes from 'up' to 'down' (**6→7→8**), similar to the [14]DBTAs.[13c] In **8** the low energy bands are at 410 and 448 nm with a cut-off of ca. 465 nm. In comparison, the analogous bands in 'down' [14]DBTA **4** are 376 and 408 nm and a cut-off of ca. 425 nm. Compound **9** has an appreciable low energy absorption band at 349 nm and overall displays different features than **6-8**. This reflects the decreased conjugation in the macrocycle due to 3,4-fusion of the two thiophene moieties. Once again, the 15-membered ring of **9** affords a band that is lower in energy than the corresponding band in the 3,4-fused [14]DBTA (339 nm), though the magnitude of this difference is smaller than the 2,3-fused systems.

FIGURE 4. UV-Vis absorption spectra of (a) **6-9** and (b) **10-11**. All spectra recorded in CH_2Cl_2 at analyte concentrations of 15-25 μM.

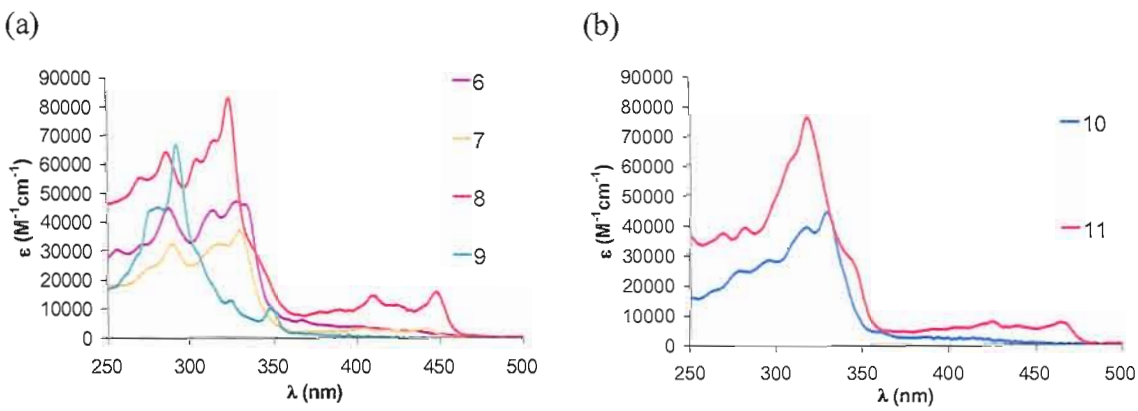

Replacing the benzene with a pyridine unit (Figure 4b) yields only minor changes to the electronic absorption data. Compounds **6** and **10** have nearly identical electronic absorption spectrum and thus identical band gaps, whereas [15]DPTA **11** red shifts to 465 nm compared to 448 for **8**. This 17 nm difference not only demonstrates that the orientation of the sulfurs plays an important role in the electronic properties of this class

of compounds, but also suggests that direct conjugation of the sulfur to the benzene (or pyridine) is a driving factor in lowering the energy of the transition states. The addition of the electron-withdrawing N-atom likely allows for a more charge separated excited state (vide infra). None of the reported macrocycles, however, displayed any appreciable solvatochromism.

The [15]DBTAs and [15]DPTAs did exhibit modest emissive properties (quantum yields of 0.03-0.17), unlike the [14]DBTAs (quantum yields less than 0.01). The emissive properties of cross-conjugated systems over directly conjugated systems is a phenomenon often observed elsewhere[23] and observed with many of our previous systems.[12a,e,24] Emission spectra and quantum yields were taken in both toluene and dichloromethane, and are summarized along with the absorption data and Stokes shifts in Table 2. [15]DPTA **11** is the only system to exhibit appreciable solvatochromism in the emission spectrum with the emission peak shifting from 471 nm to 524 nm when changing solvent from toluene to CH_2Cl_2.

TABLE 2. Photophysical Paramaters of [15]Annulenes 6-11.

	Lowest Energy Abs. λ_{max} (cut-off) [nm]	Emission Energy [nm] (CH_2Cl_2, PhMe)	Φ_f (CH_2Cl_2, PhMe)	Stokes shift, (CH_2Cl_2, PhMe) [cm^{-1}]
6	366 (450)	443, 447	0.11, 0.17	4975, 5028
7	440 (450)	449, 449	0.03, 0.03	507, 404
8	448 (460)	456, 455	0.06, 0.05	392, 244
9	349 (360)	363, 363	0.04, 0.05	1023, 1105
10	363 (460)	512, 510	0.04, 0.05	8017, 7789
11	465 (480)	524, 471	0.05, 0.06	2421, 228

2.3 Electrochemistry

Cyclic voltammograms were obtained of the [15]annulenes using a Pt disk electrode, Ag wire reference, and Pt swirl auxiliary in CH_2Cl_2 solutions of Bu_4NPF_6 and referenced to ferrocene. Electrochemical band gap values for compounds **6-8**, **10**, and **11** were discerned using previously described methods.[13c,25] Table 3 lists the oxidation and reduction onsets and the electrochemical band gap, along with the optically estimated and DFT calculated band gap values. Compound **9** was not tested, as it was too difficult to handle and thus garner reliable CV information. The CVs showed irreversible oxidation peaks and multiple irreversible, and sometimes quasi-irreversible reduction waves. In certain instances, however, multiple oxidations were found to occur. This could be due to an increased HOMO energy, allowing more electron transfer reactions to happen away from the solvent window. As was the case with the [14]annulenes, no polymer films were deposited on the electrode. The electrochemistry results match the relative trends observed in the UV-Vis absorption data. For example, sulfurs 'up' macrocycles have wider band gaps (e.g., **6**, 2.85 eV) than sulfurs 'down' (e.g., **8**, 2.70 eV), in agreement with the [14]DBTA series.[13c] Similarly, the optical and electrochemical band gaps of the [15]DPTAs are larger than those of the corresponding [15]DBTAs.

2.4 Computational Results

DFT calculations (B3LYP/6-311G**)[26] were performed on both the [15]DBTAs and [15]DPTAs. The computed HOMO/LUMO gaps are also given in Table 3, and show excellent relative agreement with the empirical trends. For instance, the largest band gap,

[15]DBTA **6** (2.85-3.39 eV), corresponds well to the calculated value (3.18 eV). In most cases the DFT computed energies are larger than the experimentally determined ones, as was found for all of the [14]DBTAs and [14]DTAs.[13c] The two exceptions in the current study are sulfurs 'up' annulenes **6** and **10**. Given their UV-Vis spectra in Figure 4, we can easily attribute this difference to unresolved low energy peaks in the data.

TABLE 3. Electrochemical Data and Band Gaps.

Cmpd	E_{pa} (ox) (vs. Fc) [V]	E_{pa} (red) (vs. Fc) [V]	Electrochemical Band Gap [eV]	Optical Band Gap [eV]	DFT Calculated Band Gap [eV]
6	1.14	–1.71	2.85	3.39	3.18
7	1.14	–1.64	2.78	2.82	3.09
8	1.13	–1.57	2.70	2.77	3.02
9	–	–	–	3.55	4.04
10	1.20	–1.86	3.06	3.42	3.06
11	0.97	–1.76	2.73	2.66	2.93

The computed HOMO/LUMO plots for **6-11** are given in Figure 5. These show little if any difference in topology with respect to the sulfur orientation in [15]DBTAs **6-8**, similar to what was previously observed in the [14]annulene series (e.g., **3-5**) when 2,3-fused thiophenes were incorporated into the macrocycle.[13c] Compound **9**, possessing 3,4-fusion, shows disruption in the continuity of electron delocalization around the macrocycle; however, it is not as dramatic and well-defined as in the plots of the corresponding [14]DBTA.[13c] DPTAs **10** and **11** also show remarkable similarity to DBTAs **6-8** with the exception of some slight additional electron density at C4 of the pyridine.

The placement of the electron density on the carbon lying between the triple bonds in the LUMOs of **6-8** and **10-11** alludes to perhaps some charge transfer effects.

Furthermore it is serendipitous that the lowering of energy of the UV absorption for the pyridine, sulfurs 'down' DPTA **11** occurs when the sulfurs are directly in conjugation with the pyridine nitrogen atom, in contrast to **10**, when the sulfur is not conjugated with the nitrogen, where no discernable change in the UV-Vis spectrum is observed. This could imply that there is some level of charge transfer component to **8** and **11** ($\pi \rightarrow n^*$)

FIGURE 5. Calculated HOMO and LUMO plots of [15]DBTAs **6-9** and [15]DPTAs **10-11**.

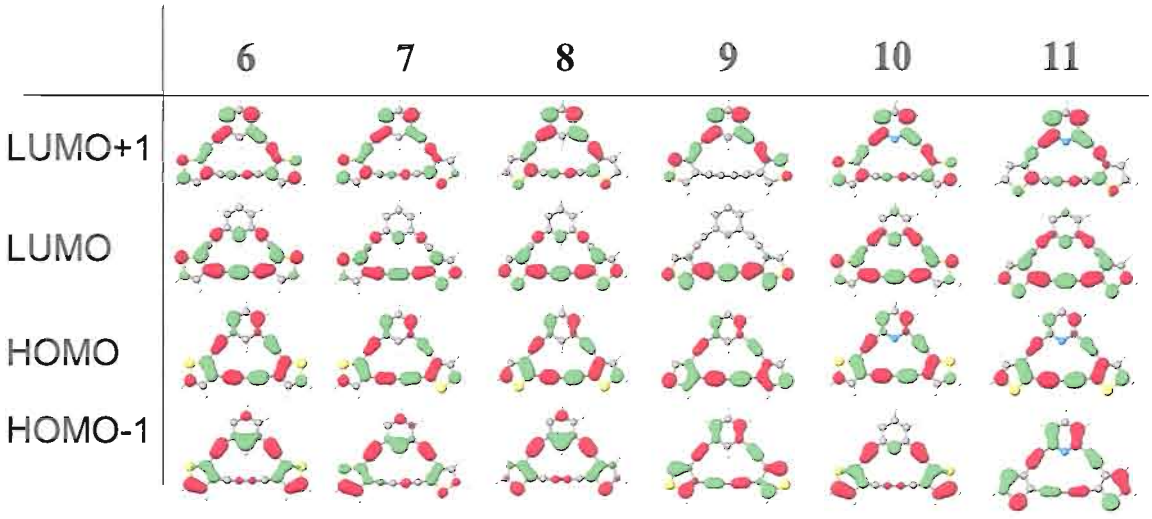

3 Conclusions

A small series of [15]DBTA and [15]DPTA hybrids composed of multiple fused thiophenes, benzenes, and/or pyridines was successfully prepared. Planarizing the thiophenes into the [15]annulene scaffold was found to increase orbital overlap even in a cross-conjugated system. Concurrently, the same relative electronic trends were observed in both the 14- and 15-membered macrocycles that are contingent on the orientation of the sulfur. When the sulfur atoms is oriented 'down' (as in **8**), the absorption bands of the

macrocycle red shift and intensify compared to when the sulfurs are oriented 'up' (as in **6**). When 3,4-fused onto the annulene scaffold, as in **9**, the net conjugation around the ring is disrupted by the increased single bond character. Incorporating pyridines in the macrocycle (DPTAs **10-11**) can significantly red shift the molecule, but only when the sulfurs are oriented down (**11**). These results as a whole are supported by DFT-B3LYP calculations of the HOMO-LUMO energy gap. Overall, the [15]annulene scaffold offers some benefits over the [14]scaffold with a wider dispersion of UV-Vis absorption energies, and increased emissive properties regardless of the loss of macrocycle aromaticity. Electrochemical measurements were performed and again failed to yield polymers typical of thiophenes, most likely due to the increased 'annulene' character of the compounds. Future reports will focus on stabilized α-alkylated thiophene targets in order to expand the scope of syntheses of these macrocycles by solubilizing the products and protecting against unwanted degradation.

4 Experimental Section

General Methods. These are described in reference 12a. Diynes **17**,[12c] **18**,[13c] and **19**[13c] and annulene **10**[12c] were prepared according to known procedures.

General Procedure For Preparation of 'Symmetrical' Annulene Precursors. To a solution of diyne (2.5 equiv.) dissolved in MeOH/THF (10:1, 0.05 M) was added K_2CO_3 (10 equiv.) and the mixture stirred for 30 min. The solution was filtered and then Et_2O added. The solution was washed successively with H_2O, 10% NaCl soln. and water, and then dried ($MgSO_4$). Solvent was removed in vacuo and the residue added to a solution of

THF/DIPA (1:1, 0.1 M) and dihaloarene (1 equiv.). The mixture was degassed under Ar for 30 min after which CuI (6 mol%) and $Pd(PPh_3)_4$ (3 mol%) were added. The sealed vessel was stirred at room temperature until TLC showed the reaction complete (12 h – 2 d). The solvent was removed in vacuo and the crude product chromatographed on silica to afford the annulene precursor.

Precursor to 6 (18/pre-6). Chromatography on silica (10:1 hexanes:CH_2Cl_2) furnished **18** (**pre-6**, 334 mg, 85%) as an orange oil. ^{1}H NMR (300 MHz, $CDCl_3$) δ 1.20 (s, 42H), 7.08 (d, J = 5.3 Hz, 2H), 7.21 (d, J = 5.3 Hz, 2H), 7.33-7.39 (m, 1H), 7.48-7.54 (m, 2H), 7.69 (t, J = 1.5 Hz, 1H); ^{13}C NMR (75 MHz, $CDCl_3$) δ 11.6, 19.0, 82.9, 95.7, 96.4, 100.9, 123.5, 126.3, 127.0, 127.6, 128.7, 130.3, 131.5, 134.9; MS (APCI) *m/z* (%) 650.8 (MH^+, 50); IR (NaCl) ν 2149, 2202, 2864, 2891, 2942 cm^{-1}.

Precursor to 8 (pre-8). Chromatography on silica (10:1 hexanes:CH_2Cl_2) furnished **pre-8** (184 mg, 47%) as an orange oil. ^{1}H NMR (300 MHz, $CDCl_3$) δ 1.17 (s, 42H), 7.09 (d, J = 5.3 Hz, 2H), 7.16 (d, J = 5.3 Hz, 2H), 7.34-7.39 (m, 1H), 7.47-7.53 (m, 2H), 7.71 (t, J = 1.4 Hz, 1H); ^{13}C NMR (75 MHz, $CDCl_3$) δ 11.3, 18.7, 84.4, 92.2, 98.2, 100.4, 132.4, 125.8, 126.7, 126.8, 128.2, 129.3, 131.2, 134.8; MS (APCI) *m/z* (%) 721.3 (MH^++THF, 100); IR (NaCl) ν 2142, 2213, 2891, 2864, 2942 cm^{-1}.

Precursor to 9 (pre-9). Chromatography on silica (10:1 hexanes:CH_2Cl_2) furnished **pre-9** (913 mg, 79%) as an orange oil. ^{1}H NMR (300 MHz, $CDCl_3$) δ 1.07 (s, 42H), 7.41-7.47 (m, 5H), 7.67 (t, J = 1.4 Hz, 1H); ^{13}C NMR (75 MHz, $CDCl_3$) δ 11.3, 18.7, 83.7, 90.4, 93.2, 100.0, 123.4, 125.0, 125.3, 128.1, 128.2, 129.0, 131.2, 135.0; MS (APCI) *m/z*

(%) 721.3 (MH^++THF, 100), 791.3 (M^++2THF, 10); IR (NaCl) ν 2155, 2219, 2960, 2863, 3109 cm^{-1}.

Precursor to 11 (pre-11). Chromatography on silica (10:1 hexanes:CH_2Cl_2) furnished **pre-11** (153 mg, 56%) as an orange oil. ^1H NMR (300 MHz, $CDCl_3$) δ 1.34 (s, 42H), 7.11 (d, J = 5.3 Hz, 2H), 7.15 (d, J = 5.3 Hz, 2H), 7.41 (d, J = 7.6 Hz, 2H), 7.63 (t, J = 7.6 Hz, 1H); ^{13}C NMR (75 MHz, $CDCl_3$) δ 11.2, 18.7, 84.0, 91.7, 97.9, 100.8, 125.9, 126.0, 126.2, 127.9, 129.7, 136.1, 143.7; MS (APCI) *m/z* (%) 651.9 (MH^+, 100); IR (NaCl) ν 2143, 2214, 2942, 3109 cm^{-1}.

Asymmetric Annulene Precursor 20 (pre-7). To a solution of diyne **15** (111 mg, 0.311 mmol) dissolved in MeOH (6 mL) and THF (0.5 mL) was added K_2CO_3 (106 mg, 0.78 mmol) and the mixture stirred for 30 min. The solution was filtered and then Et_2O was added. The solution was washed successively with H_2O, 10% NaCl soln. and water, and then dried ($MgSO_4$). Solvent was removed in vacuo and the unstable crude material (**19**) was added to a solution of THF (1.5 mL), DIPA (1.5 mL) and 1-bromo-3-iodobenzene (**13**, 80 mg, 0.282 mmol). The mixture was degassed under Ar for 30 min after which CuI (3 mg, 0.017 mmol) and $Pd(PPh_3)_4$ (10 mg, 0.008 mmol) were added. The sealed vessel was stirred at room temperature until TLC showed the reaction complete (ca. 2 d). The solvent was removed in vacuo and the crude product chromatographed on a short plug silica to afford the halodiyne precursor. This material was redissolved in THF (1.5 mL) and DIPA (1.5 mL), and then diyne **16** (153 mg, 0.429 mmol), desilylated in the manner described above, was added. The solution was degassed under Ar for 30 min and then CuI (4 mg, 0.019 mmol), $Pd(PPh_3)_2Cl_2$ (7 mg, 0.0086

mmol), and $Pd(PPh_3)_4$ (5 mg, 0.0043 mmol) were added. The reaction mixture was transferred to a sealed pressurized tube and heated at 85 °C for 18 h. The solvent was removed in vacuo and the crude product was chromatographed on silica (6:1 hexanes:CH_2Cl_2) to afford **20** (**pre-7**, 191 mg, 67%) as a dark orange oil. ^{1}H NMR (300 MHz, $CDCl_3$) δ 1.14 (s, 42H), 7.04 (d, J = 5.3 Hz, 2H), 7.16 (d, J = 5.3 Hz, 1H), 7.17 (d, J = 5.3 Hz, 1H), 7.28-7.36 (m, 1H), 7.43-7.48 (m, 2H), 7.68 (t, J = 1.5 Hz, 1H); ^{13}C NMR (75 MHz, $CDCl_3$) δ 11.3, 18.7, 84.5, 84.5, 92.2, 95.4, 96.3, 98.1, 100.5, 100.6, 123.1, 123.5, 125.8, 126.0, 126.8, 126.9, 127.2, 128.3, 129.3, 130.0, 131.0, 131.2, 131.4, 134.7; MS (APCI) *m/z* (%) 757.4 (M^++THF+2H_2O, 80); IR (NaCl) ν 2145, 2209, 2891, 2865, 2943 cm^{-1}.

General Procedure of Annulene Formation. To a solution of annulene precursor (1 equiv.) in THF (0.1 M) was added TBAF (20 equiv., 1.0 M THF). The mixture was stirred for 5 min and then Et_2O was added. The solution was washed 4–6 times with brine and then water, and the organic layer was dried ($MgSO_4$). The solution was diluted with Et_2O (to ca. 50 mL total volume) and then slowly injected over 8 h into a pyridine solution (0.01 M) of CuCl (10 equiv.) and $Cu(OAc)_2$ (10 equiv.) stirring at 45 °C. Once TLC showed completion of the reaction, the solvent was removed under reduced pressure and the residue was run through a silica plug (1:1 hexanes:CH_2Cl_2). The product was further purified on a chromatotron (8:1 hexanes:EtOAc).

[15]DBTA 6. Obtained **6** (8 mg, 55%) as a pale yellow solid. ^{1}H NMR (300 MHz, THF-d_8) δ 7.14 (d, J = 5.3 Hz, 2H), 7.25-7.40 (m, 3H), 7.47 (d, J = 5.3 Hz, 2H), 8.52 (t, J = 1.5 Hz, 1H); ^{13}C NMR (75 MHz, THF-d_8) δ 79.6, 80.0, 87.5, 101.9, 125.1, 127.1,

127.9, 129.5, 129.7, 130.1, 130.4, 146.1; MS (APCI) *m/z* (%) 406.7 (MH^++THF, 85); IR (KBr) ν 2105, 2198 cm^{-1}; UV-Vis (CH_2Cl_2) λ_{max} (log ε): 285 (4.67), 327 (4.67), 333 (4.65), 366 (3.77) nm.

[15]DBTA 7. Obtained **7** (10 mg, 29%) as a yellow solid. ^1H NMR (300 MHz, THF-d_8) δ 7.05 (d, J = 5.2 Hz, 1H), 7.15 (d, J = 5.2 Hz, 1H), 7.22-7.37 (m, 3H), 7.47 (d, J = 5.2 Hz, 1H), 7.52 (d, J = 5.2 Hz, 1H), 8.51 (bs, 1H); ^{13}C NMR (75 MHz, THF-d_8) δ 78.1, 79.7, 82.4, 83.6, 87.5, 89.4, 98.9, 102.2, 125.3, 125.6, 127.2, 127.5, 128.1 (2), 129.6, 129.8, 130.2, 130.6, 132.4, 146.8; MS (APCI) *m/z*(%) 406.9 (MH^++THF, 85); IR (KBr) ν 2130, 2190 cm^{-1}; UV-Vis (CH_2Cl_2) λ_{max} (log ε): 288.0 (4.51), 328 (4.56), 406 (3.46), 441 (3.47) nm.

[15]DBTA 8. Obtained **8** (23 mg, 50%) as a yellow solid. ^1H NMR (300 MHz, THF-d_8) δ 7.05 (d, J = 5.3 Hz, 2H), 7.22-7.36 (m, 3H), 7.53 (d, J = 5.3 Hz, 2H), 8.51 (t, J = 1.5 Hz, 1H); ^{13}C NMR (75 MHz, THF-d_8) δ 79.2, 82.4, 88.2, 98.0, 124.6, 126.5, 126.8, 127.1, 128.9, 129.1, 131.4, 146.2; MS (APCI) *m/z* (%) 407.0 (MH^++THF, 90); IR (KBr) ν 2173, 2205 cm^{-1}; UV-Vis (CH_2Cl_2) λ_{max} (log ε): 285 (4.81), 303.0 (4.78), 314 (4.83), 323.0 (4.92), 410 (4.15), 448 (4.19) nm.

[15]DBTA 9. Obtained **9** (27 mg, 53%) as an unstable white solid. ^1H NMR (300 MHz, THF-d_8) δ 7.27-7.36 (m, 3H), 7.58 (d, J = 2.9 Hz, 2H), 7.82 (d, J = 2.9 Hz, 2H), 8.47 (t, J = 1.5 Hz, 1H); ^{13}C NMR (75 MHz, THF-d_8) δ 77.0, 77.8, 88.2, 94.9, 125.0, 126.2, 126.5, 127.6, 128.1, 130.0, 132.2, 145.3; MS (APCI) *m/z* (%) 407.0 (MH^++THF, 90); IR (KBr) ν 2136, 2200 cm^{-1}; UV-Vis (CH_2Cl_2) λ_{max} (log ε): 292 (4.83), 325 (4.16), 349 (4.08) nm.

[15]DPTA 11. Obtained **11** (10 mg, 38%) as a yellow solid. ^{1}H NMR (300 MHz, THF-d_8) δ 6.99 (d, J = 5.2 Hz, 2H), 7.10 (d, J = 7.8 Hz, 2H), 7.45 (d, J = 5.2 Hz, 2H), 7.59 (t, J = 7.8 Hz, 1H); ^{13}C NMR (75 MHz, THF-d_8) δ 78.9, 85.3, 86.3, 99.2, 123.0, 129.2, 129.3, 130.3, 131.9, 138.1, 146.0; MS (APCI) *m/z* (%) 337.5 (MH^+, 100); IR (KBr) ν 2145, 2212 cm^{-1}; UV-Vis (CH_2Cl_2) λ_{max} (log ε): 281 (4.85), 317 (4.87), 345 sh (4.27), 426 (3.87), 464 (3.86) nm.

Computational Methods. Geometry optimizations were performed using the B3LYP[26] functional and 6-31G* basis set. HOMO-LUMO gaps and dipole moments were taken from single-point energy calculations which were carried out on the optimized structures using B3LYP/6-311G**, in a solvent modeled using the Cosmo reaction field model[27] with a dielectric corresponding to methylene chloride (ε = 9.08). The set of atomic radii optimized by Stefanovich and Truong[28] were used for the solvation energy calculations. The NWChem (v4.7 and v5.0)[29] program was used for all geometry optimizations and single-point energy calculations. Building and modeling of all compounds was done using the program Ecce v3.2.4.[30]

Electrochemistry. Electrochemical measurements were taken in a solution of 100 mM Bu_4NPF_6 and 1 mM macrocycle using Pt disc working electrode, Pt wire auxiliary electrode, and silver wire reference. Measurements were then referenced with respect to an internal ferrocene standard.

Acknowledgement. We thank the ACS Petroleum Research Fund and the National Science Foundation (CHE-0718242) for financial support. We thank Prof. J. E. Hutchison for use of his group's potentiostat.

Supporting Information. Available on request

5. Bridge to Chapter V

Chapters III and IV were devoted to the synthesis and characterization of thiophenes and acetylenes in an annulene scaffold. Chapter V is the work on improvements to the materials presented in Chapters III and IV by incorporating 2-butyl groups to the previous dehydrothieno[14]annulenes to stabilize the materials from undesired degradations. Further modifications were made by reaction with sodium sulfide afforded planarized terthiophenes.

CHAPTER V

SYNTHESIS AND PROPERTIES OF ALKYL-CAPPED DEYHYDROTHIENOANNULENES AND THEIR CONVERSION INTO PLANARIZED TERTHIOPHENES

This chapter contains the synthetic work and characterization by UV-Vis spectroscopy of several annulenes containing butyl capped protecting groups as well as further functionalization to form planarized 3-terthiophenes. The synthesis and characterization of the molecules presented were done by me. The manuscript was prepared by myself with editorial assistance from Prof. Michael M. Haley. After minor revisions this chapter will be submitted to Organic Letters and co-authored with Sean McClintock who will provide further computational detail.

Electron-rich unsaturated compounds have been of considerable focus in recent years.[1] Conjugated acetylene systems, in particular,[2] have garnered the bulk of this interest, which can be attributed to ease of preparation[3] and interesting materials properties such as nonlinear optical (NLO) activity,[4] liquid crystalline behavior,[5] and molecular switching.[6] The Haley group has and continues to synthesize and develop methods to prepare these highly unsaturated systems, particularly arene/acetylene systems such as dehydrobenzoannulenes (DBAs).[7-9] Concurrently, conjugated thiophene systems have also attracted much interest due to their highly conductive properties,

optical properties and relative environmental stabilities over many of their benzyl analogues that have been proposed as future cheap semi-conducting materials.[10,11]

Work performed on thiophene/acetylene-containing macrocycles by the groups of Youngs (e.g., **1**, Figure 1)[12] and Marsella (e.g., **2**)[13] produced macrocycles of higher order symmetries through intermolecular reactions of simple synthons.[12,13] Our desire for improved syntheses via intramolecular ring closure led to our initial communication which focused on the [18]annulene skeleton;[14] however, stability problems with the intermediate thienyldiynes forced us to examine 14- and 15-membered dehydrobenzothienoannulene (DBTA, e.g., **3**, **4**, **6**) and dehydrothienoannulene (DTA, e.g., **5**) topologies, with much greater success (Figure 1).[15]

FIGURE 1. Examples of previously reported thieno-fused annulenes.

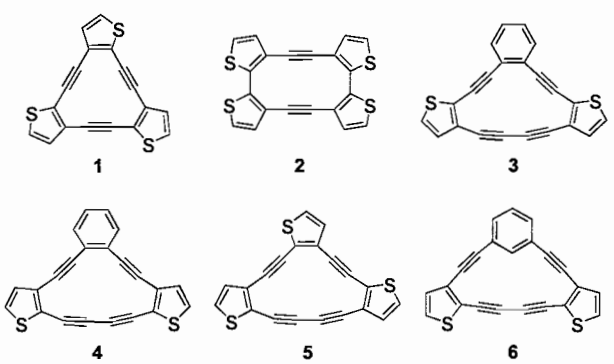

To further our understanding and scalability of thiophene-containing macrocycles, we have elected to incorporate α-alkylated thiophenes as part of the macrocycle (e.g., **7-12**) to improve solubility and, more importantly, to protect the compounds from unwanted oxidation.[11,16] The added stability conferred by the alkyl chain should also permit us to investigate the conversion of the diacetylene linker into a thiophene ring by

reaction of Na_2S.[17] The resultant terthiophenes (3TPs, e.g., **13-18**) contain more π-electron density from the thiophene sulfur atom and better electron delocalization than the diyne linker. Furthermore, the bridging 1,2-diethynylarene unit limits the rotation of the 3TPs, planarizing the 3TP moiety and thus enhancing π-orbital overlap further. We report herein the synthesis and optical properties of DBTAs/DTAs **7-12** and their conversion into 'planarized' 3TPs **13-18** (Figure 2).

FIGURE 2. Target thieno-fused dehydro[14]annulenes **7-12** and 'planarized' 3TPs **13-18**.

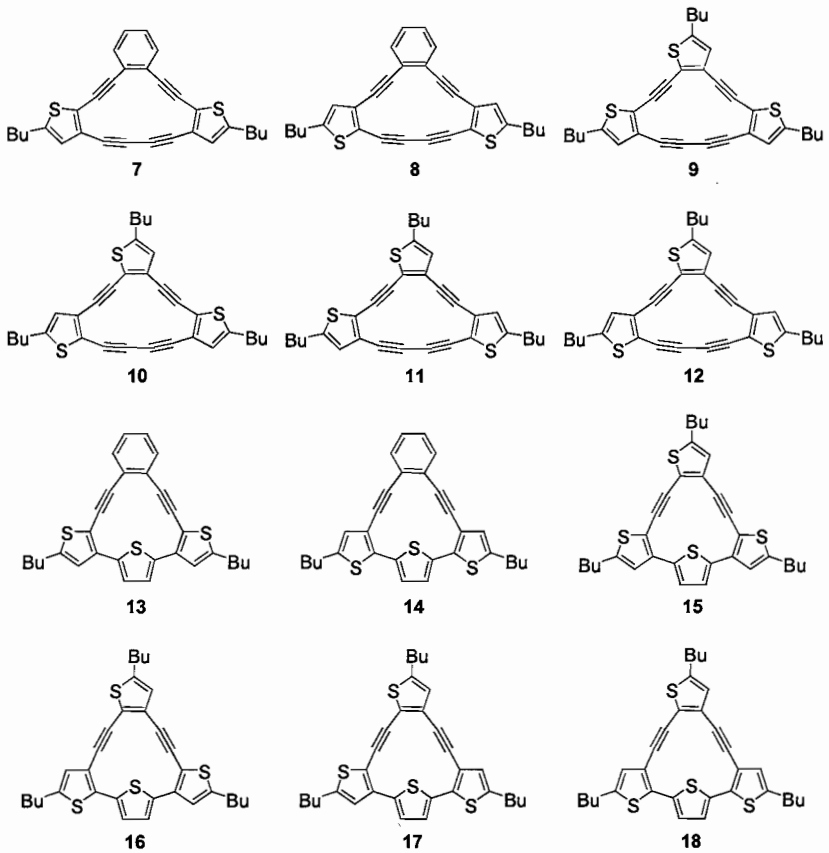

As with previous annulene works, the macrocycles were assembled from basic building blocks through a convergent design. The desire for alkylated thiophenes forced us to redesign the synthesis of our core dihaloarenes (**19**, **20**) and differentially-protected

diynes (**24**, **26**). Bromoiodothiophenes **19** and **20** were synthesized according to Scheme 1. Iodination of commercially available 2-butylthiophene furnished **21** in very good yield. Application of the lithium-halogen dance reaction[18] afforded **22** in 56% yield. This reaction proceeds much more slowly with iodoarenes than what is typically performed on bromoarenes, thus the reduced yields for iodine rearrangements.[18] NBS bromination of **22** provided multi-gram quantities of **19** in 36% overall yield. Regioisomeric **20** was easily prepared in an analogous manner: bromination of 2-butylthiophene and subsequent lithium-halogen dance reaction on **23** followed by iodine quench generated arene **20** in 90% overall yield. Halides **19** and **20** were subsequently converted into differentially-protected diynes **24** and **26** by sequential Sonogashira cross-coupling with (trimethylsilyl)acetylene (TMSA) and (triisopropylsilyl)acetylene (TIPSA) in excellent yields (vide infra).

SCHEME 1. Synthesis of dihalothiophenes **19** and **20.**

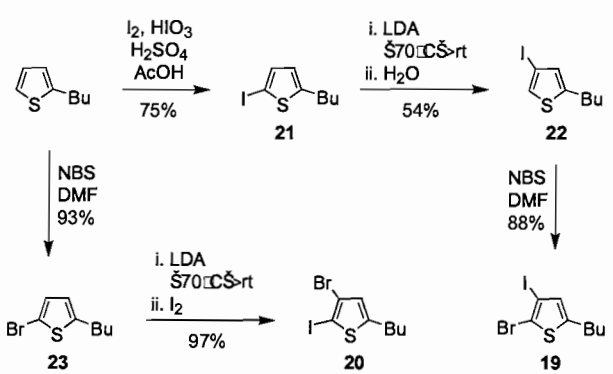

[14]DBTAs **7** and **8** and [14]DTAs **9** and **12** possess two fused thiophenes in a 'symmetrical' orientation on the lower portion of the annulene, and thus were assembled via twofold cross-coupling of the respective diyne to a central dihaloarene core. Scheme

2 illustrates a representative synthesis starting from **19**. Sequential Sonogashira reactions with TMSA and TIPSA afforded diyne **24** in 94% yield for the two steps. Selective removal of the TMS group with K_2CO_3 in MeOH followed by cross-coupling to 1,2-diiodobenzene furnished tetrayne **25** in 78% yield. Protiodesilylation with TBAF and subsequent acetylenic homocoupling utilizing $PdCl_2$(dppe) catalyst, CuI co-catalyst, and iodine as an oxidant[9a,19] gave DBTA **8** in 57% yield.

SCHEME 2. Synthesis of 'symmetrical' DBTA **8**.

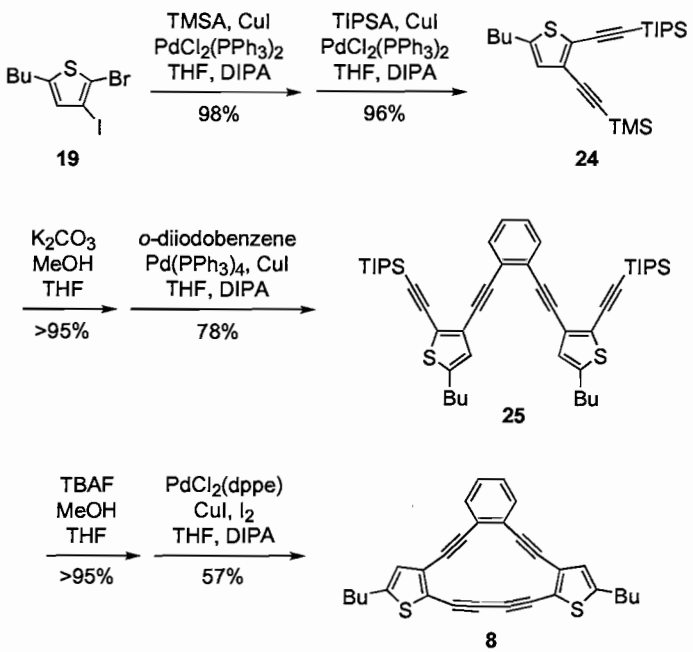

[14]DTAs **10** and **11** and possess two fused thiophenes in unsymmetrical orientations on the lower portion of the annulene, and are thus formed by sequential cross-couplings to the dihaloarene 'crown'. Scheme 3 shows a representative synthesis of 'unsymmetrical' DTA **10**. Dihalothiophene **20** was sequentially cross-coupled with TMSA and TIPSA under Sonogashira conditions to afford **26** in 91% yield. Selective

desilylation of **26** with K_2CO_3, cross-coupling to one equivalent of arene **19**, and then cross-coupling of the resultant bromodiyne to monodesilylated **24** furnished **27** in 48% combined yield. Macrocyclization was performed as before utilizing the Pd(II)/Cu(I) catalyst system under oxidizing conditions, affording **10** in 53% yield.

SCHEME 3. Synthesis of 'unsymmetrical' DTA **11**.

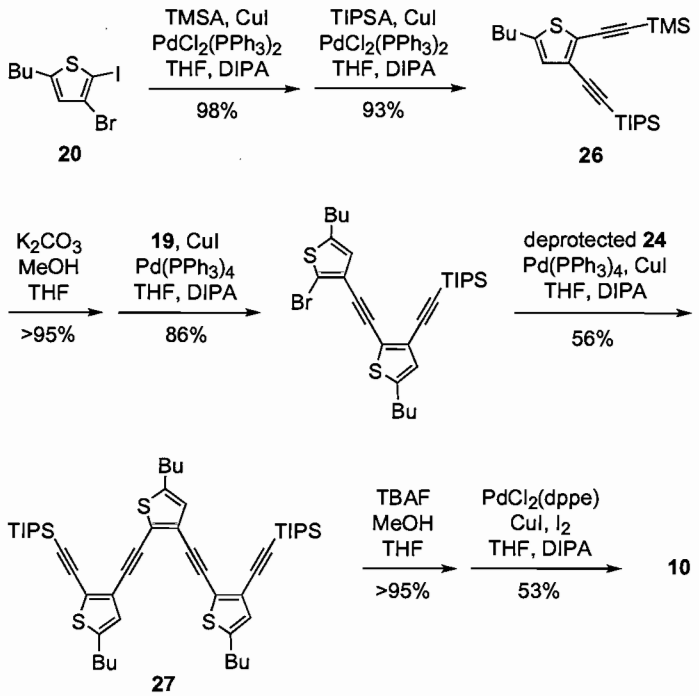

Completion of the planarized 3TPs is accomplished easily by treating the corresponding [14]annulenes with Na_2S in 2-(2-methoxyethoxy)ethanol (Scheme 4). A summary of the syntheses of all six annulenes and the 3TPs is given in Table 1. Attempting the same thiophene formation on the previously reported non-alkylated macrocycles[15a] produced promising results; however, the products were found to be extremely unstable to air and light, decomposing quite rapidly after a few hours to give

uncharacterizable mixtures. In contrast, all of the butylated products in this paper were much more stable to air, light, and silica gel, though overall yields of the DBTAs and DTAs were a bit lower than their non-butylated counterparts.[15a]

SCHEME 4. Synthesis of "planarized" terthiophene **13**.

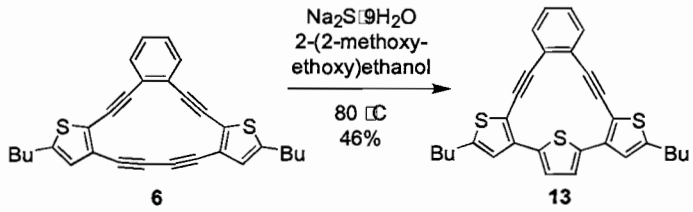

TABLE 1. Synthesis and Yields of DTAs and DBA/DTA Hybrids 3-14.

	"equivalents" of monodesilylated diyne		precursor, yield	annulene, yield	3TP, yield
dihalide	**24**	**26**			
19	2		pre**7**, 9%	**7**, 64%	**13**, 46%
19		2	pre**8** (**25**), 78%	**8**, 57%	**14**, 38%
19	2		pre**9**, 21%	**9**, 52%	**15**, 43%
20	1 (second)	1 (first)	pre**10** (**27**), 48%	**10**, 53%	**16**, 9%
20	1 (first)	1 (second)	pre**11**, 34%	**11**, 66%	**17**, 24%
19		2	pre**12**, 21%	**12**, 32%	**18**, 42%

The UV-vis spectra for [14]DBTAs **7** and **8** and the corresponding 3TPs **13** and **14** are shown in Figure 3a. Compared to **3** and **4**, electronic donation of the two butyl groups in **7** and **8** red shifts the respective peaks by 6-12 nm. The same trends with thiophene orientation are also maintained: an increased extinction coefficient and red shift are observed for both **4** (408 nm) and **8** (422 nm) with 'down' oriented thiophenes compared to **3** (374 nm) and **7** (381 nm) with 'up' thiophenes, whereas the highest intensity peak is slightly blue shifted for **4** (325 nm) and **8** (331 nm) over **3** (329 nm) and

7 (337 nm). Upon terthiophene formation, the lowest energy bands in **13** and **14** are significantly red shifted from **7** and **8** (381→415 and 422→442 nm, respectively), thus reflecting enhanced electron delocalization of the 3TP macrocycles over the diacetylenic DBTAs. Additionally, thiophene connectivity via α-α linkages as in **14** makes for a better chromophore than the α-β thiophene links in **13**; it is well established that α-α connectivity offers the narrowest energy band gap over all other possible thiophene arrangements.[11,20]

FIGURE 3. UV-vis absorption spectra of (a) **7-8**, **13-14**, (b) **9-12**, and (d) **15-18**. All spectra recorded in CH_2Cl_2 at analyte concentrations of 15-25 μM.

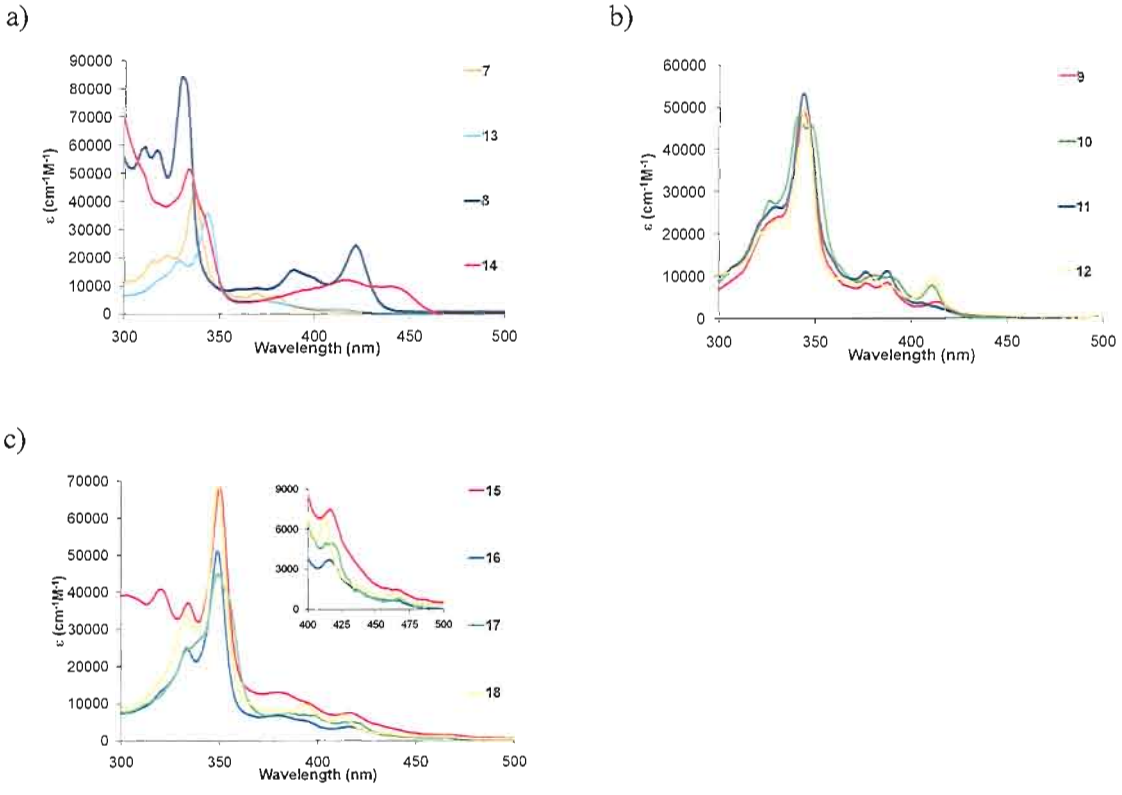

The UV-vis spectra for DTAs **9-12** are depicted in Figure 3b. The most intense peak is approximately the same for **9-12** (ca. 345 nm), with slight variations in vibronic

structure, and is red shifted compared to **5** (335 nm), again due to the electron donation of the butyl groups. In the low energy region, the most red-shifted peak belongs to **9** (415 nm) followed by DTAs **11** and **12**, with a common peak at 412 nm, and then **10** (409 nm). Analogous to what was observed with the non-alkylated [14]DTAs,[15a] there are no discernable trends of the low energy absorptions with respect to thiophene orientation.

Sulfide-induced cyclization to generate 3TPs **15-18** results in further red shifting (ca. 5 nm) of the Soret band to 350 nm, as well as a bathochromic shift and broadening of the low energy transitions (Figure 3c). In addition, there is a new, very weak, low energy transition centered around 465-470 nm, a feature unique to the all-thiophene 3TPs. Taken as a whole, the most bathochromically shifted material is compound **9**, due perhaps to the better π-orbital overlap of the benzene "crown" and the α-connected thiophenes.

In conclusion, six thieno-fused [14]annulenes were prepared that exhibit enhanced stability and synthetic scalability over their unsubstituted counterparts due to the presence of butyl groups on the α-positions. Furthermore, this enhanced stability allows for subsequent conversion to a novel class of linked terthiophenes with enhanced planarity. Future reports will discuss the electrochemical and enhanced emissive properties of the butylated DTAs and 3TPs.

CHAPTER VI

CONCLUDING SUMMARY

Dehydrobenzoannulene chemistry has evolved over the past fifty years afford a diverse array of annulenes with multiple topologies and functionalities. Initially work was pioneered by the groups of Eglinton, Nagakawa, and Staab in the 1950's through early 1970's. The 1990's were witness to a resurgence in annulene chemistry with the advent of cross-coupling techniques. Together, these compounds have demonstrated a wide array of properties ranging from probes for aromaticity, precursors for new carbon allotropes, and nonlinear optical activity. With the impressive properties as demonstrated by annulenes, the synthesis and application of these materials will be further explored.

Alternatively, conjugated and fused thiophene chemistry has made significant strides in the field of device application for organic semi-conducting and photovoltaic materials in addition to nonlinear optical effects. Fused thiophenes and thiophene incorporated macrocycles are now being explored more closely in attempts to further tailor and understand thiophene conjugation.

My dissertation evolved into a fusion of two different approaches in creating electron rich, highly reduced organic compounds. In Chapters III and IV, dehydrothienoannluenes (DTAs) and DTA/DBA hybrids were assembled using previously known DBA chemistry to afford co-planarized thiophenes that had more

annulenoid than oligo-thiophene character. These fused structures also displayed a wide array of structure property relationship stemming from the various arrangements and placement of thiophene moieties. Chapter V returns the annulenes to more oligothiophene character by first creating stabilized annulenes with 2-butyl capping groups followed by conversion to a co-planarized terthiophenes. The co-planarized terthiophenes exhibit lower energy electronic transitions due to enhanced π-orbital overlap which arise from the locked *o*-diethynylbenzene group as well as the addition of a new aromatic thiophene moiety. The development of more DTAs is particularly promising due to the inclusion of the alkyl groups which offer superior solubility and environmental stability. These new functionalities can offer further access to new topologies and substitutions which will help further the field of cyclic thiophene, oligothiophene, and annulene chemistry.

APPENDIX A

SYNTHESIS AND CHARACTERIZATION OF MULTIPLY-FUSED DEHYDROBENZOANNULENE TOPOLOGIES

This Appendix Contains Material that was coauthored with myself and Dr. Jerimiah A. Marsden. The chapter was written by Dr. Jerimiah Marsden while the bulk of the research was performed by me.

Carbon-rich materials comprise a fascinating branch of organic chemistry which has received a great amount of attention in recent years due to their unique chemical and physical properties.[1] Specifically, advances in the field of dehydroannulene chemistry have allowed the synthesis and study of a wide array of cyclic topologies including annulenes of various sizes, symmetries, shapes, and substitutions.[2] These macrocycles are often optically and non-linear optically active,[3] may polymerize topochemically to furnish polydiacetylenic tubes or "bucky" materials,[4] and have frequently been used as sensitive probes for studies of aromaticity.[5] Advances in the field of Pd-mediated alkyne cross-coupling reactions have brought about construction of increasingly larger and more complex dehydrobenzoannulene (DBA) systems.[2a] Recently, we reported an oxidative Pd-catalyzed alkyne homo-coupling procedure for the assembly of diacetylenic annulenes.[6] We now disclose the successful extension of this chemistry to the synthesis of DBA **1** (Figure 1), comprised of fused 14- and 15-membered rings and belonging to a

previously unattainable class of π-extended fenestrane-type[7] systems. We also herein describe the synthesis of a second unique DBA topology (**2**, Figure 1) from a shared precursor. There existed two main difficulties in the synthesis of macrocycle **1** which had to be overcome for its successful construction. The first obstacle was designing a system to minimize the large amount of steric bulk crowding the central ring of the precyclized material **3** (Scheme 1). The second difficulty to surmount was the closure of all four rings around the periphery of the DBA.

FIGURE 1. Compounds **1** and **2**.

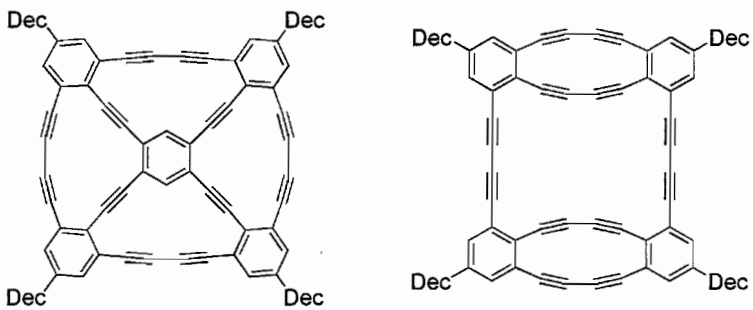

1 **2**

Our annulene syntheses typically take advantage of the difference in reactivity of trimethylsilyl (TMS) vs. triisopropylsilyl (TIPS) groups for protection of the alkynes to be used for cross-coupling vs. homo-coupling. However, the steric bulk from installing the necessary eight TIPS groups around the central ring would be impossible to achieve in this new system. The preparation of **3** instead relied upon the use of the smaller TMS groups. Triyne **4** seemed to be the ideal precursor for this synthesis, relying on only one alkyne protecting group and a terminal alkyne which was easily attached via the Stille reaction.

The synthesis proceeded by an initial triazene formation from diiodoaniline **5**[8] followed by cross-coupling of TMSA to the iodo-positions giving **6** in 96% yield (Scheme 1). Decomposition of the triazene and iodide substitution was accomplished by heating in MeI at 140 °C. A Stille cross-coupling of ethynyltributylstannane gave triyne **4** in 72% yield. Sonogashira cross-coupling of 4 with 1,2,4,5-tetraiodobenzene required heating at reflux for 60 h to give the precyclized polyyne **3** in 62%, which is a respectable 89% per cross-coupling transformation. The TMS groups were next removed with tetrabutylammonium fluoride (TBAF) and the material immediately subjected to cyclization.

No detectable annulene products were found from the Cu-mediated Glaser coupling of **3**, which gave only oligomeric byproducts. To induce ring-closure we turned to oxidative Pd-catalyzed homocoupling.[6,9] A distinct advantage of this route is the ability to tailor the reactivity of the catalyst by judicious choice of ligand. We have previously found that the cis-bidentate ligand, 1,2-diphenylphosphinoethane (dppe), favorably forms 14-membered annulenes with the geometry present in 1.6 We also determined $Pd(PPh_3)_2Cl_2$ will satisfactorily provide 15-membered DBAs, which are also present in macrocycle **1**. Initial closure of one ring should further facilitate cyclization by optimizing the geometry of terminal alkyne groups for subsequent ring closures. By using a mixture of the two aforementioned Pd-catalysts and 0.5 equiv of I_2 as an oxidant, synthesis of the first full wheel-type DBA **1** was achieved in 9% yield (55% per cyclization). To further minimize oligomer formation, polyyne **3** was slowly injected over a period of 60 h into the catalyst solution. However, with the lengthy reaction time,

we observed noticeable degradation of the Pd catalyst under the moderate temperature and oxidative conditions of the reaction. Therefore, addition of fresh catalyst at 24 h increments was required to complete the formation of the product. Material consisting of only three cyclized rings and two terminal alkynes was isolated in significant amounts if fresh Pd was not added.

SCHEME 1. Synthesis of DBA **1**

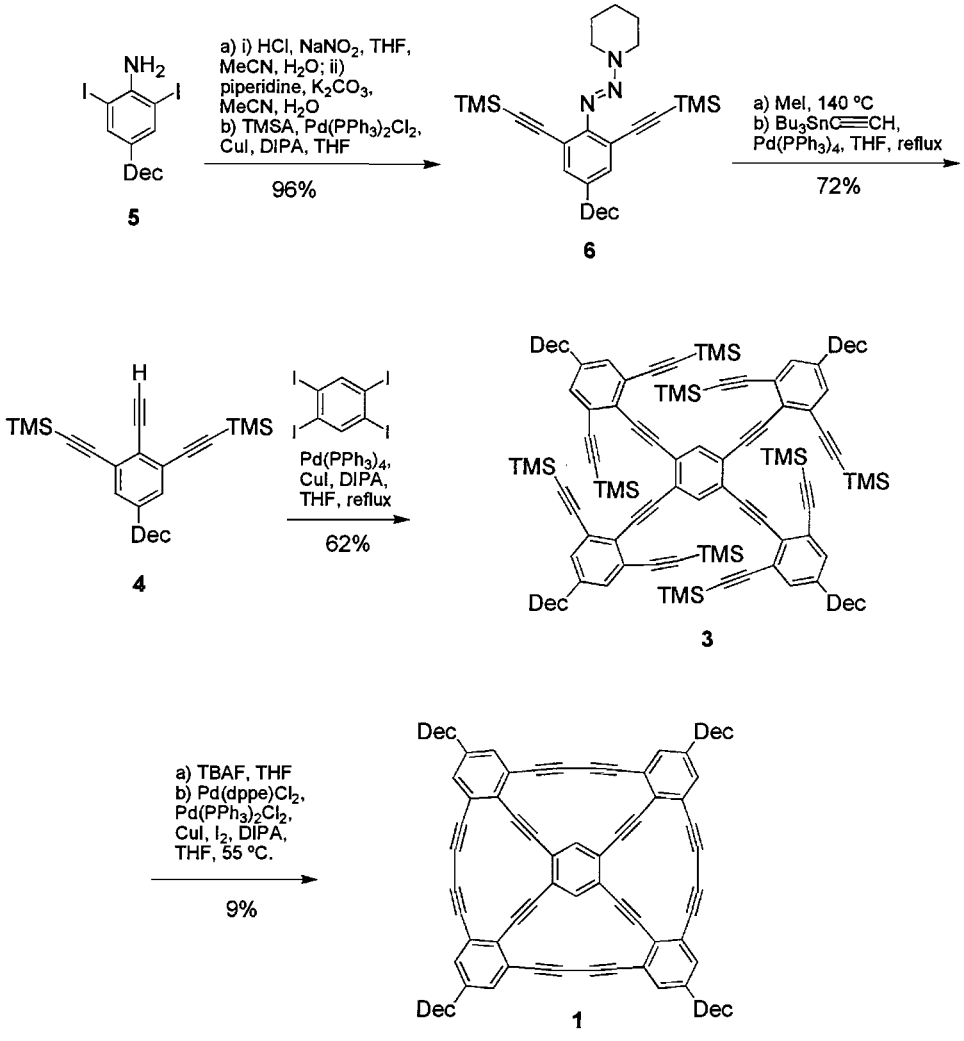

According to molecular modeling calculations,[10] fenestrane **1** should adopt a slight bowl shape which would help explain its remarkable solubility and stability. The ^{1}H NMR data was in agreement with known bis[15]- and bis[14]annulene systems (**7** and **8**, Figure 1) reported by Haley.[6] The intraannular proton confirmed a large anisotropic deshielding effect (δ = 8.41 ppm) due to their close proximity to the central alkyne bonds. The opposite effect was observed for the protons of the outer phenyls (δ = 7.06, 7.03 ppm) since these alkynes are bent away. Due to the excellent solubility of the DBA, a ^{13}C NMR spectrum was also acquired and agreed with the structural assignment. DSC data of **1** showed a broad exotherm starting ~250 °C indicative of random polymerization/decomposition.

The electronic absorption spectrum of 1 (Figure 3) displays similarities to the bis[15]- and bis[14]annulenes **7** and **8**. A red-shift of the absorption cut-off and broadening of the absorption bands due to increased overall conjugation and the more complex conjugated circuits is present in the spectrum of fenestrane **1**.

FIGURE 2. Compounds **7** and **8**.

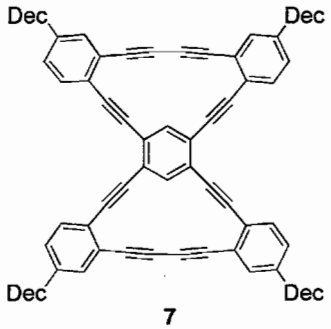

7

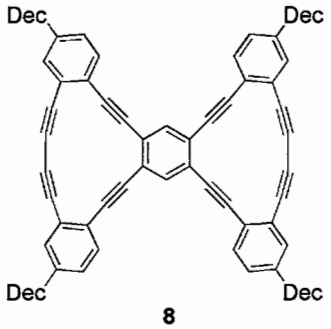

8

Through a series of intermolecular dimerizations of triyne **4**, the synthesis of another annulene of unique aesthetic appeal was possible. DBA **2** consists of two strained dehydrobenzo[12]annulenes fused to a central [24]annulene core. Triyne **4** was dimerized in quantitative yield to give **9** (Scheme 2). After removal of the TMS groups with TBAF, the polyyne was subjected to Cu-mediated homocoupling. [12]Annulenes such as **10** are known to form via this Cu/pyridine procedure.[2b,4c,11] Again in this ring system, an initial intramolecular homocoupling optimizes the geometry for subsequent cyclizations. The terminal alkynes of intermediate **10** are aligned parallel to each other and allow facile dimerization and cyclization providing the novel annulene **2** as a bright yellow solid in 13% yield.

FIGURE 3. Electronic absorption spectra of fenestrane **1** and bisannulenes **7** and **8**.

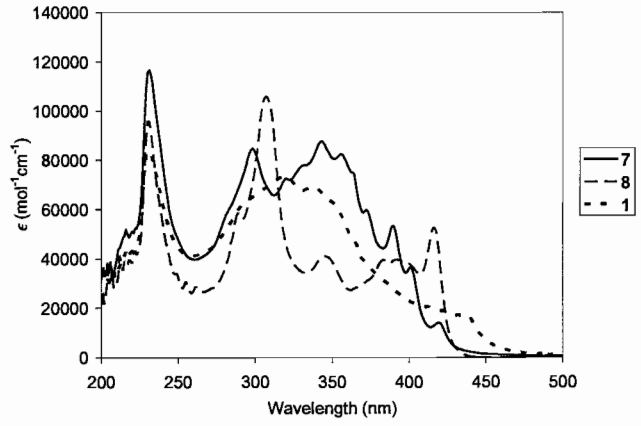

DBA **2** exhibited very low solubility in common organic solvents due to the large size and planarity of the macrocycle.[10] The solubility in $CDCl_3$ was enough to acquire ^1H NMR data, although inadequate for ^{13}C NMR characterization. Compared to **1**, the arene protons on **2** exhibit a much more significant upfield shift (δ 6.95, 6.74) due to the higher

degree of bending in the diynes as well as the presence of an anti-aromatic ring current in the two fused [12]annulenes. The DSC data of **2** displayed a broad exotherm peak similar to that of fenestrane **1**, although at a lower temperature of ~110 °C due to increased instability.

SCHEME 2. Synthesis of DBA **2**.

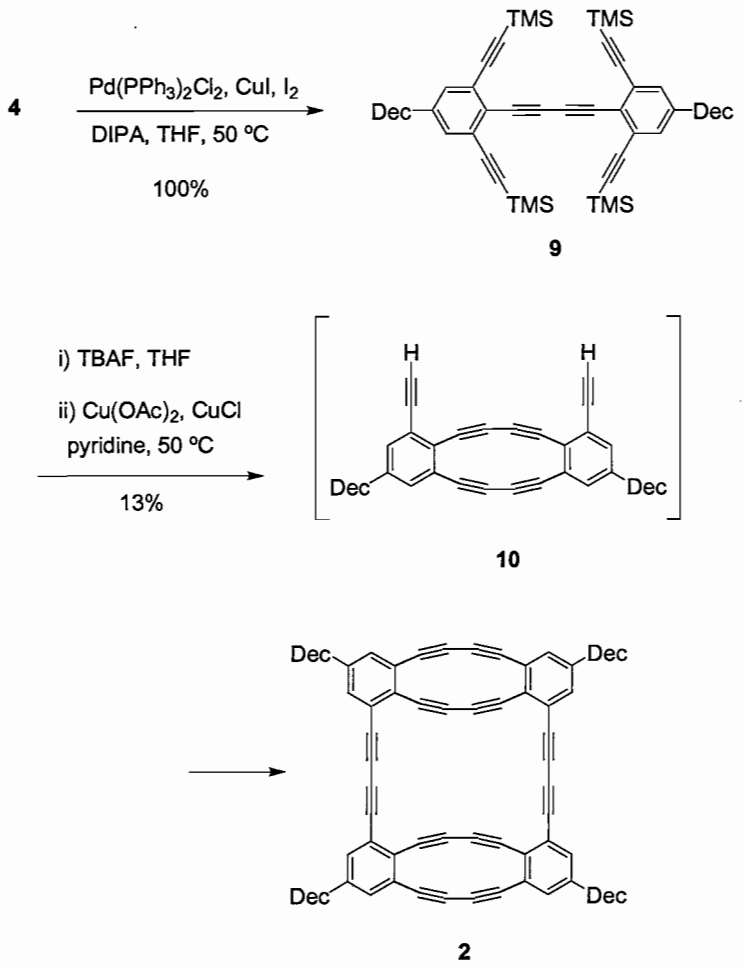

For comparison, the [12]- and [24]annulene substructures **11** and **12** were constructed.[12] The electronic absorption spectra of **2** displays similarities with both

annulene subunits. [24]Annulene **12** contains two major absorption bands also present in **2**, although the cut-off of the fused planar DBA is ~75 nm lower in energy (Figure 4). Also present in **2** are the sharp absorption peaks of **11**, though, due to the increased conjugation of the larger annulene, these peaks display an increase in absorption and a bathochromic shift of 35 nm.

FIGURE 4. Electronic absorption spectra of annulenoannulene **2** and model annulenes **11** and **12**.

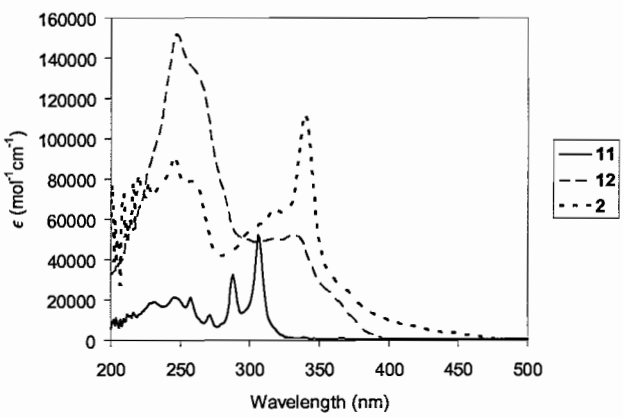

In conclusion, we have developed a straightforward synthesis of two complex dehydrobenzoannulene topologies utilizing our successful developments with oxidative Pd homocoupling chemistry. We have also demonstrated the effect of ring fusion on the electronic absorption properties of these annulenes. In the future we will continue our ongoing efforts toward the synthesis of larger and more complex DBA systems.

Acknowledgment. This work was supported by the National Science Foundation (CHE-04014175). J.A.M. acknowledges the NSF for an IGERT fellowship.

Supporting Information Available. Detailed experimental procedures and spectral data for compounds 1-4, 6, 9, 11 and 12 and their intermediates.

APPENDIX B

ISOLATION OF LINKED GOLD NANOPARTICLES VIA DIAFILTRATION

1 Introduction

This paper was co-authored with myself and Dr Scott F. Sweeney. Dr. Sweeney performed the nanoparticle work and written work while I afforded the organic synthesis of the ligand.

Nanoparticle homo- and hetero- structures, such as dimers and trimers, represent an exciting class of composite materials that are expected to have technologically useful electronic and optical characteristics. Specifically, plasmon-plasmon coupling between metal nanoparticles and plasmon-exciton coupling between metal and semiconducting nanoparticles are being actively investigated. Although a number of methods have been demonstrated for the preparation of linked nanoparticle structures, such as dimers and trimers, they are often low yielding and lead to mixed populations of monomers, aggregates and the desired structure. The presence of these impurities impedes the measurement of the electronic and optical properties of the assembled structures. Although a number of methods have been proposed for assembly, some deficiencies remain: (i) synthesis of the required linker can be difficult for routine preparations, (ii) linked nanoparticle preparations often result in mixed populations of monomers, linked

structures and aggregates and (iii) the linked structures are often prepared using citrate nanoparticles and are not functionalized, limiting their utility. Methods that provide convenient access to the desired nanostructures with useful functionality would greatly enhance our ability to measure their unique properties and allow for the further development of linked structures for a number of applications.

The assembly of nanoparticles into dimeric and trimeric structures is usually achieved by using multi-functional linkers. Feldheim et al. have shown that citrate stabilized gold nanoparticles can be linked using rigid phenylethynyl di-, tri- and tetrathiols, yielding the resultant dimers, trimers and tetramers in ~10% yield. Recent work has shown that nanoparticles can be monofunctionalized with carboxylic acid peripheral groups using Wang resins and subsequently linked using diamines to form well-defined dimer structures. Mirkin et al. have developed methods for the assembly of nanoparticles into dimeric structures through the use of complimentary base-pairing between DNA. Still others have formed nanocomposite agglomerates and aggregates through the assembly of nanoparticles using dithiols without regard for what type of structures are formed. Despite multiple preparation methods, yields of the desired linked structure are often very low.

This deficiency was quickly realized and methods for isolating or harvesting the desired nanostructures from monomers and aggregates were developed. These methods typically rely upon the use of size-exclusion chromatography or centrifugation. In the case of size-exclusion chromatography, yields of up to 55% of dimeric, 20% monomer

and 25% undefined have been obtained. Although these methods are useful, they rely upon costly chromatography supports, can require significant time, may not be applicable for the preparation of large quantities of materials and may not be applicable for the wide variety of nanostructures that are prepared. Furthermore, it has been shown that nanoparticles will often irreversibly aggregate onto chromatography supports. To avoid some of these roadblocks, we sought to leverage our existing diafiltration methods for the isolation of such nanoparticle structures.

FIGURE 1. Illustration of diafiltration, showing the elution of small impurties (organics, salts, nanoparticles) from the desired products.

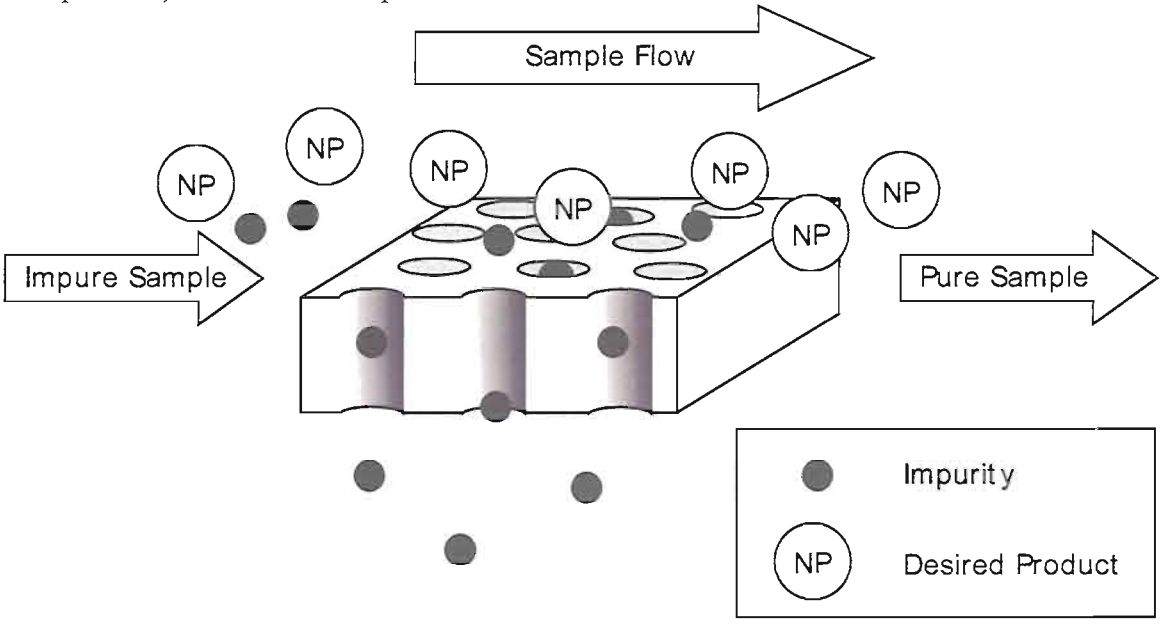

Diafiltration is a membrane-based method wherein pore size dictates the retention and elution of material from a sample (Figure 1). In the previous chapter, we showed that diafiltration was useful for both the removal of small molecule impurities as well as separating nanomaterials of disparate size. Based upon those results, we expected that diafiltration would allow for the isolation of gold nanoparticle trimers. In contrast to

previously reported methods, diafiltration offers the opportunity to separate both monomers and aggregates from the desired structure using a single approach with the additional benefits of fairly simple equipment requirements, scalability and convenience for rapid and routine separations.

Herein, we report (1) an improved, modular synthesis of rigid phenylethynyl trithiol ligands, first reported by Feldheim, for linking gold nanoparticles, (2) an improved two-step linking protocol for preparing functionalized trimeric nanoparticle structures using both 1.5 and 5-nm nanoparticles, and (3) the utilization of diafiltration to isolate linked nanoparticle structures. TEM analysis of the resultant nanoparticle structures indicates that the methods developed here may be a promising, general approach for the isolation of functionalized, linked nanoparticle structures.

2 Experimental Section

1-(4-(2-(trimethylsilyl)ethynyl)phenyl)-2-(piperidin-1-yl)diazene (4): A solution containing 11.58g (36.7mmol) of 1-(4-iodophenyl)-2-(piperidin-1-yl)diazene (**3**), 58mg (0.073mmol) of $PdCl_2(PPh_3)_2$, 27mg (0.15mmol) of CuI in 500mL of a 1:1 THF/ DIPA mixture was degassed under for 30 minutes. TMSA (5.68mL, 40.3mmol) was then added and allowed to stir overnight at room temperature. The solvent was then removed under reduced pressure and vacuum. The crude reaction mixture was run through a silica plug with 3:1 $MeCl_2$/Hexanes mixture to yield 11.52g of product in 90% yield: mp 86-88 °C; ^{1}H NMR (300 MHz, $CDCl_3$) δ 0.25 (s, 9H), 1.71 (bs, 6H), 3.79 (bs, 4H), 7.35 (d, J = 8.7Hz, 2H), 7.44 (d, J = 8.7Hz, 2H.

Three fold Symmetrical base (6): Compound **1** (5.0g, 17.5mmol) was stirred with 8.06g (58.5mmol) of K_2CO_3 for 30 minutes until terminal alkyne was deprotected. The reaction mixture was then filtered, extracted into 100mL of ether and washed successively with water, dried ($MgSO_4$), and filtered. After removing the ether under reduced pressure, the material was redissolved in toluene and degassed under argon for thirty minutes. Another vessel containing $Pd(PPh_3)_4$ (289mg, 0.25mmol), CuI (95mg, 0.50mmol), and 1,3,5-tribromobenzene (1.57g, 5.0mmol) in a 1:1 PhMe/DIPA mixture was also purged thoroughly with argon and set at reflux. The solution containing the free alkyne was slowed injected into the catalyst aryl halide mixture over 3 days. After completion, the solvent was then removed under reduced pressure and material crudely purified using a silica plug with 3:1 $MeCl_2$/hexanes to remove the catalyst and ammonium salts to yield 2.72g of three fold cross coupled product (**5**) and excess alkyne. Due to instabilities of triazenes on silica, the product was taken directly to the next step and dissolved in in 50mL of iodomethane freshly distilled over molecular sieves. Reaction mixture was sealed in pressurized flask and allowed to react overnight at 120 °C. Solvent was removed under reduced pressure and crude product run through a silica plug (1:1 $MeCl_2$/hexanes). The product was then purified by recrystallization in hexanes to yield 2.45g (3.3mmol) triiodinated product **6** in 64% overall yield. mp 265-280 °C; ^{1}H NMR (300 MHz, $CDCl_3$) δ 7.24 (d, J = 8.3Hz, 6H), 7.63 (s, 3H), 7.70 (d, J = 8.3Hz, 6H); ^{13}C NMR (75 MHz, $CDCl_3$) δ 88.99, 89.75, 94.71, 122.14, 123.80, 133.10, 134.14, 137.60; MS (APCI) *m/z* (%) 827 (100, M^++THF); IR (NaCl) ν 2151, 2208, 2845, 2953, 3042 cm^{-1}.

Three fold Symmetrical TMS ethynylated arene(7): Triidotriiyne **6** (200mg, 0.27mmol), $PdCl_2(PPh_3)_2$ (2.1mg, 0.0026mmol), and CuI (1.0mg, 0.0059mmol) was dissolved in 5mL of 1:1 THF/DIPA solution and purged for 30 minutes under argon. TMSA (0.15mL, 1.056mmol) was then added via syringe and the solution stirred overnight. The solvent was then removed under reduced pressure and material ran through a plug of silica with 1:1 $MeCl_2$/Hexanes. Hexayne **7** was isolated in 97% yield (172mg, 0.26mmol). mp 159-166 °C; ^{1}H NMR (300 MHz, $CDCl_3$) δ 0.271 (s, 27H), 7.46 (s, 12H), 7.63 (s, 3H); ^{13}C NMR (75 MHz, $CDCl_3$) δ –0.11, 89.50, 90.26, 96.54, 104.48, 122.70, 123.34, 123.86, 131.46, 131.94, 134.13; MS (APCI) *m/z* (%) 737 (100, MH^++THF); IR (NaCl) ν cm^{-1}.

Three Fold Ligand (1): Hexayne **7** (100mg, 0.149mmol) was reacted with 1.0mL 1.0M TBAF solution (1.0mmol) in 5mL of THF. The reaction was stirred for 20 minutes and then extracted into ether. The ethereal solution was then washed with water, dried over $MgSO_4$, and solvent removed under reduced pressure. The fully deprotected hexayne was then added to the arene **8** (145mg, 0.521mmol) and CuI (3mg, 0.0149mmol) and dissolved in 2.5mL of 2:1 DMF/THF solution and 0.75mL Hunnig's base. The solution was then freeze pump thawed for 3 cycles before adding the $Pd(PPh_3)_4$ (9mg, 0.00745mmol) and freeze pump thawed one additional cycle. The reaction was allowed to react at room temperature overnight. The solvent was then reduced under reduced pressure and material extracted into $MeCl_2$ (15mL) before being washed with water (5mL, 4x), dried ($MgSO_4$), and solvent removed under reduced pressure. The three fold symmetrical ligand **1** was isolated in 34% yield (50mg) as a white solid. mp 169-171 °C;

^{1}H NMR (300 MHz, $CDCl_3$) δ 2.45 (s, 9H), 7.4 (d, J = 8.4Hz, 6H), 7.53 (s, 12H), 7.56 (d, J = 8.4Hz, 6H), 7.67 (s, 3H); ^{13}C NMR (75 MHz, $CDCl_3$) δ 30.29, 89.64, 90.32, 90.61, 90.67, 122.77, 123.14, 123.88, 125.17, 128.32, 131.66, 132.17, 134.23, 193.39.

Extended iodide (9): A solution of **4** (603g, 2.12mmol) was first stirred with 10mL of 1.0M TBAF solution in 30mL of THF for 20 minutes and ether added. The resulting solution was then washed several times with 10% NaCl and then water, dried over $MgSO_4$, and solvent removed under reduced pressure. The free alkyne was then added to the triyne **6** (603mg, 2.1mmol) in 40mL 1:1 THF/DIPA mixture and purged with argon for 30 min. $Pd(PPh_3)_4$ (31mg, .026mmol) and CuI (10mg, 0.0529mmol) were then added and reaction sealed and reacted overnight at room temperature. The solvent was then removed under reduced pressure and material ran through a silica plug with 3:1 $MeCl_2$:hexanes. The material was immediately taken to the next step due to instabilities of triazenes in chromatography and dissolved in MeI (freshly distilled over dry molecular sieves) and reacted overnight in a pressurized vessel at 120 °C. The solvent was then removed under reduced pressure and material flash chromatographed with 10% $MeCl_2$: Hexanes. Material can be recrystallized with hexanes to yield **9** 365 mg in 65% yield. mp 169-171 °C; ^{1}H NMR (300 MHz, $CDCl_3$) δ 7.25 (d, J = 8.3Hz, 6H), 7.52 (s, 12H), 7.66 (s, 3H), 7.70 (d, J = 8.4Hz, 6H.

Extended Three fold Symmetrical TMS ethynylated arene(10): Triidotriiyne **9** (100mg, 0.095mmol), $PdCl_2(PPh_3)_2$ (5mg, 0.0057mmol), and CuI (3.0mg, 0.0114mmol) was dissolved in 5mL of 1:1 THF/DIPA solution and purged for 30 minutes under argon. TMSA (0.053mL, 0.38mmol) was then added via syringe and the

solution stirred overnight. The solvent was then removed under reduced pressure and material ran through a plug of silica with 1:1 $MeCl_2$/Hexanes. **10** can be further purified by recrystallizing in hexanes. Nonayne **10** was isolated in 92% yield (91mg). mp 159-166 °C; ^{1}H NMR (300 MHz, $CDCl_3$) δ 0.271 (s, 27H), 7.46 (bs, 12H), 7.52 (bs, 12H), 7.66 (s, 3H.

Three Fold Extended Ligand (2): Nonayne **10** (54mg, 0.056mmol) was reacted with 1.0mL 1.0M TBAF solution (1.0mmol) in 5mL of THF. The reaction was stirred for 20 minutes and then extracted into ether. The ethereal solution was then washed with water, dried over $MgSO_4$, and solvent removed under reduced pressure. The fully deprotected hexayne was then added to the arene **8** (93mg, 0335mmol) and CuI (1mg, 0.0056mmol) and dissolved in 1.5mL of 2:1 DMF/THF solution and 0.25mL Hunnig's base. The solution was then freeze pump thawed for 3 cycles before adding the $Pd(PPh_3)_4$ (3mg, 0.0028mmol) and freeze pump thawed one additional cycle. The reaction was allowed to react at room temperature overnight. The solvent was then reduced under reduced pressure and material extracted into $MeCl_2$ (15mL) before being washed with water (5mL, 4x), dried ($MgSO_4$), and solvent removed under reduced pressure. The three fold symmetrical ligand **7** was isolated in 75% yield (50mg) as a white solid. mp 169-171 °C; ^{1}H NMR (300 MHz, $CDCl_3$) δ 2.45 (s, 9H), 7.40 (d, J = 8.3Hz, 6H), 7.53 (m, 24H), 7.56 (d, J = 8.3Hz, 6H), 7.68 (s, 3H.

TOAB Nanoparticle Synthesis. In a 200 mL round-bottom flask, dissolved 1.1136 g tetraoctylammonium bromide in 80 mL toluene. To this, added 0.3266 g HAuCl4 in 20 mL Nanopure water. This was stirred until all of the gold was transferred to the toluene

layer. 0.4665 g of NaBH4 was dissolved in 30 mL of water. 25 mL of this NaBH4 solution was added to to the biphasic reaction mixture. Within 30 s, the solution had become a rich, ruby red color. This solution was allowed to stir for thirty minutes, then the aqueous layer was separated from the toluene dispersed nanoparticles. The nanoparticles in toluene were stored at 4C until use.

Trimer Synthesis. To a 20 mL scintillation vial, added 938 uL of as prepared gold nanoparticles was diluted in 8.5 mL of toluene. In a 1 mL Eppendorf tube, 24 uL of a 10 mg/mL (100:1 linker:nanoparticle ratio) solution of the trithiol molecule in THF:ethanol (70:30) was diluted to 500 uL in the same THF:ethanol mixture. Trithiol mixture was added dropwise to the gold nanoparticle solution with vigorous stirring. Following addition, the linking was allowed to continue for 4 hrs or overnight. In the case of deprotection, a couple of drops of ammonium hydroxide were added to the trithiol linker prior to addition to the nanoparticle sample.

Ligand Exchange. Water soluble, linked gold nanoparticles were prepared by adding an excess of mercaptoethanesulfonate, 2,2'-mercaptoethoxyethoxy ethanol or dimethaylaminopyridine to the nanoparticle solutions. In general, the mass of nanoparticles in solution was estimated and an equivalent mass of ligand was added to the solution. Following addition, the ligand exchange was allowed to proceed until full exchange was noted (almost immediately for DMAP, ~4 hrs for MEE). Following exchange, the aqueous layer was separated from the toluene and washed with methylene chloride. The stream of N2 gas was bubbled through the solution to remove any residual methylene chloride.

Diafiltration. To isolate the linked structures from monomers in solution, ligand exchanged products were diafiltered on a 300 kDa diafiltration membrane until no remaining color could be seen in the retentate, indicating that all nanoparticles or structures smaller than the pores had been eluted.

TEM Inspection. Samples for TEM inspection were aerosoled onto SiO TEM grids and imaged. Collected images were inspected manually for the presence of dimeric and trimeric species. Generally, more than 500 individual particles and linked structures were counted to determine the percentage of linked structures in a sample.

3 Results and Discussion

The work described here is based upon previous work by Feldheim et al. using rigid arylethynyl-thiolate ligands. In their work, large citrate stabilized gold nanoparticles of 8 to 10-nm obtained commercially were linked using di-, tri- and tetrathiols. To carry out the procedure, the linker dissolved in EtOH:THF was added dropwise to an aqueous dispersion of the nanoparticles. As prepared, the yield of linked structures is ~5-15%. Follow-up work by their group showed that size-exclusion chromatography could be used to enrich the population of linked structures to ~55%. Despite some improvement, we sought to improve this existing method by: (1) Developing an improved, modular synthesis of the trithiol ligand used to link the nanoparticles, allowing for more convenient access and allowing for easy tailoring of the terminal functional group allowing for the linking of diverse classes of nanomaterials. (2) Developing a novel linking approach that allows for homogeneous linker-nanoparticle mixing and also allows

for convenient functionalization following linking. (3) Leveraging our existing diafiltration platform to isolate the linked nanoparticle structures from monomers and aggregates. Our previous results suggest that diafiltration is well suited to the separation of linked structures from impurities such as excess linker, monomers and aggregates. It was anticipated that the approach developed here would allow for more convenient access to the desired linked nanoparticle structures at higher yields than previously reported.

3.1 Ligand Synthesis

The previous reports of the three fold symmetrical ligands **1** and **2** do not detail the synthesis nor full characterization of the molecules.[1] In this report we provide a detailed and improved synthetic report of both ligands as shown in Figure B.1 and B.2 (Appendix B). Due to additional stability, the diethylamine derived triazene was replaced with the piperdine derived triazene **3**. Trimethylsilyl acetylene was cross coupled to **3** under Sonogashira cross coupling conditions to produce monoyne **4** in 87% yield. Monoyne **4** was deprotected using mild base in 1:1 THF/ MeOH affording the free alkyne and taken to the next step. Slow injecting the free alkyne into a solution containing the cocatalysts $Pd(PPh_3)_4$ and CuI, 1,3,5-tribromobenzene in refluxing 1:1 PhMe/DIPA (diisopropylamine) mixture afforded the three fold cross coupled product **5** and excess free alkyne with little formation of dimer. Taking the reaction mixture to the next step was found to minimize degradation of **5** in chromatography. Triazene **5** was then dissolved in freshly distilled MeI and heating to 120 °C overnight to produce the triiodo-

triyne **6** which could be easily isolated chromatographically in overall 64% yield (3 steps). TMSA cross coupling of **6** under Sonogashira cross coupling conditions easily afforded the hexayene **7** in 94% yield.

FIGURE 2. Structure of the three-fold linkers **1** and **2** used in this study.

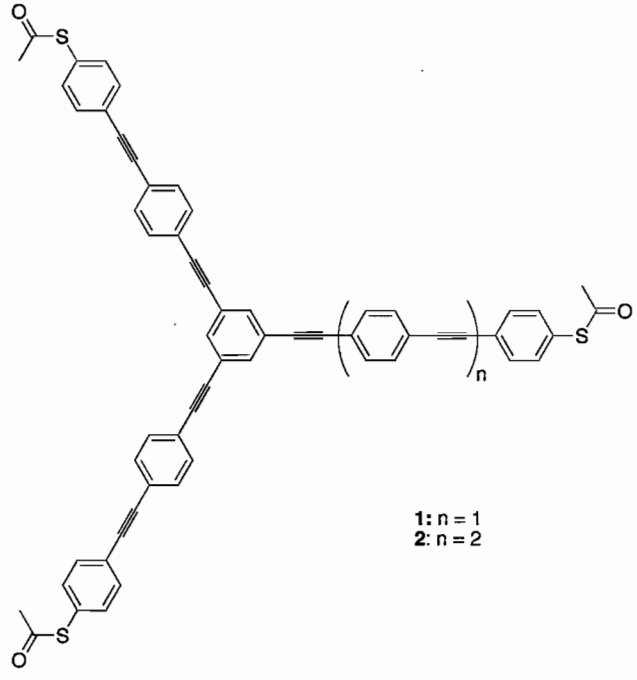

Figure B.2 shows the synthesis of the final protected thiol capped ligands **1** and **2.** In order to increase yield, 4-Bromophenylthioacetate was replaced with 4-iodophenylthioacetate[3] (**8**). Hexayene **7** was first deprotected with TBAF and then cross coupled to **8** under ambient conditions with a modified preparation reported by Hortholary and Coudret[3b] using Hunnig's base, DMF, and THF forming ligand **1** in 50% yield.

The extended ligand **2** was synthesized from triyne **6** which was cross coupled to deprotected **4** then iodinated in MeI to form **9** in 65% overall yield. Cross coupling

TMSA to the terminal iodides produces **10** in 94% yield (Figure B.1). Final cross coupling of **10** was done under identical conditions as **7** to generate **2** in 45% yield (Figure B.2).

3.2 Linked Nanoparticle Preparation

In Feldheim's original report, citrate stabilized gold nanoparticle were linked with rigid linkers in water. The linkers were dissolved in THF:ethanol and added dropwise to the aqueous nanoparticle solutions, yielding a low population of the desired structures. A couple of factors may have led to the low yields of the desired material. First, citrate nanoparticles are notoriously difficult to functionalize with thiols and only very recently have efficient functionalization methods been developed. Second, the linkers are not soluble in water and the volume of co-solvent added is quite small with respect to the overall volume. This heterogeneity could lead to difficulties in the linking procedure. Taken together, these factors would lead to low yields overall.

To overcome these issues, we attempted a number of alternative preparative strategies, including (i) amide coupling of carboxylic and amine stabilized nanoparticles, (ii) coupling of carboxylic acid stabilized nanoparticles with diamines, (iii) coupling of thiol stabilized and citrate stabilized nanoparticles with water soluble dithiols. In all cases, very little of the desired dimeric species were attained either because of poor sterics (i.e. the linker was too short) or because of poor coupling efficiency. As a result, methods for taking advantage of the rigid linkers used by Feldheim were sought.

As a first improvement, the citrate nanoparticles were substituted with 5-nm tetraoctylammonium bromide stabilized nanoparticles. These particles are very easy to functionalize with thiols, and should provide for easy linking. Furthermore, these nanoparticles are organic soluble, which would allow for the linker to be in the homogenous environment with the nanoparticles and hopefully increasing linking efficiency with a resultant increase in linked nanoparticle yield. As a final improvement, it was envisioned that the existing, labile ligand shell could be exchanged for thiols bearing another functionality, yielding linked, thiol functionalized nanoparticle structures (Figure 3).

FIGURE 3. Trimer formation scheme. Initial TOAB stabilized nanoparticles are linked with either **1** or **2**, followed by ligand exchange to form the functional linked structure.

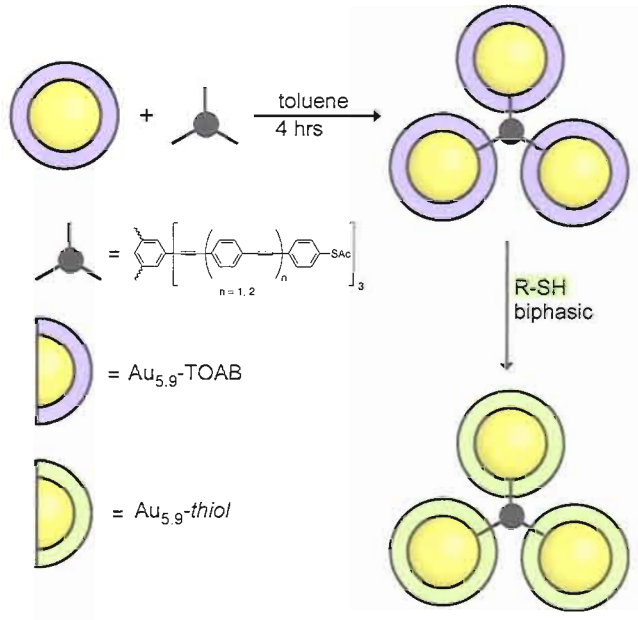

As a first step, TOAB stabilized nanoparticles in toluene were mixed at ratios of 6:1, 3:1, 1:1, 1:3 and 1:6 (nanoparticle:linker) with the rigid linker. After mixing for two

hours, the nanoparticles were inspected via TEM. Although it was expected that changes in the ligand to gold ratio would impact the yield of linked structures, TEM inspection showed no discernible difference amongst the samples. Further studies at more extreme nanoparticle:linker ratios (up to 1:1000) showed similar results. In all cases, trimer yields were ~2-3% of the total species present, and all linked structures (dimers and trimers) ranged from ~10 to 15%. Because linker concentration did not affect linked structure formation, it was hypothesized that the acetyl protecting group on the linker was interfering with the linking procedure (despite evidence from Feldheim's group that it didn't). Deprotection under mild, basic conditions prior to the linking reaction yielded no further improvements in linking. Although it had been envisioned that the use of labile ligands, under homogenous reaction conditions would improve linked nanoparticle structure yield, in fact, no appreciable improvement was realized.

3.3 Ligand Exchange and Diafiltration

As a result, diafiltration was attempted to increase the population of linked structures. Since the linking was carried out in toluene, the linked structures were transferred to the aqueous phase via a ligand exchange reaction. This was done by adding an excess of a water soluble ligand to the linked nanoparticles in a biphasic water/toluene system, separation and solvent washes to remove excess toluene. Ligand exchange was attempted with mercaptoethane sulfanate, mercaptoethoxyethanol and dimethylaminopyridine. MES exchange was unsuccessful, likely due to interactions between the MES and TOAB. However, both DMAP and MEE exchange were

successful. TEM inspection following the exchange showed similar 10-15% yields of linked structures.

A 300 kDa diafiltration membrane was used to isolate the linked structures from monomers in solution. Diafiltration was carried out until no color was seen in the permeate, indicating that all species smaller than the pore size had been eluted. Following the diafiltration step, the diafiltered sample was inspected via TEM. Manual counting of the linked species indicated an enrichment of total linked structures to ~36%, with ~6% of those being trimeric species (Figure 4). Although this was an improvement, the overall yield of trimers was far short of what is possible using diafiltration. Based upon this, it was theorized that perhaps there were some inherent limitations to this approach.

FIGURE 4. TEM images of ligand exchanged (A) and diafiltered (B) linked structure samples. Dimers are in squares, trimers are circled.

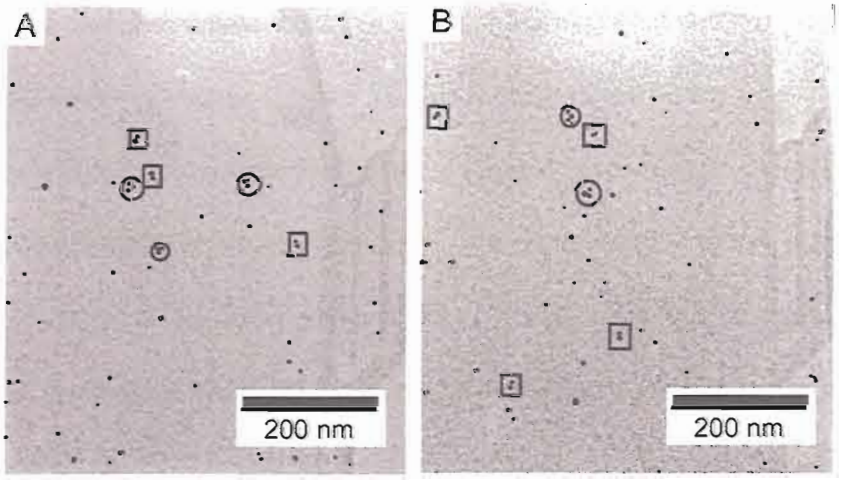

3.4 Ligand Exchange / Linking Dynamics

In order to gain a greater understanding of the linking chemistry, the dynamics of ligand exchange were studied. Ligand exchange is the most common method for

introducing peripheral functionality to gold nanoparticles, and allows for control over both solubility and over the reactivity of the nanoparticles. Generally, the gold nanoparticles are dispersed in a suitable solvent, and then an incoming ligand either under monophasic or biphasic conditions is added. This is allowed to stir for several hours or days either under ambient conditions or at elevated temperatures. Following the exchange, excess and exchanged ligand are removed via suitable purification methods. The exact mechanistic details are not understood, however for 1.5-nm TPP nanoparticles it has been shown that ligand dissociation occurs via the formation of a PPh_3AuCl salt followed by further dissociation of triphenyl phosphine to form higher order TPP-Au salts. In thiol stabilized nanoparticles, it has been suggested that ligand dissociation occurs via a concerted mechanism whereby an incoming ligand transfers a proton to the sulfur of an outgoing ligand.

It has been further hypothesized that certain locations on a nanoparticle are more reactive during ligand exchange (Figure 5). Vertex sites (areas where gold atoms have few nearest neighbors) are expected to have the highest reactivity, followed by edge sites, near edge face sites and then interior face sites. It is likely that the vertex sites are the most reactive because (1) the gold atoms at the vertex have the highest potential, and therefore show the highest reactivity (i.e. for redox chemistry) and (2) ligands at these sites are not stabilized by Van der Waals interactions. By the same arguments, interior surface sites show the greatest stability because the gold surface is more uniform and there is much higher ligand packing density, which increases the stability of the monolayer.

FIGURE 5. (A) General scheme for ligand exchange on a thiol stabilized gold nanoparticle. (B) Hypothesized truncated-cube structure of a gold nanoparticle. (C) Exchange rates for different sites on a gold nanoparticle with a truncated-cube like structure.

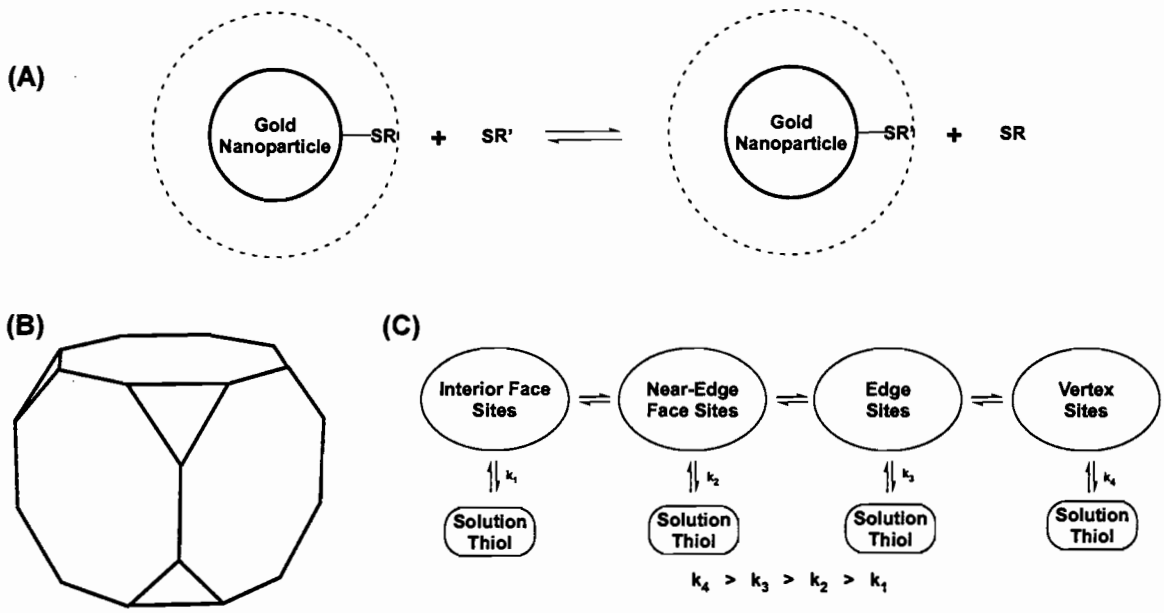

Several other factors have been shown to be important during the ligand exchange process. First, it has been shown that ligand exchange occurs most readily when the precursor particle has a ligand shell that is composed of short chain length and that is labile. Longer chain lengths lead to greater monolayer stability and lower exchange rates. It has also been shown that for the same reasons, incoming ligands that have favorable Van der Waal or hydrogen bonding interactions will show higher exchange rates. The concentration of incoming ligand also plays a large role. Although there is a 1:1 ligand exchange ratio, a high concentration of incoming linker is required to force the ligand exchange reaction to completion. The reason for this is that there is significant interchange of thiols both on the surface and in solution. As with any equilibrium

situation, pushing the reaction towards completion requires a significant excess of the incoming thiol. As well, time and temperature play a role in forcing the reaction.

The linking reaction used to from a gold nanoparticle trimer is similar to a ligand exchange reaction. Based upon this, some reasons for the low yield of linked structures include: (i) instability of the linker on the surface of the nanoparticle. Because the linker likely associates at a vertex or edge site, it can be very quickly exchanged. Furthermore, there are no favorable interactions between it and other molecules on the surface to stabilize it, thus linkers more than likely exchange very quickly on the surface of the particle. (ii) While association of a linker on a particle is probable, the association of this species with a second nanoparticle is expected to be limited due to size and sterics. The probability of this dimeric species interacting favorably with a third nanoparticle is even less likely, thus the trend of monomers > dimers > trimers observed in the work here. These results suggest that other approaches, based upon external linking mechanisms, may be more useful in the synthesis of linked nanoparticle structures.

4 Conclusion

Herein were described attempts at increasing the yield of linked gold nanoparticle structures through the use of rigid trithiolate linkers. Specifically, we described an improved synthesis of the linkers, allowing for a modular approach to their synthesis and a likely ability to tailor the peripheral functionality to diverse classes of materials. We described attempts at the linking of TOAB stabilized nanoparticles that could have led to greater yields of linked nanoparticle species, but remained limited to ~15% as previously

reported. Diafiltration of these linked structures allowed for an enrichment of up to 36% for both dimers and trimers in solution. Unfortunately, the low yields were likely due to the dynamics of ligand exchange on gold nanoparticles, which can place limits on the introduction of molecules on the surface of nanoparticles. Although not proven here, diafiltration remains a promising choice for the isolation of linked nanoparticle structures. Future work should focus upon increasing the yields of linked nanoparticle structures through alternative linking schemes. For example the use of base-pairing in DNA, as described by Mirkin et al., the use of chelating moieties as described for plasmon resonance based sensors or the use of coupling chemistry are all promising alternatives to the methods for nanoparticle linking described here.

APPENDIX C

CRYASTALLOGRAPHIC DATA FOR FIGURE 3.4

X-ray Crystallography. X-Ray diffraction intensities for 8 and 13 were collected on a Bruker SMART APEX CCD diffractometer at 173(2) K with MoKa radiation (l = 0.71073 Å). The crystallographic data for 8 and 13 and summary of the data collection and structure refinement are given in Table 1. Absorption correction was applied by SADABS [*]. The structure was solved using direct methods and completed by subsequent difference Fourier syntheses and refined by full matrix least-squares procedures on F2. All non-hydrogen atoms were refined with anisotropic displacement coefficients. H atoms were placed in calculated positions and refined in a riding group model. In both crystal structures there are two symmetrically independent molecules. The five-member C(9)-C(12),S(3) ring in both molecules of 13 are disordered over two positions corresponding two opposite orientations of the molecules. Atoms in the disordered rings were refined with restrictions: the standard S-C and C-C distances were used as targets for the corresponding bond lengths. All software and sources scattering factors are contained in the SHELXTL (6.10) program package [**].

X-Ray Data for 8

TABLE 1. Crystal data and structure refinement for 8.

Identification code	mh12	
Empirical formula	C22 H8 S2	
Formula weight	336.40	
Temperature	173(2) K	
Wavelength	0.71073 Å	
Crystal system	Monoclinic	
Space group	P2(1)/c	
Unit cell dimensions	a = 16.752(3) Å	α= 90°.
	b = 12.248(2) Å	β= 109.933(3)°.
	c = 16.951(3) Å	γ = 90°.
Volume	3269.7(10) $Å^3$	
Z	8	
Density (calculated)	1.367 Mg/m^3	
Absorption coefficient	0.323 mm^{-1}	
F(000)	1376	
Crystal size	0.22 x 0.12 x 0.03 mm^3	
Theta range for data collection	2.10 to 25.00°.	
Index ranges	-19<=h<=19, -14<=k<=14, -20<=l<=20	
Reflections collected	30979	
Independent reflections	5756 [R(int) = 0.0770]	
Completeness to theta = 25.00°	100.0 %	
Absorption correction	Semi-empirical from equivalents	
Max. and min. transmission	0.9904 and 0.9322	
Refinement method	Full-matrix least-squares on F^2	
Data / restraints / parameters	5756 / 0 / 497	
Goodness-of-fit on F^2	1.059	
Final R indices [I>2sigma(I)]	R1 = 0.0564, wR2 = 0.1112	
R indices (all data)	R1 = 0.0946, wR2 = 0.1291	
Largest diff. peak and hole	0.313 and -0.362 $e.Å^{-3}$	

TABLE 2. Atomic coordinates (x 10^4) and equivalent isotropic displacement parameters ($Å^2$x 10^3) for 8 (mh12). U(eq) is defined as one third of the trace of the orthogonalized U^{ij} tensor.

	x	y	z	U(eq)
S(1)	1098(1)	5646(1)	131(1)	41(1)
S(2)	516(1)	11399(1)	3395(1)	42(1)
C(1)	2050(2)	5306(3)	47(2)	42(1)
C(2)	2678(3)	6013(3)	444(2)	38(1)
C(3)	2387(2)	6884(2)	837(2)	32(1)
C(4)	1530(2)	6782(2)	720(2)	30(1)
C(5)	1318(3)	12297(3)	3870(2)	44(1)
C(6)	2022(2)	12112(3)	3675(2)	36(1)
C(7)	1933(2)	11197(2)	3130(2)	30(1)
C(8)	1136(2)	10734(2)	2918(2)	31(1)
C(9)	856(2)	9833(3)	2374(2)	32(1)
C(10)	782(2)	9083(3)	1898(2)	33(1)
C(11)	867(2)	8233(3)	1412(2)	32(1)
C(12)	1087(2)	7510(3)	1047(2)	31(1)
C(13)	2905(2)	7762(3)	1281(2)	31(1)
C(14)	3352(2)	8505(2)	1631(2)	30(1)
C(15)	3986(2)	9334(2)	1955(2)	27(1)
C(16)	4753(2)	9203(3)	1807(2)	36(1)
C(17)	5382(2)	9966(3)	2044(2)	42(1)
C(18)	5276(2)	10899(3)	2459(2)	45(1)
C(19)	4543(2)	11040(3)	2629(2)	40(1)
C(20)	3882(2)	10276(2)	2390(2)	29(1)
C(21)	3143(2)	10495(2)	2602(2)	31(1)
C(22)	2583(2)	10805(2)	2834(2)	32(1)
S(1')	9333(1)	8671(1)	3101(1)	48(1)
S(2')	8714(1)	2870(1)	6315(1)	59(1)
C(1')	8569(2)	9629(4)	2704(2)	47(1)
C(2')	7851(2)	9450(3)	2876(2)	38(1)

C(3')	7920(2)	8474(3)	3373(2)	34(1)
C(4')	8701(2)	7972(3)	3537(2)	36(1)
C(5')	7834(3)	2694(3)	6594(3)	58(1)
C(6')	7238(3)	3453(3)	6264(3)	52(1)
C(7')	7474(2)	4223(3)	5751(2)	42(1)
C(8')	8274(2)	4005(3)	5722(2)	44(1)
C(9')	8678(2)	4640(3)	5282(2)	46(1)
C(10')	8883(2)	5321(3)	4876(2)	47(1)
C(11')	8984(2)	6187(3)	4402(2)	45(1)
C(12')	8947(2)	7003(3)	4005(2)	40(1)
C(13')	7282(2)	8088(3)	3686(2)	35(1)
C(14')	6748(2)	7820(3)	3973(2)	34(1)
C(15')	6054(2)	7689(3)	4273(2)	32(1)
C(16')	5444(2)	8528(3)	4096(2)	43(1)
C(17')	4765(2)	8484(3)	4371(2)	50(1)
C(18')	4667(2)	7598(3)	4835(2)	47(1)
C(19')	5243(2)	6757(3)	5006(2)	41(1)
C(20')	5950(2)	6783(3)	4745(2)	33(1)
C(21')	6539(2)	5895(3)	5015(2)	38(1)
C(22')	6965(2)	5121(3)	5338(2)	40(1)

TABLE 3. Bond lengths [Å] and angles [°] for 8 (mh12).

S(1)-C(1)	1.700(4)
S(1)-C(4)	1.722(3)
S(2)-C(5)	1.711(4)
S(2)-C(8)	1.724(3)
C(1)-C(2)	1.352(5)
C(1)-H(1)	0.93(3)
C(2)-C(3)	1.429(4)
C(2)-H(2)	0.91(3)
C(3)-C(4)	1.386(4)
C(3)-C(13)	1.426(4)
C(4)-C(12)	1.390(4)
C(5)-C(6)	1.348(5)
C(5)-H(5)	0.91(3)
C(6)-C(7)	1.427(4)
C(6)-H(6)	0.87(3)
C(7)-C(8)	1.382(4)
C(7)-C(22)	1.428(4)
C(8)-C(9)	1.412(4)
C(9)-C(10)	1.201(4)
C(10)-C(11)	1.364(5)
C(11)-C(12)	1.208(4)
C(13)-C(14)	1.200(4)
C(14)-C(15)	1.435(4)
C(15)-C(16)	1.398(4)
C(15)-C(20)	1.412(4)
C(16)-C(17)	1.363(5)
C(16)-H(16)	0.86(3)
C(17)-C(18)	1.384(5)
C(17)-H(17)	0.91(3)
C(18)-C(19)	1.365(5)
C(18)-H(18)	0.91(4)
C(19)-C(20)	1.401(4)

C(19)-H(19)	0.90(3)
C(20)-C(21)	1.426(4)
C(21)-C(22)	1.197(4)
S(1')-C(1')	1.696(4)
S(1')-C(4')	1.713(3)
S(2')-C(5')	1.710(5)
S(2')-C(8')	1.726(4)
C(1')-C(2')	1.350(5)
C(1')-H(1')	0.84(4)
C(2')-C(3')	1.444(5)
C(2')-H(2')	0.77(3)
C(3')-C(4')	1.385(4)
C(3')-C(13')	1.427(5)
C(4')-C(12')	1.408(5)
C(5')-C(6')	1.338(5)
C(5')-H(5')	0.94(4)
C(6')-C(7')	1.427(5)
C(6')-H(6')	0.88(3)
C(7')-C(8')	1.383(5)
C(7')-C(22')	1.422(5)
C(8')-C(9')	1.402(5)
C(9')-C(10')	1.204(5)
C(10')-C(11')	1.376(6)
C(11')-C(12')	1.195(5)
C(13')-C(14')	1.199(4)
C(14')-C(15')	1.428(4)
C(15')-C(16')	1.408(4)
C(15')-C(20')	1.414(4)
C(16')-C(17')	1.369(5)
C(16')-H(16')	0.98(3)
C(17')-C(18')	1.382(5)
C(17')-H(17')	0.91(3)
C(18')-C(19')	1.373(5)
C(18')-H(18')	0.95(3)

C(19')-C(20')	1.398(4)
C(19')-H(19')	0.97(3)
C(20')-C(21')	1.434(5)
C(21')-C(22')	1.201(4)

C(1)-S(1)-C(4)	91.49(17)
C(5)-S(2)-C(8)	91.25(18)
C(2)-C(1)-S(1)	113.3(3)
C(2)-C(1)-H(1)	129(2)
S(1)-C(1)-H(1)	118(2)
C(1)-C(2)-C(3)	112.2(3)
C(1)-C(2)-H(2)	123.8(18)
C(3)-C(2)-H(2)	124.0(18)
C(4)-C(3)-C(13)	123.9(3)
C(4)-C(3)-C(2)	111.6(3)
C(13)-C(3)-C(2)	124.5(3)
C(3)-C(4)-C(12)	123.6(3)
C(3)-C(4)-S(1)	111.4(2)
C(12)-C(4)-S(1)	125.0(2)
C(6)-C(5)-S(2)	112.9(3)
C(6)-C(5)-H(5)	126(2)
S(2)-C(5)-H(5)	121(2)
C(5)-C(6)-C(7)	112.6(3)
C(5)-C(6)-H(6)	125(2)
C(7)-C(6)-H(6)	122(2)
C(8)-C(7)-C(6)	111.6(3)
C(8)-C(7)-C(22)	123.8(3)
C(6)-C(7)-C(22)	124.6(3)
C(7)-C(8)-C(9)	124.6(3)
C(7)-C(8)-S(2)	111.6(2)
C(9)-C(8)-S(2)	123.8(2)
C(10)-C(9)-C(8)	166.3(3)
C(9)-C(10)-C(11)	168.9(3)
C(12)-C(11)-C(10)	169.0(3)

C(11)-C(12)-C(4)	166.4(3)
C(14)-C(13)-C(3)	177.6(3)
C(13)-C(14)-C(15)	168.9(3)
C(16)-C(15)-C(20)	118.2(3)
C(16)-C(15)-C(14)	117.1(3)
C(20)-C(15)-C(14)	124.7(3)
C(17)-C(16)-C(15)	122.3(4)
C(17)-C(16)-H(16)	120.8(19)
C(15)-C(16)-H(16)	116.8(19)
C(16)-C(17)-C(18)	119.6(4)
C(16)-C(17)-H(17)	121(2)
C(18)-C(17)-H(17)	119(2)
C(19)-C(18)-C(17)	119.5(4)
C(19)-C(18)-H(18)	123(2)
C(17)-C(18)-H(18)	117(2)
C(18)-C(19)-C(20)	122.2(4)
C(18)-C(19)-H(19)	122(2)
C(20)-C(19)-H(19)	115(2)
C(19)-C(20)-C(15)	118.1(3)
C(19)-C(20)-C(21)	118.0(3)
C(15)-C(20)-C(21)	123.9(3)
C(22)-C(21)-C(20)	170.9(3)
C(21)-C(22)-C(7)	178.2(3)
C(1')-S(1')-C(4')	91.36(19)
C(5')-S(2')-C(8')	91.4(2)
C(2')-C(1')-S(1')	114.2(3)
C(2')-C(1')-H(1')	127(3)
S(1')-C(1')-H(1')	119(3)
C(1')-C(2')-C(3')	111.1(4)
C(1')-C(2')-H(2')	126(3)
C(3')-C(2')-H(2')	122(3)
C(4')-C(3')-C(13')	123.6(3)
C(4')-C(3')-C(2')	111.6(3)
C(13')-C(3')-C(2')	124.8(3)

C(3')-C(4')-C(12')	124.3(3)
C(3')-C(4')-S(1')	111.8(3)
C(12')-C(4')-S(1')	123.9(3)
C(6')-C(5')-S(2')	112.8(4)
C(6')-C(5')-H(5')	123(3)
S(2')-C(5')-H(5')	124(3)
C(5')-C(6')-C(7')	113.1(4)
C(5')-C(6')-H(6')	121(2)
C(7')-C(6')-H(6')	126(2)
C(8')-C(7')-C(22')	123.9(3)
C(8')-C(7')-C(6')	111.5(3)
C(22')-C(7')-C(6')	124.5(4)
C(7')-C(8')-C(9')	124.1(3)
C(7')-C(8')-S(2')	111.2(3)
C(9')-C(8')-S(2')	124.7(3)
C(10')-C(9')-C(8')	166.7(4)
C(9')-C(10')-C(11')	169.8(4)
C(12')-C(11')-C(10')	168.9(4)
C(11')-C(12')-C(4')	166.1(4)
C(14')-C(13')-C(3')	176.2(4)
C(13')-C(14')-C(15')	169.9(3)
C(16')-C(15')-C(20')	118.2(3)
C(16')-C(15')-C(14')	117.5(3)
C(20')-C(15')-C(14')	124.3(3)
C(17')-C(16')-C(15')	121.7(4)
C(17')-C(16')-H(16')	121.5(18)
C(15')-C(16')-H(16')	116.8(18)
C(16')-C(17')-C(18')	119.9(4)
C(16')-C(17')-H(17')	123(2)
C(18')-C(17')-H(17')	117(2)
C(19')-C(18')-C(17')	119.7(4)
C(19')-C(18')-H(18')	120(2)
C(17')-C(18')-H(18')	120(2)
C(18')-C(19')-C(20')	121.8(3)

C(18')-C(19')-H(19')	119.7(18)
C(20')-C(19')-H(19')	118.4(18)
C(19')-C(20')-C(15')	118.6(3)
C(19')-C(20')-C(21')	116.5(3)
C(15')-C(20')-C(21')	124.8(3)
C(22')-C(21')-C(20')	169.0(4)
C(21')-C(22')-C(7')	177.7(4)

Symmetry transformations used to generate equivalent atoms:

TABLE 4. Anisotropic displacement parameters ($Å^2 x\ 10^3$)for 8 (mh12). The anisotropic displacement factor exponent takes the form: $-2\pi^2[\ h^2 a^{*2} U^{11} + ... + 2\ h\ k\ a^*\ b^*\ U^{12}\ ]$

	U^{11}	U^{22}	U^{33}	U^{23}	U^{13}	U^{12}
S(1)	51(1)	30(1)	37(1)	-7(1)	10(1)	-14(1)
S(2)	46(1)	38(1)	48(1)	2(1)	26(1)	12(1)
C(1)	60(3)	29(2)	35(2)	-7(2)	15(2)	-3(2)
C(2)	41(2)	32(2)	41(2)	-5(2)	15(2)	-2(2)
C(3)	38(2)	26(2)	29(2)	-1(1)	9(2)	-2(2)
C(4)	38(2)	23(2)	30(2)	-2(1)	10(2)	-6(2)
C(5)	61(3)	32(2)	39(2)	-2(2)	18(2)	12(2)
C(6)	38(2)	27(2)	35(2)	1(2)	5(2)	2(2)
C(7)	33(2)	27(2)	27(2)	4(1)	8(2)	5(2)
C(8)	36(2)	25(2)	32(2)	2(2)	12(2)	7(2)
C(9)	28(2)	35(2)	37(2)	8(2)	15(2)	0(2)
C(10)	29(2)	33(2)	40(2)	4(2)	15(2)	-4(2)
C(11)	30(2)	29(2)	37(2)	4(2)	12(2)	-9(2)
C(12)	29(2)	31(2)	30(2)	3(2)	8(2)	-10(2)
C(13)	32(2)	28(2)	33(2)	1(2)	9(2)	2(2)
C(14)	30(2)	26(2)	35(2)	-1(2)	14(2)	2(2)
C(15)	25(2)	27(2)	27(2)	4(1)	5(1)	-1(1)
C(16)	33(2)	40(2)	36(2)	-2(2)	12(2)	5(2)
C(17)	25(2)	53(3)	50(2)	3(2)	14(2)	-2(2)
C(18)	29(2)	48(2)	51(2)	2(2)	7(2)	-15(2)
C(19)	38(2)	32(2)	46(2)	-4(2)	8(2)	-5(2)
C(20)	26(2)	27(2)	32(2)	-1(1)	6(2)	-3(1)
C(21)	32(2)	25(2)	34(2)	-2(1)	8(2)	-2(2)
C(22)	37(2)	23(2)	31(2)	0(1)	7(2)	-1(2)
S(1')	36(1)	66(1)	44(1)	-5(1)	16(1)	-4(1)
S(2')	79(1)	41(1)	45(1)	0(1)	5(1)	26(1)
C(1')	44(2)	55(3)	38(2)	6(2)	8(2)	-4(2)
C(2')	29(2)	42(2)	44(2)	-2(2)	15(2)	-4(2)
C(3')	28(2)	39(2)	34(2)	-8(2)	10(2)	-2(2)

C(4')	34(2)	42(2)	33(2)	-7(2)	13(2)	0(2)
C(5')	74(3)	40(2)	48(3)	4(2)	5(2)	5(2)
C(6')	55(3)	41(2)	51(3)	-2(2)	6(2)	1(2)
C(7')	53(2)	29(2)	34(2)	-4(2)	1(2)	6(2)
C(8')	63(3)	30(2)	31(2)	-7(2)	4(2)	13(2)
C(9')	54(3)	41(2)	36(2)	-10(2)	8(2)	22(2)
C(10')	51(2)	49(2)	40(2)	-7(2)	14(2)	24(2)
C(11')	43(2)	55(3)	38(2)	-12(2)	15(2)	17(2)
C(12')	38(2)	47(2)	37(2)	-13(2)	16(2)	4(2)
C(13')	31(2)	35(2)	36(2)	0(2)	6(2)	4(2)
C(14')	32(2)	32(2)	37(2)	1(2)	8(2)	2(2)
C(15')	27(2)	37(2)	31(2)	-1(2)	7(2)	2(2)
C(16')	39(2)	41(2)	49(2)	12(2)	17(2)	8(2)
C(17')	41(2)	57(3)	55(3)	10(2)	20(2)	20(2)
C(18')	36(2)	61(3)	48(2)	9(2)	20(2)	6(2)
C(19')	41(2)	43(2)	40(2)	5(2)	16(2)	-3(2)
C(20')	30(2)	35(2)	29(2)	1(2)	6(2)	0(2)
C(21')	38(2)	35(2)	36(2)	1(2)	7(2)	-2(2)
C(22')	49(2)	31(2)	35(2)	-6(2)	7(2)	0(2)

TABLE 5. Hydrogen coordinates (x 10^4) and isotropic displacement parameters ($Å^2$x 10^3) for 8 (mh12).

	x	y	z	U(eq)
H(1)	2070(20)	4680(30)	-250(20)	50(10)
H(2)	3226(18)	5930(20)	474(16)	18(8)
H(5)	1250(20)	12820(30)	4220(20)	47(10)
H(6)	2494(19)	12480(20)	3868(19)	29(9)
H(16)	4804(17)	8620(20)	1539(17)	20(8)
H(17)	5870(20)	9880(30)	1920(20)	46(10)
H(18)	5710(20)	11390(30)	2600(20)	60(12)
H(19)	4460(20)	11610(30)	2920(20)	49(11)
H(1')	8660(20)	10140(30)	2410(20)	68(14)
H(2')	7460(20)	9830(30)	2760(20)	44(12)
H(5')	7790(30)	2150(40)	6970(30)	89(16)
H(6')	6760(20)	3450(30)	6360(20)	32(10)
H(16')	5517(19)	9130(30)	3749(19)	40(9)
H(17')	4370(20)	9020(30)	4270(20)	42(10)
H(18')	4170(20)	7540(30)	4980(20)	48(10)
H(19')	5165(19)	6120(30)	5318(19)	36(9)

APPENDIX D

CRYASTALLOGRAPHIC DATA FOR FIGURE 3.5

X-ray Crystallography. X-Ray diffraction intensities for 8 and 13 were collected on a Bruker SMART APEX CCD diffractometer at 173(2) K with MoKa radiation (l = 0.71073 Å). The crystallographic data for 8 and 13 and summary of the data collection and structure refinement are given in Table 1. Absorption correction was applied by SADABS [*]. The structure was solved using direct methods and completed by subsequent difference Fourier syntheses and refined by full matrix least-squares procedures on F2. All non-hydrogen atoms were refined with anisotropic displacement coefficients. H atoms were placed in calculated positions and refined in a riding group model. In both crystal structures there are two symmetrically independent molecules. The five-member C(9)-C(12),S(3) ring in both molecules of 13 are disordered over two positions corresponding two opposite orientations of the molecules. Atoms in the disordered rings were refined with restrictions: the standard S-C and C-C distances were used as targets for the corresponding bond lengths. All software and sources scattering factors are contained in the SHELXTL (6.10) program package [**].

X-ray Data for 13

TABLE 1. Crystal data and structure refinement for 13 (mha14).

Identification code	mha14	
Empirical formula	C20 H6 S3	
Formula weight	342.43	
Temperature	173(2) K	
Wavelength	0.71073 Å	
Crystal system	Monoclinic	
Space group	P2(1)/n	
Unit cell dimensions	a = 17.698(2) Å	α= 90°.
	b = 10.0144(13) Å	β= 113.957(2)°.
	c = 19.344(3) Å	γ = 90°.
Volume	3133.2(7) $Å^3$	
Z	8	
Density (calculated)	1.452 Mg/m^3	
Absorption coefficient	0.467 mm^{-1}	
F(000)	1392	
Crystal size	0.09 x 0.06 x 0.03 mm^3	
Theta range for data collection	1.32 to 25.00°.	
Index ranges	-21<=h<=21, -11<=k<=11, -22<=l<=22	
Reflections collected	29359	
Independent reflections	5495 [R(int) = 0.1088]	
Completeness to theta = 25.00°	100.0 %	
Absorption correction	Semi-empirical from equivalents	
Max. and min. transmission	0.9861 and 0.9592	
Refinement method	Full-matrix least-squares on F^2	
Data / restraints / parameters	5495 / 26 / 471	
Goodness-of-fit on F^2	1.032	
Final R indices [I>2sigma(I)]	R1 = 0.0576, wR2 = 0.1028	
R indices (all data)	R1 = 0.1088, wR2 = 0.1221	
Largest diff. peak and hole	0.353 and -0.302 $e.Å^{-3}$	

TABLE 2. Atomic coordinates (x 10^4) and equivalent isotropic displacement parameters ($Å^2$x 10^3) for 13 (mha14). U(eq) is defined as one third of the trace of the orthogonalized U^{ij} tensor.

	x	y	z	U(eq)
S(1)	12821(1)	12696(1)	1145(1)	54(1)
S(2)	10940(1)	4665(1)	2142(1)	43(1)
C(1)	12219(3)	14047(4)	751(2)	47(1)
C(2)	11411(3)	13847(4)	586(2)	42(1)
C(3)	11251(3)	12525(4)	788(2)	36(1)
C(4)	11973(2)	11796(4)	1101(2)	35(1)
C(5)	9936(2)	4274(4)	1946(2)	41(1)
C(6)	9398(3)	5292(4)	1607(2)	37(1)
C(7)	9822(2)	6437(4)	1504(2)	32(1)
C(8)	10665(2)	6238(4)	1757(2)	33(1)
C(9)	9024(3)	11174(4)	561(2)	33(1)
C(10)	8713(2)	9966(4)	677(2)	32(1)
C(11)	7834(8)	10040(19)	486(11)	60(8)
C(12)	7500(7)	11268(10)	238(7)	37(3)
S(3)	8263(2)	12375(3)	253(2)	38(1)
C(9A)	9024(3)	11174(4)	561(2)	33(1)
C(10A)	8713(2)	9966(4)	677(2)	32(1)
C(11A)	8410(14)	12160(30)	287(17)	120(20)
C(12A)	7686(14)	11691(18)	273(17)	24(6)
S(3A)	7715(6)	10033(13)	490(6)	40(3)
C(13)	11228(2)	7186(4)	1718(2)	37(1)
C(14)	11585(2)	8148(4)	1628(2)	36(1)
C(15)	11867(2)	9361(4)	1489(2)	37(1)
C(16)	12006(2)	10460(4)	1337(2)	38(1)
C(17)	10466(3)	12009(4)	693(2)	37(1)
C(18)	9823(3)	11544(4)	643(2)	34(1)
C(19)	9139(2)	8754(4)	946(2)	33(1)
C(20)	9441(2)	7682(4)	1197(2)	35(1)
S(1')	8118(1)	2488(1)	2149(1)	36(1)

S(2')	5188(1)	8699(1)	-1468(1)	46(1)
C(1')	7930(2)	2163(4)	2932(2)	38(1)
C(2')	7242(2)	2765(4)	2917(2)	33(1)
C(3')	6834(2)	3550(4)	2250(2)	30(1)
C(4')	7259(2)	3504(3)	1780(2)	27(1)
C(5')	4384(2)	9602(4)	-1461(2)	43(1)
C(6')	4178(2)	9282(4)	-880(2)	39(1)
C(7')	4688(2)	8262(4)	-410(2)	33(1)
C(8')	5273(2)	7831(4)	-668(2)	34(1)
C(9')	4781(2)	5686(4)	1889(2)	27(1)
C(10')	4375(2)	6682(4)	1379(2)	27(1)
C(11')	3695(13)	7090(30)	1551(15)	35(7)
C(12')	3575(15)	6490(20)	2120(13)	36(5)
S(3')	4336(4)	5331(6)	2496(3)	30(1)
C(9B)	4781(2)	5686(4)	1889(2)	27(1)
C(10B)	4375(2)	6682(4)	1379(2)	27(1)
C(11B)	4391(15)	5470(20)	2400(13)	69(12)
C(12B)	3731(15)	6280(20)	2230(12)	42(6)
S(3'B)	3530(5)	7290(8)	1478(4)	33(1)
C(13')	5846(2)	6814(4)	-321(2)	35(1)
C(14')	6274(3)	5934(4)	61(2)	36(1)
C(15')	6710(2)	4979(4)	578(2)	36(1)
C(16')	7023(2)	4230(4)	1101(2)	33(1)
C(17')	6100(2)	4302(4)	2083(2)	31(1)
C(18')	5495(2)	4957(4)	1962(2)	29(1)
C(19')	4555(2)	7201(4)	782(2)	32(1)
C(20')	4618(2)	7697(4)	240(2)	33(1)

TABLE 3. Bond lengths [Å] and angles [°] for 13 (mha14).

S(1)-C(1)	1.699(4)
S(1)-C(4)	1.722(4)
S(2)-C(5)	1.705(4)
S(2)-C(8)	1.726(4)
C(1)-C(2)	1.348(5)
C(2)-C(3)	1.440(5)
C(3)-C(4)	1.381(5)
C(3)-C(17)	1.423(6)
C(4)-C(16)	1.407(6)
C(5)-C(6)	1.367(5)
C(6)-C(7)	1.429(5)
C(7)-C(8)	1.383(5)
C(7)-C(20)	1.428(5)
C(8)-C(13)	1.400(5)
C(9)-C(10)	1.385(5)
C(9)-C(18)	1.408(6)
C(9)-S(3)	1.721(4)
C(10)-C(19)	1.411(5)
C(10)-C(11)	1.449(14)
C(11)-C(12)	1.364(15)
C(12)-S(3)	1.737(9)
C(11A)-C(12A)	1.355(19)
C(12A)-S(3A)	1.708(16)
C(13)-C(14)	1.204(5)
C(14)-C(15)	1.380(6)
C(15)-C(16)	1.190(5)
C(17)-C(18)	1.195(5)
C(19)-C(20)	1.209(5)
S(1')-C(1')	1.709(4)
S(1')-C(4')	1.724(4)
S(2')-C(5')	1.692(4)
S(2')-C(8')	1.727(4)

C(1')-C(2')	1.348(5)
C(2')-C(3')	1.431(5)
C(3')-C(4')	1.396(5)
C(3')-C(17')	1.420(5)
C(4')-C(16')	1.408(5)
C(5')-C(6')	1.353(5)
C(6')-C(7')	1.420(5)
C(7')-C(8')	1.388(5)
C(7')-C(20')	1.428(5)
C(8')-C(13')	1.402(5)
C(9')-C(10')	1.382(5)
C(9')-C(18')	1.416(5)
C(9')-S(3')	1.696(6)
C(10')-C(19')	1.414(5)
C(10')-C(11')	1.432(16)
C(11')-C(12')	1.343(17)
C(12')-S(3')	1.700(16)
C(11B)-C(12B)	1.342(17)
C(12B)-S(3'B)	1.689(15)
C(13')-C(14')	1.200(5)
C(14')-C(15')	1.373(6)
C(15')-C(16')	1.199(5)
C(17')-C(18')	1.196(5)
C(19')-C(20')	1.206(5)

C(1)-S(1)-C(4)	91.1(2)
C(5)-S(2)-C(8)	91.6(2)
C(2)-C(1)-S(1)	113.5(3)
C(1)-C(2)-C(3)	112.3(4)
C(4)-C(3)-C(17)	123.1(4)
C(4)-C(3)-C(2)	110.9(4)
C(17)-C(3)-C(2)	126.0(4)
C(3)-C(4)-C(16)	123.6(4)
C(3)-C(4)-S(1)	112.2(3)

C(16)-C(4)-S(1)	124.2(3)
C(6)-C(5)-S(2)	113.4(3)
C(5)-C(6)-C(7)	111.2(4)
C(8)-C(7)-C(20)	122.2(4)
C(8)-C(7)-C(6)	112.8(4)
C(20)-C(7)-C(6)	125.0(4)
C(7)-C(8)-C(13)	124.9(4)
C(7)-C(8)-S(2)	111.0(3)
C(13)-C(8)-S(2)	124.1(3)
C(10)-C(9)-C(18)	131.2(4)
C(10)-C(9)-S(3)	111.1(3)
C(18)-C(9)-S(3)	117.7(3)
C(9)-C(10)-C(19)	128.6(4)
C(9)-C(10)-C(11)	111.7(8)
C(19)-C(10)-C(11)	119.7(8)
C(12)-C(11)-C(10)	113.7(14)
C(11)-C(12)-S(3)	110.3(11)
C(9)-S(3)-C(12)	93.1(5)
C(11A)-C(12A)-S(3A)	113(2)
C(14)-C(13)-C(8)	168.0(4)
C(13)-C(14)-C(15)	170.2(4)
C(16)-C(15)-C(14)	171.4(4)
C(15)-C(16)-C(4)	166.9(4)
C(18)-C(17)-C(3)	177.1(5)
C(17)-C(18)-C(9)	172.2(4)
C(20)-C(19)-C(10)	173.6(4)
C(19)-C(20)-C(7)	178.2(4)
C(1')-S(1')-C(4')	91.36(19)
C(5')-S(2')-C(8')	91.7(2)
C(2')-C(1')-S(1')	113.2(3)
C(1')-C(2')-C(3')	112.7(3)
C(4')-C(3')-C(17')	123.6(4)
C(4')-C(3')-C(2')	111.2(3)
C(17')-C(3')-C(2')	125.2(3)

C(3')-C(4')-C(16')	123.8(3)
C(3')-C(4')-S(1')	111.5(3)
C(16')-C(4')-S(1')	124.7(3)
C(6')-C(5')-S(2')	113.0(3)
C(5')-C(6')-C(7')	112.8(4)
C(8')-C(7')-C(6')	111.4(3)
C(8')-C(7')-C(20')	122.4(4)
C(6')-C(7')-C(20')	126.1(4)
C(7')-C(8')-C(13')	123.7(4)
C(7')-C(8')-S(2')	111.1(3)
C(13')-C(8')-S(2')	125.2(3)
C(10')-C(9')-C(18')	128.8(4)
C(10')-C(9')-S(3')	113.2(4)
C(18')-C(9')-S(3')	118.0(4)
C(9')-C(10')-C(19')	128.7(4)
C(9')-C(10')-C(11')	106.2(11)
C(19')-C(10')-C(11')	125.1(12)
C(12')-C(11')-C(10')	119(2)
C(11')-C(12')-S(3')	107(2)
C(9')-S(3')-C(12')	94.0(10)
C(11B)-C(12B)-S(3'B)	115.4(18)
C(14')-C(13')-C(8')	168.8(4)
C(13')-C(14')-C(15')	170.9(4)
C(16')-C(15')-C(14')	168.9(4)
C(15')-C(16')-C(4')	166.1(4)
C(18')-C(17')-C(3')	178.0(4)
C(17')-C(18')-C(9')	174.3(4)
C(20')-C(19')-C(10')	172.7(4)
C(19')-C(20')-C(7')	179.0(4)

Symmetry transformations used to generate equivalent atoms:

TABLE 4. Anisotropic displacement parameters ($Å^2$x 10^3)for 13 (mha14). The anisotropic displacement factor exponent takes the form: $-2\pi^2[h^2a^{*2}U^{11} + ... + 2\ h\ k\ a^*\ b^*\ U^{12}]$

	U^{11}	U^{22}	U^{33}	U^{23}	U^{13}	U^{12}
S(1)	43(1)	50(1)	74(1)	11(1)	29(1)	-7(1)
S(2)	47(1)	33(1)	54(1)	5(1)	27(1)	5(1)
C(1)	51(3)	36(3)	61(3)	0(2)	29(3)	-11(2)
C(2)	50(3)	39(3)	37(3)	2(2)	19(2)	-1(2)
C(3)	42(3)	38(3)	32(2)	-4(2)	19(2)	-1(2)
C(4)	41(3)	33(2)	35(3)	0(2)	21(2)	-5(2)
C(5)	45(3)	33(3)	50(3)	-3(2)	24(2)	-4(2)
C(6)	39(3)	33(2)	40(3)	-9(2)	17(2)	-6(2)
C(7)	38(3)	31(2)	26(2)	-5(2)	12(2)	1(2)
C(8)	38(3)	29(2)	37(3)	-1(2)	21(2)	2(2)
C(9)	29(3)	40(3)	28(3)	0(2)	9(2)	6(2)
C(10)	25(2)	42(3)	28(2)	-1(2)	10(2)	4(2)
C(11)	83(15)	37(10)	69(12)	1(8)	41(10)	-3(8)
C(12)	22(5)	53(7)	34(5)	9(6)	10(4)	-13(5)
S(3)	30(1)	40(1)	44(2)	9(1)	13(1)	11(1)
C(9A)	29(3)	40(3)	28(3)	0(2)	9(2)	6(2)
C(10A)	25(2)	42(3)	28(2)	-1(2)	10(2)	4(2)
C(11A)	170(50)	170(50)	70(30)	0(30)	90(30)	-60(30)
C(12A)	7(12)	16(11)	47(12)	-5(10)	9(9)	-7(9)
S(3A)	18(3)	64(7)	31(5)	3(4)	5(3)	12(3)
C(13)	36(3)	37(3)	42(3)	0(2)	21(2)	7(2)
C(14)	31(2)	36(3)	47(3)	3(2)	22(2)	8(2)
C(15)	27(2)	44(3)	44(3)	4(2)	18(2)	3(2)
C(16)	32(2)	43(3)	47(3)	3(2)	24(2)	-2(2)
C(17)	37(3)	40(3)	35(3)	-1(2)	16(2)	3(2)
C(18)	37(3)	33(2)	32(3)	1(2)	15(2)	4(2)
C(19)	28(2)	38(3)	31(3)	-6(2)	11(2)	-3(2)
C(20)	32(2)	43(3)	33(3)	-8(2)	15(2)	-6(2)
S(1')	38(1)	34(1)	39(1)	7(1)	18(1)	11(1)

S(2')	58(1)	43(1)	43(1)	17(1)	29(1)	11(1)
C(1')	46(3)	33(2)	33(3)	6(2)	15(2)	8(2)
C(2')	43(3)	26(2)	35(3)	5(2)	20(2)	5(2)
C(3')	32(2)	23(2)	36(3)	1(2)	14(2)	1(2)
C(4')	32(2)	19(2)	31(2)	3(2)	13(2)	5(2)
C(5')	44(3)	39(3)	43(3)	15(2)	16(2)	8(2)
C(6')	37(3)	34(3)	49(3)	6(2)	20(2)	5(2)
C(7')	39(2)	27(2)	32(2)	4(2)	14(2)	-4(2)
C(8')	41(2)	28(2)	36(3)	7(2)	20(2)	3(2)
C(9')	24(2)	33(2)	24(2)	-3(2)	10(2)	-5(2)
C(10')	25(2)	34(2)	23(2)	-2(2)	11(2)	-6(2)
C(11')	29(11)	34(10)	35(10)	14(6)	7(8)	24(7)
C(12')	13(7)	51(9)	41(11)	-14(7)	8(7)	4(6)
S(3')	27(2)	38(2)	32(2)	0(2)	18(2)	-3(2)
C(9B)	24(2)	33(2)	24(2)	-3(2)	10(2)	-5(2)
C(10B)	25(2)	34(2)	23(2)	-2(2)	11(2)	-6(2)
C(11B)	63(18)	60(14)	66(17)	25(10)	8(11)	19(11)
C(12B)	28(11)	83(13)	25(8)	10(7)	20(8)	7(8)
S(3'B)	31(2)	41(3)	30(2)	6(2)	16(2)	10(2)
C(13')	39(3)	37(3)	33(3)	4(2)	20(2)	2(2)
C(14')	43(3)	41(3)	31(3)	4(2)	22(2)	8(2)
C(15')	43(3)	35(3)	36(3)	-2(2)	23(2)	6(2)
C(16')	35(2)	27(2)	38(3)	-1(2)	16(2)	6(2)
C(17')	34(2)	23(2)	37(3)	3(2)	17(2)	-2(2)
C(18')	32(2)	29(2)	29(2)	2(2)	16(2)	-5(2)
C(19')	21(2)	34(2)	36(3)	-3(2)	7(2)	2(2)
C(20')	28(2)	35(2)	34(3)	4(2)	11(2)	0(2)

TABLE 5. Hydrogen coordinates (x 10^4) and isotropic displacement parameters ($Å^2$x 10^3) for 13 (mha14).

	x	y	z	U(eq)
H(1A)	12431	14865	656	57
H(2A)	10994	14502	361	50
H(5A)	9767	3432	2060	49
H(6A)	8817	5244	1460	45
H(11A)	7518	9302	529	72
H(12A)	6932	11487	80	44
H(11B)	8490	13029	133	146
H(12B)	7208	12231	154	29
H(1'A)	8276	1614	3338	45
H(2'A)	7050	2677	3307	40
H(5'A)	4105	10266	-1827	51
H(6'A)	3740	9695	-795	47
H(11C)	3330	7770	1264	42
H(12C)	3147	6677	2282	43
H(11D)	4574	4849	2805	83
H(12D)	3401	6273	2513	50

BIBLIOGRAPHY

Chapter I

(1) (a) *Modern Acetylene Chemistry*; Stang, P. F.; Diederich, F., Eds.; VCH: Weinheim, 1995. (b) *Acetylene Chemistry – Chemistry, Biology, and Materials Science*; Diederich, F.; Tykwinski, R. R.; Stang, P. J., Eds.; Wiley-VCH: Weinheim, 2005.

(2) (a) *Metal-Catalyzed Cross-Coupling Reactions*; Diederich, F.; Stang, P. J., Eds, Wiley-VCH: Weinheim, 1998. (b) *Transition Metal Catalyzed Reactions-IUPAC Monographs Chemistry for the 21st Century*; Davies, S. G.; Murahashi, S., Eds, Blackwell Science: Oxford, 1998. (c) *Handbook of Organopalladium Chemistry for Organic Synthesis*; Negishi, E., Ed, Wiley: New York, 2002. (d) *Metal-Catalyzed C-C and C-N Coupling Reactions*; de Meijere, A.; Diederich, F., Eds, Wiley-VCH: Weinheim, 2004.

(3) (a) Marsden, J. A.; Haley, M. M. in reference 2d; (b) Sonogashira, K. *J. Organomet. Chem.* **2002**, *653*, 46-49. (c) Negishi, E.; Anastasia, L. *Chem. Rev.* **2003**, *103*, 1979-2017.

(4) Siemsen, P.; Livingston, R. C.; Diederich, F. *Angew. Chem.* **2000**, *112*, 2740-2767. *Angew. Chem. Int. Ed.* **2000**, *39*, 2632-2657.

(5) (a) Haley, M. M.; Pak, J. J.; Brand, S. C. *Top. Curr. Chem.* **1999**, *201*, 81-129. (b) Bunz, U. H. F.; Y. Rubin, Tobe. Y. *Chem. Soc. Rev.* **1999**, *28*, 107-119. (c) Zhao, D.; Moore, J. S. *Chem. Commun.* **2003**, 807-818. (d) Marsden, J. A.; Palmer, G. J.; Haley, M. M.;, *Eur. J. Org. Chem.* **2003**, 2355-2369.

(6) (a) Grave, C.; Schlüter, A. D. *Eur. J. Org. Chem.* **2002**, 3075-3098. (b) Yamaguchi, Y.; Yoshida, Z. *Chem. Eur. J.* **2003**, *9*, 5430-5440. (c) Bunz, U. H. F. *J. Organomet. Chem.* **2003**, *683*, 269-287.

(7) Eglinton, G.; Galbraith, A. R. *Proc. Chem. Soc.* **1957**, 350-351.

(8) (a) Behr, O. M.; Eglinton, G.; Raphael, R. A. *Chem. Ind.* **1959**, 699-700. (b) Behr, O. M.; Eglinton, G. E.; Galbraith, A. R..; Raphael, R. A. *J. Chem. Soc.* **1960**, 3614-3625.

(9) Grant, W. K.; Speakman, J. C. *Proc. Chem. Soc.* **1959**, 231.

(10) Zhou, Q.; Carrol, P. C.; Swager, T. M. *J. Org. Chem.* **1994**, *59*, 1294-1301.

(11) Campbell, I. D.; Eglinton, G.; Henderson, W.; Raphael, R. A. *J. Chem. Soc., Chem. Commun.* **1966**, 87-89.

(12) (a) Castro, C. E.; Stephens, R. D. *J. Org. Chem.* **1963**, *28*, 2163. (b) Sladkov, A. M., Golding, I. R.;, *Russ. Chem. Rev.* **1979**, *48*, 868-896.

(13) Solooki, D.; Ferrara, J. D.; Malaba, D.; Bradshaw, J. D.; Tessier, C. A.; Youngs, W. J. *Inorg. Synth.* **1997**, 31, 122-128.

(14) Hunyh, C.; Linstrumelle, G. *Tetrahedron* **1988**, *44*, 6337-6344.

(15) Pham, S.; Haley, M. M. unpublished observations.

(16) Miljanic, O. S.; Vollhardt, K. P. C.; Whitener, G. D. *Synlett* **2003**, 29-34.

(17) Staab, H. A.; Graf, F. *Tetrahedron Lett.* **1966**, 751-757.

(18) Iyoda, M.; Vorasingha, A.; Kuwatani, Y.; Yoshida, M.; *Tetrahedron Lett.* **1998**, 39, 4701-4704.

(19) (a) Baldwin, K. P.; Bradshaw, J. D.; Tessier, C. A.; Youngs, W. J. *Synlett* **1993**, 853-855. (b) Baldwin, K. P.; Simons, R. S.; Rose, J.; Zimmerman, P.; Hercules, D. M.; Tessier, C. A.; Youngs, W. J. *Chem. Commun.* **1994**, 1257-1258.

(20) Kehoe, J. M.; Kiley, J. H.; English, J. J.; Johnson, C. A.; Petersen, R. C.;Haley, M. M. *Org. Lett.* **2000**, *2*, 969-972.

(21) Behr, O. M.; Eglinton, G.; Lardy, I. A.; Raphael, R. A. *J. Chem. Soc.* **1964**, 1151-1154.

(22) Guo, L.; Bradshaw, J. D.; Tessier, C. A.; Youngs, W. J. *Chem. Commun.* **1994**, 243-244.

(23) Baldwin, K. P.; Matzger, A. J.; Scheiman, D. A.;Tessier, C. A.; Vollhardt, K. P. C.; Youngs, W. J. *Synlett* **1995**, 1215-1218.

(24) Marsden, J. A.; Miller, J. J.; Haley, M. M. *Angew. Chem.* **2004**, *116*, 1726-1729; *Angew. Chem. Int. Ed.* **2004**, *43*, 1694-1697.

(25) Wong, H. N. C.; Garratt, P. J.; Sondheimer, F. *J. Am. Chem. Soc.* **1974**, *96*, 5604-5605.

(26) (a) Chaffins, S.; Brettreich, M.; Wudl, F. *Synthesis* **2002**, 1191-1194. (b) Orita, A.; Hasegawa, D.; Nakano, T.; Otera, J. *Chem. Eur. J.* **2002**, *8*, 2000-2004.

(27) (a) Sirinintasak, S.; Sultana, F.; Nishiyama, T. Vorasingha, A.; Miyake, Y.; Kuwatani, Y. Yoshida, M.; Iyoda, M. *Tetrahedron Let.* **2007**, 1527-1531. (b) Zhang, D.; Tessier, C. A.; Youngs, W. J. *Chem. Mater.* **1999**, *11*, 3050-3057.

(28) (a) Eickmeier, C.; Junga, H.; Matzger, A. J.; Scherhag, F.; Shim, M.; Vollhardt, K. P. C. *Angew. Chem.* **1997**, *109*, 2194-2199. *Angew. Chem. Int. Ed. Engl.* **1997**, *36*, 2103-2108. (b) Matzger, A. J.; Shim, M.; Vollhardt, K. P. C. *Chem. Commun.* **1999**, 1871-1872.

(29) Kinder, J. D.; Tessier, C. A.; Youngs, W. J. *Synlett* **1993**, 149-150.

(30) Djebli, A.; Ferrara, J. D.; Tessier-Youngs, C.; Youngs, W. J. *J. Chem. Soc., Chem. Commun.* **1988**, 548-549.

(31) (a) Ferrara, J. D.; Tessier-Youngs, C.; Youngs, W. J. *J. Am. Chem. Soc.* **1985**, *107*, 6719-6721. (b) Ferrara, J. D.;, Tanaka, A. A.; Fierro, C.; Tessier-Youngs, C.; Youngs, W. J. *Organometallics* **1989**, *8*, 2089-2098. (c) Youngs, W. J.; Kinder, J. D.; Bradshaw, J. D.; Tessier, C. A. *Organometallics* **1993**, *12*, 2406-2407.

(32) (a) Ferrara, J. D.; Tessier-Youngs, C.; Youngs, W. J. *Organometallics* **1987**, *6*, 676-678. (b) Ferrara, J. D.; Tessier-Youngs, C.; Youngs, W. J. *Inorg. Chem.* **1988**, *27*, 2201-2202.

(33) Ferrara, J. D.; Djebli, A.; Tessier-Youngs, C.; Youngs, W. J. *J. Am. Chem. Soc.* **1988**, *110*, 647-649.

(34) Ohkoshi, M.; Horino, T.; Yoshida, M.; Iyoda, M.; *Chem. Commun.* **2003**, 2586-2587.

(35) (a) Youngs, W. J.; Djebli, A.; Tessier, C. A. *Organometallics* **1991**, *10*, 2089-2090. (b) Malaba, D.; Djebli, A.; Chen, L.; Zarate, E. A.; Tessier, C. A.; Youngs, W. J. *Organometallics* **1993**, *12*, 1266-1276.

(36) (a) Baughman, R. H.; Eckhardt, H.; Kertesz, M. *J. Chem. Phys.* **1987**, *87*, 6687-6699. (b) Narita, N.; Nagai, S.; Suzuki, S.; Nakao, K. *Phys. Rev. B* **1998**, *58*, 11009-11014.

(37) Zhou, Y.; Feng, S. *Solid State Commun.* **2002**, *122*, 307-310.

(38) Sonoda, M.; Sakai, Y.; Yoshimura, T.; Tobe, Y.; Komada, K. *Chem. Lett.* **2004**, *33*, 972-973.

(39) (a) Bradshaw, J. D.; Solooki, D.; Tessier, C. A.;, Youngs, W. J.;, *J. Am. Chem. Soc.* **1994**, *116*, 3177-3179; (b) Solooki, D.; Bradshaw, J. D.; Tessier, C. A.;, Youngs, W. J.; See, R. F.; Churchill, M.; Ferrara, J. D. *J. Organomet. Chem.* **1994**, *470*, 231-236.

(40) Kawase, T.; Ueda, N.; Oda, M. *Tetrahedron Lett.* **1997**, *38*, 6681-6684.

(41) Kawase, T.; Ueda, N.; Darabi, H. R.; Oda, M. *Angew. Chem.* **1996**, *108*, 1658-1660; *Angew. Chem. Int. Ed. Engl.* **1996**, *35*, 1556-1558.

(42) Kawase, T.; Hosokawa, Y.; Kurata, H.; Oda, M. *Chem. Lett.* **1999**, 745-746.

(43) Zhang, J.; Pesak, D. J.; Ludwick, J. L.; Moore, J. S. *J. Am Chem. Soc,* **1994**, *116*, 4227-4239.

(44) Staab, H. A.; Neunhoeffer, K. *Synthesis* **1974**, 424.

(45) Ge, P.-H.; Fu, W.; Herrmann, W.A.; Herdtweck, E.; Campana, C.; Adams, R. D.; Bunz, U. H. F. *Angew. Chem.* **2000**, *112*, 3753-3756; *Angew. Chem. Int. Ed.* **2000**, *39*, 3607-3610.

(46) (a) Moore, J. S.; *Acc. Chem. Res.* **1997**, *30*, 402-413; (b) Zhang, J.; Moore, J. S.; Xu, Z.; Aguirre, R. *J. Am. Chem. Soc.* **1992**, *114*, 2273-2274; (c) Shetty, A. S.; Fischer, P. R.; Stork, K. F.; Bohn, P. W.; Moore, J. S. *J. Am. Chem Soc.* **1996**, *118*, 9409-9414; (d) Lahiri, S.; Thompson, J. L.; Moore, J. S. *J. Am. Chem. Soc.* **2000**, *122*, 11315-11319.

(47) Shetty, A. S.; Zhang, J.; Moore, J. S. *J. Am. Chem. Soc.* **1996**, *118*, 1019-1027.

(48) Zhang, J.; Moore, J. S. *J. Am. Chem. Soc.* **1992**, *114*, 9701-9702.

(49) Zhang, J.; Moore, J. S. *J. Am. Chem. Soc.* **1994**, *116*, 2655-2656.

(50) Höger, S.; Enkelmann, V.; Borad, K.; Tschierske, C.; *Angew. Chem.* **2000**, *112*, 2355-2358; *Angew. Chem. Int. Ed.* **2000**, *39*, 2267-2270.

(51) Hosokawa, Y.; Kawase, T.; Oda, M.; *Chem. Commun.* **2001**, 1948-1949.

(52) Pyun, O. S.; Yang, W.; Jeong, M.-J.; Lee, S. H.; Kang, K. M.; Jeon, S. -J.; Cho, B. R. *Tetrahedron Lett.* **2003**, *44*, 5179-5182.

(53) Wu, Z.; Lee, S.; Moore, J. S.; *J. Am. Chem. Soc.* **1992**, *114*, 8730-8732.

(54) Wu, Z.; Moore, J. S.; *Angew. Chem.* **1996**, *108*, 320-322; *Angew. Chem. Int. Ed. Engl.* **1996**, *35*, 297-299.

(55) Kawase, T.; Darabi, H. R.; Oda, M.; *Angew. Chem.* **1996**, *108*, 2803-2805; *Angew. Chem. Int. Ed. Engl.* **1996**, *35*, 2664-2666.

(56) Kawase, T.; Ueda, N.; Tanaka, K.; Seirai, Y.; Oda, M. *Tetrahedron Lett.* **2001**, *42*, 5509-5511.

(57) Kawase, T.; Seirai, Y.; Darabi, H. R.; Oda, M.; Y. Sarakai, Tashiro, K.; *Angew. Chem.* **2003**, *115*, 1659-1662; *Angew. Chem. Int. Ed.* **2003**, *42*, 1621-1624.

(58) Kawase. T.; Tanaka, K.; Fujiwara, N.; Darabi, H. R.; Oda, M.; *Angew. Chem.* **2003**, *115*, 1662-1666. *Angew. Chem. Int. Ed.* **2003**, *42*, 1624-1628.

(59) Kawase, T.; Tanaka, K.; Shiono, N.; Seirai, Y.; Oda, M.; *Angew. Chem.* **2004**, *116*, 1754-1756. *Angew. Chem. Int. Ed.* **2004**, *43*, 1722-1724.

(60) Kawase, T.; Tanaka, K.; Seirai, Y.; Shiono, N.; Oda, M.; *Angew. Chem.* **2003**, *115*, 5755-5758; *Angew. Chem. Int. Ed.* **2003**, *42*, 5597-5560.

(61) Ohkita, M.; Ando, K.; Suzuki, T.; Tsuji, T.; *J. Org. Chem.* **2000**, *65*, 4385-4390.

(62) Young, J. K.; Moore, J. S.; in reference [1a], p 415.

(63) Moore, J. S.; Zhang, J.; *Angew. Chem.* **1992**, *104*, 873-875; *Angew. Chem., Int. Ed. Engl.* **1992**, *31*, 922-924.

(64) Bedard, T. C.; Moore, J. S.; *J. Am. Chem. Soc.* **1995**, *117*, 10662-10671.

(65) (a) Wegner, G.; *Z. Naturforsch. B* **1969**, *24*, 824-832; (b) Enkelmann, V.; *Adv. Polym. Sci.* **1984**, *63*, 91-136.

(66) Bunz, U. H. F.; Enkelmann, V.; *Chem. Eur. J.* **1999**, *5*, 263-266.

(67) Nishinaga, T.; Nodera, N.; Miyata, Y.; Komatsu, K. *J. Org. Chem.* **2002**, *67*, 6091-6096.

(68) Coates, G. W.; Dunn, A. R.; Henling, L. M.; Dougherty, D. A.; Grubbs, R. H. *Angew. Chem.* **1997**, *109*, 290-293; *Angew. Chem., Int. Ed. Engl.* **1997**, *36*, 248-251.

(69) Boese, R.; Matzger, A. J.; Vollhardt, K. P. C.; *J. Am. Chem. Soc.* **1997**, *119*, 2052-2053.

(70) (a) Haley, M. M.; Bell, M. L.; English, J. J.;, Johnson, C. A.; Weakley, T. J. R. *J. Am. Chem. Soc.* **1997**, *119*, 2956-2957; (b) Bell, M. L.; Chiechi, R. C.; Johnson, C. A.;

Kimball, D. B.; Matzger, A. J.; Wan, W. B.; Weakley, T. J. R.; Haley, M. M. *Tetrahedron* **2001**, *57*, 3507-3520.

(71) (a) Ott, S.; Faust, R.; *Chem. Commun.* **2004**, 388-389. (b) Ott, S.; Faust, R.; *Synlett* **2004**, 1509-1512.

(72) Gallagher, M. E.; Anthony, J. E.; *Tetrahedron Lett.* **2001**, *42*, 7533-7536.

(73) (a) Dosa, P. I.; Erben, C.; Iyer, V. S.; Vollhardt, K. P. C.; Wasser, I. M. *J. Am. Chem. Soc.* **1999**, *121*, 10430-10431. (b) Laskoski, M.; Steffen, W.; Morton, J. G. M.; Smith, M. D.; Bunz, U. H. F. *J. Am. Chem. Soc.* **2002**, *124*, 13814-13818. (c) Iyer, V. S.; Vollhardt, K. P. C.; R. Wilhelm, R. *Angew. Chem.* **2003**, *115*, 4515-4519. *Angew. Chem. Int. Ed.* **2003**, *42*, 4379-4383.

(74) (a) Tovar, J. D.; Jux, N.; Jarrosson, T.; Khan, S. I.; Rubin, Y. *J. Org. Chem.* **1997**, *62*, 3432-3433; (b) corrections: *J. Org. Chem.* **1997**, *62,* 5656 and **1998**, *63*, 4856.

(75) Wan, W. B.; Haley, M. M. in *Advances in Strained and Interesting Molecules*; Halton, B., Ed.; JAI Press: Stamford, CT, 2000, pp 1-41.

(76) Haley, M. M.; Brand, S. B.; Pak, J. J. *Angew. Chem.* **1997**, *109*, 863-866. *Angew. Chem. Int. Ed. Engl.* **1997**, *36*, 835-838.

(77) Wan, W. B.; Brand, S. B.; Pak, J. J.; Haley, M. M. *Chem. Eur. J.* **2000**, *6*, 2044-2052.

(78) Wan, W. B.; Haley, M. M. *J. Org. Chem.* **2001**, *66*, 3893-3901.

(79) Marsden, J. A.; Haley, M. M. *J. Org. Chem.* **2005**, *70*, 10213-10226.

(80) Pak, J. J.; Weakley, T. J. R.; Haley, M. M. *J. Am. Chem. Soc.* **1999**, *121*, 8182-8192.

(81) Sarkar, A.; Pak, J. J.; Rayfield, G. W.; Haley, M. M. *J. Mater. Chem.* **2001**, *11*, 2943-2945.

(82) Kimball, D. B.; Boydston, A. J.; Haley, M. M. unpublished results.

(83) (a) Tobe. Y.; Utsumi, N.; Kawabata, K.; Naemura, K. *Tetrahedron Lett.* **1996**, *37*, 9325-9328. (b) Tobe. Y.; Utsumi, N.; Kawabata, K.; Nagano, A.; Adachi, K.; Araki, S.; Sonoda, M.; Hirose, K.; Naemura, K. *J. Am. Chem. Soc.* **2002**, *124*, 5350-5364.

(84) Tobe. Y.; Utsumi, N.; Nagano, A.; Sonoda, M.; Naemura, K. *Tetrahedron* **2001**, *57*, 8075-8083.

(85) Tobe. Y.; Utsumi, N.; Nagano, A.; Naemura, K. *Angew. Chem.* **1998**, *110*, 1347-1349. *Angew. Chem. Int. Ed.* **1998**, *37*, 1285-1287.

(86) Mayor, M.; Lehn, J.-M. *J. Am. Chem. Soc.* **1999**, *121*, 11231-11232.

(87) Ohkita, M.; Ando, K.; Tsuji, T. *Chem. Commun.* **2001**, 2570-2571.

(88) Höger, S. In *Acetylene Chemistry – Chemistry, Biology, and Materials Science*, Diederich, F.; Tykwinski, R. R.; and Stang P. J., Eds., Wiley-VCH: Weinheim, 2005, pp. 427-452.

(89) (a) Höger, S.; Enkelmann, V. *Angew. Chem.* **1995**, *107*, 2917-2919; *Angew. Chem., Int. Ed. Engl.* **1995**, *34*, 2713-2716. (b) Höger, S.; Meckenstock, A.-D.; Müller, S. *Chem. Eur. J.* **1998**, *4*, 2423-2434.

(90) Morrison, D. L.; Höger, S. *Chem. Commun.* **1996**, 2313-2314.

(91) Höger, S.; Bonrad, K.; Karcher, L.; Meckenstock, A.-D. *J. Org. Chem.* **2000**, *65*, 1588-1589.

(92) (a) Höger, S.; Meckenstock, A.-D.; Pellen, H. *J. Org. Chem.* **1997**, *62*, 4556-4557. (b) Höger, S.; Meckenstock, A.-D. *Tetrahedron Lett.* **1998**, *39*, 1735-1736. (c) Höger, S.; Meckenstock, A.-D. *Chem. Eur. J.* **1999**, *5*, 1686-1691.

(93) Collins, S. K.; Yap, G. P. A.; Fallis, A. G. *Angew. Chem.* **2000**, *112*, 393-396. *Angew. Chem. Int. Ed.* **2000**, *39*, 385-388.

(94) Collins, S. K.; Yap, G. P. A.; Fallis, A. G. *Org. Lett.* **2000**, *2*, 3189-3192.

(95) Heuft, M. A.; Collins, S. K.; Fallis, A. G. *Org. Lett.* **2003**, *5*, 1911-1914.

(96) Marsden, J. A.; O'Connor, M. J.; Haley, M. M. *Org. Lett.* **2004**, *6*, 2385-2388.

(97) Collins, S. K.; Yap, G. P. A.; Fallis, A. G.; *Org. Lett.* **2002**, *4*, 11-14.

(98) Tobe. Y.; Kishi, J.; Ohki, I.; Sonoda, M.; *J. Org. Chem.* **2003**, *68*, 3330-3332.

(99) Parker, T. C.; Khan, S. I.; Holliman, C. L.; McElvany, S. W.; Rubin, Y. unpublished results; cited in: Rubin, Y.; *Chem. Eur. J.* **1997**, *3*, 1009-1016.

(100) Rubin, Y.; Parker, T. C.; Khan, S. I.; Holliman, C. L.; McElvany, S. W.; *J. Am. Chem. Soc.* **1996,** *118*, 5308-5309.

(101) (a) Tobe. Y.; Ohki, I.; Sonoda, M.; Niino, H.; Sato, T.; Wakabayashi, T.; *J. Am. Chem. Soc.* **2003**, *125*, 5614-5615. (b) Hisaki, I.; Eda, T.; Sonoda, M.; Tobe, Y. *Chem. Lett.* **2004**, *33*, 620-621. (b) Hisaki, I.; T. Eda, Sonoda, M.; Niino, H.; Sato, T.; Wakabayashi, T.; Tobe. Y. *J. Org. Chem.* **2005**, *70*, 1853-1864.

(102) Wan, W. B.; Kimball, D. B.; Haley, M. M. *Tetrahedron Lett.* **1998**, *39*, 6795-6798.

(103) Haley, M. M.; Bell, M. L.; Brand, S. B.; Kimball, D. B.; Pak, J. J.; Wan, W. B. *Tetrahedron Lett.* **1997**, *38*, 7483-7486.

(104) Heuft, M. A.; Collins, S. K.; Yap, G. P. A.; Fallis, A. G. *Org. Lett.* **2001**, *3*, 2883-2886.

(105) Haley, M. M.; Langsdorf, B.L. *Chem. Commun.* **1997**, 1121-1222.

(106) (a) Tobe. Y.; Nakagawa, N.; Naemura, K.; Wakabayashi, T.; Shida, T.; Achiba, Y. *J. Am. Chem. Soc.* **1998**, *120*, 4544-4545. (b) Tobe. Y.; Nakagawa, N.; Kishi, J.; Sonoda, M.; Naemura, K.; Wakabayashi, T.; Shida, T.; Achiba, Y. *Tetrahedron* **2001**, *57*, 3629-3636. (c) Tobe. Y.; Furukawa, R.; Sonoda, M.; Wakabayashi, T. *Angew. Chem.* **2001**, *113*, 4196-4198. *Angew. Chem. Int. Ed.* **2001**, *40*, 4072-4074.

(107) Rubin, Y.; Parker, T. C.; Pastor, S. J.; Jalisatgi, S.; Boulle, C.; Wilkins, C. L. *Angew. Chem.* **1998**, *110*, 1353-1356. *Angew. Chem. Int. Ed.* **1998**, *37*, 1226-1229.

(108) Tobe. Y.; Wakabayashi, T. In *Acetylene Chemistry – Chemistry, Biology, and Materials Science*, Diederich, F.; Tykwinski, R. R.; Stang, P. J., Eds.; Wiley-VCH: Weinheim, 2005, pp. 387-426.

Chapter II

(1) *Inter alia*: (a) *Topics in Current Chemistry (Carbon Rich Compounds I)*; de Meijere, A., Ed.; Springer-Verlag: Berlin, 1998; Vol. 196. (b) *Topics in Current Chemistry (Carbon Rich Compounds II)*; de Meijere, A., Ed.; Springer-Verlag: Berlin, 1999; Vol. 201. (c) Watson, M. D.; Fechtenkötter, A.; Müllen, K. *Chem Rev.* **2001**, *101*, 1267-1300. (d) Grimsdale, A. C.; Müllen, K. *Angew. Chem. Int. Ed.* **2005**, *44*, 5592-5629. (e) *Carbon-Rich Compounds: From Molecules to Materials*; Haley, M. M.; Tykwinski, R. R., Eds.; Wiley-VCH: Weinheim, 2006.

(2) *Inter alia:* (a) *Handbook of Oligo- and Poly-thiophenes*; Fichou, D., Ed.; Wiley-VCH: Weinheim, **1999**. b) Katz, H. E.; Bao, Z.; Gilat, S. L. *Acc. Chem. Res.* **2001**, *34*, 359-369. (c) *Electronic Materials: The Oligomeric Approach*; Müllen, K.; Wegner, G.,

Eds. Wiley-VCH: Weinheim, 1998. (b) "Sulfur-Containing Oligomers", Bäuerle, P. in *Electronic Materials: The Oligomer Approach*, Müllen, K.; Wegner, G., Eds. Wiley-VCH: Weinheim, **1998**, pp. 105-231.

(3) Izumi, T.; Kobashi, S.; Takimiya, K.; Aso, K.; Otsubo. T. *J. Am. Chem. Soc.* **2003**, *125*, 5286 –5287.

(4) (a) Jen, A. K. Y.; Pushkara, R. V.; W. K. Y.; Drost, K. J. *J. Chem. Soc. Chem. Comm.* **1993**, 90-92. (b) Zamboni, R.; Danieli, R.; Ruini, G.; Taliana, C. *Opt. Lett.* **1989**, *14*, 1321-1323.

(5) Mazaki, Y.; Kobayashi, K. *Tetrahedron Lett.* **1989**, *30*, 3315-3318.

(6) Zhang, Z.; Coté, A. P.; Matzger, A. J. *J. Am. Chem. Soc.* **2005**, *127*, 10502-10503.

(7) Roncali, J. *J. Chim. Phys.* **1995**, *95*, 1155-1160.

(8) Roncali, J.; Thobie-Gautier, C. *Adv. Mater.* **1994**, *6*, 846-847.

(9) Wex, B.; Kaafarani, B. R.; Kirschbaum, K.; Neckers, D. C. *J. Org. Chem.* **2005**, *70*, 4502-4505.

(10) Sirringhuas, H.; Friend, R. H.; Wang, C.; Leuninger, J.; Müllen, K. *J. Mater. Chem.* **1999**, *9*, 2095-2101.

(11) Wang, C.-H.; Hu, R.-R.; Liang, S.; Chen, J.-H.; Yang, Z.; Pei, J. *Tetrahedron Lett.* **2005**, *46*, 8153-8157.

(12) Yue, D.; Larock, R. C. *J. Org. Chem.* **2002**, *67*, 1905-1909.

(13) Krömer, J.; Idoia Rios-Carreras, I.; Fuhrmann, G.; Musch, C.; Wunderlin, M.; Debaerdumaeker, T.; Mena-Osteritz, E.; Bäuerle, P. *Angew. Chem. Int. Ed.* **2000**, *39*, 3481-3486

(14) (a) Bednarz, M.; Reineker, P.; Mena-Osteritz, E.; Bäuerle P. *J. Lumin.* **2004**, *110*, 225-231. (b) Mena-Osteritz, E.; Bäuerle, P. *Adv. Mater.* **2001**, *13*, 243-246. (b) Mena-Osteritz, E.; Bäuerle, P. *Adv. Mater.* **2006**, *18*, 447-451.

(15) Zhang, J.; Pesak, D. J.; Ludwick, J. L.; Moore, J. S. *J. Am Chem. Soc.* **1994**, *116*, 4227-4239.

(16) Ammann, M.; Rang, A.; Schalley, C. A.; Bäuerle, P. *Eur. J. Org. Chem.* **2006**, 1940-1948.

(17) Ammann, M.; Bäuerle, P. *Org. Biomol. Chem.* **2005**, *3*, 4143-4152.

(18) Kauffmann, M. J.; Greving, B.; Kriegesmann, R.; Mitschker, A.; Woltermann, A. *Chem. Ber.* **1978**, *111*, 1330-1336.

(19) Kabir, S. M. K.; Miura, M.; Sasaki, S.; Harada, G.; Kuwatani, Y.; Yoshida, M.; Iyoda, M. *Heterocycles* **2000**, *52*, 761-774.

(20) Marsella, M. J.; Kim, I. T.; Tham, F. *J. Am. Chem. Soc.* **2000**, *122*, 974-975.

(21) Marsella, M. J.; Reid, R. J.; Estassi, S.; Wang, L.-S. *J. Am. Chem. Soc.* **2002**, *124*, 12507-12510.

(22) Marsella, M. J.; Yoon, K.; Tham, F. S. *Org. Lett.* **2001**, *3*, 2129-2131.

(23) Chernichenko, Yu. K.; Sumerin, V. V.; Shpanchenko, R. V.; Balenkova, E. S.; Nenajdenko, V. G. *Angew. Chem. Int. Ed.* **2006**, *45*, 7367-7370.

(24) (a) Vogel, E. *Phosphorus, Sulfur, and Silicon* **1994**, *95*, 509-510. (b) Vogel, E.; Pohl, M.; Herrmann, A.; Wiss, T.; König, C.; Lex, J.; Gross, M.; Gisselbrecht, J. P. *Angew. Chem. Int. Ed. Engl.* **1996**, *35*, 1520-1524.

(25) (a) Sprutta, N.; Latos-Grażyński, L. *Org. Lett.* **2001**, *3*, 1933-1936. (b) Berlicka, A; Latos-Grażyński, L; Tadeusz, Liz. *Angew. Chem. Int. Ed.* **2005**, *44*, 5288-5291. (c) Agarwal, N.; Mishra, S. P.; Kumar, A.; Hung, C.-H.; Ravikanth, M. *Chem. Commun.* **2002**, 2642-2643. (d) Punidha, S.; Agarwal, N.; Ravikanth, M. *Eur. J. Org. Chem.* **2005**, 2500-2517.

(26) (a) Hu, Z.; Atwood, J. L.; Cava, M. P. *J. Org. Chem.* **1994**, *59*, 8071-8074. (b) Hu, Z.; Kelley, Kelly, C. -S.; Cava, M.P. *Tetrahedron Lett.* **1993**, *34*, 1879-1881. (c) Hu, Z.; Cava, M. P. *Tetrahedron Lett.* **1994**, *34*, 3493-3496.

(27) Ellinger, F.; Gieren, A.; Hübner, Th.; Lex.J.; Lucchesini, F.; Merz, A. Neidlein, R.; Salbeck, J. *Montash. Chem.* **1993**, *124*, 931-943.

(28) Marsella, M. J.; Piao, G.; Tham, F. *Synthesis* **2002**, *9*, 1133-1135..

(29) Marsella, M. J.; Kim, I. T.; Tham, F. *J. Am. Chem. Soc.* **2000**, *122*, 974-975.

(30) Mayor, M.; Didschies, C. *Angew. Chem. Int. Ed.* **2003**, *42*, 3176-3179.

(31) (a) Solooki, D.; Bradshaw, J. D.; Tessier, C. A.; Youngs, W.J. *Organometallics* **1994**, *13*, 451-455. (b) Solooki, D.; Kennedy, V. O.; Tessier, C. A.; Youngs, W. J. *Synlett* **1990**, 427-428.

(32) Zhang, D.; Tessier, C. A., Youngs, W. J. *Chem. Mater.* **1999**, *11*, 3050-3057.

(33) Baldwin, J. P.; Matzger, A. J.; Scheiman, D. A.; Tessier, C. A.; Vollhardt, K. P. C.; Youngs, W. J. *Synlett* **1995**, 1215-1218.

(34) Iyoda, M.; Vorasingha, A.; Kuwatani, Y.; Yoshida, M. *Tetrahedron Lett.* **1998**, *39*, 4701-4704.

(35) Boydston, A. J.; Haley, M. M.; Williams, R. V.; Armantrout, J. R. *J. Org. Chem.* **2002**, *67*, 8812-8819.

(36) Sarkar, A.; Haley, M. M. *Chem. Commun.* **2000**, 1733-1734.

(37) (a) Sarkar, A; Haley, M. M. unpublished results. (b) Marsden, J.; Haley, M. M. unpublished results.

Chapter III

(1) *Inter alia*: (a) *Topics in Current Chemistry (Carbon Rich Compounds I)*; de Meijere, A., Ed.; Springer-Verlag: Berlin, 1998; Vol. 196. (b) *Topics in Current Chemistry (Carbon Rich Compounds II)*; de Meijere, A., Ed.; Springer-Verlag: Berlin, 1999; Vol. 201. (c) Watson, M. D.; Fechtenkötter, A.; Müllen, K. *Chem Rev.* **2001**, *101*, 1267-1300. (d) Grimsdale, A. C.; Müllen, K. *Angew. Chem.. Int. Ed.* **2005**, *44*, 5592-5629. (e) *Carbon-Rich Compounds: From Molecules to Materials*; Haley, M. M.; Tykwinski, R. R., Eds.; Wiley-VCH: Weinheim, 2006.

(2) *Inter alia*: (a) *Modern Acetylene Chemistry*; Stang, P. J.; Diederich, F., Eds.; VCH: Weinheim, 1995. (b) Bunz, U. H. F.; Rubin, Y.; Tobe, Y. *Chem. Soc. Rev.* **1999**, *28*, 107-119. (c) Bunz, U. H. F. *Chem. Rev.* **2000**, *100*, 1605-1644. (d) Nielsen, M. B.; Diederich, F. In *Modern Arene Chemistry;* Astruc, D., Ed.; Wiley-VCH: Weinheim, 2002; pp 196-216. (e) *Acetylene Chemistry: Chemistry, Biology, and Material Science*; Diederich, F.; Stang, P. J.; Tykwinski, R. R., Eds.; Wiley-VCH: Weinheim, 2005.

(3) (a) *Metal Catalyzed Cross-Coupling Reactions (2nd Ed)*; de Meijere, A.; Diederich, F., Eds.; Wiley-VCH: Weinheim, 2004. (b) *Transition Metal Catalyzed Reactions – IUPAC Monographs Chemistry for 21st Century*; Davies, S. G.; Murahashi, S., Eds.; Blackwell Science: Oxford, 1998.

(4) (a) Spreiter, R.; Bosshard, C.; Knöpfle, G.; Günter, P.; Tykwinski, R. R.; Schreiber, M.; Diederich, F. *J. Phys. Chem. B* **1998**, *102*, 29-32. (b) Tykwinski, R. R.; Gubler, U.; Martin, R. E.; Diederich, F.; Bosshard, C.; Günter, P. *J. Phys. Chem. B* **1998**, *102*, 4451-4465. (c) Sarkar, A.; Pak J. J.; Rayfield, G. W.; Haley, M. M. *J. Mater. Chem.* **2001**, *11*, 2943-2945. (d) Slepkov, A.; Hegmann, F. A.; Tykwinski, R. R.; Kamada, K.; Ohta, K.; Marsden, J. A.; Spitler, E. L.; Miller, J. J.; Haley, M. M. *Opt. Lett.* **2006**, *31*, 3315-3317. (e) Bhaskar, A.; Guda, R.; Haley, M. M.; Goodson III, T. *J. Am. Chem. Soc.* **2006**, *128*, 13972-13973.

(5) (a) Zhang, J.; Moore, J. S. *J. Am. Chem. Soc.* **1994**, *116*, 2655-2656. (b) Pesak, D. J.; Moore, J. S. *Angew. Chem., Int. Ed. Engl.* **1997**, *36*, 1636-1639. (c) Seo, S. H.; Jones, T. V.; Seyler, H.; Peters, J. O.; Kim, T. H.; Chang, J. Y.; Tew, G. N. *J. Am. Chem. Soc.* **2006**, *128*, 9264-9265.

(6) (a) Gobbi, L.; Seiler, P.; Diederich, F. *Angew. Chem. Int. Ed.* **1999**, *38*, 674-678. (b) Gobbi, L.; Seiler, P.; Diederich, F.; Gramlich, V. *Helv. Chim. Acta* **2000**, *83*, 1711-1723.

(7) (a) Marsden, J. A.; Palmer, G. J.; Haley, M. M. *Eur. J. Org. Chem.* **2003**, 2355-2369. (b) Spitler, E. L.; Johnson, C. A.; Haley, M. M. *Chem. Rev.* **2006**, *106*, 5344-5386.

(8) (a) Jones, C. S.; O'Connor, M. J.; Haley, M. M. In Reference 2e; pp. 303-385. (b) Zhao, D.; Moore, J. S. *Chem. Commun.* **2003**, 807-818. (c) Zhang, W.; Moore, J. S. *Angew. Chem. Int. Ed.* **2006**, *45*, 4416-4439.

(9) Baldwin, J. P.; Matzger, A. J.; Scheiman, D. A.; Tessier, C. A.; Vollhardt, K. P. C.; Youngs, W. J. *Synlett* **1995**, 1215-1218.

(10) Zhou, Q.; Carroll, P. J.; Swager, T. M. *J. Org. Chem.* **1994**, *59*, 1294-1301.

(11) (a) Boese, R.; Matzger, A. J.; Vollhardt, K. P. C. *J. Am. Chem. Soc.* **1997**, *119*, 2052-2053. (b) Tobe, Y.; Nakagawa, N.; Naemura, K.; Wakabayashi, T.; Shida, T.; Achiba, Y. *J. Am. Chem. Soc.* **1998**, *120*, 4544-4545. (c) Rubin, Y.; Parker, T. C.; Pastor, S. J.; Jalisatgi, S.; Boulle, C.; Wilkins, C. L. *Angew. Chem. Int. Ed.* **1998**, *37*, 1226-1229. (d) Laskoski, M.; Steffen, W.; Morton, J. G. M.; Smith, M. D.; Bunz, U. H. F. *J. Am. Chem. Soc.* **2002**, 124, 13814-13818.

(12) Recent contributions, *inter alia*: (a) Marsden, J. A.; Miller, J. J.; Shirtcliff, L. D.; Haley, M. M. *J. Am. Chem. Soc.* **2005**, *127*, 2464-2476. (b) Marsden, J. A.; Haley, M. M. *J. Org. Chem.* **2005**, *70*, 10213-10226. (c) Johnson, C. A.; Baker, B. A.; Berryman, O. B.; Zakharov, L. N.; O'Connor, M. J.; Haley, M. M. *J. Organomet. Chem.* **2006**, *691*, 413-421. (d) Anand, S.; Varnavski, O.; Marsden, J. A.; Haley, M. M.; Schlegel, H. B.; Goodson III, T. *J. Phys. Chem. A* **2006**, *110*, 1305-1318. (e) Spitler, E. L.; McClintock, S. P.; Haley, M. M. *J. Org. Chem.* **2007**, *72*, 6692-6699. (f) Johnson II, C. A.; Lu, Y.; Haley, M. M. *Org. Lett.* **2007**, *9*, 3725-3728. (g) Tahara, K.; Johnson II, C. A.; Fujita, T.; Sonoda, M.; De Schryver, F.; De Feyter, S.; Haley, M. M.; Tobe, Y. *Langmuir* **2007**, *23*, 10190-10197.

(13) (a) Sarkar, A.; Haley, M. M. *Chem. Commun.* **2000**, 1733-1734. (b) Sarkar, A.; Marsden, J. A.; Haley. M. M., unpublished results.

(14) (a) Roncali, J. *Chem. Rev.* **1992**, *92*, 711-738. (b) Jen, A. K.; Rao, V. P.; Wong, K. Y.; Drost, K. J. *Chem. Commun.* **1993**, 90-91. (c) Zamboni, R.; Danieli, R.; Ruini, G.; Taliani, C. *Opt. Lett.* **1989**, *14*, 1321-1323.

(15) (a) Krömer, J.; Rios-Carreras, I.; Fuhrmann, G.; Musch, C.; Wunderlin, M.; Debärdemäker, T.; Mena-Osteritz, E.; Bäuerle, P. *Angew. Chem. Int. Ed.* **2000**, *39*, 3481-3486. (b) Bednarz, M.; Reineker, P.; Mena-Osteritz, E.; Bäuerle, P. *J. Lumin.* **2004**, *110*,

225-231. (c) Kozaki, M.; Parakka, J. P.; Cava, M. P. *J. Org. Chem.* **1996**, *61*, 3657-3661. (b) Hu, Z.; Scordilis-Kelley, C.; Cava, M. P. *Tetrahedron Lett.* **1993**, *34*, 1879-1882.

(16) (a) Mayor, M.; Didschies, C. *Angew. Chem. Int. Ed.* **2003**, *42*, 3176-3179. (b) Nakao, K.; Nishimura, M.; Tamachi, T.; Kuwatani, Y.; Miyasaka, H.; Nishinaga, T.; Iyoda, M. *J. Am. Chem. Soc.* **2006**, 128, 16740-16747.

(17) (a) Solooki, D.; Bradshaw, J. D.; Tessier, C. A.; Youngs, R. J. *Organometallics* **1994**, *13*, 451-455. (b) Zhang, D.; Tessier, C. A.; Youngs, W. J. *Chem. Mater.* **1999**, *11*, 3050-3057. (c) See also: Iyoda, M.; Vorasingha, A; Kuwatani, Y.; Yoshida, M. *Tetrahedron Lett.* **1998**, *39*, 4701-4704.

(18) (a) Marsella, M. J.; Kim, I. T.; Tham, F. *J. Am. Chem. Soc.* **2000**, *122*, 974-975. (b) Marsella, M. J.; Wang, Z.-Q.; Reid, R. J.; Yoon, K. *Org. Lett.* **2001**, *3*, 885-887. (c) Marsella, M. J.; Piao, G.; Tham, F. S. *Synthesis* **2002**, 1133-1135. (d) Marsella, M. J.; Reid, R. J.; Estassi, S.; Wang, L.-S. *J. Am. Chem. Soc.* **2002**, *124*, 12507-12510.

(19) (a) Takahashi, T.; Matsuoka, K Takimiya, K.; Otsubo, T.; Aso, Y. *J. Am. Chem. Soc.* **2005**, *127*, 8928-8929. (b) Kozaki, M.; Isoyama, A.; Okada, K. *Org. Lett.* **2005**, *7*, 115-118.

(20) (a) Gronowitz, S.; Vilks, V. *Arkiv. Kem.* **1964**, *21*, 191-196. (b) Gronowitz, S.; Holm, B. *Acta Chem. Scand. B* **1976**, *30*, 423-429. (c) Consiglio, G.; Gronowitz, S.; Hörnfeldt, A.-B.; Noto, R.; Spinelli, D. *Chem. Scr.* **1980**, *16*, 117-121. (d) Spagnoto, P.; Zaniroto, P.; Gronowitz, S. *J. Org. Chem.* **1982**, *47*, 3177-3180.

(21) (a) Haley, M. M.; Bell, M. L.; English, J. J.; Johnson, C. A.; Weakley, T. J. R.; *J. Am. Chem. Soc.* **1997**, *119*, 2956-2957. (b) Bell, M. L.; Chiechi, R. C.; Johnson, C. A.; Kimball, D. A.; Matzger, A. J.; Wan, W. B.; Weakley, T. J. R.; Haley, M. M. *Tetrahedron* **2001**, *57*, 3507-3520.

(22) (a) Marsden, J. A.; Miller, J. J.; Haley, M. M. *Angew. Chem. Int. Ed.* **2004**, *43*, 1694-1697. (b) See also: Siemsen, P.; Livingston, R. C.; Diederich, F. *Angew. Chem. Int. Ed.* **2000**, *39*, 2632-2657.

(23) Guru Row, T. N.; Parthasarathy, R. *J. Am. Chem. Soc.* **1981**, *103*, 477-479.

(24) Enkelmann, V. *Adv. Polym. Sci.* **1984**, *63*, 91-136.

(25) Baldwin, K. P.; Matzger, A. J.; Scheiman, D. A.; Tessier, C. A.; Vollhardt, K. P. C.; Youngs, W. J. *Synlett* **1995**, 1215-1218.

(26) Blanchette, H. S.; Brand, S. C.; Naruse, H.; Weakley, T. J. R.; Haley, M. M. *Tetrahedron* **2000**, *56*, 9581-9588.

(27) (a) Boydston; A. J.; M. M. Haley, M. M. *Org. Lett.* **2001**, *3*, 3599-3601. (b) Boydston, A. J.; Haley, M. M.; Williams, R. V.; Armantrout, J. R. *J. Org. Chem.* **2002**, *67*, 8812-8819.

(28) (a) Matzger, A. J.; Vollhardt, K. P. C. *Tetrahedron Lett.* **1998**, *39*, 6791-6794. (b) Wan, W. B.; Kimball, D. B.; Haley, M. M. *Tetrahedron Lett.* **1998**, *39*, 6795-6798.

(29) Baldwin, K. P.; Bradshaw, J. D.; Tessier C. A.; Youngs, W. J. *Synlett* **1993**, 853-855.

(30) Mitchell, R. H. *Chem. Rev.* **2001**, *101*, 1301-1316.

(31) Fringuelli, F.; Marino, G.; Taticchi, A. *J. Chem. Soc., Perkin Trans. 2* **1974**, 332-337.

(32) (a) Becke, A. D. *Phys. Rev. A* **1988**, *38*, 3098-3100. (b) Lee, C.; Yang, W.; Parr, R. G. *Phys. Rev. B* **1988**, *37*, 785-789. (c) Becke, A. D. *J. Chem. Phys.* **1993**, *98*, 5648-5652. (d) Becke, A. D. *J. Chem. Phys.* **1993**, *98*, 1372-1377.

(33) Sheldrick, G. M. Bruker/Siemens Area Detector Absorption Correction Program; Bruker AXS; Madison, WI, 1998.

(34) SHELXTL-6.10 "Program for Structure Solution, Refinement and Presentation" BRUKER AXS Inc., 5465 East Cheryl Parkway, Madison, WI 53711-5373 USA.

(35) (a) Becke, A. D. *Phys. Rev. A* **1988**, *38*, 3098-3100. (b) Lee, C.; Yang, W.; Parr, R. G. *Phys. Rev. B* **1988**, *37*, 785-789. (c) Becke, A. D. *J. Chem. Phys.* **1993**, *98*, 5648-5652. (d) Becke, A. D. *J. Chem. Phys.* **1993**, *98*, 1372-1377.

(36) Klamt, A.; Schürmann, G. *J. Chem. Soc., Perkin Trans.* **1993**, 799-806.

(37) Stefanovich, E. V.; Truong, T. N. *Chem. Phys. Lett.* **1995**, *244*, 65-74.

(38) (a) Kendall, R. A.; Apra, E.; Bernholdt, D. E.; Bylaska, E. J.; Dupuis, M.; Fann, G. I.; Harrison, R. J.; Ju, J.; Nichols, J. A.; Nieplocha, J.; Straatsma, T. P.; Windus, T. L.; Wong, A. T. *Computer Phys. Comm.* **2000**, *128*, 260-283. (b) Aprà, E.; Windus, T. L.; Straatsma, T. P.; Bylaska, E. J.; Jong, W. A. de; Hirata, S.; Valiev, M.; Hackler, M.; Pollack, L.; Kowalski, K.; Harrison, R.; Dupuis, M.; Smith, D. M. A.; Nieplocha, J.; Tipparaju, V.; Krishnan, M.; Auer, A. A.; Brown, E.; Cisneros, G.; Fann, G. I.; Früchtl, H.; Garza, J.; Hirao, K.; Kendall, R.; Nichols, J. A.; Tsemekhman, K.; Wolinski, K.; Anchell, J.; Bernholdt, D.; Borowski, P.; Clark, T.; Clerc, D.; Dachsel, H.; Deegan, M.; Dyall, K.; Elwood, D.; Glendening, E.; Gutowski, M.; Hess, A.; Jafe, J.; Johnson, B.; Ju, J.; Kobayashi, R.; Kutteh, R.; Lin, Z.; Littlefield, R.; Long, X.; Meng, B.; Nakajima, T.; Niu, S.; Rosing, M.; Sandrone, G.; Stave, M.; Taylor, H.; Thomas, G.; Lenthe, J. van;

Wong, A.; Zhang, Z. "NWChem, A Computational Chemistry Package for Parallel Computers, Version 4.7." Pacific Northwest National Laboratory, Richland, Washington, **2005**. (c) Bylaska, E. J.; Jong, W. A. de; Kowalski, K.; Straatsma, T. P.; Valiev, M.; Wang, D.; Aprà, E.; Windus, T. L.; Hirata, S.; Hackler, M. T.; Zhao, Y.; Fan, P.-D.; Harrison, R. J.; Dupuis, M.; Smith, D. M. A.; Nieplocha, J.; Tipparaju, V.; Krishnan, M.; Auer, A. A.; Nooijen, M.; Brown, E.; Cisneros, G.; Fann, G. I.; Früchtl, H.; Garza, J.; Hirao, K.; Kendall, R.; Nichols, J. A.; Tsemekhman, K.; Wolinski, K.; Anchell, J.; Bernholdt, D.; Hess, P. A.; Jaffe, J.; Johnson, B.; Ju, J.; Kobayashi, R.; Kutteh, R.; Lin, Z.; Littlefield, R.; Long, X.; Meng, B.; Wong, T. A.; Zhang, Z. "NWChem, A Computational Chemistry Package for Parallel Computers, Version 5.0." Pacific Northwest National Laboratory, Richland, Washington, **2006**.

(39) (a) Schuchardt, K. L., Didier, B. T.; Black, G. D. *Concurrency and Computation: Practice and Experience* **2002**, *14*, 1221-1239. (b) Black, G. D.; Didier, B. T.; Elsethagen, T.; Feller, D.; Gracio, D.; Hackler, M.; Havre, S.; Jones, D.; Jurrus, E.; Keller, T.; Lansing, C.; Matsumoto, S.; Palmer, B.; Peterson, M.; Schuchardt, K.; Stephan, E.; Taylor, H.; Thomas, G.; Vorpagel, E.; Windus, T. "ECCE, A Problem Solving Environment for Computational Chemistry, Software Version 3.2." Pacific Northwest National Laboratory, Richland, Washington, **2004**.

Chapter IV

(1) *Inter alia*: (a) *Topics in Current Chemistry (Carbon Rich Compounds I)*; de Meijere, A., Ed.; Springer-Verlag: Berlin, 1998; Vol. 196. (b) *Topics in Current Chemistry (Carbon Rich Compounds II)*; de Meijere, A., Ed.; Springer-Verlag: Berlin, 1999; Vol. 201. (c) Watson, M. D.; Fechtenkötter, A.; Müllen, K. *Chem Rev.* **2001**, *101*, 1267-1300. (d) Grimsdale, A. C.; Müllen, K. *Angew. Chem.. Int. Ed.* **2005**, *44*, 5592-5629. (e) *Carbon-Rich Compounds: From Molecules to Materials*; Haley, M. M.; Tykwinski, R. R., Eds.; Wiley-VCH: Weinheim, 2006.

(2) *Inter alia*: (a) *Modern Acetylene Chemistry*; Stang, P. J.; Diederich, F., Eds.; VCH: Weinheim, 1995. (b) Bunz, U. H. F.; Rubin, Y.; Tobe, Y. *Chem. Soc. Rev.* **1999**, *28*, 107-119. (c) Bunz, U. H. F. *Chem. Rev.* **2000**, *100*, 1605-1644. (d) Nielsen, M. B.; Diederich, F. In *Modern Arene Chemistry;* Astruc, D., Ed.; Wiley-VCH: Weinheim, 2002; pp 196-216. (e) *Acetylene Chemistry: Chemistry, Biology, and Material Science*; Diederich, F.; Stang, P. J.; Tykwinski, R. R., Eds.; Wiley-VCH: Weinheim, 2005.

(3) (a) *Metal Catalyzed Cross-Coupling Reactions (2nd Ed)*; de Meijere, A.; Diederich, F., Eds.; Wiley-VCH: Weinheim, 2004. (b) *Transition Metal Catalyzed Reactions – IUPAC Monographs Chemistry for 21st Century*; Davies, S. G.; Murahashi, S., Eds.; Blackwell Science: Oxford, 1998.

(4) (a) Spreiter, R.; Bosshard, C.; Knöpfle, G.; Günter, P.; Tykwinski, R. R.; Schreiber, M.; Diederich, F. *J. Phys. Chem. B* **1998**, *102*, 29-32. (b) Tykwinski, R. R.; Gubler, U.; Martin, R. E.; Diederich, F.; Bosshard, C.; Günter, P. *J. Phys. Chem. B* **1998**, *102*, 4451-4465. (c) Sarkar, A.; Pak J. J.; Rayfield, G. W.; Haley, M. M. *J. Mater. Chem.* **2001**, *11*, 2943-2945. (d) Slepkov, A.; Hegmann, F. A.; Tykwinski, R. R.; Kamada, K.; Ohta, K.; Marsden, J. A.; Spitler, E. L.; Miller, J. J.; Haley, M. M. *Opt. Lett.* **2006**, *31*, 3315-3317. (e) Bhaskar, A.; Guda, R.; Haley, M. M.; Goodson III, T. *J. Am. Chem. Soc.* **2006**, *128*, 13972-13973.

(4) (a) Zhang, J.; Moore, J. S. *J. Am. Chem. Soc.* **1994**, *116*, 2655-2656. (b) Pesak, D. J.; Moore, J. S. *Angew. Chem., Int. Ed. Engl.* **1997**, *36*, 1636-1639. (c) Seo, S. H.; Jones, T. V.; Seyler, H.; Peters, J. O.; Kim, T. H.; Chang, J. Y.; Tew, G. N. *J. Am. Chem. Soc.* **2006**, *128*, 9264-9265.

(5) (a) Gobbi, L.; Seiler, P.; Diederich, F. *Angew. Chem. Int. Ed.* **1999**, *38*, 674-678. (b) Gobbi, L.; Seiler, P.; Diederich, F.; Gramlich, V. *Helv. Chim. Acta* **2000**, *83*, 1711-1723.

(6) (a) Marsden, J. A.; Palmer, G. J.; Haley, M. M. *Eur. J. Org. Chem.* **2003**, 2355-2369. (b) Spitler, E. L.; Johnson, C. A.; Haley, M. M. *Chem. Rev.* **2006**, *106*, 5344-5386.

(7) (a) Jones, C. S.; O'Connor, M. J.; Haley, M. M. In Reference 2e; pp. 303-385. (b) Zhao, D.; Moore, J. S. *Chem. Commun.* **2003**, 807-818. (c) Zhang, W.; Moore, J. S. *Angew. Chem. Int. Ed.* **2006**, *45*, 4416-4439.

(8) Baldwin, J. P.; Matzger, A. J.; Scheiman, D. A.; Tessier, C. A.; Vollhardt, K. P. C.; Youngs, W. J. *Synlett* **1995**, 1215-1218.

(9) Zhou, Q.; Carroll, P. J.; Swager, T. M. *J. Org. Chem.* **1994**, *59*, 1294-1301.

(10) (a) Boese, R.; Matzger, A. J.; Vollhardt, K. P. C. *J. Am. Chem. Soc.* **1997**, *119*, 2052-2053. (b) Tobe, Y.; Nakagawa, N.; Naemura, K.; Wakabayashi, T.; Shida, T.; Achiba, Y. *J. Am. Chem. Soc.* **1998**, *120*, 4544-4545. (c) Rubin, Y.; Parker, T. C.; Pastor, S. J.; Jalisatgi, S.; Boulle, C.; Wilkins, C. L. *Angew. Chem. Int. Ed.* **1998**, *37*, 1226-1229. (d) Laskoski, M.; Steffen, W.; Morton, J. G. M.; Smith, M. D.; Bunz, U. H. F. *J. Am. Chem. Soc.* **2002**, 124, 13814-13818.

(11) Recent contributions, *inter alia*: (a) Marsden, J. A.; Miller, J. J.; Shirtcliff, L. D.; Haley, M. M. *J. Am. Chem. Soc.* **2005**, *127*, 2464-2476. (b) Marsden, J. A.; Haley, M. M. *J. Org. Chem.* **2005**, *70*, 10213-10226. (c) Johnson, C. A.; Baker, B. A.; Berryman, O. B.; Zakharov, L. N.; O'Connor, M. J.; Haley, M. M. *J. Organomet. Chem.* **2006**, *691*, 413-421. (d) Anand, S.; Varnavski, O.; Marsden, J. A.; Haley, M. M.; Schlegel, H. B.; Goodson III, T. *J. Phys. Chem. A* **2006**, *110*, 1305-1318. (e) Spitler, E. L.; McClintock, S. P.; Haley, M. M. *J. Org. Chem.* **2007**, *72*, 6692-6699. (f) Johnson II, C. A.; Lu, Y.;

Haley, M. M. *Org. Lett.* **2007**, *9*, 3725-3728. (g) Tahara, K.; Johnson II, C. A.; Fujita, T.; Sonoda, M.; De Schryver, F.; De Feyter, S.; Haley, M. M.; Tobe, Y. *Langmuir* **2007**, *23*, 10190-10197.

(12) (a) Sarkar, A.; Haley, M. M. *Chem. Commun.* **2000**, 1733-1734. (b) Sarkar, A.; Marsden, J. A.; Haley. M. M., unpublished results. (c) O'Connor, M. J.; Yelle, R. B.; Zakharov, L. N.; Haley, M. M. *J. Org. Chem.* submitted.

(13) (a) Roncali, J. *Chem. Rev.* **1992**, *92*, 711-738. (b) Jen, A. K.; Rao, V. P.; Wong, K. Y.; Drost, K. J. *Chem. Commun.* **1993**, 90-91. (c) Zamboni, R.; Danieli, R.; Ruini, G.; Taliani, C. *Opt. Lett.* **1989**, *14*, 1321-1323. (d) Varnavski, O.; Bauerle, P.; Goodson III, T. *Opt. Lett.* **2007**, *32*, 3083-3085. (e) Bhaskar, A.; Ramakrishna, G.; Hagedorn, K.; Varnavski, O.; Mena-Osteritz, E.; Baeuerle, P.; Goodson III, T. *J. Phys Chem. B.* **2007**, *111*, 946-954.

(14) (a) Krömer, J.; Rios-Carreras, I.; Fuhrmann, G.; Musch, C.; Wunderlin, M.; Debärdemäker, T.; Mena-Osteritz, E.; Bäuerle, P. *Angew. Chem. Int. Ed.* **2000**, *39*, 3481-3486. (b) Bednarz, M.; Reineker, P.; Mena-Osteritz, E.; Bäuerle, P. *J. Lumin.* **2004**, *110*, 225-231. (c) Kozaki, M.; Parakka, J. P.; Cava, M. P. *J. Org. Chem.* **1996**, *61*, 3657-3661. (b) Hu, Z.; Scordilis-Kelley, C.; Cava, M. P. *Tetrahedron Lett.* **1993**, *34*, 1879-1882.

(15) (a) Mayor, M.; Didschies, C. *Angew. Chem. Int. Ed.* **2003**, *42*, 3176-3179. (b) Nakao, K.; Nishimura, M.; Tamachi, T.; Kuwatani, Y.; Miyasaka, H.; Nishinaga, T.; Iyoda, M. *J. Am. Chem. Soc.* **2006**, 128, 16740-16747.

(16) (a) Solooki, D.; Bradshaw, J. D.; Tessier, C. A.; Youngs, R. J. *Organometallics* **1994**, *13*, 451-455. (b) Zhang, D.; Tessier, C. A.; Youngs, W. J. *Chem. Mater.* **1999**, *11*, 3050-3057. (c) See also: Iyoda, M.; Vorasingha, A; Kuwatani, Y.; Yoshida, M. *Tetrahedron Lett.* **1998**, *39*, 4701-4704.

(17) (a) Marsella, M. J.; Kim, I. T.; Tham, F. *J. Am. Chem. Soc.* **2000**, *122*, 974-975. (b) Marsella, M. J.; Wang, Z.-Q.; Reid, R. J.; Yoon, K. *Org. Lett.* **2001**, *3*, 885-887. (c) Marsella, M. J.; Piao, G.; Tham, F. S. *Synthesis* **2002**, 1133-1135. (d) Marsella, M. J.; Reid, R. J.; Estassi, S.; Wang, L.-S. *J. Am. Chem. Soc.* **2002**, *124*, 12507-12510.

(18) Nakao, K.; Nishimura, M.; Tamachi, T.;Kuwatani, Y.; Miyasaka, H.; Nishinaga, T.; Iyoda, M. *J. Am. Chem. Soc.* **2006**, *128*, 16741-16747.

(19) (a) Takahashi, T.; Matsuoka, K Takimiya, K.; Otsubo, T.; Aso, Y. *J. Am. Chem. Soc.* **2005**, *127*, 8928-8929. (b) Kozaki, M.; Isoyama, A.; Okada, K. *Org. Lett.* **2005**, *7*, 115-118.

(20) Turbiez, M.; Fre`re, P.; Roncali, J. *J. Org. Chem.* **2003**, *68*, 5357-5360.

(21) (a) Collins, S. K.; Yap, G. P. A.; Fallis, A. G. *Org. Lett.* **2002**, *4*, 11-14. (b) Tobe, Y.; Kishi, J.; Ohki, I.; Sonoda, M. *J. Org. Chem.* **2003**, *68*, 3330-3332.

(22) Thompson, A. L.; Ahn, T-S.; Thomas, K. R. J.; Thayumanavan, S.; Martinez, T. J.; Bardeen, C. J. *J. Am. Chem. Soc.* **2005**, *127*, 1634-1635.

(23) Spitler, E. L.; Shirtcliff, L. D.; Haley, M. M. *J. Org. Chem.* **2007**, *72*, 5344-5386.

(24) (a) Pei, J.; Ni, J.; Zhoa, X-Y.; Cao, X-Y.; Lai, Y-H. *J. Org. Chem.* **2002**, *67*, 8104-8113. (b) Raposo, M. M. M.; Sousa, A. M. R. C.; Kirsch, G.; Cardoso, P.; Belsley, M.; Gomes, E. d. M.; Fonseca, A. M. C. *Org. Lett.* **2006**, *8*, 3681-3684.

(25) (a) Becke, A. D. *Phys. Rev. A* **1988**, *38*, 3098-3100. (b) Lee, C.; Yang, W.; Parr, R. G. *Phys. Rev. B* **1988**, *37*, 785-789. (c) Becke, A. D. *J. Chem. Phys.* **1993**, *98*, 5648-5652. (d) Becke, A. D. *J. Chem. Phys.* **1993**, *98*, 1372-1377.

(26) Klamt, A.; Schürmann, G. *J. Chem. Soc., Perkin Trans.* **1993**, 799-806.

(26) Stefanovich, E. V.; Truong, T. N. *Chem. Phys. Lett.* **1995**, *244*, 65-74.

(27) (a) Kendall, R. A.; Apra, E.; Bernholdt, D. E.; Bylaska, E. J.; Dupuis, M.; Fann, G. I.; Harrison, R. J.; Ju, J.; Nichols, J. A.; Nieplocha, J.; Straatsma, T. P.; Windus, T. L.; Wong, A. T. *Computer Phys. Comm.* **2000**, *128*, 260-283. (b) Aprà, E.; Windus, T. L.; Straatsma, T. P.; Bylaska, E. J.; Jong, W. A. de; Hirata, S.; Valiev, M.; Hackler, M.; Pollack, L.; Kowalski, K.; Harrison, R.; Dupuis, M.; Smith, D. M. A.; Nieplocha, J.; Tipparaju, V.; Krishnan, M.; Auer, A. A.; Brown, E.; Cisneros, G.; Fann, G. I.; Früchtl, H.; Garza, J.; Hirao, K.; Kendall, R.; Nichols, J. A.; Tsemekhman, K.; Wolinski, K.; Anchell, J.; Bernholdt, D.; Borowski, P.; Clark, T.; Clerc, D.; Dachsel, H.; Deegan, M.; Dyall, K.; Elwood, D.; Glendening, E.; Gutowski, M.; Hess, A.; Jafe, J.; Johnson, B.; Ju, J.; Kobayashi, R.; Kutteh, R.; Lin, Z.; Littlefield, R.; Long, X.; Meng, B.; Nakajima, T.; Niu, S.; Rosing, M.; Sandrone, G.; Stave, M.; Taylor, H.; Thomas, G.; Lenthe, J. van; Wong, A.; Zhang, Z. "NWChem, A Computational Chemistry Package for Parallel Computers, Version 4.7." Pacific Northwest National Laboratory, Richland, Washington, **2005**. (c) Bylaska, E. J.; Jong, W. A. de; Kowalski, K.; Straatsma, T. P.; Valiev, M.; Wang, D.; Aprà, E.; Windus, T. L.; Hirata, S.; Hackler, M. T.; Zhao, Y.; Fan, P.-D.; Harrison, R. J.; Dupuis, M.; Smith, D. M. A.; Nieplocha, J.; Tipparaju, V.; Krishnan, M.; Auer, A. A.; Nooijen, M.; Brown, E.; Cisneros, G.; Fann, G. I.; Früchtl, H.; Garza, J.; Hirao, K.; Kendall, R.; Nichols, J. A.; Tsemekhman, K.; Wolinski, K.; Anchell, J.; Bernholdt, D.; Hess, P. A.; Jaffe, J.; Johnson, B.; Ju, J.; Kobayashi, R.; Kutteh, R.; Lin, Z.; Littlefield, R.; Long, X.; Meng, B.; Wong, T. A.; Zhang, Z. "NWChem, A Computational Chemistry Package for Parallel Computers, Version 5.0." Pacific Northwest National Laboratory, Richland, Washington, **2006**.

(28) (a) Schuchardt, K. L., Didier, B. T.; Black, G. D. *Concurrency and Computation: Practice and Experience* **2002**, *14*, 1221-1239. (b) Black, G. D.; Didier, B. T.; Elsethagen, T.; Feller, D.; Gracio, D.; Hackler, M.; Havre, S.; Jones, D.; Jurrus, E.; Keller, T.; Lansing, C.; Matsumoto, S.; Palmer, B.; Peterson, M.; Schuchardt, K.; Stephan, E.; Taylor, H.; Thomas, G.; Vorpagel, E.; Windus, T. "ECCE, A Problem Solving Environment for Computational Chemistry, Software Version 3.2." Pacific Northwest National Laboratory, Richland, Washington, **2004**.

Chapter V

(1) *Inter alia*: (a) *Topics in Current Chemistry (Carbon Rich Compounds I)*; de Meijere, A., Ed.; Springer-Verlag: Berlin, 1998; Vol. 196. (b) *Topics in Current Chemistry (Carbon Rich Compounds II)*; de Meijere, A., Ed.; Springer-Verlag: Berlin, 1999; Vol. 201. (c) Watson, M. D.; Fechtenkötter, A.; Müllen, K. *Chem Rev.* **2001**, *101*, 1267-1300. (d) Grimsdale, A. C.; Müllen, K. *Angew. Chem.. Int. Ed.* **2005**, *44*, 5592-5629. (e) *Carbon-Rich Compounds: From Molecules to Materials*; Haley, M. M.; Tykwinski, R. R., Eds.; Wiley-VCH: Weinheim, 2006.

(2) *Inter alia*: (a) *Modern Acetylene Chemistry*; Stang, P. J.; Diederich, F., Eds.; VCH: Weinheim, 1995. (b) Bunz, U. H. F.; Rubin, Y.; Tobe, Y. *Chem. Soc. Rev.* **1999**, *28*, 107-119. (c) Bunz, U. H. F. *Chem. Rev.* **2000**, *100*, 1605-1644. (d) Nielsen, M. B.; Diederich, F. In *Modern Arene Chemistry;* Astruc, D., Ed.; Wiley-VCH: Weinheim, 2002; pp 196-216. (e) *Acetylene Chemistry: Chemistry, Biology, and Material Science*; Diederich, F.; Stang, P. J.; Tykwinski, R. R., Eds.; Wiley-VCH: Weinheim, 2005.

(3) (a) *Metal Catalyzed Cross-Coupling Reactions (2nd Ed)*; de Meijere, A.; Diederich, F., Eds.; Wiley-VCH: Weinheim, 2004. (b) *Transition Metal Catalyzed Reactions – IUPAC Monographs Chemistry for 21st Century*; Davies, S. G.; Murahashi, S., Eds.; Blackwell Science: Oxford, 1998.

(4) (a) Spreiter, R.; Bosshard, C.; Knöpfle, G.; Günter, P.; Tykwinski, R. R.; Schreiber, M.; Diederich, F. *J. Phys. Chem. B* **1998**, *102*, 29-32. (b) Tykwinski, R. R.; Gubler, U.; Martin, R. E.; Diederich, F.; Bosshard, C.; Günter, P. *J. Phys. Chem. B* **1998**, *102*, 4451-4465. (c) Sarkar, A.; Pak J. J.; Rayfield, G. W.; Haley, M. M. *J. Mater. Chem.* **2001**, *11*, 2943-2945. (d) Slepkov, A.; Hegmann, F. A.; Tykwinski, R. R.; Kamada, K.; Ohta, K.; Marsden, J. A.; Spitler, E. L.; Miller, J. J.; Haley, M. M. *Opt. Lett.* **2006**, *31*, 3315-3317. (e) Bhaskar, A.; Guda, R.; Haley, M. M.; Goodson III, T. *J. Am. Chem. Soc.* **2006**, *128*, 13972-13973.

(5) (a) Zhang, J.; Moore, J. S. *J. Am. Chem. Soc.* **1994**, *116*, 2655-2656. (b) Pesak, D. J.; Moore, J. S. *Angew. Chem., Int. Ed. Engl.* **1997**, *36*, 1636-1639. (c) Seo, S. H.; Jones,

T. V.; Seyler, H.; Peters, J. O.; Kim, T. H.; Chang, J. Y.; Tew, G. N. *J. Am. Chem. Soc.* **2006**, *128*, 9264-9265.

(6) (a) Gobbi, L.; Seiler, P.; Diederich, F. *Angew. Chem. Int. Ed.* **1999**, *38*, 674-678. (b) Gobbi, L.; Seiler, P.; Diederich, F.; Gramlich, V. *Helv. Chim. Acta* **2000**, *83*, 1711-1723.

(7) (a) Marsden, J. A.; Palmer, G. J.; Haley, M. M. *Eur. J. Org. Chem.* **2003**, 2355-2369. (b) Spitler, E. L.; Johnson, C. A.; Haley, M. M. *Chem. Rev.* **2006**, *106*, 5344-5386.

(8) (a) Jones, C. S.; O'Connor, M. J.; Haley, M. M. In Reference 2e; pp. 303-385. (b) Zhao, D.; Moore, J. S. *Chem. Commun.* **2003**, 807-818. (c) Zhang, W.; Moore, J. S. *Angew. Chem. Int. Ed.* **2006**, *45*, 4416-4439.

(9) Recent contributions, *inter alia*: (a) Marsden, J. A.; Miller, J. J.; Shirtcliff, L. D.; Haley, M. M. *J. Am. Chem. Soc.* **2005**, *127,* 2464-2476. (b) Marsden, J. A.; Haley, M. M. *J. Org. Chem.* **2005**, *70*, 10213-10226. (c) Johnson, C. A.; Baker, B. A.; Berryman, O. B.; Zakharov, L. N.; O'Connor, M. J.; Haley, M. M. *J. Organomet. Chem.* **2006**, *691,* 413-421. (d) Anand, S.; Varnavski, O.; Marsden, J. A.; Haley, M. M.; Schlegel, H. B.; Goodson III, T. *J. Phys. Chem. A* **2006**, *110*, 1305-1318. (e) Spitler, E. L.; McClintock, S. P.; Haley, M. M. *J. Org. Chem.* **2007**, *72*, 6692-6699. (f) Johnson II, C. A.; Lu, Y.; Haley, M. M. *Org. Lett.* **2007**, *9*, 3725-3728. (g) Tahara, K.; Johnson II, C. A.; Fujita, T.; Sonoda, M.; De Schryver, F.; De Feyter, S.; Haley, M. M.; Tobe, Y. *Langmuir* **2007**, *23*, 10190-10197.

(10) (a) Roncali, J. *Chem. Rev.* **1992**, *92*, 711-738. (b) Jen, A. K.; Rao, V. P.; Wong, K. Y.; Drost, K. J. *Chem. Commun.* **1993**, 90-91. (c) Zamboni, R.; Danieli, R.; Ruini, G.; Taliani, C. *Opt. Lett.* **1989**, *14*, 1321-1323. (d) Varnavski, O.; Bauerle, P.; Goodson III, T. *Opt. Lett.* **2007**, *32*, 3083-3085. (e) Bhaskar, A.; Ramakrishna, G.; Hagedorn, K.; Varnavski, O.; Mena-Osteritz, E.; Baeuerle, P.; Goodson III, T. *J. Phys Chem. B.* **2007**, *111*, 946-954.

(11) (a) *Handbook of Oligo- and Poly-thiophenes*, Fichou, D., ed.; Wiley-VCH: Weinham, 1999; b) Katz, H. E.; Bao, Z., Gilat, S. L. *Acc. Chem. Res.* **2001**, *34*, 359-369, (c) "Sulfur-Containing Oligomers" Bäuerle, P. in *Electronic Materials: The Oligomer Approach*, Müllen K.; Wegner, G.; eds. Wiley-VCH: Weinheim, 1998, pp. 105-231.

(12) (a) Solooki, D.; Bradshaw, J. D.; Tessier, C. A.; Youngs, R. J. *Organometallics* **1994**, *13*, 451-455. (b) Zhang, D.; Tessier, C. A.; Youngs, W. J. *Chem. Mater.* **1999**, *11*, 3050-3057. (c) See also: Iyoda, M.; Vorasingha, A; Kuwatani, Y.; Yoshida, M. *Tetrahedron Lett.* **1998**, *39*, 4701-4704.

(13) (a) Marsella, M. J.; Kim, I. T.; Tham, F. *J. Am. Chem. Soc.* **2000**, *122*, 974-975. (b) Marsella, M. J.; Wang, Z.-Q.; Reid, R. J.; Yoon, K. *Org. Lett.* **2001**, *3*, 885-887. (c)

Marsella, M. J.; Piao, G.; Tham, F. S. *Synthesis* **2002**, 1133-1135. (d) Marsella, M. J.; Reid, R. J.; Estassi, S.; Wang, L.-S. *J. Am. Chem. Soc.* **2002**, *124*, 12507-12510.

(14) (a) Sarkar, A.; Haley, M. M. *Chem. Commun.* **2000**, 1733-1734. (b) Sarkar, A.; Marsden, J. A.; Haley. M. M., unpublished results.

(15) (a) O'Connor, M. J.; Yelle, R. B.; Zakharov, L. N.; Haley, M. M. *J. Org. Chem.*, submitted. (b) O'Connor, M. J.; Yelle, R. B.; Linz, T. M.; Haley, M. M., to be submitted.

(16) (a) Hotta, S.; Waragi, K. *J. Mater. Chem.* **1991**, *1*, 835-842. (b) Mohanakrishnan, A. K.; Amaladass, P.; Clement, J. A. *Tetrahedron Lett.* **2007**, *48*, 779-784. (c) Wakamiya, A.; Daisuke, Y.; Nishinaga, T.; Kitagawa, T.; Komatsu, K. *J. Org. Chem.* **2003**, *68*, 8305-8314. (d) Turbiez, M.; Frére, P.; Roncali, J. *J. Org. Chem.* **2003**, *68*, 5357-5360.

(17) (a) Krömer, J.; Rios-Carreras, I.; Fuhrmann, G.; Musch, C.; Wunderlin, M.; Debärdemäker, T.; Mena-Osteritz, E.; Bäuerle, P. *Angew. Chem. Int. Ed.* **2000**, *39*, 3481-3486. (b) Bednarz, M.; Reineker, P.; Mena-Osteritz, E.; Bäuerle, P. *J. Lumin.* **2004**, *110*, 225-231.

(18) (a) Torrado, A.; Lamas, C.; Agejas, J.; Jiménez, A.; Díaz, N.; Gilmore, J.; Boot, J.; Findlay, J.; Hayhurst, L.; Wallace, L.; Broadmore, R.; Tomlinson, R. *Biorg. Med. Chem.* **2004**, *12*, 5277-5295. (b) Kano, S.; Yuasa, Y. Yokomatsu, T.; Shibuya, S. *Heterocycles* **1983**, *20*, 2035-2037. (c) Schnürch, M. L.; Spina, M.; Khan, A. F.; Mihovilovic, M. D.; Stanetty, P. *Chem. Soc. Rev.* **2007**, *36*, 1046-1057.

(19) Marsden, J. A.; Miller, J. J.; Haley, M. M. *Angew. Chem. Int. Ed.* **2004**, *43*, 1694-1697.

(20) Bredas, J. L.; Street, G. B.; Themans, B.; Andre, J.-M. *J. Chem. Phys.* **1985**, *83*, 1323-1329.

Appendix A

(1) For recent reviews: (a) Schwab, P. F. H.; Levin, M. D.; Michl, J. *Chem. Rev.* **1999**, *99*, 1863-1933. (b) Young, J. K.; Moore, J. S. In *Modern Acetylene Chemistry* VCH: Weinheim, 1995, pp 415-442. (c) Tour, J. M. *Chem. Rev.* **1996**, *96*, 537-554. (d) de Meijere, A. (Ed.) *Topics in Current Chemistry (Carbon Rich Compounds I)* Springer: Berlin, 1998, vol. 196. (e) de Meijere, A. (Ed.) *Topics in Current Chemistry (Carbon Rich Compounds II)* Springer: Berlin, 1999, vol. 201.

(2) (a) Marsden, J. A.; Palmer, G. J.; Haley, M. M. *Eur. J. Org. Chem.* **2003**, 2355-2369. (b) Balaban, A. T.; Banciu, M.; Ciorba, V. In *Annulenes, Benzo-, Hetero-, Homo-Derivatives and their Valence Isomers,* CRC Press: Boca Raton, FL, 1987, vol. 1-3.

(3) (a) Sarkar, A.; Pak, J. J.; Rayfield, G. W.; Haley, M. M. *J. Mater. Chem.* **2001**, *11*, 2943-2945. (b) *Conjugated Polymers and Related Materials: The Interconnection of Chemical and Electronic Structure* (Eds.: Saleneck, W. R.; Lundström, I.; Ranby, B.), Oxford University Press, Oxford, UK, 1993. (c) *Photonic and Optoelectronic Polymers* (Eds.: Jenekhe, S. A.; Wynne, K. J.), American Chemical Society, Washington, DC, 1995. (d) *Nonlinear Optics of Organic Molecules and Polymers* (Eds.: Nalwa, H. S.; Miyata S.), CRC Press, New York, 1997. (e) *Electronic Materials: The Oligomer Approach* (Eds.: Müllen, K.; Wegner, G.), Wiley-VCH, Weinheim, Germany, 1998. (f) Nagamura, T. *Molec. Supramol. Photochem.* **2001**, *7*, 387-427.

(4) (a) Baldwin, K. P.; Matzger, A. J.; Scheiman, D. A.; Tessier, C. A.; Vollhardt, K. P. C.; Youngs, W. J. *Synlett* **1995**, 1215-1218. (b) Boese, R.; Matzger, A. J.; Vollhardt, K. P. C. *J. Am. Chem. Soc.* **1997**, *119*, 2052-2053. (c) Zhou, Q.; Carroll, P. J.; Swager, T. M. *J. Org. Chem.* **1994**, *59*, 1294-1301.

(5) (a) Mitchell, R. H. *Chem. Rev.* **2001**, *101*, 1301-1315. (b) Laskoski, M.; Smith, M. D.; Morton, J. G. M.; Bunz, U. H. F. *J. Org. Chem.* **2001**, *66*, 5174-5181. (c) Kimball, D. B.; Haley, M. M.; Mitchell, R. H.; Ward, T. J.; Bandyopadhyay, S.; Williams, R. V.; Armantrout, J. A. *J. Org. Chem.* **2002**, *67*, 8798-8811. (d) Boydston, A. J.; Haley, M. M.; Williams, R. V.; Armantrout, J. R. *J. Org. Chem.* **2002**, *67*, 8812-8819.

(6) Marsden, J. A.; Miller, J. J.; Haley, M. M. *Angew. Chem., Int. Ed.* **2004**, *43*, 1694-1697.

(7) (a) Laskoski, M.; Steffen, W.; Morton, J. G. M.; Smith, M. D.; Bunz, U. H. F. *J. Organomet. Chem.* **2003**, *673*, 25-39. (b) Kuck, D. In *Theoretically Interesting Molecules* (Ed. Thummel, R. P.) JAI Press, Greenwich, CT, 1998, vol. 4, pp 81-155. (c) Hopf, H. *Classics in Hydrocarbon Chemistry*, Wiley-VCH: Weinheim, Germany, 2000, pp 88-98.

(8) (a) W. B. Wan, M. M. Haley, *J. Org. Chem.* **2001**, *66*, 3893-3901. (b) Wan, W. B.; Brand, S. C.; Pak, J. J.; Haley, M. M. *Chem. Eur. J.* **2000**, *6*, 2044-2052.

(9) (a) Liu, Q.; Burton, D. J. *Tetrahedron Lett.* **1997**, *38*, 4371-4374. (b). Takano, S.; Sugihara, T.; Ogasawara, K. *Synlett* **1990**, 453-454. (c) Rossi, R.; Carpita, A.; Bigelli, C. *Tetrahedron Lett.* **1985**, *26*, 523-526. (d) Lei, A.; Srivastava, M.; Zhang, X. *J. Org. Chem.* **2002**, *67*, 1969-1971.

(10) PM3(*tm*) calculations performed on an SGI Octane workstation using Spartan SGI version 5.1.3 by Wavefunction Inc., **1998**. See Supporting Information for minimized structures.

(11) (a) Bunz, U. H. F.; Enkelmann, V. *Chem. Eur. J.* **1999**, *5*, 263-266. (b) Guo, L.; Bradshaw, J. D.; Tessier, C. A.; Youngs, W. J. *J. Chem. Soc., Chem. Commun.* **1994**, 243-244. (c) Behr, O. M.; Eglinton, G.; Galbraith, A. R.; Raphael, R. A. *J. Chem. Soc.*

1960, 3614-3625. (d) Behr, O. M.; Eglinton, G.; Raphael, R. A. *Chem. Ind.* **1959**, 699-700.

(12) See Supporting Information for details.

Appendix B

(1) Novak, J. P.; Brousseau, L. C.; Vance, F. W.; Johnson, R. C.; Lemon, B. I.; Hupp, J. T.; Feldheim, D. L. *J. Am. Chem. Soc.* **2000**, *122*, 12029; McConnell, W. P.; Novak, J. P.; Brousseau, L. C.; Fuierer, R. R.; Tenent, R. C.; Feldheim, D. L. *J. Phys. Chem. B* **2000**, *104*, 8925.

(2) Reinhard, B. M.; Siu, M.; Agarwal, H.; Alivisatos, A. P.; Liphardt, J. *Nano Lett.* **2005**, *5*, 2246.

(3) Nikoobakht, B.; Burda, C.; Braun, M.; Hun, M.; El-Sayed, M. A. *Photo. Chem. Photo. Bio.* **2004**, *75(6)*, 591.

(4) Novak, J. P.; Feldheim, D. L. *J. Am. Chem. Soc.* **2000**, *122*, 3979-3980; Brousseau, L. C.; Novak, J. P.; Marinakos, S. M.; Feldheim, D. L. *Adv. Mater.* **1999**, *11*, 447.

(5) Sung, K.-M.; Mosley, D. W.; Peelle, B. R.; Zhang, S.; Jacobson, J. M. *J. Am. Chem. Soc.* **2004**, *126*, 5064.

(6) Alivisatos, A. P.; Johnsson, K. P.; Peng, X.; Wilson, T. E.; Loweth, C. J.; Bruchez, M. P.; Schultz, P. G. *Nature* **1996**, *382*, 609-611; Loweth, C. J.; Caldwell, W. B.; Peng, X.; Alivisatos, A. P.; Schultz, P. G. *Ang. Chem. Int. Ed.* **1999**, *38*, 1808.

(7) Cumberland, S. L.; Berrettini, M. G.; Javier, A.; Strouse, G. F. *Chem. Mater.* **2003**, *15*, 1047-1056; Mirkin, C. A.; Letsinger, R. L.; Mucic, R. C.; Storhoff, J. J. *Nature* **1996**, *382*, 607-609; Mitchell, G. P.; Mirkin, C. A.; Letsinger, R. L. *J. Am. Chem. Soc.* **1999**, *121*, 8122-8123; Park, S. Y.; Lee, J. S.; Georganopoulou, D.; Mirkin, C. A.; Schatz, G. C. *J. Phys. Chem. B* **2006**, *110*, 12673.

(8) Novak, J. P.; Nickerson, C.; Franzen, S.; Feldheim, D. L. *Anal. Chem.* **2001**, *73*, 5758.

(9) Taher, D.; Walfort, B.; Lang, H. *Inorg. Chim. Act.* **2006**, *359*, 1899; Hortholary, C.; Coudret, C. *J. Org. Chem.* **2003**, *68*, 2167.

(10) Brust, M.; Walker, M.; Bethell, D.; Schiffrin, D. J.; Whyman, R. J. *J. Chem Soc.,*

Chem. Commun. **1994**, *5*, 801.

(11) Rucareanu, S.; Gandubert, V. J.; Lennox, R. B. *Chem. Mater.* **2006**, *18*, 4674.

(12) Tour, J.; Jones, L.; Pearson, D.; Lamba, J.; Burgin, T.; Whitesides, G.; Allara, D.; Parikh, A.; Atre, S. *J. Am. Chem. Soc.* **1995**, *117*, 9529.

(13) Hostetler, M. J.; Templeton, A. C.; Murray, R. W. *Langmuir* **1999**, *15*, 3782; Montalti, M.; Prodi, L.; Zaccheroni, N.; Baxter, R.; Teobaldi, G.; Zerbetto, F. *Langmuir* **2003**, *19(12)*, 5172.